Development and evaluation of innovative tuberculosis diagnostics and study of the cross-impact of Sars-CoV-2 pandemic

Mame Diarra Bousso Ndiaye

université PARIS-SACLAY

Development and evaluation of innovative tuberculosis diagnostics and study of the cross-impact of SARS-CoV-2 pandemic

Développement et évaluation de tests de diagnostic innovants pour la tuberculose et étude de l'impact croisé de la pandémie de SARS-CoV-2

Thèse de doctorat de l'université Paris-Saclay

École doctorale n° 577, structure et dynamique des systèmes vivants (SDSV)
Spécialité de doctorat : Microbiologie
Graduate School : Sciences de la vie et santé. Référent : Faculté des sciences d'Orsay

Thèse préparée dans les unités de recherche : unité des Mycobactéries et unité de l'Immunologie des Maladies Infectieuses (Institut Pasteur de Madagascar), sous la direction de **Voahangy RASOLOFO, DR**, la co-direction de **Jonathan HOFFMANN**, **PhD,** Le co-encadrement de **Niaina RAKOTOSAMIMANANA, PhD,** et de **Matthieu SCHOENHALS, PhD**

Thèse soutenue à l'Institut Pasteur à Paris, le 26 Avril 2023, par

Mame Diarra Bousso NDIAYE

Composition du Jury

Jean-Louis HERRMANN PU-PH, INSERM U1173, Université Versailles Saint-Quentin en Yvelines	Président de Jury
Maryline BONNET DR, Institut de recherche pour le développement (IRD), Université de Montpellier	Rapporteure & Examinatrice
Oana DUMITRESCU MCU-PH, UFR médecine Lyon-Sud	Rapporteure & Examinatrice
Jérôme NIGOU DR, Institut de pharmacologie et de biologie structurale (IPBS), Université de Toulouse	Examinateur
Priscille BRODIN DR, Institut Pasteur de Lille	Examinatrice

THESE DE DOCTORAT

NNT : 2023UPASL034

université PARIS-SACLAY

ÉCOLE DOCTORALE
Structure et dynamique des systèmes vivants (SDSV)

Titre : Développement et évaluation de tests diagnostiques innovants pour la tuberculose et étude de l'impact croisé de la pandémie de SARS-CoV-2

Mots clés : Biomarqueurs, Diagnostic, Co-Infection SARS-CoV-2, Progression de la tuberculose latente, Suivi du Traitement, Tuberculose

Résumé : La tuberculose (TB) reste une des maladies infectieuses les plus mortelles au monde. Compte tenu des limites que connaissent les tests de diagnostic existants, basés sur l'expectorât, tant au niveau de la collection du spécimen qu'au niveau des performances diagnostic, l'Organisation Mondiale de la Santé (OMS) a déclaré urgent de trouver des nouveaux tests non basés sur l'expectorât pour le diagnostic mais également le suivi de l'efficacité du traitement de la TB.

L'objectif de cette thèse était d'évaluer et de développer de nouveaux outils de diagnostic de la TB conformément aux critères de l'OMS en termes de sensibilité et de spécificité pour le diagnostic et le traitement de la TB. Ainsi, nous avons évalué des biomarqueurs de l'hôte basé sur des approches plus simples et plus rapide.

Dans un premier temps, nous avons évalué la signature de gènes de l'hôte RISK6. Cette dernière a été évalué par PCR quantitative en temps réel et la performance du test estimé en analysant l'aire sous la courbe d'efficacité du récepteur (AUC ROC) sur des patients atteints de la TB active (ATB), des patients d'une infection tuberculeuse latente (ITL), et des donneurs sains (HD). La performance de RISK6 pour discriminer des ATB des HD a atteint une AUC de 0,94, une sensibilité de 90,9 % et une spécificité de 87,8 %, atteignant ainsi les critères de l'OMS pour un test de dépistage de la tuberculose non basé sur l'expectoration.

Dans un deuxième temps, le dosage par Luminex de 7 biomarqueurs protéiques de l'hôte, à partir du plasma a permis d'identifier une signature de 4 protéines capable de discriminer entre différents groupes cliniques (ATB, TBI et HD) de Madagascar. La signature (CLEC3B-ECM1-IP10-SELL) permet de discriminer les ATB des HD avec une AUC de 0,96, une sensibilité de 95,6 % et une spécificité de 91,7 %. Cette signature permet également de différencier des patients qui répondent rapidement au traitement TB et des patients qui répondent tardivement à leurs traitements avec une AUC de 0,87, avec une sensibilité de 83,3 % et une spécificité de 84 %.

Enfin, nous avons développé et évalué un test de sérodiagnostic pour la détection des anticorps spécifiques anti-SARS-COV-2 basé sur la technologie Luminex. Grâce à cet outil, nous avons montré que le virus SARS-CoV-2 avait fortement circulé chez les patients tuberculeux de la cohorte de Madagascar et leurs contacts entre décembre 2020 et décembre 2021 avec une séroprévalence de 77,16% en IgG et 51,84% en IgM. En comparant les données de séroprévalence par rapport à la progression de la TB, aucune différence significative n'a été observé pour la réponse humorale anti-SARS-CoV-2 entre les patients ayant progressé vers une TB et les non progresseurs de la cohorte de contacts étudiée.

Les résultats de cette thèse fournissent des preuves solides que les tests basés sur des biomarqueurs sanguins sont des alternatives prometteuses pour améliorer le diagnostic et le suivi du traitement de la TB. Ces résultats soutiennent les efforts visant à traduire de tels outils en tests simplifié, moins couteux et plus accessible, garantissant une détection rapide et précoce de l'infection tuberculeuse mais aussi un suivi de la réponse au traitement de la TB.

université PARIS-SACLAY

ÉCOLE DOCTORALE
Structure et dynamique des systèmes vivants (SDSV)

Title: Development and evaluation of innovative tuberculosis diagnostics and study of the cross-impact of SARS-CoV-2 pandemic

Keywords: Biomarkers, Co-infection SARS-CoV-2, Diagnosis, latent tuberculosis progression, Tuberculosis, Treatment monitoring

Abstract: Tuberculosis (TB) remains one of the deadliest infectious diseases in the world. Given the limitations of existing sputum-based diagnostic tests in terms of specimen collection and diagnostic performance, the World Health Organization (WHO) has declared an urgent need to find new non-sputum-based tests for the diagnosis and monitoring of treatment efficacy of TB.

The objective of this thesis was to evaluate and develop new TB diagnostic tools in accordance with WHO criteria for sensitivity and specificity for the diagnosis and treatment of TB. Thus, we evaluated host biomarkers based on a simplified and more rapid approach.

Firstly, we evaluated the host gene signature RISK6. The latter was assessed by quantitative real-time PCR and the performance of the assay estimated by analysing the area under the receiver operating curve (AUC ROC) on active TB patients (ATB), TB infection patients (TBI), and healthy donors (HD). The performance of RISK6 in discriminating TBI from HDs achieved an AUC of 0.94, a sensitivity of 90.9% and a specificity of 87.8%, thus meeting the WHO criteria for a non-sputum-based TB test.

Secondly, of 7 host protein biomarkers evaluated from plasma using Luminex assay, we identified a signature of 4 proteins discriminating between different clinical groups (ATB, TBI and HD) recruited in Madagascar. The signature (CLEC3B-ECM1-IP10-SELL) allows to discriminate ATB from HD with an AUC of 0.96, a sensitivity of 95.6% and a specificity of 91.7%. This signature also enables us to differentiate between patients who respond rapidly to TB treatment and patients who respond late to their treatments with an AUC of 0.87, a sensitivity of 83.3% and a specificity of 84%.

Finally, we developed and evaluated a serodiagnostic tool for the detection of specific anti-SARS-CoV-2 antibodies based on Luminex technology. Using this tool, we showed that SARS-CoV-2 virus circulated strongly in the Madagascar cohort of TB patients and their contacts between December 2020 and December 2021 with a seroprevalence of 77.16% in IgG and 51.84% in IgM. When comparing seroprevalence data with TB progression, no significant difference was observed for the anti-SARS-CoV-2 humoral response between patients who progressed to TB and non-progressors in the contact cohort studied.

The results of this thesis provide strong evidence that non-sputum-based tests are promising alternatives to improve TB diagnosis and treatment monitoring. These results support efforts to translate such tools into simplified, less expensive and more accessible tests, ensuring rapid and early detection of TB infection and monitoring of response to TB treatment.

Acknowledgment

Au terme de cette aventure, je tiens à adresser mes sincères remerciements aux personnes qui ont contribué à la réalisation de ces travaux de thèse.

Aux membres du jury,

Dr. Oana Dumitrescu et Dr. Maryline Bonnet, pour avoir accepté d'évaluer mon travail de thèse en tant que rapporteures.

Dr. Priscille Brodin, Pr. Jean-Louis Hernann et Dr. Jerome Nigou, pour avoir accepté d'évaluer ma thèse en tant qu'examinateurs.

A mon encadrement,

A ma directrice et mon co-directeur de thèse,

Mes sincères remerciements à Dr Voahangy Rasolofo et à Dr Jonathan Hoffmann, pour m'avoir fait confiance et permis de mener à bien ce projet durant ces 3 années. Elles ont permis d'acquérir de nombreuses compétences tant sur le plan scientifique qu'humain. Merci à vous deux d'avoir été présents à chaque étape pour m'encourager et me pousser à aller de l'avant.

Je tiens à remercier le Dr Niaina Rakotosamimanana et le Dr Matthieu Schoenhals pour m'avoir accueilli dans leur unité de recherche, pour leur encadrement, leur disponibilité et leurs conseils.

A la Fondation Mérieux et au réseau GABRIEL, pour m'avoir accordé une bourse doctorale me permettant de réaliser cette thèse dans les meilleures conditions.

A la direction de l'Institut Pasteur de Madagascar, merci de m'avoir accueilli et de m'avoir permis d'effectuer cette thèse à l'IPM.

A mes collègues des Unités Mycobactéries et Immunologie des Maladies Infectieuses, Merci de m'avoir accueilli parmi vous ces 3 dernières années. 3 années qui auront marqué toute une vie et que je n'oublierai jamais. Merci pour la gentillesse et la bonne humeur. Misaotra Tompoko daholo !

A mes amis, pour le soutien inconditionnel et les encouragements qui m'ont poussé jusqu'à l'aboutissement de ce projet.

A ma famille, les SEYE, les NDIAYE, les MBAYE.

Je dédie ce travail à ces personnes qui me sont chères et sans qui rien de tout ceci n'aurait été possible. A Papa, Maman, Mourtada, Fatime, Kabir, Bachir merci de m'avoir toujours soutenu. Sans vous, je ne serais pas là aujourd'hui. Vous êtes ma force !

A ma grand-mère Alima SEYE, mon père Mor Gora NDIAYE et ma grande sœur Anta NDIAYE, il ne se passe pas un jour sans que je pense à vous. Que la terre de Touba vous soit légère.

A ces enseignants, professeurs, tuteurs et encadrants qui ont tous, à un moment ou à un autre, participé à mon éducation et à la construction de la personne que je suis devenue, qui ont forgé cette curiosité intellectuelle et cet amour pour la science et la recherche.

Alhamdoulilahi Rabil Alamina!

"It always seems impossible until it's done"

Madiba Mandela

Table of Content

List of figures

List of abbreviations

AFB: acid-fast bacillus
AFB−: negative acid-fast bacillus smear microscopy
Ag85: antigen 85
AlereLAM: Alere Determine TB LAM Ag
ATB: active tuberculosis
AUC: areas under the curve
BC: before Christ
BCG: bacille Calmette–Guérin
BMI: body mass index
C1q: complement component 1q
CBC: blood cell count
sCD14: monocyte differentiation antigen sCD14 soluble
cDNA: complementary DNA
CFP: culture filtrate protein
CFU: colony forming units
CI: confidence interval
CLEC3B: c-type lectin domain family 3 member B/Tetranectin
CLT+: positive sputum culture
COVID-19: coronavirus disease 2019
CRP: C-reactive protein
CSF: cerebrospinal fluid
Ct: cycle threshold
DBS: dried blood spots
DOTS: directly observed treatment
DR-TB: drug-resistant tuberculosis
DST: drug susceptibility testing
EBC: exhaled breath condensate
ECM1: Extracellular Matrix Protein 1
ELISA: enzyme linked immunosorbent assay
ELISPOT: enzyme-linked immunospot
ESAT-6: 6-kDa early secretory antigenic target
ESX1: five type VII secretion systems
FIND: foundation for innovative new diagnostics
HBHA: heparin-binding hemagglutinin antigen
HD: healthy donors
HHCs: household contacts
HIV: human immunodeficiency virus
IFN-γ: interferon-gamma
IGFBP3: Insulin-like growth factor-binding protein 3
IGRAs: interferon-gamma release assays
IP10: Interferon gamma-induced protein 10/CXCL10
IQR: interquartile range
LAM: lipoarabinomannans
L-J: Lowenstein–Jensen

LTBI: latent tuberculosis infection
LTFU: lost to follow-up
MDR-TB: multidrug-resistant tuberculosis
MHC-I: major histocompatibility complex I
M.tb: Mycobacterium tuberculosis
M. tuberculosis: Mycobacterium tuberculosis
MTBC*: Mycobacterium tuberculosis* complex
NK: natural killer
NPV: negative predictive value
OL: outermost layer
ORD: other respiratory diseases
PBMC: peripheral blood mononuclear cell
PBS: phosphate buffer saline
PG: peptidoglycan
POC: point-of-care
PPD: purified protein derivative
PPV: positive predictive value
PTB: pulmonary TB
QFT: QuantiFERON
QFT-G-IT: QuantiFERON TB-Gold-In-Tube
QFT-P: QuantiFERON TB Plus
qRT-PCR: quantitative real time PCR
RIF: rifampicin
rmsHBHA: recombinant *Mycobacterium tuberculosis* HBHA expressed in *Mycobacterium smegmatis*
ROC: receiver operating characteristic curve
ROS: reactive oxygen species
RR-TB: rifampicin-resistant tuberculosis
SARS-CoV-2: severe acute respiratory syndrome coronavirus 2
SELL: selectin L
TB: tuberculosis
TB-LAMP: tuberculosis- loop mediated isothermal amplification
TBI: tuberculosis infection
TNF: tumor necrosis factor
TPP: target product profiles
TST: tuberculin skin test
WBC: white blood cell
WGS: whole-genome sequencing
WHO: world health organization
XDR-TB: extensively drug-resistant tuberculosis

Introduction

Before the emergence of the COVID-19 pandemic that has up to date killed 6.8 million of people, tuberculosis (TB) was the leading cause of death from a single infectious agent, ahead of HIV[1]. In 2021, 10.6 million people contracted the disease and 1.6 million people died from it, including 187,000 co-infected with HIV[2]. About 20% of individuals exposed to a *Mycobacterium tuberculosis* complex bacillus will develop an active TB disease[3]. The World Health Organisation (WHO) estimates that between a quarter and a third of the world's population is infected with *Mycobacterium tuberculosis (M. tuberculosis)*, without developping any symptoms, in a state in which viable bacteria persist under immune control without clinically active TB. The infection will most often be latent, with about 5-10% risk of developing an active form of the disease during their lifetime. Latent tuberculosis infection (TBI) constitutes a reservoir from which TB disease will continue to emerge, and thus represents a major challenge to the global effort to end the TB epidemic. This risk is much higher in children and in people with a weakened immune system: people living with HIV, in a state of malnutrition, or with diabetes; as it is mostly observed in southern countries[2].

The WHO has adopted the "End TB" strategy, which aims to reduce the number of TB deaths by 95% and the incidence rate by 90% by 2035[4]. The aim is to achieve records similar to those observed in countries with a low incidence of TB (less than 8 cases per 100 000 inhabitants). To reach this goal, WHO advocates, intensified research into new prognostic tools for the evolution of latent infection and diagnostics for TB in order to overcome the current limitations in this area.

Current TB diagnosis relies on sputum-based tests, including smear microscopic and culture, which are also used to monitor response to TB treatment [2,5]. Molecular tests, such as GeneXpert MTB/RIF or ULTRA, are also performed on sputum samples[6]. However, sputum-based TB tests have limitations, including the long culture time and lack of sensitivity and specificity of smear microscopy[7]. In addition, although molecular

tests are more sensitive for the diagnosis of pulmonary TB, they still have limited sensitivity in patients with paucibacillary TB[8]. It is therefore essential to rely not only on early diagnosis, but also on biomarkers to monitor the effectiveness of treatment[9,10]. Moreover, sputum samples may be difficult to obtain in certain populations (e.g. children). In this context, WHO has stated that there is an urgent need for alternative non-sputum-based TB tests, with a set of Target Product Profiles (TPP) detailing the minimum and optimal criteria to be met for a diagnosis or for monitoring response to TB treatment test[11–13]. Developing new biomarker-based TB tests from samples other than sputum is thus needed in order to develop rapid and inexpensive tools. These should be based on more accessible biological samples such as blood or urine, convenient for field applications, and should be implementable in low-resource settings[14].

As the world is facing the COVID-19 pandemic, it is important to ensure that services and operations essential to address long-standing health problems continue to protect the lives of people with tuberculosis and other diseases or health conditions[15]. Our knowledge of COVID-19 and TB coinfection is however limited. It is thus important to investigate the concomitence of these two diseases. In this manuscript, the literature presenting tuberculosis and its main issues in this particular pantemic time was reviewed. The objectives of this PhD have been stated and the results obtained published / or not were presented and discussed.

Chapter 1: Generalities on tuberculosis: facts and context

1. The history of tuberculosis

Tuberculosis is an ancient disease. Studies on human skeletons showed that TB has affecting humans for thousands of years[16,17]. Its cause remained unknown until March 1882, when Dr Robert Koch announced the discovery of the causative bacillus, later named *M. tuberculosis*[18].

Already described in ancient times, several authors recorded a long-term weight loss disease, also called "phthisis". Hippocrates, in the 5th-4th century BC., described the symptoms, such as progressive weight loss, fatigue, coughing[19]. He also described other forms of tuberculosis, such as the bone and lymph node forms. In the eleventh century, the Uzbek physician Ibn Sina, also known as Avicenna, devoted a chapter in his famous encyclopaedic work on medicine, the *Qanûn*, to describing pulmonary tuberculosis and the different stages of the disease[20].

In 1818, René Laennec invented the stethoscope, which greatly facilitated the diagnosis of tuberculosis[19]. In 1819, Laennec was convinced that the tubercle was the common factor in all forms of the disease, that tuberculosis was an infectious disease without knowing that it was also contagious. He died of this disease in 1826[19]. The physician Jean-Antoine Villemin reproduced the lesions of human tuberculosis in animals (rabbits, guinea pigs) by inoculation of altered human tissue in the 1860s. From these observations, he asserted that this disease, was caused by a microbe that was inoculable and invisible by the technical means of the time. He demonstrated in 1865 that the transmission of bacilli occurs through the air[18].

Finally, in 1882, Robert Koch discovered the tubercle bacillus from human lesions and published an article on the etiology of tuberculosis in the *Berliner klinische Wochenschrift*. He also demonstrated the presence of the bacillus in human sputum and tubercular lesions. It was on March 24th, 1882 that Koch announced the discovery of the tuberculosis bacillus at the monthly meeting of the Berlin Physiological Society. This date is now remembered as the World TB Day. Koch continued his work on the tuberculosis pathogen, also known as Koch's bacillus. In 1890, Koch announced the

discovery of a substance that inhibited the growth of the tubercle bacillus, cured tuberculosis in infected guinea pigs and would probably be useful in treating the disease, called tuberculin. Later, it was found that tuberculin was a very useful diagnostic tool to distinguish infected from uninfected people, but it could not be used as a treatment because it was proven to be harmful for human health[18].

The Austrian paediatrician Clemens Von Pirquet used tuberculin as early as 1907 to detect a tuberculosis infection by means of a cuti-reaction test[21]. This test consists of placing a drop of tuberculin on a scarification of the skin. The test is positive when a skin reaction occurs, indicating a bacillary infection. Subsequently, Charles Mantoux advocated the administration of tuberculin by intradermal injection[22].

This technique is still the reference method used in humans today and is known as the Mantoux test or tuberculin sensitivity test (TST)[23].

In 1921, Albert Calmette and Camille Guérin first described the use of an attenuated vaccine against tuberculosis[24]. They made this discovery by working with *Mycobacterium bovis*, the pathogen of animal tuberculosis, and carried out 230 passages on the bacteria until they obtained an attenuated version of the bacillus, called Bacille Calmette Guérin (BCG). They tested their candidate vaccine on laboratory animals, but also on cattle, the natural host of *M. bovis*, and found that the vaccine was effective, protected against TB and was safe[24]. In 1943, with the advent of antibiotics in the 1940s, the use of streptomycin for the treatment of tuberculosis was described by Selman A Waksman[25]. In 1952, isoniazid, (INH) was introduced as the new wonder drug. Then pyrazinamide (PZA) and rifampicin (RIF) were developed, thus considerably reducing the duration of TB chemotherapy[26].

In 1993, tuberculosis was declared a global public health concern by the WHO. The WHO estimated at the time that one third of the world's population was infected with TB, of which about 8.8 million people developed the disease each year and 3 million died[27].

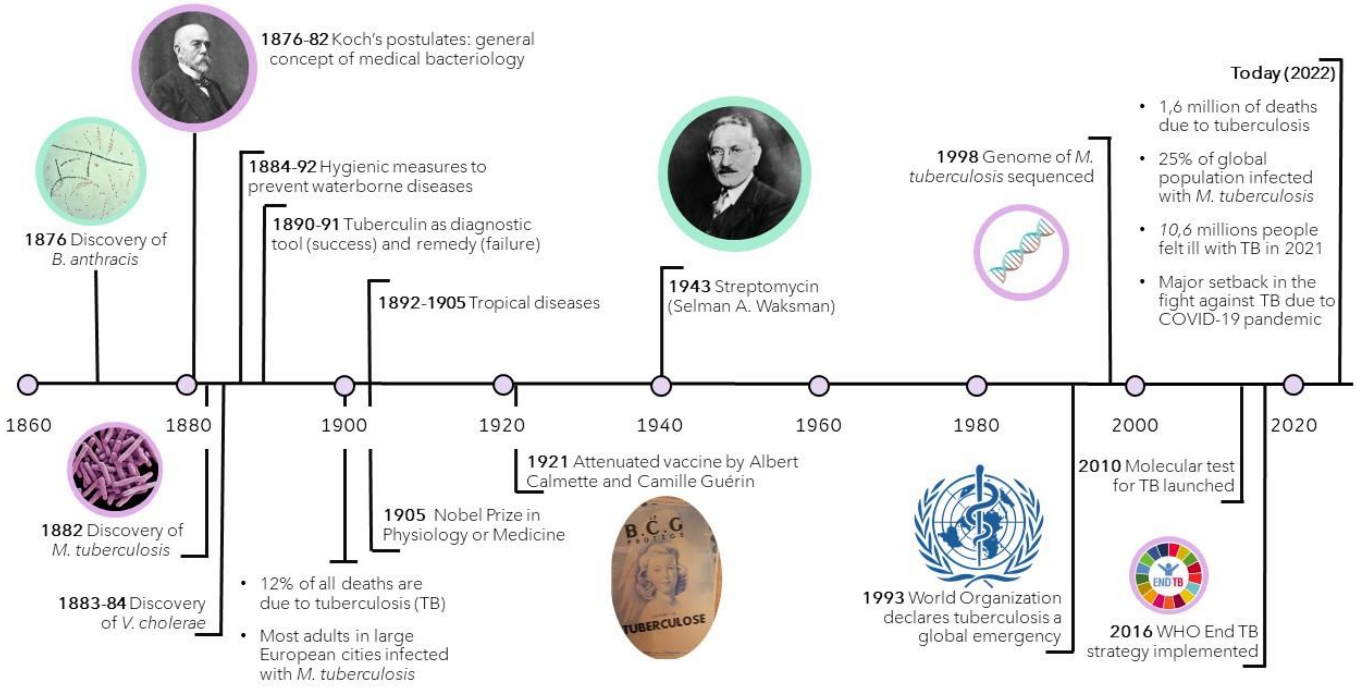

Figure 1: Chronological overview of the main discoveries in the history of tuberculosis, adapted from chronological overview of the major discoveries in the history of tuberculosis. Adapted from Oxford Immunotech: TB timeline[28].

Advances in genomics have made it possible to sequence *M. tuberculosis* H37Rv[28] (Cole et al., 1998). Thus, *M. tuberculosis* DNA shows more than 99.9% identity with other members of the tubercle bacillus complex: *M. bovis*; BCG; *M. africanum*, a human pathogen of African origin; *M. canettii*, an atypical human tuberculosis bacillus; and *M. microti*, which causes tuberculosis in some rodents[29]. These findings also show that modern pathogenic *M. tuberculosis* strains are thought to be derived from a clone that emerged 15,000 to 20,000 years ago, or 11,000 years ago, from an ancestral strain of *M. tuberculosis*[29].

2. Epidemiology of tuberculosis

2.1. Tuberculosis in the world

Tuberculosis (TB) is one of the top 10 causes of death worldwide. About 10.6 million people contract the disease annually. In 2021, 1.6 million people died from it[2]. The World Health Organisation (WHO) estimates that about one out of 4 individuals (about 2 billion people) are infected with *M. tuberculosis*, the causative agent of TB[2]. These people are carriers of the disease and therefore likely to develop an active form of TB at some point in their lives.

It is astimated that most people who develop the disease (about 90%) are adults and there are more cases in men than in women. Indeed, adult males accounted for 56.5% of TB cases in 2021, adult females accounted for 32.5% while 11% of cases were children[2]. The incidence of TB is higher in economically disadvantaged areas. In 2021, most people who developed TB were located in the WHO regions of South-East Asia (45%), Africa (23%) and the Western Pacific (18%), with smaller proportions in the Eastern Mediterranean (8.1%), the Americas (2.9%) and Europe (2.2%). The 30 high-incidence countries accounted for 87% of all estimated incident cases worldwide, and eight of them accounted for more than two-thirds of the total: India (28%), Indonesia (9.2%), China (7.4%), the Philippines (7.0%), Pakistan (5.8%), Nigeria (4.4%), Bangladesh (3.6%) and the Democratic Republic of Congo (2.9%)[2] (Figure 2).

In 2021, the number of new cases of multidrug-resistant tuberculosis (MDR-TB) (resistant to isoniazid and rifampicin) has been estimated at 450,000, up from 437,000 in 2020. The number of TB cases caused by an extensively drug resistant strain (XDR) (resistant to isoniazid, rifampicin, a fluoroquinolone and an injectable antibiotic) was estimated at 381,600 in 2021. About 6.7% of all incident TB cases that same year, were in people living with HIV. The proportion of individuals with a new episode of TB co-infected with HIV was higher in African Region, exceeding 50% in parts of southern Africa (Figure 3).

The epidemiology of TB highlights the major gaps and challenges that lie ahead in achieving global TB elimination, such as the COVID-19 pandemic.

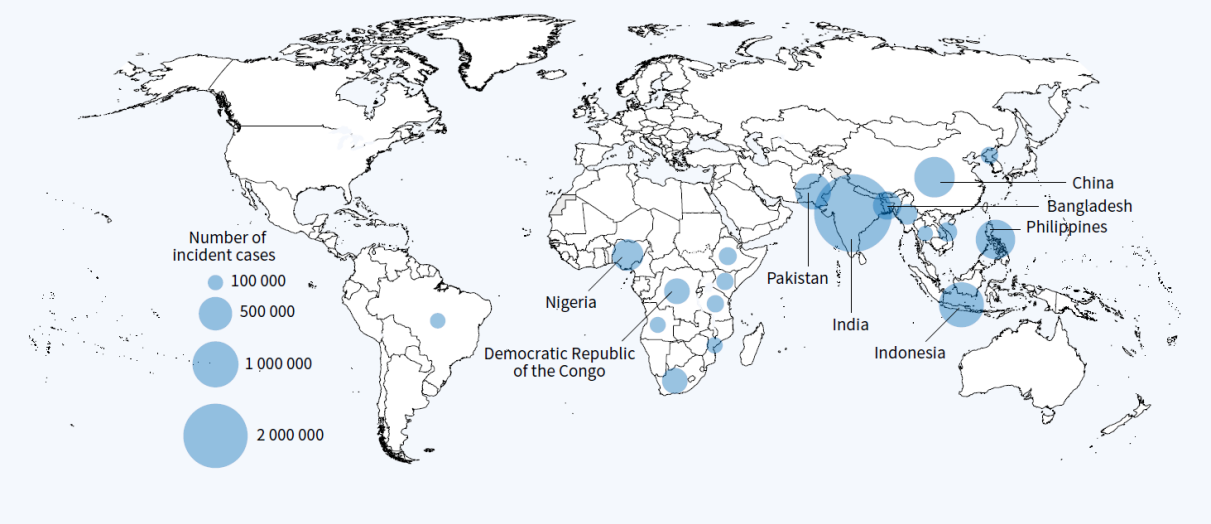

Figure 2 : Estimated incidence of tuberculosis in 2021: Countries that rank from first to eighth in terms of number of cases, and that accounted for about two-thirds of global cases in 2021, are shown[2].

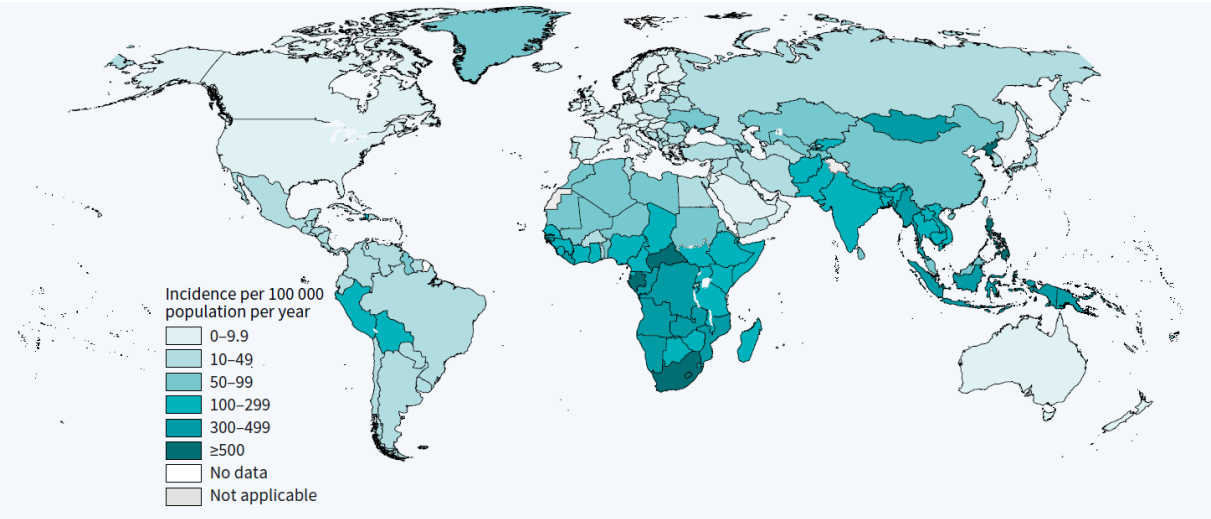

Figure 3 : Countries displayed according to incidence rate (cases per 100,000 population). More than two-thirds of the world's TB cases are concentrated in the 22 high burden countries[2].

2.2. Tuberculosis in Madagascar

TB remains a major public health problem in Madagascar. Madagascar is among the countries where the incidence remains high. The WHO estimates the burden of TB to reach 67,000 new TB infections in 2021, representing 233 incident cases per 100,000

inhabitants[30]. In 2021, the number of detected and notified TB cases, all forms combined, was 41,128, corresponding to a notification rate of 138 cases per 100,000 inhabitants[30]. This reflects the gap that needs to be filled between the estimated and reported TB cases. The majority of cases occur in young adults aged 25-34 years. As for the results regarding the treatment notified in 2020, the treatment success rate for new cases and relapsed cases is 83% compared to 84% in 2018, which is below the WHO target of 90%. Over 13,400 people have died according to the report published by WHO in 2022[30].

According to the World Bank, in 2020, Madagascar's poverty rate was 81.9% and more than 8 million people across the country (about 33 percent of the population) are food insecure[31]. Malnutrition is a risk factor that predisposes a person to develop ATB, while TB often leads to acute malnutrition and micronutrient deficiencies[32,33]. Regarding HIV coinfection, less than 1.3% of TB patients are HIV+, which is not the case in other African countries where the rate of TB-HIV co-infection is very high (Malagasy Ministry of Health data 2019).

3. Pathophysiology of *M. tuberculosis* infection

3.1. Symptoms

The clinical signs of pulmonary TB are persistent cough with sputum sometimes accompanied by blood, chest pain and more general symptoms such as fever, night sweats, fatigue, loss of appetite, and weight loss[3].

3.2. Transmission

Tuberculosis is usually transmitted by air. A patient with active pulmonary TB (PTB) emits fine droplets of bacteria into the air through coughing, sneezing or other forceful exhalation movements that produce respiratory secretions[34,35]. It is through the inhalation of these airborne droplets that a healthy individual becomes infected. The droplets can remain in the air for a long time and could be inhaled by a new host

reaching the lungs and causing an infection[36]. Crowded places (i.e., prisons, mines) favour contamination which is proportional to the confinement of the air[37]. Contamination can also occur as a result of aerosol formation when handling TB lesions or soiled objects in hospitals and laboratories[38]. The disease mainly affects the lungs, causing pulmonary tuberculosis (PTB), but it can also affect other organs (bone, pleura, lymph nodes, abdomen, skin, joints, genitourinary tract and brain), causing extra-pulmonary tuberculosis (EPTB)[39].

3.3. The spectrum of TB infection

When the *M. tuberculosis* bacillus, is inhaled into the lungs, it encounters alveolar macrophages, spreads to the lymph nodes and may enter the bloodstream with a period of bacillemia[3]. Some exposed individuals are able to resist the infection immediately or clear it quickly, others become persistently infected and develop symptoms over a period of weeks to months, and finally some individuals have a silent infection and are likely to reactivate later[3]. As the bacteria replication begins, the infection progresses and causes symptoms, most commonly in the lungs, but it can affect almost any organ in the body[39]. Nevertheless, the active phase of the disease mostly affects the lung. It is characterised by bronchopneumonia with a trend to cavitation[40].

M. tuberculosis infection and disease is a complex spectrum, which is not simply defined as TBI or active TB. Following infection with *M. tuberculosis*, some people will successfully eliminate the infection through their immune system. A second category of individuals will clear the inhaled bacteria, with an immune response that leads to the priming of T cells, and these individuals will present immunological evidence of being exposed to *M. tuberculosis*[3]. For those that have controlled the infection, the bacteria captured in a granuloma persist in a non-replicative form. These people have no symptoms and will have a negative sputum smear. The fourth category of this spectrum is the so-called incipient TB or emerging tuberculosis which refers to an intermediate

pathobiological state characterised by a higher bacterial load than in tuberculosis infection, but lower than in subclinical of active TB. Subclinical TB is a clinical state in which individuals have few or no symptoms, and intermittently the bacteria can be found in their sputum. There may be a stepwise progression of the infection or individuals may stagnate at each step for months or years[41]. Alternatively, the progression of TBI may lead to active tuberculosis. Active TB state refers to the classic form of the disease. These people have symptoms such as cough, weight loss and fever, and *M. tuberculosis* can be grown from their sputum[41]. The different stages of the TB spectrum are displayed in the figure 4.

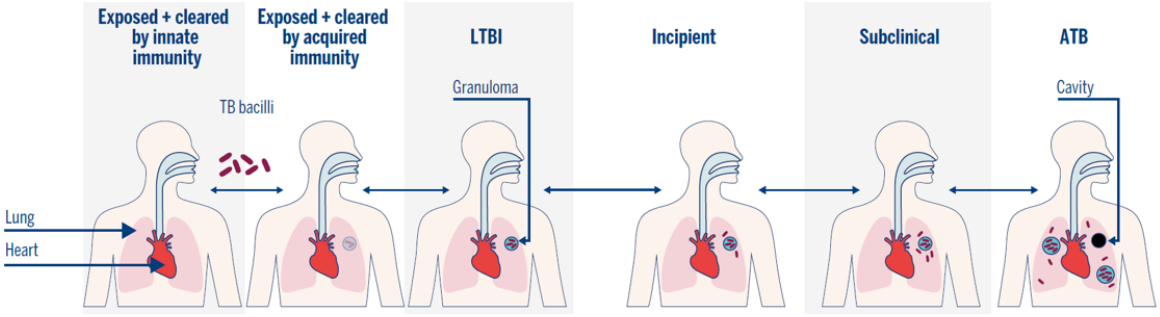

TST	Negative	Positive	Positive	Positive	Positive	Usually Positive
IGRA	Negative	Positive	Positive	Positive	Positive	Usually Positive
Culture	Negative	Negative	Negative	Negative	Intermittently positive	Positive
Sputum Smear	Negative	Negative	Negative	Negative	Usually negative	Positive or negative
Sputum molecular testing	Negative	Negative	Negative	Negative	Usually negative	Positive
Infectious	No	No	No	Likely No	Sporadically	Yes
Symptoms	None	None	None	None	None to mild	Mild to severe
Preferred treatment	None	None	Preventative therapy	Preventative therapy	Multidrug therapy	Multidrug therapy

Figure 4: The Spectrum of TB. Adapted from Pai et al.,2016 and Biomerieux Tuberculosis booklet 2022[3,41]. TST: Tuberculin Skin Test. IGRA Interferon Gamma Release Assay

3.4. A naturally resistant bacterium: structural and genomic characteristics of M. tuberculosis

3.4.1. Mycobacterium tuberculosis complex

Mycobacterium tuberculosis complex (*MTBC*) refers to a group of species (*M. tuberculosis, M. canettii, M. africanum, M. microti, M. bovis, M. caprae* and *M. pinnipedii*) that are genetically very similar[29]. Of these species, *M. tuberculosis* is the most popular

member, infecting more than a third of the world's human population; it is also capable of infecting animals in contact with humans and vice versa. *M. canettii* and *M. africanum*, closely related to *M. tuberculosis*, and can also cause tuberculosis in humans. They are usually isolated from African patients or those of African origin[42–44]. *M. bovis* has a broad spectrum of host infection, affecting humans, domestic and wild cattle and goats. In addition, a laboratory-selected mutant of *M. bovis*, isolated by Calmette and Guérin and known as *M. bovisvar* BCG, is the only vaccine used for the prevention of tuberculosis in early childhood. *M. microti* is a rodent pathogen, usually isolated from moles (rodents of the genus *Microtus*) that can also cause disease in immunocompromised human patients[45]. *M. caprae* is endemic in Europe and is usually isolated from livestock, but has recently been isolated from red fox[46,47]. Finally, *M. pinnipedii* infects seals, birds and marine mammals[48].

M. tuberculosis are acid-fast, immobile, aerobic, nonsporulating, bacilli that appear under the microscope as straight or slightly curved rods, about 4µm long and 0.4µm wide, hence the name 'bacillus' (Figure 5). The growth of *M. tuberculosis* is particularly slow with a generation time of 18 to 24 h in stationary cultures and 10 to 12 h in shaking cultures[49].

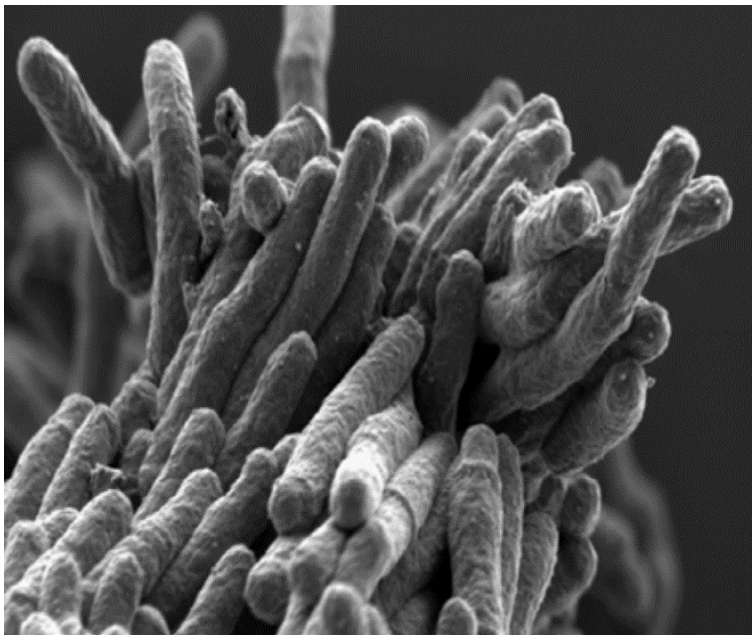

Figure 5 : Scanning Electron Microscopy (SEM) image of Mycobacterium tuberculosis [46]

3.4.2. Virulence factors

Virulence factors are the molecules that allow the bacterium to infect the host and cause disease. Those molecules of *M. tuberculosis* can be classified into two groups: secreted proteins by the bacteria and cell wall components[50].

3.4.2.1. Cell wall of mycobacteria

The cell envelope is mainly composed by a large core or cell wall complex that contains three different covalently bound structures: the peptidoglycan, the arabinogalactan and the mycolic acids[51,52]. The covalent bonding of the mycolic acids results in a hydrophobic layer of extremely low fluidity. This layer is also called the mycomembrane. This fatty acid layer is responsible for the low permeability of the membrane which protects the bacteria from many host factors and also from many antibiotics, including beta-lactamases[53]. The outer part of the mycomembrane contains various free lipids, such as phenolic glycolipids, phthiocerol dimycocerosates, cord factor or dimycolyltrehalose, sulfolipids and phosphatidylinositol mannosides, which are intercalated with the mycolic acids. Most of these lipids are specific to mycobacteria[51]. The outer layer, usually called the capsule, contains mainly polysaccharides (glucan and arabinomannan) (Figure 6). All these molecules are capable of inducing host immune responses[51].

The best-characterized virulence factor of *M. tuberculosis*, lipoarabinomannan (LAM), binds to the plasma membrane via a glycosylphosphatidylinositol (GPI) anchor and extends through the bacterial cell wall. The surface of *M. tuberculosis* harbors mannose-capped LAMs (ManLAMs), while other less pathogenic mycobacteria contain phospho-myo-inositol-capped LAMs (PILAMs). These molecules play important role in immune system failure by interfering with phagosomal maturation, the autophagy, the apoptosis, MHC antigen processing and presentation, granuloma formation, macrophage activation, protection from IFN-γ, inhibition of protein kinase C activity, and blocking transcription of IFN-γ-inducible genes[54–56].

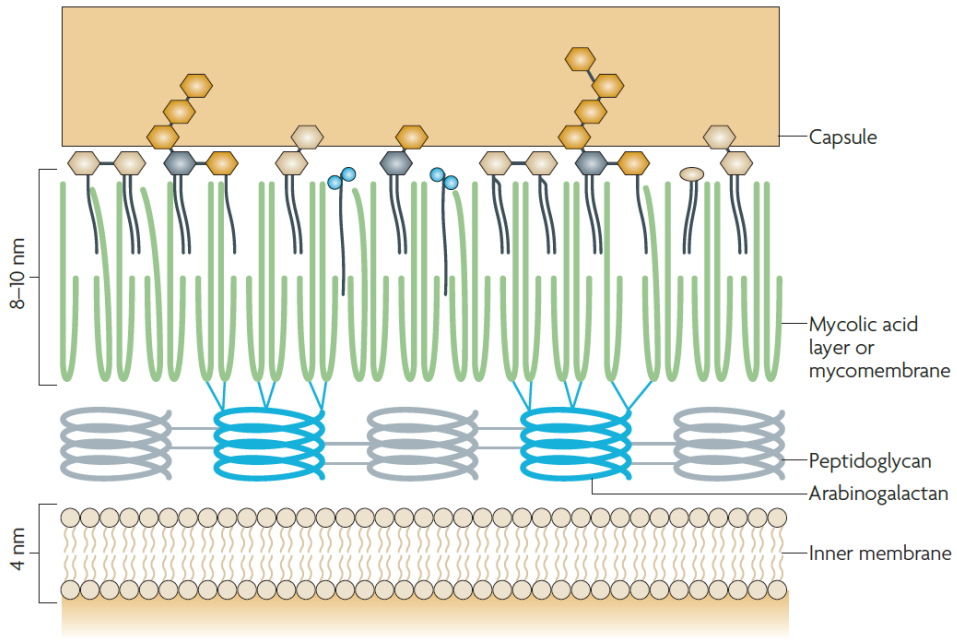

Figure 6 : Schematic representation of the cell envelope of *Mycobacterium tuberculosis*. Composed of a large cell-wall core or complex that contains three different covalently linked structures (peptidoglycan (grey), arabinogalactan (blue) and mycolic acids (green)). The covalent linkage of mycolic acids results in a hydrophobic layer of extremely low fluidity. This layer is also referred to as the mycomembrane. The outer part of the mycomembrane contains various free lipids, such as phenolic glycolipids, phthiocerol dimycocerosates, cord factor or dimycolyltrehalose, sulpholipids and phosphatidylinositol mannosides, that are intercalated with the mycolic acids. Most of these lipids are specific for mycobacteria. The outer layer, which is generally called the capsule, mainly contains polysaccharides (glucan and arabinomannan).[57]

3.4.2.2. *M. tuberculosis* and ESX1: an escape mechanism

ESX1 is a type VII secretion system involved in the virulence of the bacteria[57]. Once bacteria have been internalised into a phagosome by host macrophages, the ESX-1 secretion system ensures delivery of bacterial products into the cytoplasm of macrophages[58]. This system is carried by the secretion locus called RD1. This locus encodes 9 genes including those coding for the ESAT-6 (early secreted antigenic target of 6 kDa) and CFP-10 (culture filtrate protein of 10 kDa) proteins[57]. Both of these proteins are important antigenic targets for T cells and are essential for the virulence of *M. tuberculosis*. Without the ESX 1 system, tuberculosis is attenuated. For example,

the BCG vaccine strain lacks *Esx*1[24]. The absence of RD1 in BCG strains has allowed the development of immunoassays to distinguish the host response to *M. tuberculosis* infection from the BCG vaccine-induced response[59]. Hence, many non-tuberculous mycobacteria also lack RD1, these tests can also distinguish M. tuberculosis infection from infection with commonly encountered environmental mycobacteria such as *M. avium*[59]. The ESX 1 is also a potent inducer of type I IFN, meaning that without this type VII secretion system, the innate immune response that is triggered is much less robust[50].

4. The immune response to tuberculosis infection

During infection, bacilli contained in small droplets reach the pulmonary alveoli where they are absorbed by different cell types including alveolar macrophages, interstitial macrophages, local dendritic cells and epithelial cells. If this first line of defense fails to eliminate the bacteria, *M. tuberculosis* invades the interstitial tissue of the lungs, either by directly infecting the alveolar epithelium or by migrating infected alveolar macrophages to the lung parenchyma. These cells carry *M. tuberculosis* to the draining lymph nodes where the dendritic cells, in cooperation with the macrophages, stimulate T-cells, which mediate protective immunity against tuberculosis. Macrophages and other immune cells are recruited during the early innate response to infection. The resulting cellular infiltrates become organized as primary granulomas. The secretion of cytokines such as IL-12 and IL-23 by dendritic cells, leads to the activation of T cells which produce IFN-γ. *M. tuberculosis*-infected macrophages which are also antigen-presenting cells, secrete bacteria peptides, that would be presented in the major histocompatibility complex (MHC). MHC class I present peptides to CD8 T cells and MHC class II present peptides to CD4 T cells.

Both CD4 and CD8 T cells are involved in protective immunity against TB[60]. CD4 T cells are mainly helper cells. Th1 cells will produce IFN-γ and other cytokines such as IL2,

and TNFα, that are crucial for protective immunity against mycobacterial infections[61]. Th17 cells, which produces IL-17A, IL-17F, and IL-22[62,63].

CD8 T cells secrete granules that contain cytotoxic molecules such as perforin, granzymes, and granulysin[60]. These molecules confer CD8 T cells ability to lyse infected host cells, including *M. tuberculosis*-infected macrophages. In addition, CD8 T cells can induce apoptosis of infected target cells. Apoptosis may be activated to control *M. tuberculosis* infection[64]. CD8 T cells produce cytokines similar to those of CD4 T cells, that are IL-2, IFN-γ and TNF, thus activating other T cells and macrophages[56].

After being activated, T cells migrate into the lung where *M. tuberculosis* is located. T lymphocytes start infiltrating the granuloma; this leads to the formation of larger, well-organized, solid granulomas in which *M. tuberculosis* organisms typically are mostly located centrally. From the host's point of view, the granuloma is a bacterial "prison" that allows the infection to be "isolated" from the rest of the body; however, from the bacterium's point of view, it may be a growing collection of phagocytic cells to infect and replicate[3]. Granulomas may kill, limit replication of *M. tuberculosis* or evolve into permissive granulomas with increased bacterial growth, limited destruction and further spread to form new granulomas. Those structures harbour a wide variety of immune cells and immunological factors such as macrophages, epithelioid macrophages, CD4 and CD8 T cells, cytotoxic granules and cytokines, B cells, NK cells and antibodies. These compounds' interactions likely govern whether the lesions progress or not[65]. When the granuloma is restrictive, the infection is under control, but the pathogen is not completely eradicated. At this stage, the infected individual is healthy and will not transmit the infectious agent. The successful containment depends on the full activity of the T-cell response[56]. This T cell function can be compromised if they are confronted with co-infections, for example HIV. These co-infections prevent an immune response; that can result in the secretion of anti-inflammatory cytokines, such as IL-10 and TGF-β. When the immune response is impaired, which is the case in about 10% of infected individuals, disease may occur. The infection is not contained anymore, and the bacteria

can multiply in the granuloma. The granuloma becomes caseous and ruptures, enabling the pathogen to spread and the TB infection is now contagious[3] (Figure 7). In some cases, this bacterial spread can occur through the capillaries, thus infecting other organs.

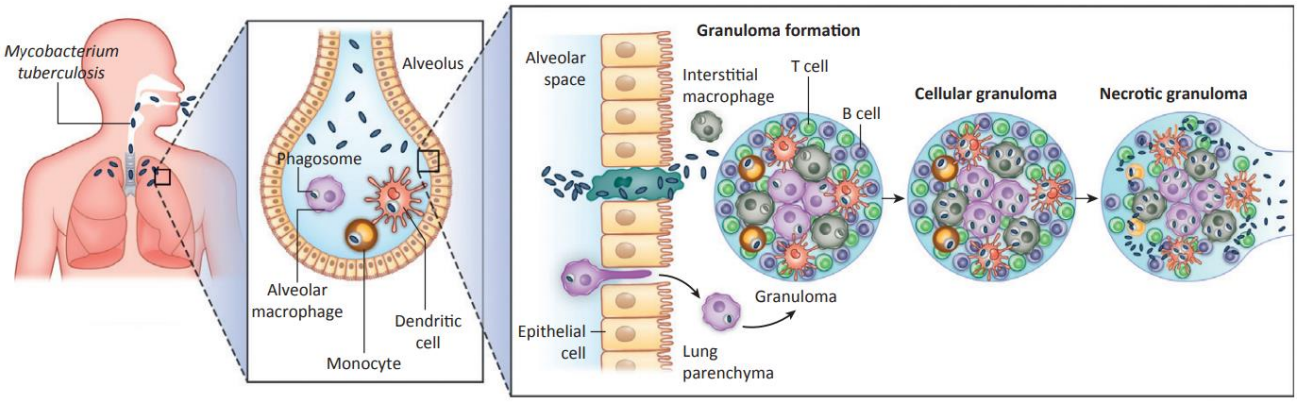

Figure 7: Granuloma formation. When *M. tuberculosis* enters the lungs by inhalation, it reaches the alveolar space and encounters the resident alveolar macrophages. If this first line of defense fails to eliminate the bacteria, *M. tuberculosis* invades the interstitial tissue of the lungs, either by directly infecting the alveolar epithelium or by migrating infected alveolar macrophages to the lung parenchyma. Subsequently, dendritic cells or inflammatory monocytes transport *M. tuberculosis* to the pulmonary lymph nodes for T cell priming. This leads to the recruitment of immune cells, including T cells and B cells, into the lung parenchyma to form a granuloma. The bacteria replicate in the growing granuloma. If the bacterial load becomes too great, the granuloma cannot contain the infection leading to the spread to other organs, including the brain. At this stage, the bacteria can enter the bloodstream or re-enter the respiratory tract and be released; this leaves the infected host with active TB. [66]

5. Treatment and prevention of tuberculosis

5.1. Treatment of drug-sensitive tuberculosis

The standard treatment for new cases of tuberculosis involves first-line antibiotics: isoniazid, rifampicin, pyrazinamide and ethambutol[2]. The standard treatment duration is 6 to 8 months and consists of 2 successive phases. The initial phase lasts 2 months and consists of the administration of these four antibiotics. The second phase of 4-6 months, also known as the 'continuation phase', consists of dual therapy with isoniazid and a second antibiotic, rifampicin or ethambutol[67]. The drugs are taken orally every day. In order to fight the disease more effectively, the Directly observed treatment

(DOTS), strategy is recommended by the WHO. This involves direct observation and monitoring by a third party of every antibiotic taken by the patient treated for at least the first two months of treatment.

5.2. Preventive treatment

The main health intervention for TB prevention is the treatment of people at high risk of developing TB. WHO has recommended that certain high-risk groups, tested for TB infection, to be targeted for preventive therapy. Those groups include people living with HIV, children and adults who have been in contact with patients with TB disease (household contacts), patients starting anti-TNF therapy or dialysis, those preparing for organ or haematological transplantation, or those with silicosis. WHO-recommended preventive treatment regimens include: 6 or 9 months of daily isoniazid, or a 3-month regimen of weekly rifapentine plus isoniazid, or a 3-month regimen of daily isoniazid plus rifampin[2]. A one-month regimen of daily rifapentine plus isoniazid or 4 months of daily rifampicin alone can also be proposed as alternatives. In settings with high TB transmission, adults and adolescents living with HIV should receive at least 36 months of isoniazid preventive therapy[2].

5.3. Drug-resistance of *M. tuberculosis*

TB can be treated with first-line antibiotics. However, this treatment is long (6-9 months), and as a result of poorly followed treatment, the bacilli may become resistant to one or more first-line drugs. Treatment of people diagnosed with rifampicin-resistant TB (RR-TB) and multidrug-resistant TB (MDR-TB, defined as resistance to isoniazid and rifampicin) takes longer, and requires drugs that are more expensive (≥US$1,000 per person) and cause more side effects. Multidrug-resistant TB is a form of the disease caused by a bacillus that is resistant to isoniazid and rifampicin, the two most effective first-line TB drugs. However, multidrug-resistant TB can be treated and cured with second-line drugs. Nevertheless, these treatment options require long-term administration (9 months) of drugs that are both expensive and toxic.

5.4. Challenges of treating pulmonary tuberculosis

The main challenges of TB treatment are the duration and intensity of drug regimens, both of which affect adherence to treatment, toxicity, especially of second-line drugs used to treat resistant TB, and the limited availability of drugs for the treatment of resistant TB in children. The treatment of TB in people living with HIV is further complicated by drug interactions between anti-TB drugs and antiretrovirals[2,67].

There is a pressing need for more effective, affordable and less toxic regimens that shorten the duration of treatment, especially for drug-resistant TB. Therefore, WHO promotes the funding and research of new molecules to treat TB. The figure 8 shows the pipeline of new TB drugs but also the new TB treatment regimens being tested in 2022[68].

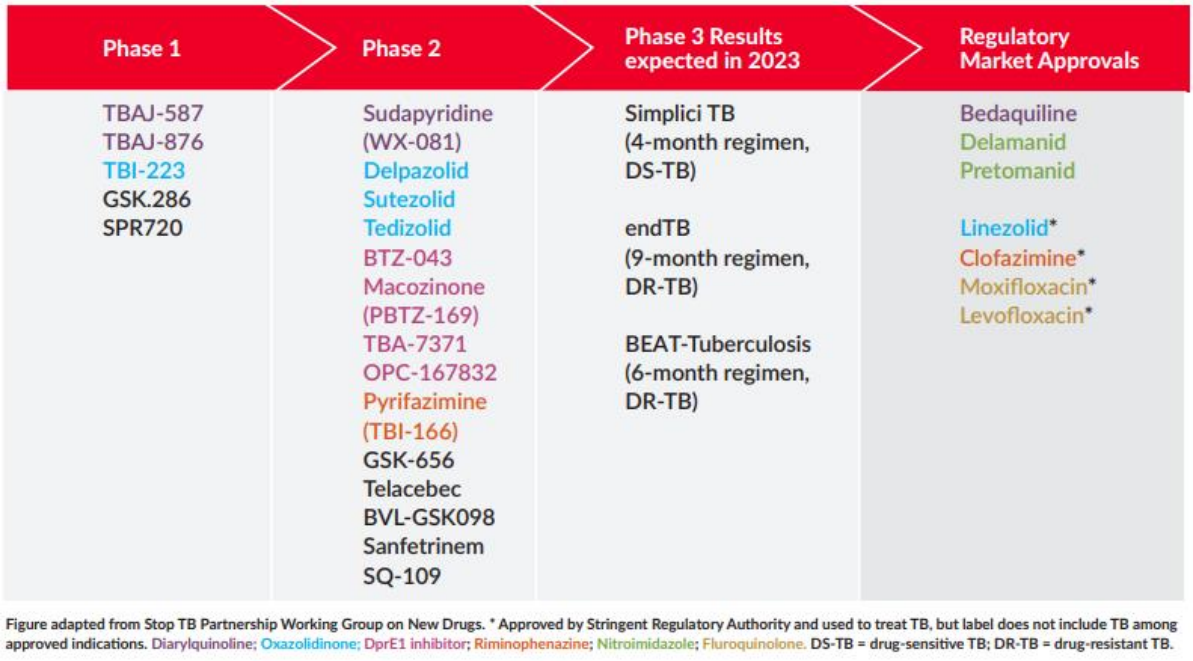

Figure 8 : Overview of the pipeline of new TB drugs in Clinical Development[68].

5.5. Current methods of monitoring the treatment of TB: challenges and needs

Smear microscopy is the most widely used method to date for diagnosing pulmonary TB and monitoring response to treatment[6]. However, sputum smears have a low sensitivity (20% to 66%). The GeneXpert system is more sensitive, but is not

recommended for treatment monitoring as it may detect remnant DNA from dead bacteria. In this context, there is a need to improve monitoring of treatment efficacy[69]. Immunoassays can be complementary tools for monitoring the effectiveness of TB treatment[70]. These tools could allow early identification of TB patients non responding to treatment and therefore require timely adjustment during antibiotic therapy, those who require longer treatment or those who do not respond to treatment[71,72]. Existing blood tests, such as IFN-γ release assays (IGRA), measure IFN-γ production in response to stimulation by the *M. tuberculosis*-specific antigens ESAT6 and CFP10. But these tests do not provide information on the efficacy of TB treatment.

5.6. Vaccination against tuberculosis

Currently, the Bacille Calmette-Guérin (BCG) vaccine remains the only vaccine licensed for the prevention of TB disease[2]. It is a live attenuated bacterial vaccine derived from *M. bovis*. BCG was first used in humans in 1921[24]. It provides significant protection to children, particularly against severe forms such as meningeal and miliary tuberculosis[73]. The protective effect of BCG in children is likely to last up to 10 years[73]. However, BCG vaccination is not recommended for the prevention of pulmonary tuberculosis in adults because of its variable efficacy. This variability depends on multiple factors such as geographical location, exposure to environmental mycobacteria, age at vaccination, variation in HLA alleles, etc.[74,75]. There is therefore an urgent need for new, highly effective vaccines that offer protection against all forms of TB in all population groups[2]. Currently, 16 vaccine candidates are in clinical trials: four in phase I, two in phase IIa, four in phase IIb, and six in phase III. These include candidates that prevent TB infection and disease, as well as those that improve TB treatment outcomes[68] (Figure 9). In September 2022, a new innovative TB vaccine candidate known as BNT164 entered clinical trials. The company BioNTech registered a phase I study of two investigational mRNA vaccines under the common name BNT164: BNT164a1 and BNT164b1[68]. This Phase I safety and immunogenicity study will evaluate three different dose levels of the

two vaccines in male subjects. Other mRNA vaccines from IAVI/Moderna and the WHO mRNA vaccine technology transfer centre are in the pipeline[68] (Figure 9).

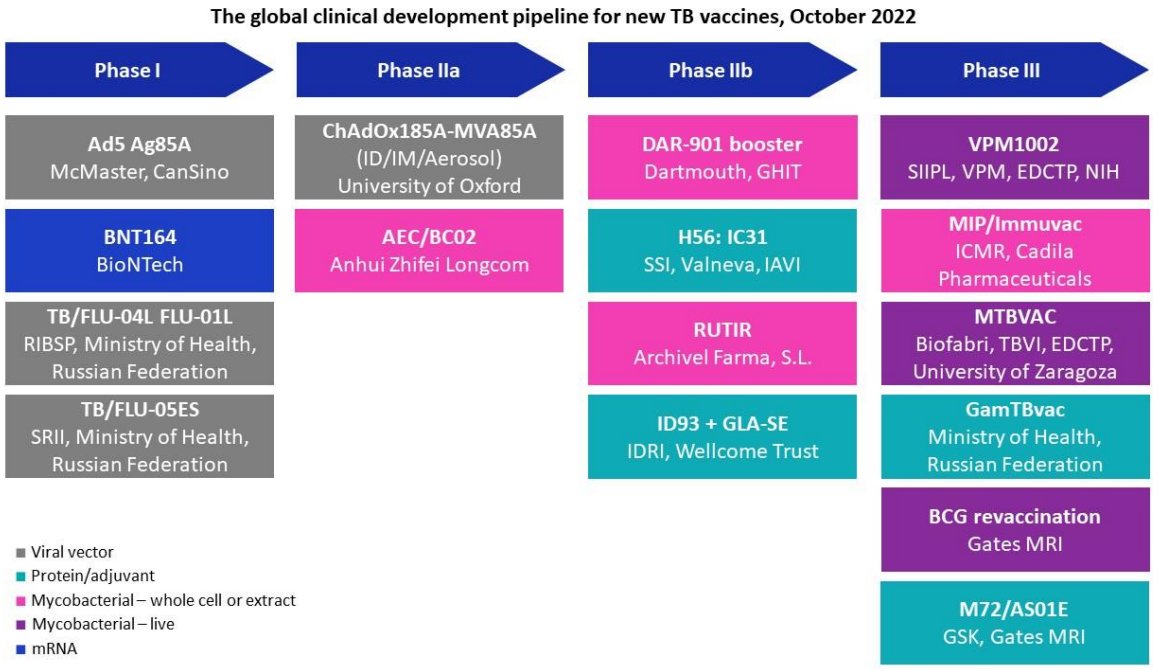

Figure 9 : Diagrams of new vaccines in development classified by vaccine type and evaluation phase. Adapted from the TAG pipeline report 2022 and the WHO global report on TB in 2020[15,68].

6. Diagnosis of pulmonary tuberculosis

6.1. Screening for tuberculosis infection

The diagnosis of TB infection is based on specific cell-mediated immune response (Figure 10).

6.1.1. Tuberculin Skin Test (TST)

The TST is based on delayed hypersensitivity reaction that develops 48-72 hours after intradermal administration of the purified protein derivative (PPD)[76] A positive test is indicated by the size of the induration larger than 5 mm diameter. The main disadvantage of the TST is its lack of specificity in people who have been vaccinated with BCG and those with exposition to non-tuberculosis mycobacteria. Moreover, this test requires at least two visits with the patient.

In order to improve the specificity of the test, the RD-1 skin-specific intradermal test has recently been developed[77]. This test would be more specific as it is based on proteins carried by the RD-1 loci encoding two immunogenic proteins, namely early secreted antigenic target 6 (ESAT-6) and culture filtrate protein 10 (CFP-10)[57].

Therefore, tests containing only RD-1 associated proteins have improved specificity hence these proteins are absent in BCG [77].

6.1.2. Interferon-gamma release assays (IGRA)

IGRAs are in vitro blood tests that measure T-cell release of IFN-γ following stimulation by antigens specific to the *M. tuberculosis* such as ESAT6 and CFP10[59]. To our knowledge, 5 of these tests are commercialized and currently available in three different formats. One is a whole blood test ELISA format. The most used and known is the QuantiFERON-TB Gold Plus assay (Cellestis/Qiagen, Carnegie, Australia). The assay contains 4 blood stimulation tubes: negative control tube, positive control tube and 2 TB antigen tubes TB1 and TB2. TB1 contains ESAT-6 and CFP-10 antigens that stimulates CD4 T cells. TB2 contains in addition to those 2 antigens, new peptides that stimulate the IFN-γ production by both CD4 and CD8 T-cells. The Standard TB Feron ELISA assay uses three tube-based IGRAs including a single TB antigen tube containing ESAT-6, CFP-10 and TB7.7. There is also the LIOFeron TB/TBI test (LIONEX GmbH, Braunschweig, Germany), which is a new developed IGRA for the diagnosis of TBI and TB[78]. This assay contains four blood stimulation tubes including 2 TB antigen tubes including TB A and TB B. This assay contains, alanine dehydrogenase (Ala-DH) antigen in addition to ESAT-6, CFP-10, and TB7.7 which induces (MHC) class I-restricted T CD8+ lymphocytes to produce IFN-γ[79].

The second format of assays is a whole blood test using chemiluminescent immunoassay (CLIA), the LIAISON QuantiFERON-TB Gold Plus assay. This is an in vitro diagnostic test using QuantiFERON-TB Gold Plus collection Tube by Qiagen (Qiagen, Carnegie, Australia) and the CLIA reagents by LIASON (DiaSorin, Saluggia VC, Italia)[80].

The third format is an enzyme-linked immunospot (ELISPOT) using peripheral blood mononuclear cells (PBMC) and consists of cytokine fingerprints of a gamma interferon-producing T cell and counting of spot. This test is called T-SPOT.TB assay (Oxford Immunotec, Abingdon, United Kingdom)[81].

The three technologies involve overnight incubation with *M. tuberculosis* specific antigens, sample processing, and the use of instruments to generate a readout.

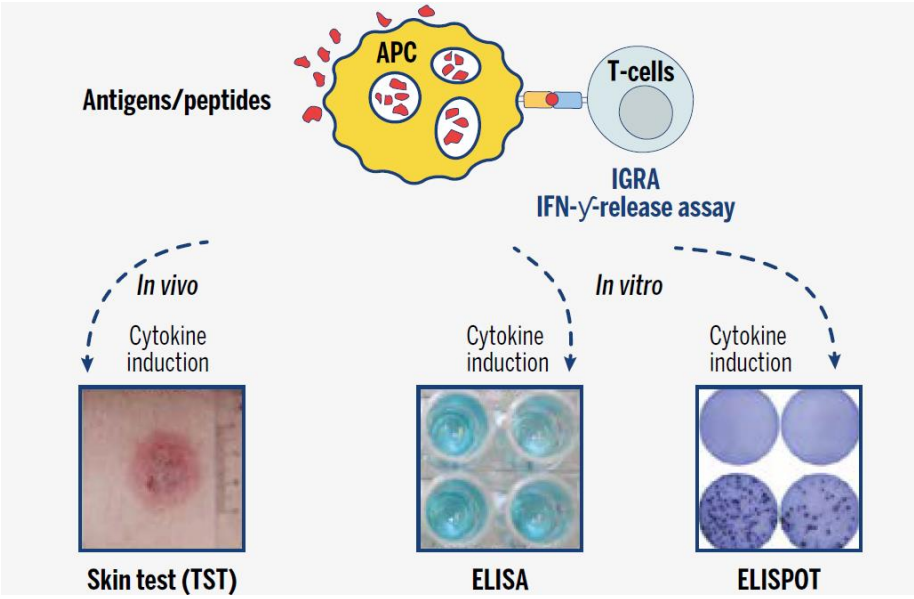

Figure 10 Tests based on specific T-cell immunity for the diagnosis of infection. All tests rely on stimulation with a purified protein derivative (PPD) or specific *M. tuberculosis* antigens (in red) that cause induction of cytokines in specific T cells. Cytokines can be detected in vivo by skin tests or in vitro by gamma interferon release assays: ELISA or ELISPOT[41].

6.2. Diagnosis of tuberculosis disease

Suspicion of TB disease in a patient requires confirmation through clinical and bacteriological examinations.

6.2.1 Radiological examination

It allows the pulmonary forms of the disease to be identified. Radiological abnormalities can be very variable. Infiltrates (white areas on the X-ray), isolated or grouped nodules and excavated lesions (caverns) in the upper lobes and posterior segments of the chest are usually present (Figure 11)[3].

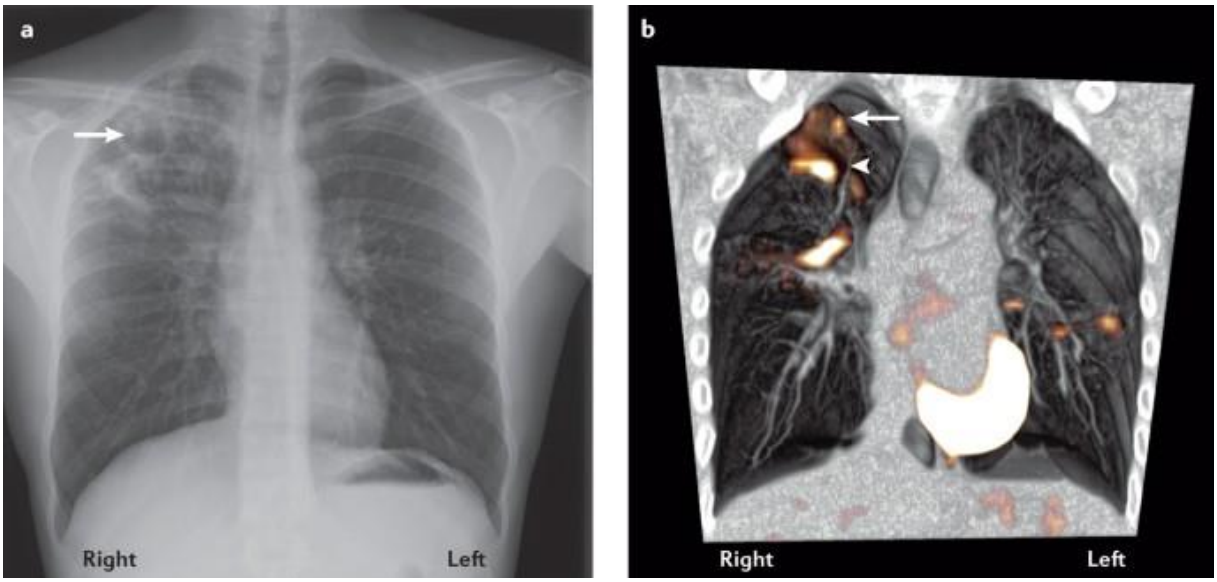

Figure 11: Conventional chest X-ray and High-resolution PET scan. a. Conventional chest X-ray. The image shows the typical features of active pulmonary tuberculosis: a large cavity in the right upper lobe of the lung indicated by the arrow with surrounding infiltrates or consolidation (due to inflammation and oedema). B. High-resolution PET scan. Image showing the posterior half of the chest cavity of a person recently diagnosed with bilateral pulmonary tuberculosis. The orange colour represents areas with abnormalities[3].

6.2.2. Bacteriological examination

6.2.2.1. Direct examination under the microscope

Microscopic examination of clinical sputum samples has been the mainstay of TB case detection for over 100 years. As such, the microscopic smear is the most widely used test for active TB. It is rapid, relatively inexpensive and less labour intensive than other technologies[82]. It allows the detection of acid-fast bacilli (AFB) after Ziehl-Nielsen staining or by using auramine stanning in fluorescence microscopy[83,84] (Figure 12). However, smear microscopy lacks of sensibility and specificity.

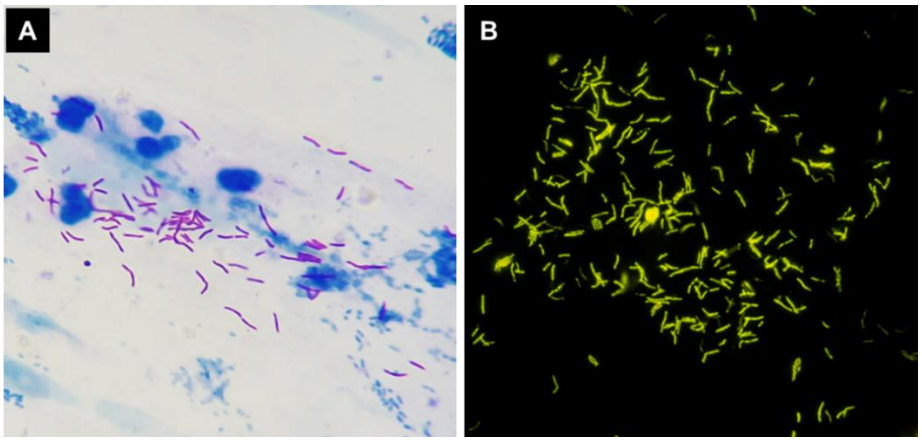

Figure 12: *M. tuberculosis* staining methods. A: Ziehl-Neelsen stain of a sputum smear showing long, thin, curved, purple acid-fast bacilli (AFB). B: Auramine-phenol stain of a sputum smear showing tubercle bacilli in bright green on a dark background.

6.2.2.2. Culture

Isolation of *M. tuberculosis* is usually performed by culture on specific solid media, most commonly Löwenstein-Jensen (LJ), an egg based solid medium, containing glycerol and supplemented with sodium pyruvate to promote the growth of *M. bovis* and *M. africanum*[85]. On solid media, *M. tuberculosis* strains appear as rough, beige cabbage like colonies (Figure 12). Three to seven weeks are required to obtain a result. Mycobacteria grow more rapidly in liquid than in solid media[7]. Although manual methods exist, automated methods with permanent control systems have been developed, such as the Bactec 9000MB (Becton Dickinson, Sparks, MD), the Bactec 960 Mycobacterial Growth Indicator Tube (MGIT960; Becton Dickinson), the ESP II Culture System (Trek Diagnostic Systems; Cleveland, OH) and the MB/BacT Alert 3D (bioMérieux, France)[86]. However, performing smear culture requires high-level laboratory facilities (BSL3), is expensive and takes weeks to obtain colonies.

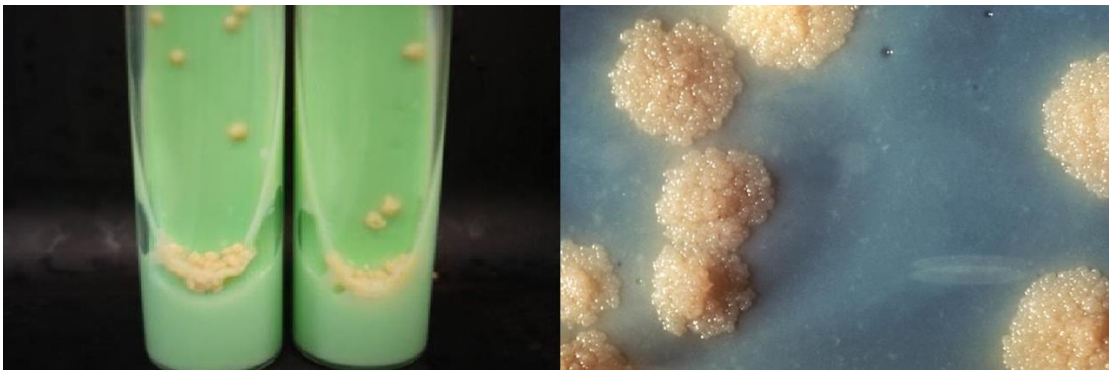

Figure 13: Lowenstein-Jensen medium culture of Mycobacterium tuberculosis showing typical dry, clustered, yellow to beige colonies.[87]

6.2.3. DNA based molecular test

These techniques can be used for the identification of germs after culture or directly from pathological specimen. One example is the GeneXpert (Cepheid, Sunnyvale, CA, USA). This real-time PCR-based technique allows both the detection of mycobacteria of the tuberculosis complex and the detection of rifampicin resistance in biological samples (sputum).

The GenoType MTBDRplus test (Hain Lifescience GmbH, Nehren, Germany) is a PCR-based technique for the detection of mycobacteria of the MTBC and MDR strains, identifying atypical mycobacteria.

The LAMP test (Loop Mediated isothermal Amplification Test) (Eiken Chemical Company Ltd, Tokyo, Japan, 2005) is based on isothermal amplification, not requiring a thermal cycler to detect the MTBC.

6.2.4. Urine tests

The commercially available Alere Determine TB LAM (AlereLAM; Abbott, Chicago, IL, USA) detects lipoarabinomannan (LAM) in urine using polyclonal antibodies on a simple lateral flow test, providing a point-of-care (POC) reading in 20 minutes[88]. The current format is only useful for HIV-infected individuals, particularly those with a CD4 count <200[89]. A more sensitive platform is under development, has shown encouraging results and is being commercialised, the Fujifilm SILVAMP TB LAM (FujiLAM; Fujifilm,

Tokyo, Japan) which have a 30% improved sensitivity for detecting TB (independent of whether it is PTB or EPTB) compared to the AlereLAM[90].

6.2.5. Genomic sequencing

Whole genome sequencing (WGS) is a current alternative to the WHO-approved probe-based methods for TB diagnosis and detection of drug resistance.

The Deeplex® Myc-TB assay (Genoscreen, Lille, France) is the most well-described commercially available targeted sequencing assay. Deeplex is usable directly on sputum samples but has also recently been applied successfully to stool samples[91,92]. The main disadvantage of these techniques is the high cost of the equipment and technical expertise required to interpret WGS data, making them difficult to implement in resource-limited countries.

7. Innovation and research in biomarkers of pulmonary *M. tuberculosis* infection

Biomarkers are indicators of a particular biological, physiological and/or pathological state. In the context of this thesis, they can indicate whether a person is infected with *M. tuberculosis*, and could potentially identify the state in which is an individual in the spectrum of TB presentations. Biomarkers can also be useful tools to monitor treatment and enable early detection of TB progression[9]. Indeed, even though single/fewer markers are easier to test for, many studies have shown the increased effectiveness of a biomarker in combination to other molecules compared to a single biomarker[93,94]. Those biosignature of markers should make it possible to overcome the limitations of existing diagnostic tools based on sputum and to answer several biological questions related to TB infection, such as the diagnosis, the risk of progression to active TB, and the treatment monitoring. Biomarkers can be either arise from the host or from a pathogen (Figure 14)[9].

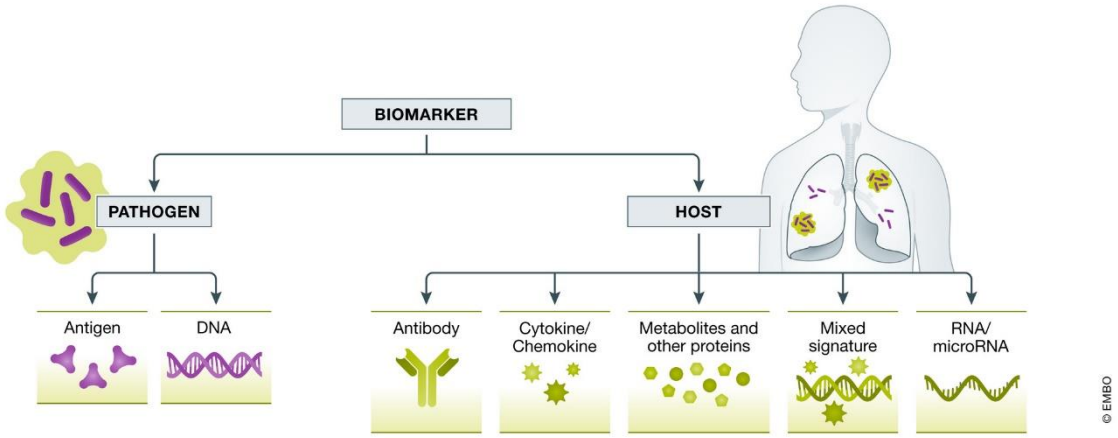

Figure 14: Spectrum of host and pathogen biomarkers commonly studied for the diagnosis of TB.[9]

7.1. Biomarkers from the bacteria

7.1.1. DNA

The DNA of *M. tuberculosis is* the target of several molecular tests such as GeneXpert or WGS based assays. These tests, based on the detection of the DNA of the bacteria, can also detect resistance to one or more antibiotics by targeting several gens or the whole genome. Several of these tests are commercially available.

7.1.2. Lipoarabinomannan LAM

LAM is an antigen that can be detected rapidly, its low sensitivity in individuals other than immunocompromised persons living with HIV (PLWH) limits its use[89]. A recent publication described an assay for serum LAM using single-molecule array anti-LAM monoclonal antibodies and evaluated the performance on serum samples from patients with and without active TB and/or HIV[95]. Results showed that mycobacterial LAM is detectable in serum with high specificity (100%) and variable sensitivity: test sensitivity was 37% in all TB+ subjects, 47% in TB+/HIV+ subjects and 60% in TB+/HIV+/smear+ subjects[95]. Further improvements in clinical sensitivity can be achieved by optimizing the test and reagents[96].

7.1.3. Secretory protein of M. tuberculosis

Other *M. tuberculosis* secretory protein, the 85-antigen complex (Ag85A, Ag85B and Ag85C), ESAT-6, CFP-10 and MPT64[97–99] have also been evaluated for their suitability as diagnostic tools. The Ag85 complex is present in sputum from patients with PTB as well as in cerebrospinal fluid (CSF) from patients with tuberculous meningitis, but sensitivity is not consistent[98,99]. ESAT-6, CFP-10, CFP-21, and MPT-64 face a similar problem. The detection of these antigen on sputum of AFB smear positive and AFB smear negative patients showed 56% and 52% sensitivity respectively for a specificity of 90%[97]. In one study, Turbawaty et al. attempted to detect the presence of these three antigens (ESAT-6, CFP-10 and MPT64) in urine using cocktail of polyclonal antibodies. The authors reported that the sensitivity and the specificity of urinary *M. tuberculosis* antigens cocktail were 68.2% and 33% respectively[100]. Their strategy allowed for an increase in sensitivity to 90%, although the specificity was reduced.

7.1.4. Heparin-binding hemagglutinin antigen (HBHA)

During infection, M. tuberculosis adhesion to epithelial cells is primarily mediated by the heparin-binding haemagglutinin adhesin (HBHA)[101,102]. HBHA is a, structural antigen localised at the surface of *M. tuberculosis* and has been identified in 1996 by Menozzi et al.[103]. Actually, it was shown that most of the TB patients produced anti-HBHA IgG in contrast to healthy infected subjects ($p<0.01$), and in comparison to negative control subjects and to BCG vaccinees[104], and compared to both unvaccinated control PPD^+ and PPD^-[104,105]. It has been reported in a study the use of ELISA to measure levels of IgA, IgG, and IgM from sera of PTB patients and household contacts (HHCs) at baseline, and at 6 and 12 months. The results showed that IgA and IgG antibody levels against HBHA decreased over treatment, while IgM did not show any significant variation during follow up[106]. Moreover it was also shown in immunoblot analysis study that, compared to the IgG antibodies, IgM of the TB patients reacted strongly with recombinant *M. smegmatis* HBHA (rmsHBHA)[107]. This high sensitivity of IgM of TB patients to rmsHBHA was confirmed, compared to patients with malignant effusions[108].

HBHA has previously been shown to be a mycobacterial antigen associated with TBI[109]. Indeed, high secretion of interferon gamma (IFN-γ) is noted in LTBI patients in response to in vitro stimulation with HBHA in, whereas IFN-γ levels were significantly lower in active TB patients suggesting that HBHA-specific T cell responses may participate in the containment of TB infection[110].

7.2. Host biomarkers

7.2.1. Protein and cytokine biomarkers and markers of metabolic activity

For the diagnosis of active TB, specific cytokine biomarkers have shown sufficient performance and currently represent a leading strategy for new non-sputum-based diagnostic tools[10,111–114]. African studies using cytokine biosignatures have met the criteria defined in the WHO Target Product Profile (TPP) for the diagnosis of pulmonary TB, but showed significant variation in the discrimination between negative and positive cases on microscopy[111,112]. In many cases, cytokines are combined with other proteins to form more accurate marker biosignatures. Recently, the combination of a commercial IGRA test (QFT-TB Gold-in-tube) with another non-commercial test based on the response to the *M. tuberculosis* HBHA (hemagglutinin binding heparin) protein has been evaluated to monitor the efficacy of TB treatment[115]. This test is based on the stimulation of whole blood with the recombinant HBHA protein expressed in *M. smegmatis* (IGRAs-rmsHBHA). The white blood cell count (WBC) was also shown to be a marker of interest for monitoring treatment but also for progression to TB[116,117]. The absolute WBC decreased and the proportion of lymphocytes increased throughout the treatment[116,117]. Indeed, it has been shown that a high white blood cell count and a low lymphocyte count before treatment were associated with a risk of treatment failure[116]. In another study, a high percentage of monocytes in the peripheral blood and a high response to the TST were shown to be potential biomarkers for identifying contacts of TB patients at high risk of progressing to active disease[117].

A study published by Jacobs et al. assessed protein biomarkers in saliva[114]. The results of this study revealed an eight-marker biosignature (granzyme A,

growth/differentiation factor 15 (GDF15), serum amyloid A (SAA), interleukin-21 (IL-21), C-X-C motif chemokine 5 (CXCL5), IL-12(p40), IL-13 and plasminogen activator inhibitor-1) that was highly effective in diagnosing active TB with a sensitivity of 100% and specificity of 95%. A second five-marker biosignature including IL-1β, IL-23, extracellular matrix protein 1 (ECM-1), Hemofiltrate C-C chemokine (HCC1) and fibrinogen, diagnosed TB with a sensitivity of 88.9% and specificity of 89.7%, independent of HIV infection status[114]. In blood, Chegou et al identified a seven-marker protein signature including C-reactive protein (CRP), transthyretin, IFN-γ, complement factor H, apolipoprotein-A1, inducible protein 10, and serum amyloid A, which allowed the detection of TB, independent of HIV status or ethnicity in Africa[111].

One study reported a biosignature of 5 plasma markers consisting of neural cell adhesion molecule (NCAM), serum amyloid P (SAP), ferritin, complement factor H (CFH), and ECM-1 to diagnose active TB with a sensitivity of 95.2% and specificity of 92.9%[113].

7.2.2. Cellular biomarkers

Recently, the immunophenotyping of cells has shown promising results for the diagnosis of TB and TB treatment monotoring[118]. Such biomarkers have been identified on the basis of memory phenotypes, activation or cytokine expression profiles[119,120]. Indeed, CD4 T cells are considered as one of the main immune cells involved in the immune response against *M. tuberculosis* infection. Therefore, several studies have identified markers expressed by these cells in the context of active TB. CD69 is a co-stimulatory receptor and a marker of early activation. The increase of CD4+CD69+IFN-γ+ levels is associated with early active TB or recent TB infection[121–123].

Similarly, the frequency of CD137, a co-stimulatory molecule playing a key role in the activation cascade, proliferation and survival of T cells, has also been associated with active TB[124]. Moreover a study by Millington et al., showed that polyfunctional CD4+

IFN-γ+IL-2+TNF-α+ cells predominate in patients with active TB compared to CD4+IL-2+IFN-γ + and CD4+IFN-γ + T cells only in latent TB[125].

The activation (CD38 and HLA-DR) and proliferation (Ki-67) markers are expressed by *M. tuberculosis*-specific CD4+ T cells during TB infection[119,120]. The frequency of *M. tuberculosis*-specific IFN-γ+ CD4+ T cells expressing the immune activation markers CD38 and HLA-DR and the intracellular proliferation marker Ki-67 was significantly higher in active TB subjects than in TBI subjects[119]. These markers allowed accurate classification of these two groups, with a specificity of 100% and a sensitivity of over 96%. These markers also allowed the distinction of those with untreated TB from those who had successfully completed TB treatment correlated with a decrease in mycobacterial load during treatment[119].

In a study of 81 individuals, the authors compared differentiation makers (CD27 and KLRG1), activation markers (HLA-DR), homing potential (CCR4, CCR6, CXCR3 and CD161) and functional profiles (IFNγ, IL-2 and TNFα) of *M. tuberculosis* specific CD4 T cells using flow cytometry. They found that Active TB induced major changes in the *M. tuberculosis*-responsive CD4 T cell population, promoting memory maturation, high activation and increased inflammatory potential compared to individuals with latent TB infection. Furthermore, they described that functional profile of *M. tuberculosis* specific CD4 T cells appear to be intrinsically linked to their degree of differentiation. The best performance for TB diagnosis was obtain with HLA-DR expression showing: 82% specificity and 84% sensitivity for HIV negative individuals and 94% specificity, 93% sensitivity for HIV positive[120].

More detailed studies have shown that non-active TB including latent TB infection, BCG vaccination or treated TB are associated with a predominance of IFN-γ+IL-2+ CD4 T cells; whereas active TB is associated with a predominance of IFN-γ+IL-2+TNF-α^+ CD4 T cells[126,127]. CD38, a marker of immune activation, and CD27, a maturation marker have been shown to discriminate active TB from TBI. Indeed, the increased frequency of

CD38+ CD27low have been associated with active TB was; whereas TBI was associated with a high frequency of CD38-CD27high[128].

CD27, a member of the TNF-α receptor superfamily has been shown to be useful in differentiating between active and latent TB[129]. Indeed, a study showed that active TB patients had a significantly higher number of CD4+CD27+ T cells compared to BCG vaccinated patients and that patients with TBI had an intermediate level of CD4+CD27+ T cells.

Another study has shown that CD27 and PD-1 predicted TBI, BCG status in healthy individuals and distinguished TBI individuals from those who had clinically resolved *M. tuberculosis* infection after anti-tuberculosis treatment and could therefore serve as good biomarkers to improve our ability to evaluate true TBI status[130].

Recent studies suggest that the measurement of a single activation marker (HLA-DR) has generated excellent diagnostic potential to distinguish recent from older TB infection[131]. Hiza et al described a T cell activation marker (TAM)-TB assay to detect TB in adults from 1 mL of blood with a 24 h turnaround time. This test measure expression of CD38 or CD27 by CD4 T cells producing IFN-γ and/or TNF-α in response to a synthetic peptide pool covering the sequences of *M tuberculosis* ESAT-6, CFP-10 and TB10.4 antigens. The results from 479 GeneXpert positive and 108 symptomatic but GeneXpert negative controls reported that CD38-based TAM-TB assay was significantly superior to CD27 in accurately diagnosing TB, and the specificity reached 93.4% for a sensitivity of 82.2%, independent of HIV status[132]. Recent study demonstrated the potential biomarker of CD27−CD38+IFN-γ+ CD4 T cells for active tuberculosis diagnosis[133].

On the other hand, it has recently been shown that the assessment of CD40 ligand (CD154) expression, an activation marker expressed on the surface of central memory CD4+ T cells, could be used as a potential tool to discriminate between active TB TBI and non-infected contacts groups. Indeed, a higher expression of specific CD154+CD4

T cells was observed in patients with active TB and in TBI compared to people without TB[134].

In addition to T cells, there are cells involved in innate immunity against TB including (NK) cells, γδ T cells and mucosal-associated invariant T cells (MAIT) and Dendritic cells.

Mucosal-associated invariant T (MAIT) cells are abundant innate-like T cells, that recognize antigens presented on non-polymorphic major histocompatibility complex-related 1 (MR1) molecules. Results have shown that frequencies and functional profile of MAIT cells in response to mycobacterial stimulation are significantly decreased in HIV infected persons, active TB and HIV-associated TB, with a concomitant increase in MAIT cell activation, defined by HLA-DR expression[135].

Dendritic cells (DC), notably the percentage of circulating myeloid DC and plasmacytoid DC CD123+ was significantly reduced in patients with active TB, while the same subtypes were significantly activated in patients with TBI[136].

Experiments on primate models of *M. tuberculosis* infection revealed the expansion of γδ T cells leading to reduced *M. tuberculosis* burden in lungs as well as reduced pathology[137].

NK cells are recognized as playing a vital role in defense against *M. tuberculosis* infection. NK cells are able to kill the pathogen and infected cells using different mechanisms, including destroying infected cells via cytolysis, apoptosis, and production of cytokines (IFN-γ, TNF-α and IL-22)[138]. Moreover, there are also NK cell mechanisms that target the pathogen, including antibody-dependent NK cell cytotoxicity and generation of reactive nitrogen and oxygen species. NK cells are involved in early *M. tuberculosis* clearance[138].

7.2.3. Genetic biomarkers mRNA

In tuberculosis research, transcriptomic studies using host blood have led to considerable advances in diagnosis, through the identification of powerful gene expression signatures[139]. A recent systematic review and meta-analysis revealed that

17 transcriptomic signatures met at least one WHO minimum performance criterion for TB diagnosis and that three of them (Berry393, Kaforou27, Zak16) were validated for discrimination between TB and other respiratory diseases[140–143]. RISK11, an 11-gene transcriptomic signature, performed well as a screening test for active TB[141,144,145]but performance for asymptomatic (subclinical) TB was significantly lower [146,147]. A large study describes a 380-gene meta-signature for the diagnosis of active TB[148].

Penn Nicholson and colleagues describe RISK6, a signature of 6 genes identified by transcriptomic approach. This study showed that the RISK6 score is a biomarker of lung immunopathological activity, which also allows treatment monitoring, thus predicting treatment failure.[149,150]. The authors also demonstrated that the performance of the test from blood samples was similar to the performance using venous blood collected in PAXgene tubes[149].

In 2016, Sweeney et al developed a highly efficient three-gene signature (GBP5, DUSP3, and KLF2) for the diagnosis of pulmonary TB. The diagnostic performance of this signature has been validated to discriminate active TB from healthy controls, latent TB patients from individuals infected with other respiratory infections, in children and adults from 10 different countries[93]. A review published by Turner et al showed that in a comparison of 27 transcriptomic signatures, four of them (Sweeney3, Kaforou25, Roe3, and BATF2) showed high diagnostic accuracy, for a TB diagnostic test[151]. However, they do not meet the optimal diagnostic criteria defined by the WHO, i.e. sensitivity >95% and specificity >80% for a confirmatory test.

The Sweeney3 signature has now been developed into a prototype "the Xpert MTB Host Response [MTB-HR]" cartridge by Cepheid which measures the signature on capillary blood taken from a fingerpick[152,153]. This prototype test has been evaluated as a triage test and has met the minimum criteria set by WHO using the Xpert Ultra test as a reference test in a prospective cohort[154]. QuantuMDx and bioMérieux are also developing diagnostic platforms using mRNA signatures, but no data has yet been published[155].

A large number of studies are being set up to investigate biomarkers for the detection of TB[10,118]. However, only a small proportion of the markers are clinically tested, thus progress towards a useful point-of-care (POC) test is slow. In order to overcome this, it would be necessary to move towards studies with larger cohort sizes, more focused scientific questions and in countries with different TB realities.

7.3. Respiratory tests

Human exhaled breath contains disease biomarkers and has potential to be used as a non-invasive sample collection method for a diagnostic investigation. Exhaled breath condensate (EBC) is a method of sampling airway lining fluid. Several biomarkers can be measured in the EBC[156]. The concentration of biomarkers is directly influenced by cells composition and activity.

The principal is based on the fact that the fully saturated air is exhaled from the lungs and then comes into contact with the EBC cold collection device cold collection device, which condenses into liquid or ice, depending on the cooling temperature[156–158].

EBC has been used in TB diagnosis for the detection of *M. tuberculosis* DNA, and LAM. Interestingly, a recent study demonstrated the identification of LAM in EBC of TB patients by an immunoassay using the anti-LAM antibody[159]. They found the presence of lipids, LAM and *M. tuberculosis*-specific proteins in EBC allowing an effectively discrimination TB patients from controls.

Another quite similar approach is Exhaled breath particle collection. This has been used to detect TB using high-resolution mass spectrometry[160].

Another interesting tool that has been developed and evaluated to detect *M. tuberculosis* from exhaled air is a modified face mask to easily collect aerosols[161]. It has been shown that face mask sampling offers a highly efficient and non-invasive method of detecting *M. tuberculosis* in breath, informing of the presence of active infection with greater consistency and at an earlier stage of disease compared to sputum samples[161].

This kind of tools need to be evaluated in larger cohort of patients. Once confirmed, they could be a huge turning point in the diagnosis of TB.

8. Tuberculosis and COVID-19

8.1. Impact of COVID-19 pandemic in tuberculosis management

Since late 2019, the world has had to face the emergence of a new coronavirus disease pandemic (COVID-19), caused by the Severe Acute Respiratory Syndrome Coronavirus 2 (SARS-CoV-2). Since the start of the pandemic, 650 million people have been infected with SARS-CoV-2 and more than 6 million people have died[162]. WHO has declared COVID-19 a global public health problem and has warned of the negative impact this pandemic could have on health care facilities and thus on the management of TB in general, from screening to treatment and follow-up of infected individuals[15]. The most significant impact is the dramatic increase of misdiagnosis. The number of notified TB cases dropped from 7.1 million in 2019 to 5.8 million in 2020, representing an 18% decline and a return to 2012 level[2] (Figure 15).

Globally, the estimated number of TB deaths increased between 2019 and 2021, reversing the dropping numbers achieved between 2005 and 2019. In 2021, 1.4 million deaths among HIV-negative people and 187 000 deaths among HIV-positive people, for a combined total of 1.6 million have been notified. This is increasing from estimates of 1.5 million in 2020 and 1.4 million in 2019, returning to 2017 numbers. There has been a clear set back from 2015 to 2021 of 5.9%, or about one-sixth of the WHO End TB Strategy target[2]. There is an increase of 4.5% from 10.1 million in 2020, as the estimated TB cases is 10.6 million people in 2021. The incidence rate of TB increased by 3.6% between 2020 and 2021 after a decline of about 2% over the previous 2 decades[2].

Other impacts include a reduction between 2019 and 2020 in the number of people treated for drug-resistant TB (-17%, from 181,533 to 150,469, or about 1 in 3 people in need) with a partial improvement (+7.5%) of 161,746 in 2021; and on preventive TB treatment (-21%, from 3.6 million to 2.8 million)[2].

The COVID-19 pandemic has reversed years of progress in providing essential TB services and reducing TB deaths. Urgent action is needed to mitigate and counteract these effects.

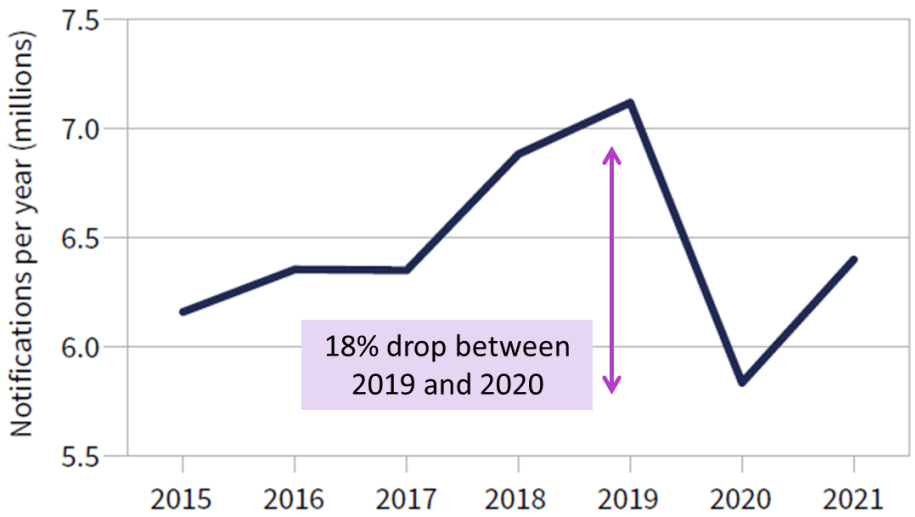

Figure 15: Global trend in case notifications of persons newly diagnosed with TB, 2015-2021. Adapted from WHO Global TB report 2022

8.2. TB and COVID-19 co-infection

To date, there is very limited information on the concomitance of these two respiratory diseases. Clinical studies conducted to date have shown that COVID-19 can occur before, during or even after tuberculosis. Factors such as HIV, poverty and malnutrition seem to play an important role in mortality.

The results of a first publication on 49 cases in eight countries show the importance of having different time frames for the diagnosis of COVID-19 and TB[163]. This study describes a fairly high mortality rate (6/49, 12.3%). In another study, it was shown that high mortality following COVID-19 was noted in people with HIV or active TB with an adjusted risk index of 2.14 and 2.70 respectively[164]. The authors conclude that people living with HIV and/or TB should be considered a high-risk group for COVID-19 management, especially if they have other comorbidities[164].

Researchers in the Philippines have shown that co-infection with TB increases morbidity and mortality in patients with COVID-19[165]. The risk of death in TB patients with COVID-

19 was 2.17 times higher than in those without TB, and the risk of recovery in these patients was 25% lower compared to those without the disease. Similarly, the time to cure from COVID-19 was significantly longer for TB patients[165].

Song and colleagues published a meta-analysis of 36 studies. The results show that out of 89 patients with COVID-TB, 19 (23.46%) died, and 72 (80.90%) were men[166]. Their conclusion suggested that patients with COVID-TB are more likely to suffer a severe form or to die than patients with COVID-19 alone[166].

Given the limited information available, there are still many unanswered research questions about the interaction of these two diseases: one of the most intriguing being the potential role of COVID-19 in the risk of progression from TB infection to active TB.

8.3. Immune response to TB and COVID-19

The immune response, has been investigated in order to better understand the immunity underlining the coinfection. In this study by Rajamanickam et al, patients with asymptomatic COVID-19 and latent TB infection showed serum levels of cytokines including IFN-γ, TNF-α, IL-1α, IL-1β, IL-2, IL-6, IL-12, IL-15, IL-17, IFN-α, IFN-β, IL-3, GM-CSF, IL-10, IL-25 and IL-33, the chemokines CCL3 and CXCL10, and the growth factors VEGF and TGF-α, higher compared to patients with COVID-19 alone[167]. This study also described a high level of SARS-CoV-2 specific IgM, IgG, IgA neutralising antibodies in patients with COVID-19 and latent TB infection compared to patients with COVID-19 alone. Higher C-reactive protein (CRP) and α-2 microglobulin levels were reported in co-infected patients compared to those with COVID-19 alone.[167]

The lymphocyte response appears to differ according to the infection profile. Madan et al. evaluated lymphocyte counts in patients with both latent TB infection and COVID-19[168]. They found higher lymphocyte and monocyte counts in coinfected patients compared to patients with COVID-19 infection only. They also found that coinfection was associated with lower CRP levels and a lower neutrophil/lymphocyte ratio compared to the COVID-19 alone group[168].

Riou et al evaluated the specific CD4 T cells and their functionality. They showed that COVID-19 patients alone had a higher polyfunctional CD4 T cell (IFN-γ, IL-2 and TNF-α) capacity. They also highlighted a difference in the overall phenotype of SARS-CoV-2 specific CD4 T cells compared to patients coinfected with active TB[169]. Indeed, COVID-19 patients had lower numbers of specific CD4 T cells compared to non-COVID-19 patients, which could mean that cellular defence against M. tuberculosis is diminished in SARS-CoV-2 co-infection. However, among the groups of patients with COVID-19 infection, no significant differences were found in the expression of the *M. tuberculosis*-specific CD4 T cell activation and proliferation markers HLA-DR, CD38 and Ki67[169].

Petrone et al found that patients with symptomatic COVID-19 and latent or active TB infection had significantly higher IFN-γ levels in response to the TB1 and TB2 antigens of QuantiFERON-TB Gold plus, compared with patients with COVID-19 alone[170]. On the other hand, patients with COVID-19 or COVID-19 and TBI expressed significantly more IFN-γ in response to SARS-CoV-2 antigen compared to patients with COVID-19/active TB co-infection[170].

Data from the current literature suggest that in patients with TBI, positive immunomodulation against COVID-19 may occurs and on the other hand, patients with active TB would have a weaker specific response to SARS-CoV-2 and weaker lymphocyte function, which would not allow effective control of the infection[171].

9. Research objectives

This thesis project regroups findings of two independent studies described in the next chapter : HINTT and APRECIT. The overall objective of this thesis was to evaluate and develop new non-sputum based diagnostic tools for tuberculosis, in accordance with the priority needs of tuberculosis research advised by the WHO. Thus, we focused on the evaluation of new blood tests for the diagnosis of tuberculosis and on the identification of simple and rapid biomarkers for the diagnosis of tuberculosis infection (TBI and active TB) but also for monitoring the response to tuberculosis treatment in adults. Beside, the impact of ongoing COVID-19 pandemic and coinfection has made necessary to take an interest in the evaluation of biomarkers associated with COVID-19 and TB coinfection but also in the risk of TB progression following COVID-19 coinfection. To this end, we evaluated the performance of a novel blood-to-man transcriptomic signature, RISK6, in the context of TB diagnosis and treatment monitoring. Next, we identified plasma biomarker assays using the Luminex x-MAP® platform, for the TB treatment monitoring and to discriminated between active TB and TBI. Next, we developed a serodiagnosis tool for COVID-19 and described a statistical model to date SARS-CoV-2 infection and clinical presentation. This tool was used retrospectively to determine COVID-19 seroprevalence and date SARS-CoV-2 infection in household contacts of the APRECIT project. Using these data, we assessed the risk of progression of TB patients in the APRECIT cohort.

I believe that the results of this doctoral thesis provide new advances in the field of tuberculosis research by proposing new, simple and rapid tools for the diagnosis and monitoring of tuberculosis treatment, which could move from clinical research to clinical applications, but also help in understanding COVID-19 tuberculosis infection.

10. Description of the research projects

10.1. HINTT

The HINTT (HBHA IGRA New Tool for Tuberculosis diagnosis) project is a multicentre study aiming to identify and evaluate immunological biomarkers for monitoring the efficacy of TB treatment. This project was launched in 2017 in 5 countries of the GABRIEL network, which are Madagascar, Georgia, Bangladesh, Lebanon and Paraguay. The objective is to assess the diagnostic and prognostic value of new TB biomarkers in monitoring treatment efficacy.

This project was triggered by the high rate of treatment failure in patients infected with so-called multidrug-resistant strains of Mycobacterium tuberculosis is partly related to adverse side effects and the duration of treatment. The tendency to withdraw and discontinue treatment undermines all efforts to control the spread of the epidemic.

HINTT was set up to identify and evaluate immunological tools developed to screen for TB and monitor the effectiveness of TB treatment, in order to help clinical practitioners, provide adequate treatment to those most at risk, improve patient outcomes and reduce the spread of multidrug-resistant forms of TB.

10.2. APRECIT

The APRECIT project (Amélioration de la prise en charge de l'infection tuberculeuse) aims to evaluate strategies to improve the overall management of tuberculosis infection by national tuberculosis control programmes (NTPs) in Cameroon and Madagascar. This project focuses on a community-based household survey with the evaluation of 3 immunological tests: the TST, the QuantiFERON-TB Gold Plus and the T-Spot TB, to determine the incidence rate of TB in a prospective cohort of people in contact with people with TB.

With the pandemic caused by SARS COV-2 virus, an expansion was made in the project.

This is a strategy to include COVID-19 diagnostic activities in the APRECIT project. The community-based intervention, which is at the heart of the APRECIT project, is an asset for the detection and management of vulnerable populations at risk of TB and COVID-19. The aim is also to better understand the interactions between the two diseases.

Chapter 2: Results and publications

1. Study 1: Evaluation of transcriptomic biomarkers for diagnosis and monitoring of treatment response

Summary

In this study, we evaluate the performance of RISK6, a human-blood transcriptomic signature, for TB screening, triage and treatment monitoring. RISK6 performance was evaluated in a multicentric prospective nested case–control study conducted in Bangladesh, Georgia, Lebanon and Madagascar. Adult non-immunocompromised patients with bacteriologically confirmed active pulmonary TB (ATB), latent TB infection (LTBI) and healthy donors (HD) were enrolled. ATB patients were followed-up during and after treatment. Blood RISK6 scores were assessed using quantitative real-time PCR and evaluated by area under the receiver-operating characteristic curve (ROC AUC). RISK6 performance to discriminate ATB from HD reached an AUC of 0.94 (95% CI 0.89–0.99), with 90.9% sensitivity and 87.8% specificity, thus achieving the minimal WHO target product profile for a non-sputum-based TB screening test. Besides, RISK6 yielded an AUC of 0.93 (95% CI 0.85–1) with 90.9% sensitivity and 88.5% specificity for discriminating ATB from LTBI. Moreover, RISK6 showed higher performance (AUC 0.90, 95% CI 0.85–0.94) than IGRA-rmsHBHA (AUC 0.75, 95% CI 0.69–0.82) to differentiate TB infection stages. Finally, RISK6 signature scores significantly decreased after 2 months of TB treatment and continued to decrease gradually until the end of treatment reaching scores obtained in HD.

scientific reports

Check for updates

OPEN

Multi-country evaluation of RISK6, a 6-gene blood transcriptomic signature, for tuberculosis diagnosis and treatment monitoring

Rim Bayaa[1,2,15]✉, Mame Diarra Bousso Ndiaye[1,3,15], Carole Chedid[1,4,5], Eka Kokhreidze[6], Nestani Tukvadze[6], Sayera Banu[7], Mohammad Khaja Mafij Uddin[7], Samanta Biswas[7], Rumana Nasrin[7], Paulo Ranaivomanana[3], Antso Hasina Raherinandrasana[8], Julio Rakotonirina[8], Voahangy Rasolofo[3], Giovanni Delogu[9], Flavio De Maio[9], Delia Goletti[10], Hubert Endtz[11], Florence Ader[12], Monzer Hamze[2], Mohamad Bachar Ismail[2], Stéphane Pouzol[1], Niaina Rakotosamimanana[3,16], Jonathan Hoffmann[1,16]✉ & The HINTT working group within the GABRIEL network*

There is a crucial need for non-sputum-based TB tests. Here, we evaluate the performance of RISK6, a human-blood transcriptomic signature, for TB screening, triage and treatment monitoring. RISK6 performance was also compared to that of two IGRAs: one based on RD1 antigens (QuantiFERON-TB Gold Plus, QFT-P, Qiagen) and one on recombinant *M. tuberculosis* HBHA expressed in *Mycobacterium smegmatis* (IGRA-rmsHBHA). In this multicenter prospective nested case–control study conducted in Bangladesh, Georgia, Lebanon and Madagascar, adult non-immunocompromised patients with bacteriologically confirmed active pulmonary TB (ATB), latent TB infection (LTBI) and healthy donors (HD) were enrolled. ATB patients were followed-up during and after treatment. Blood RISK6 scores were assessed using quantitative real-time PCR and evaluated by area under the receiver-operating characteristic curve (ROC AUC). RISK6 performance to discriminate ATB from HD reached an AUC of 0.94 (95% CI 0.89–0.99), with 90.9% sensitivity and 87.8% specificity, thus achieving the minimal WHO target product profile for a non-sputum-based TB screening test. Besides, RISK6 yielded an AUC of 0.93 (95% CI 0.85–1) with 90.9% sensitivity and 88.5% specificity for discriminating ATB from LTBI. Moreover, RISK6 showed higher performance (AUC 0.90, 95% CI 0.85–0.94) than IGRA-rmsHBHA (AUC 0.75, 95% CI 0.69–0.82) to differentiate TB infection stages. Finally, RISK6 signature scores significantly decreased after 2 months of TB treatment and continued to decrease gradually until the

[1]Medical and Scientific Department, Fondation Mérieux, Lyon, France. [2]Laboratoire Microbiologie, Santé et Environnement (LMSE), Doctoral School of Sciences and Technology, Faculty of Public Health, Lebanese University, Tripoli, Lebanon. [3]Institut Pasteur de Madagascar, Antananarivo, Madagascar. [4]Department of Biology, Ecole Normale Supérieure de Lyon, Lyon, France. [5]Equipe Pathogénèse des Légionelles, International Center for Research in Infectiology, INSERM U1111, University Lyon 1, CNRS UMR5308, École Normale Supérieure de Lyon, Lyon, France. [6]National Center for Tuberculosis and Lung Diseases (NCTLD), Tbilisi, Georgia. [7]International Centre for Diarrhoeal Disease Research, Bangladesh (icddr,b), Dhaka, Bangladesh. [8]Centre Hospitalier Universitaire de Soins et Santé Publique Analakely (CHUSSPA), Antananarivo, Madagascar. [9]Dipartimento di Scienze di Laboratorio e Infettivologiche, Fondazione Policlinico Universitario "A. Gemelli", IRCCS, Rome, Italy. [10]Translational Research Unit, Department of Epidemiology and Preclinical Research, "L. Spallanzani" National Institute for Infectious Diseases (INMI), IRCCS, Rome, Italy. [11]Erasmus MC, Medical Microbiology and Infectious Diseases, University Medical Center Rotterdam, Rotterdam, The Netherlands. [12]Service des Maladies Infectieuses et Tropicales, Hospices Civils de Lyon, Lyon, France. [15]These authors contributed equally: Rim Bayaa and Mame Diarra Bousso Ndiaye. [16]These authors jointly supervised this work: Niaina Rakotosamimanana and Jonathan Hoffmann. *A list of authors and their affiliations appears at the end of the paper. ✉email: bayaarim@gmail.com; jonathan.hoffmann@fondation-merieux.org

end of treatment reaching scores obtained in HD. We confirmed the performance of RISK6 signature as a triage TB test and its utility for treatment monitoring.

One fourth of the world population is estimated to be infected with *Mycobacterium tuberculosis* (*Mtb*) that causes approximately 10 million cases of tuberculosis (TB) yearly. This disease ranks among the leading causes of death worldwide, resulting in 1.4 million deaths in 2019[1]. Five to 10% of infected individuals develop the contagious, active form of TB (ATB) disease, while most of them (90%) control the infection and develop asymptomatic latent TB infection (LTBI). However, a small proportion (10%) of LTBI individuals will develop ATB during their lifetime[2]. TB can be treated with a regimen of several antibiotics for a minimum of 6 months. In most patients, TB therapy provides cure[3] but treatment failure and relapse can occur. These outcomes are associated with severe adverse effects and long treatment durations that induce a lack of patient adherence to the treatment regimen thus promoting the emergence of drug-resistance[4].

Current ATB diagnostic tests include sputum-based culture and acid-fast Bacillus (AFB) smear microscopy which are also used for monitoring TB treatment response[1,3]. Molecular tests like the GeneXpert MTB/RIF or ULTRA, are also performed using sputum samples[5]. Interferon (IFN)-γ release assays (IGRAs) such as QuantiFERON-TB Plus (QFT-P; Qiagen) are blood-based tests used for the detection of *Mtb* infection, yet cannot discriminate ATB from LTBI[6–9]. However, the combined use of QFT-P with the heparin-binding hemagglutinin antigen; HBHA-based IGRAs, that relies on the stimulation of whole blood with recombinant *Mtb* HBHA protein expressed in *Mycobacterium smegmatis* (IGRAs-rmsHBHA)[10], recently revealed the potential for the stratification of TB stages (e.g. ATB vs LTBI)[11–14].

Sputum-based TB tests are associated with several limitations including the long-time of culture and the lack of sensitivity and specificity of smear microscopy[15]. Besides, although molecular tests are more sensitive for diagnosing pulmonary TB, they still have limited sensitivity in paucibacillary pulmonary TB patients[16,17]. In addition, sputum samples may be difficult to obtain in some populations (e.g. children and HIV co-infected TB patients) as well as in ATB patients after symptom improvement[18]. In this context, the World Health Organization (WHO) has declared an urgent need for alternative non-sputum-based TB tests with a series of target product profiles (TPPs) which detailed the minimal and optimal criteria that should be met to diagnose and monitor TB treatment response[19–21]. Those new TB tests need to be based on accessible biological samples such as whole blood or urine, and must be practical for field applications[22].

Currently, there is much active research[23,24] on human blood transcriptomic TB biomarkers[25]. A six whole blood gene transcriptomic signature (RISK6) has been recently described and validated in 7 independent cohorts, demonstrating its utility to predict the risk of progression from TB infection to ATB disease, as a screening test for TB, and to monitor TB treatment response[19,26]. The present study aims: to evaluate the robustness of the RISK6 signature in four additional independent cohorts from different countries and ethnicities; to assess its performance for TB screening and triage; to compare its performance to that of two IGRAs (QFT-P and IGRAs-rmsHBHA); and to evaluate its utility for monitoring treatment outcome.

Results

Sociodemographic and clinical characteristics. A total of 141 patients with bacteriologically confirmed pulmonary ATB were included in the study. Their sociodemographic and clinical characteristics were compared at baseline. The median age was 28 years, 66% were male, and 51.8% were smokers. Among them, 48.2% had a positive sputum smear microscopy with a high grade at baseline (2+ or 3+). 97 of these patients were followed at least until the end of treatment and have been successfully treated for TB. The remaining participants included 26 individuals with LTBI and 71 healthy donors (Table 1).

Performance of the RISK6 signature as a screening and triage test for pulmonary TB disease. To investigate the use of RISK6 score as a screening and triage test for TB, we compared RISK6 scores between patients with ATB disease (n = 141), treated TB patients who have been successfully treated for TB (TREATED, n = 97, with negative sputum culture at T2 and/or T3), the individuals with LTBI (n = 26), and healthy donors (HD, n = 71). In all cohorts, RISK6 scores were significantly higher in ATB patients at baseline compared to HD ($p < 0.001$) and TREATED TB patients ($p < 0.001$) (Fig. 1a). Moreover, RISK6 score levels of TREATED patients became indistinguishable from HD. Remarkably, in the Madagascar cohort that includes the enrolled LTBI individuals, we observed a significant difference for the RISK6 scores between ATB and LTBI group ($p < 0.001$) but not between the LTBI group and the TREATED TB patients or the HD group. Remarkably, when we compared the RISK6 scores levels between study sites, we found that the RISK6 scores levels in ATB, TREATED TB patients and the HD recruited from Bangladesh were higher than the levels observed in the other study sites (Fig. 1a).

We then generated a receiver operating characteristic curve (ROC) and the respective areas under the curve (AUC) for each cohort to evaluate, by country, the performance of RISK6 signature as screening or triage test (Fig. 1b). First, we assessed the performance of RISK6 as a screening test for the discrimination between ATB patients and HD. Remarkably, the performance of the RISK6 signature was similar in the four different cohorts, with outstanding AUC values ranging from 90.1% (Bangladesh; 95% CI 80.7–99.4) to 96.4% (Georgia; 95% CI 90.5–100) (Fig. 1b). Secondly, ROC analysis was also performed to determine the potential of RISK6 signature as a triage test to discriminate between different stages of TB infection. Results demonstrated a powerful classifying potential to discriminate patients with ATB from LTBI or TREATED TB patients with an AUC of 92.8% (95% CI 85.6–100) and 96.1% (95% CI 91.7–100) respectively (Fig. 1b). Remarkably, we also found that the discrimination between ATB and HD was lowest in the cohort of Bangladesh when compared to other study sites (Fig. 1b).

	Georgia	Madagascar	Lebanon	Bangladesh	Total
ATB (N)	32	44	21	44	141
ATB patient demographics					
Age (years)	33.5 (26.75–44.5)	29.5 (21.75–43.25)	30 (22–37)	23.5 (20.75–30.5)	28 (22–39)
Gender (male)	81.2% (26/32)	59.1% (26/44)	47.6% (10/21)	70.5% (31/44)	66% (93/141)
BMI at baseline	20.06 (18.65–21.67)	17.19 (16.31–18.67)	20.94 (19.59–21.41)	18.28 (16.2–20.79)	18.68 (16.89–20.95)
Vaccination					
BCG vaccination	40.6% (13/32)	88.6% (39/44)	19% (4/21)	75% (33/44)	63.1% (89/141)
Risk factors					
Smoking habit	59.4% (19/32)	43.2% (19/44)	57.1% (12/21)	52.3% (23/44)	51.8% (73/141)
Alcohol consumption	9.7% (3/31)	45.5% (20/44)	9.5% (2/21)	11.4% (5/44)	21.4% (30/140)
Injecting drug users	–	–	–	9.3% (4/43)	2.9% (4/138)
Jail detention history	6.2% (2/32)	2.4% (1/42)	14.3% (3/21)	4.5% (2/44)	5.8% (8/139)
Other pathologies					
HCV positive	9.4% (3/32)	2.3% (1/44)	–	–	2.8% (4/141)
Other underlying disease	–	9.1% (4/44)	9.5% (2/21)	2.3% (1/44)	5.5% (7/127)
Sputum smear microscopy at baseline					
Low grade (1+ or scanty)	37.5% (12/32)	25% (11/44)	28.6% (6/21)	27.3% (12/44)	29.1% (41/141)
High grade (2+ or 3+)	25% (8/32)	54.5% (24/44)	38.1% (8/21)	63.6% (28/44)	48.2% (68/141)
Negative	34.4% (11/32)	20.5% (9/44)	19% (4/21)	9.1% (4/44)	19.9% (28/141)
Not evaluated	3.1% (1/32)	–	14.3% (3/21)	–	2.8% (4/141)
TB treatment					
Treated	26	33	15	23	97
LTBI (N)	–	26	–	–	26
Healthy donors (N)	7	23	25	16	77

Table 1. Baseline sociodemographic and clinical characteristics of ATB patients in the four cohorts. *TB* Tuberculosis, *BMI* Body Mass Index, *LTBI* latent TB infection, *IQR* interquartile range. Data were given as % (N) or median (IQR).

Performance of RISK6 signature benchmarked against the WHO TPP for a non-sputum based diagnostic test. Our findings were then benchmarked against the WHO TPP for a screening/triage test for TB that should have a minimum sensitivity of > 90% and specificity of ≥ 70%[19,27]. At a sensitivity set to > 90%, the performance of RISK6 signature as screening/triage test demonstrated specificity scores of > 70% in all cohorts, except for Bangladesh (Table 2). This shows that RISK6 signature achieves the minimal WHO TPP for non-sputum-based screening and triage tests discriminating patients with ATB from both HD and LTBI groups.

Performance of RISK6 as a confirmatory test for pulmonary TB disease. Our next aim was to evaluate the performance of RISK6 signature in sputum smear-negative and culture-confirmed TB individuals. Based on the TPP criteria set by the WHO as a reference[19,27], we found that RISK6 achieved the minimal sensitivity of > 60% with 100% specificity for an initial TB diagnostic test for sputum smear-negative TB to replace smear microscopy in the cohort from Georgia (Table 2). Similarly, in the same cohort, RISK6 signature also reached the minimum criteria of 65% sensitivity and 100% specificity for a confirmatory test. However, RISK6 signature detection failed to meet these WHO requirements in the other study sites (Table 2).

As most ATB patients had a positive sputum smear microscopy with a high grade at baseline, we wondered if RISK6 scores and mycobacterial loads were correlated. We therefore performed a sub-analysis on stratified sputum smear microscopy results among ATB patients, defined as follow: negative smears, low-grade positive smears (1+ or scanty) and high-grade positive smears (2+ or 3+). RISK6 scores in the negative smear group showed a significant difference ($p < 0.001$) compared to HD (Fig. 2). Moreover, RISK6 scores were significantly lower (median = 0.31, IQR 0.22–0.40) in negative smears than in individuals with low- or high-grade positive smears ($p < 0.001$). While not statistically different ($p > 0.05$), RISK6 scores in the high-grade smear group were higher (median = 0.5, IQR 0.40–0.56) than in the low-grade mycobacterial load group (median = 0.46, IQR 0.38–0.52).

Performance of RISK6 signature compared to IGRAs. Next, we assessed the performance of RISK6 signature compared to two assays based on IFN-γ release: the commercial QFT-P, and the non-commercial IGRAs-rmsHBHA. Compared to the QFT-P assay, the RISK6 signature achieved better performance in AUC (94.1% vs 57.2%), sensitivity (90.9% vs 50.9%) and specificity (87.8% vs 57.2%) to discriminate ATB patients from an asymptomatic population (LTBI + HD) (Table 3). However, a comparative sub-analysis indicated a lower positive (79.7%) and negative (50%) predictive values of the RISK6 signature when compared to QFT-P assay (100% and 63.9%, respectively) in detection of *Mtb*-infected individuals (ATB + LTBI) from uninfected ones (HD). Notably, the RISK6 signature showed a higher performance (AUC 90.9%, 95% CI 87.2–94.5), with 90.1% sensitivity and 72.2% specificity than the IGRAs-rmsHBHA (AUC 75.3%, 95% CI 68.6–82) that achieved

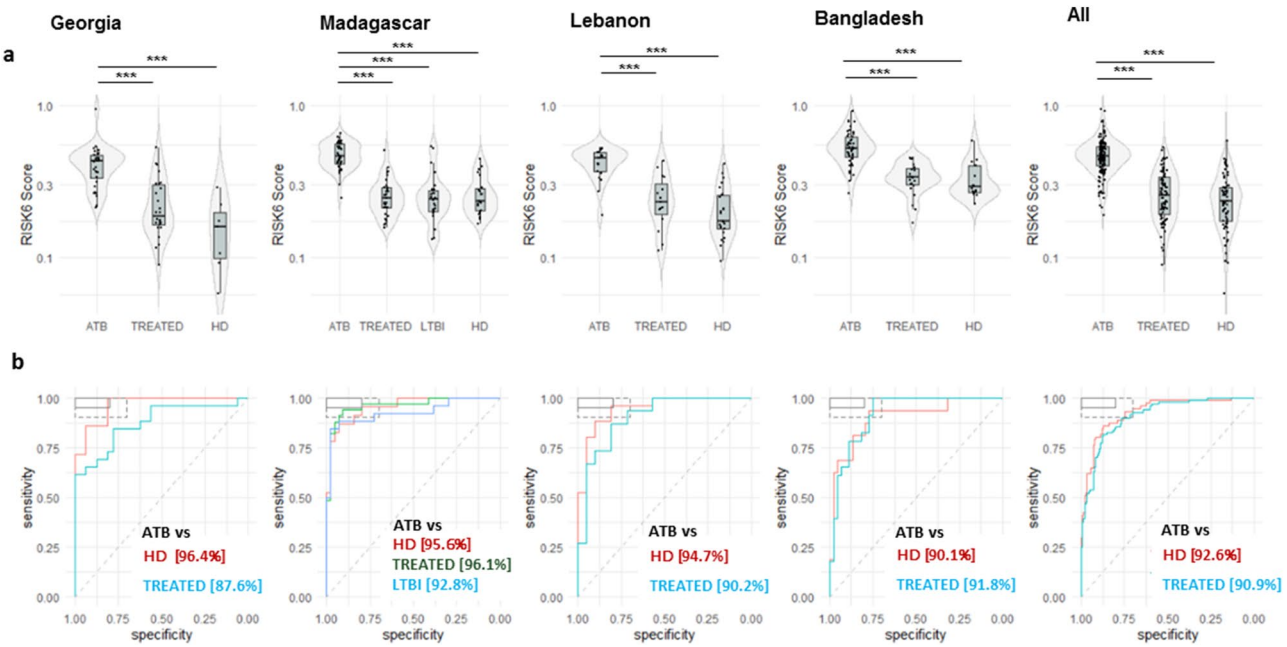

Figure 1. Validation of the performance of a multi-cohort 6-gene signature; RISK6 as a screening and triage test in patients with pulmonary TB. (**a**) Violin plots showing the differences in the levels of RISK6 signature scores from patients with active TB at baseline (ATB, n = 141), treated TB patients (TREATED, n = 97; patients with a negative sputum culture at T2 and/or T3), individuals with a latent TB infection (LTBI, n = 26), and healthy donors (HD, n = 71) from Georgia, Madagascar, Lebanon, Bangladesh and in all sites. Horizontal lines designate medians, boxes represent the inter-quartile ranges (IQR) and the ranges are represented by whiskers. Single patient results are represented by each dot in the graph. Statistical significance was calculated using Mann–Whitney U test. *Indicates a p-value < 0.05, **indicates a p-value < 0.01, and ***indicates a p-value < 0.001. (**b**) Receiver operating characteristic (ROC) curve analysis and the respective areas under the curve (AUC) with 95% confidence intervals showing the performance of the RISK6 signature to discriminate between ATB patients at baseline, HD and LTBI. In the top left box, the solid and dashed lines represent the respective optimal and minimum criteria set by the WHO in the target product profile (TPP) for a screening/triage test for TB.

lower sensitivity and specificity (83.8% and 59.8% respectively) to differentiate *Mtb*-infection status (i.e. ATB vs TREATED TB patients) (Table 3).

RISK6 as a biomarker for TB treatment monitoring. Patients with successful treatment (defined as negative sputum culture at T2) were selected to determine whether RISK6 signature was a clinically relevant biomarker for TB treatment monitoring. Overall, in all cohorts combined, we observed a significant drop in RISK6 scores after two months of treatment (T1, $p < 0.001$) and until treatment completion (T2, $p < 0.001$). Moreover, RISK6 scores were significantly higher in cured TB patients (T2, $p > 0.05$) when compared to HD, however, in each of the four cohorts, there were no significant difference between these two groups ($p > 0.05$) (Fig. 3a). Similarly, analytical performance demonstrated capacity of RISK6 signature to significantly discriminate patients at baseline and two months after treatment initiation (AUC 69.7%, 95% CI 57.1–79.6) (Fig. 3b and Supplementary Table 6). Noticeably, by the end of treatment, the majority of patients had lower RISK6 score levels, further enhancing the discriminatory power between ATB patients at T0 and T2 (AUC 87.1, 95% CI 77.6–94.3) and at T3 (AUC 90.4, 95% CI 82.6–96.6) (Fig. 3b and Supplementary Table 6).

Furthermore, we evaluated whether RISK6 allows the discrimination of cured TB patients (n = 104) from those with a treatment failure (defined as positive sputum culture at T2, n = 2). Thereafter, patients were stratified into drug-sensitive (DS) and drug-resistant TB (DR-TB) cases and the RISK6 signature scores were compared within these groups. We found that RISK6 scores decreased throughout treatment among DS-TB patients independently of treatment outcome (Supplementary Fig. 1). In contrast, the RISK6 score remained stable at baseline and during treatment in a DR-TB patient with a treatment failure. Importantly, RISK6 score levels during TB treatment seem to be higher in patients with treatment failure among both DS and DR-TB cases. However, in a univariate or multivariate analyses, no significant association of the RISK6 score at baseline with treatment failure was found (Supplementary Table 8).

TPP requirement		Cut-off	Sensitivity%	Specificity%	Cases, n	Controls, n	AUC	AUC 95%CI
Screening test (ATB vs HD)								
Georgia	Sensitivity > 90%	> 0.2583	90.6	85.7	32	7	96.4%	90.5–100%
Madagascar		> 0.3697	90.9	87	44	23	95.6%	90.9–100%
Lebanon		> 0.3171	90.5	88	21	25	94.7%	88.6–100%
Bangladesh		> 0.3625	90.9	68.8	44	16	90.1%	80.7–99.4%
All		> 0.3209	90.1	80.3	141	71	92.6%	88.8–96.3%
Triage test (ATB vs LTBI)								
Madagascar	Sensitivity > 90%	> 0.3697	90.9	88.5	44	26	92.8%	85.6–100%
Initial TB diagnostic test to replace smear microscopy (ATB (CLT^+ AFB^-) vs HD)								
Georgia	Sensitivity ≥ 60%	> 0.3514	63.6	100	11	7	94.8%	85.1–100%
Madagascar		> 0.4298	66.7	95.7	9	23	96.1%	90.1–100%
Lebanon		> 0.3217	75	88	4	25	90%	78.2–100%
Bangladesh		> 0.3541	75	68.8	4	16	79.7%	58.8–100%
All		> 0.3823	60.7	88.7	28	71	87.7%	80.6–94.8%
Confirmatory test (ATB (CLT^+ AFB^-) vs HD)								
Georgia	Sensitivity ≥ 65%	> 0.3131	72.7	100	11	7	94.8%	85.1–100%
Madagascar		> 0.4298	66.7	95.7	9	23	96.1%	90.1–100%
Lebanon		> 0.3217	75	88	4	25	90%	78.2–100%
Bangladesh		> 0.3541	75	68.8	4	16	79.7%	58.8–100%
All		> 0.3674	67.9	87.3	28	71	87.8%	80.6–94.8%

Table 2. Receiver operating characteristic curve analysis of the performance of the RISK6 signature to distinguish active TB cases (ATB) from healthy donors (HD) and from latent TB infected individuals (LTBI) in cohorts from Georgia, Madagascar, Lebanon, and Bangladesh. The performance of the signature is benchmarked against the WHO TPP for a non-sputum based screening/triage test (at a sensitivity of > 90%, the minimum specificity as set out in this TPP should be ≥ 70%), for an initial TB diagnostic test to replace sputum smear (at minimum 60% sensitivity, the minimum specificity as set out in this TPP should be > 98%) and for a confirmatory test (at minimum 65% sensitivity, the minimum specificity as set out in this TPP should be > 98%)[19]. *ATB* active TB, *LTBI* latent TB infection (were only recruited from Madagascar), *HD* healthy donors, CLT^+ positive sputum culture, AFB^- negative AFB smear microscopy, *AUC* area under the curve, *CI* confidence interval, *Vs* versus.

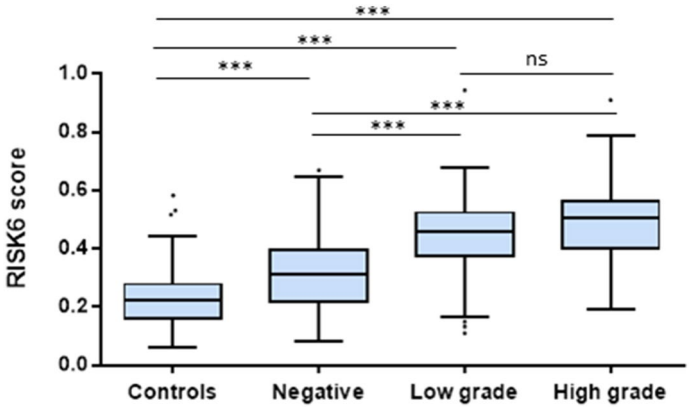

Figure 2. Correlation between RISK6 signature scores and mycobacterial loads determined by sputum smear microscopy in ATB patients. Boxplots comparing the RISK6 score levels stratified according to sputum smear grade: Negative smears, low grade positive smears (1+ or scanty) and high grade positive smears (2+ or 3+). Horizontal lines designate medians, boxes represent the inter-quartile ranges (IQR) and the ranges are represented by whiskers. Individual dots represent the results of patients with a RISK6 scores out of IQR. Statistical significance was calculated using Mann–Whitney U test. *Ns* non-significant, ***indicates a p-value < 0.001. *HD* Healthy donors.

Intended application	Test	Sensitivity%	Specificity%	PPV%	NPV%	Cases, n	Controls, n	AUC	AUC 95%CI
ATB vs (LTBI + HD)	RISK6	90.90	87.7	87	91.5	44	49	94.1	89.3–98.8
	QFT-P	67.50	46.9	50.9	63.9	40	49	57.2	45.2–69.1
(ATB + LTBI) vs HD	RISK6	90.00	30.4	79.7	50	66	23	77.8	68.5–87.1
	QFT-P	80.30	100	100	63.9	70	23	90.1	83.9–96.3
ATB vs treated TB	RISK6	90.1	72.2	82.5	83.3	141	97	90.9	87.2–94.5
	IGRAs-rmsHBHA	83.8	59.8	70.3	76.5	136	87	75.3	68.6–82

Table 3. Performance of RISK6 signature compared to Interferon-γ release assays: QuantiFERON-TB Gold Plus (QFT-P) and recombinant *Mtb*-HBHA expressed in *Mycobacterium smegmatis* (IGRAs-rmsHBHA). *ATB* active TB, *LTBI* latent TB infection, *HD* healthy donors, *vs* versus, *rmsHBH* recombinant *Mtb* HBHA expressed in, *PPV* positive predictive value, *NPV* negative predictive value.

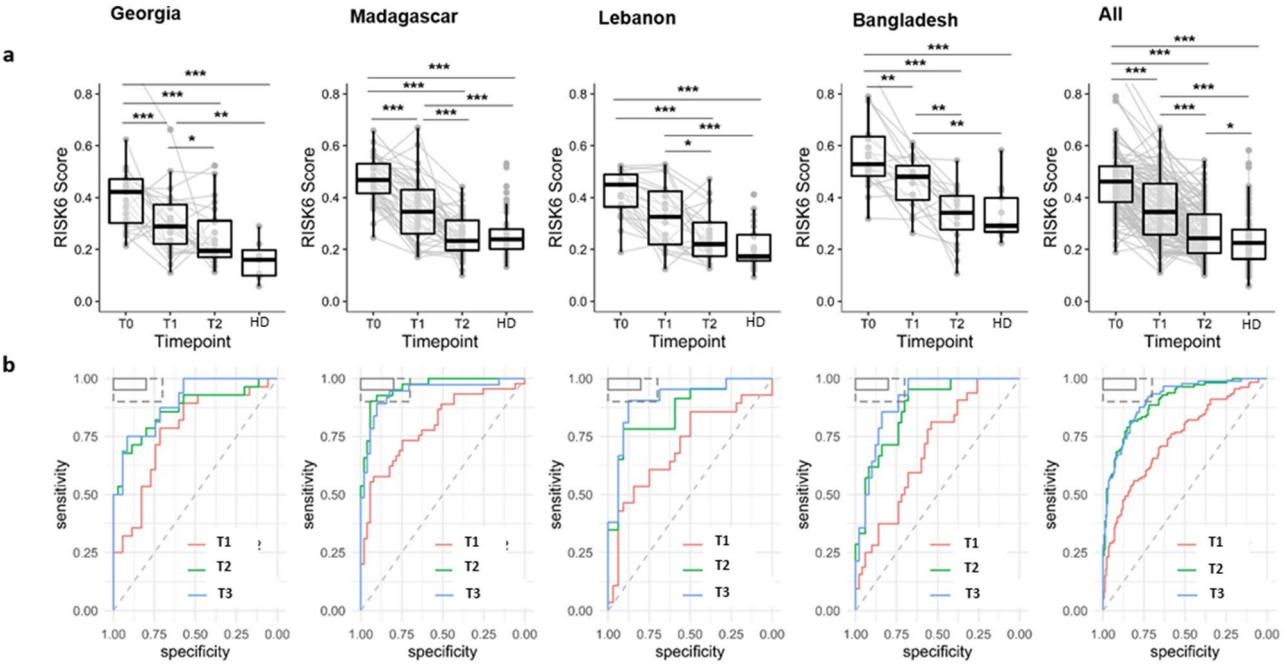

Figure 3. Validation of the performance of RISK6 signature as a biomarker for monitoring TB treatment response in four distinct geographical countries. (**a**) RISK6 scores were evaluated in whole blood of patients with active TB who had successfully completed their TB treatment until T2 (n = 104). Evaluation was done at baseline (T0), 2 months after treatment initiation (T1), and at the end of treatment (T2). RISK6 scores in healthy donors (HD: n = 71) were also evaluated. Horizontal lines designate medians, boxes represent the inter-quartile ranges (IQR) and the ranges are represented by whiskers. Single patient results are represented by each dot in the graph. Plotlines (grey) represent the RISK6 scores of the same patient at the three different time points. Statistical significance was calculated using Mann–Whitney U test. *Indicates a p-value < 0.05, **indicates a p-value < 0.01, and ***indicates a p-value < 0.001. (**b**) Receiver operating characteristic (ROC) curve analysis and the respective areas under the curve (AUC) with 95% confidence intervals (CI) showing the ability of the RISK6 signature to discriminate between active TB patients at baseline (T0, n = 141) and at month 2 after treatment initiation (T1, n = 117), at the end of treatment (T2, n = 104) and 2 months after treatment completion (T3, n = 79).

Discussion

TB remains one of the major infectious causes of death globally. In this study, we aimed to evaluate the relevance of RISK6, a PCR-based six-gene blood transcriptomic signature[26], in the context of TB diagnosis and treatment monitoring. This was conducted in four independent cohorts enrolling ethnically and geographically diverse participants, including ATB patients, LTBI individuals, and HD, in both high- and low-TB incidence settings.

We first evaluated the performance of RISK6 signature as a screening test for TB and showed that it displayed similar performance in the four different cohorts with excellent near-identical ROC AUC values (> 90.1%). Furthermore, RISK6 signature satisfied the minimum criteria set by the WHO TPP for a non–sputum-based screening test[19]. Notably, our findings suggest that, compared to IGRAs, the RISK6 signature showed a better performance as a screening test for discriminating between ATB patients and HD. Importantly, compared to previous RISK6 results reported by Penn-Nicholson et al.[26], our study found similar data in terms of score range

and score changes over time despite the heterogeneity of both cohorts and study designs. In addition, marked technical differences are also apparent between our studies: we performed the RISK6 scores measurements on RNA manually isolated from whole blood collected directly in Tempus Blood RNA tubes and from blood samples first collected in lithium heparin tube and then transferred in Tempus Blood RNA Tubes, while this measurement was done by Penn-Nicholson et al. using RNA extracted manually or by an automated processes from whole blood collected in PAXgene Blood RNA tubes. Collectively, these results highlight the robustness of this PCR-based host-blood transcriptomic signature.

Besides, the higher RISK6 score levels detected in the cohort of Bangladesh compared to the other study sites was a remarkable result. We hypothesized that these RISK6 scores observed in Bangladesh may be influenced by the differing epidemiology, geographical locations as well as differences in gene expression levels between ethnic populations that may have contributed to a stronger transcriptomic signal in Bangladesh.

Our AUC data showed that RISK6 scores had a powerful ability to distinguish ATB from HD, with better or equal results to what was found with other transcriptomic signatures[28–34]. Moreover, while these previous signatures have shown promise as diagnostic tests, it should be noted that results of a three gene signature were not generalizable[28,34], while other signatures[33] require measurement of a high number of genes, thus limiting their possible application in resource-limited settings. Moreover, while RISK6 signature seems to meet or exceeded the TPP criteria based on each of our four cohorts, only two among the previous signatures (Sweeney3[28] and Sambarey10[32]) satisfied the sensitivity and specificity TPP criteria set by the WHO for a triage test[35]. However, it would be interesting to validate those signatures in other independent cohorts[28,36].

An important finding of our study is that RISK6 signature allowed to stratify TB patient's stages. Thus, when applied to the cohort of Madagascar, the only one including LTBI cases, the RISK6 signature demonstrated a significantly higher score in ATB individuals at baseline compared to those with LTBI. This is consistent with a previous study showing that a 3-gene transcriptomic signature was significantly higher in ATB patients versus LTBI[28] individuals, in addition to a 20-gene signature set that also discriminated ATB patients from LTBI and healthy controls[18]. In the same way, some gene-signatures were also evaluated[18] and showed high specificity and sensitivity to distinguish ATB patients from those with LTBI[23,28,31,33]. In our study, at > 90% sensitivity, RISK6 signature discriminated ATB from both LTBI and HD with a specificity > 70% which met the WHO TPP for a triage test for TB. Besides, no significant differences in the classification performance of RISK6 signature were observed between LTBI and HD, in line with recent transcriptomic studies demonstrating failure in discriminating LTBI from HD[18,28]. Moreover, while no previous studies has compared the levels of a transcriptomic signature between LTBI and treated TB patients, our data showed that the RISK6 signature reached the same score levels in treated TB patients when compared to LTBI individuals. Hence, it will be of interest to validate RISK6 signature in cohorts with larger number of latently infected individuals.

An additional finding of our study is that RISK6 signature also achieved the minimal WHO criteria in the Georgia cohort, for (i) an initial TB diagnostic test for sputum smear-negative TB to replace smear microscopy, using culture-confirmed TB as a gold standard (ii) and a non-sputum-based confirmatory test for sputum smear-negative TB. In this context, Turner et al.[37] reported a comparison of 27 signatures in cohorts of 181 patients for discriminating TB and no TB disease. They found that no previously published signatures achieved the minimal WHO sensitivity (65%) and specificity (98%) performance for a non-sputum-based confirmatory test for sputum smear-negative TB. Thus, our results are promising but further validation of RISK6 signature in larger cohorts will allow testing such performance. Furthermore, we found that ATB patients with low- or high-grade positive smears had significantly higher RISK6 scores compared with those with negative smears. Similarly to previous reported results with either Xpert MTB/RIF test or the C-reactive protein (CRP) concentration measurements[38,39], our findings suggest that RISK6 signature scores directly correlate with sputum smear grade, and may possibly represent a useful tool in the identification of patients with high transmission risk.

In the present study, we also attempted to compare the performance of different TB blood-based tests; RISK6 versus two IGRAs (QFT-P and IGRAs-rmsHBHA). Our results indicate that the performance of RISK6 was greater than that of QFT-P assay for ATB case-finding. Given that QFT-P was not recommended for the diagnosis of ATB but for LTBI diagnosis, we and others have shown that this assay is a better indicator for the detection of *Mtb* infection[12,40,41].

Our next aim was to evaluate variations in the RISK6 scores throughout successful treatment. We found that the RISK6 signature scores were significantly higher in ATB at baseline compared to HD, and continued to decrease progressively until the end of treatment reaching scores obtained in HD. Moreover, we also demonstrated that the RISK6 signature enables discrimination with high accuracy between untreated (T0), treated (T1 and T2), and post-treated (T3) TB patients who achieved a clinical cure. Taken together, these results showed the RISK6 genes might be modulated during anti-TB treatment as early as 2 months. Notably, the well-established data by Penn Nicholson et al.[26] also included additional earlier time points (week 1 and week 4) and found that RISK6 signature scores decrease over the course of successful treatment as early as 1 week. Data obtained with RISK6 is consistent with previous studies showing that transcriptomic signatures could be used as a powerful tool to monitor TB treatment response[30,42–46]. In this context, it has been previously reported that reduced gene expression levels occurred rapidly during the first and the second weeks of TB treatment[47,48]. An additional report showed that ATB gene set decreased after 4 months of anti-TB treatment, however, no tests were performed at earlier time points, or during TB treatment course[49]. To note, we showed that the RISK6 signature scores returned to normal levels (compared to HD) after 6 months of treatment, which confirmed previous data[26] but contrasted with another transcriptomic study showing that normal levels were reached 12 months after the treatment initiation[30]. Subsequently, these results indicate that RISK6 scores significantly stratified end of treatment from pre-treatment baseline. Taken together, our findings suggest that RISK6 signature could be used as a useful tool to monitor the response to anti-TB treatment. It may represent a potential alternative of the current tests used

to assess TB treatment efficacy and used comparing its result with those obtained by sputum culture that are crucial to evaluate drug resistance occurrence.

Remarkably, RISK6 relies on the use of qRT-PCR that could detect low levels of gene expression[50] and could be integrated into clinical poor settings in contrast to other complex methods. Besides, this signature requires the measurement of a small number of genes with subsequent reduced complexity and costs. Moreover, a key advantage of RISK6 is that it is a blood-based test, which is an easily accessible sample. Blood transcriptomic tests will improve the diagnosis of TB allowing faster treatment and thus reduction of transmission, especially in children, HIV co-infected TB patients and paucibacillary pulmonary TB patients. In such populations, microbiological tests are not always feasible due to the limited ability to produce good quality sputum samples or due to low bacterial loads in their samples. In the future, it will be of interest (i) to evaluate if RISK6 is able to predict the risk of progression to TB as demonstrated by the RISK11 signature[25] and (ii) to assess the diagnostic performance of RISK6 signature as a prototype cartridge assay as it has already been evaluated for the 3-gene signature against a microbiological reference standard[51].

This study was subject to several limitations. Indeed, the sample size was relatively small and LTBI individuals were recruited from only one country. Hence, validation of our findings in cohorts with larger number of LTBI individuals is required to better estimate specificities and sensitivities for a triage test. Moreover, only two patients had failed treatment. Therefore, further validation is required to better understand how RISK6 signature tracks with response to treatment. Additionally, we excluded diabetic and HIV-positive patients and immunosuppressed individuals in general and our study was restricted to adults. Thus, similar validation studies are needed for children and HIV-positive patients. Moreover, in future studies, it would be relevant to evaluate the specificity of the RISK6 scores in comparison to other respiratory diseases than TB, which is considered as most difficult to distinguish with.

In conclusion, data from this study provide strong proof that RISK6 can be applied as a non-sputum-based screening and triage test that met the WHO TPP benchmarks. This host response-based gene signature may be used for stratifying patients according to their TB infection status, as well as for monitoring patients over the course of treatment. RISK6 signature is applicable using a robust and simple qRT-PCR platform which facilitates its implementation in the clinical laboratories located in resource-poor settings. Our overall findings support the efforts to incorporate RISK6 signature into a point-of-care test ensuring rapid and accurate detection of ATB cases. Indeed, such simple tests are highly needed to reduce TB spread and transmission especially in areas with high TB burden that are usually disturbed with poverty.

Methods

Study design and population. This evaluation of the RISK6 signature was a nested case–control multicenter prospective cohort study evaluating the prognostic value of blood-based immunological biomarkers for monitoring TB treatment outcome. It was conducted within the GABRIEL Network[52] in four different countries including Bangladesh, Georgia, Lebanon and Madagascar.

In total, 238 participants were recruited and followed-up between August 2018 and September 2020. Participants included patients with ATB disease (n = 141), HD (n = 71) and individuals with LTBI (n = 26). Enrolled ATB patients aged ≥ 15 years old, newly diagnosed with pulmonary ATB: scoring positive for TB following bacteriological (culture positive and/or sputum smear microscopy positive) and/or molecular analysis (GeneXpert positive results) were recruited at primary healthcare TB clinics in each country: National Center for Tuberculosis and Lung Diseases (NCTLD) in Tbilisi, Georgia; Tuberculosis screening and treatment center (CHUSSPA) related to National Tuberculosis Programs (NTPs) in Antananarivo, Madagascar; NTP centers in Tripoli and Akkar, Lebanon and International Centre for Diarrhoeal Disease Research, Bangladesh (icddr,b) in Dhaka, Bangladesh. Clinically asymptomatic healthy donors; who do not have a previous TB history and who have no recent TB contacts were also recruited in all sites. In Madagascar, participants with positive QFT-P results (IFN-γ production ≥ 0.35 IU/mL) were defined as latently *Mtb* infected individuals. Patients with negative cultures at inclusion, ATB patients with Human Immunodeficiency Virus (HIV) or with diabetes mellitus comorbidities and patients under immunocompromising treatment were excluded (Fig. 4).

Enrolled ATB patients were followed-up during the treatment course at four different time points and classified as follow: (i) ATB at baseline T0: patients who didn't start TB treatment; (ii) treated active TB at T1 and T2: patients with ATB followed-up during the treatment and tested after 2 months of the start of the treatment (T1), and at the end of treatment (T2); (iii) treated active TB at T3: treated TB patients tested at 2 months after treatment completion.

Ethics statement. The study protocols were reviewed and approved by the human research ethics committees in each country; Georgia, the Institutional Review Board of the National Center for Tuberculosis and Lung Diseases (NTCLD) (Reference number: IORG0009467), Madagascar, the Ministry of Public Health and the Ethical Committee for Biomedical Research (Reference number: n°099-MSANP/CERBM), Lebanon, the institutional review board of NINI hospital (Reference number: IRB-F-01) and Bangladesh, the Research Review Committee and the Ethical Review Committee of International center for diarrheal diseases and research (icddr,b). All study participants provided written informed consent. All research was performed in accordance with relevant guidelines/regulations.

Diagnostic assessment and follow-up. ATB diagnosis was based on both bacteriological and molecular parameters. At least one sputum sample was collected at inclusion (T0) for culture testing (liquid culture media: MGIT mycobacterial growth indicator tube, BD BioSciences, NJ, USA and/or solid culture media: L–J (Lowenstein–Jensen) and also tested by microscopy for the presence of acid-fast bacilli (AFB) using the Ziehl–Neelsen

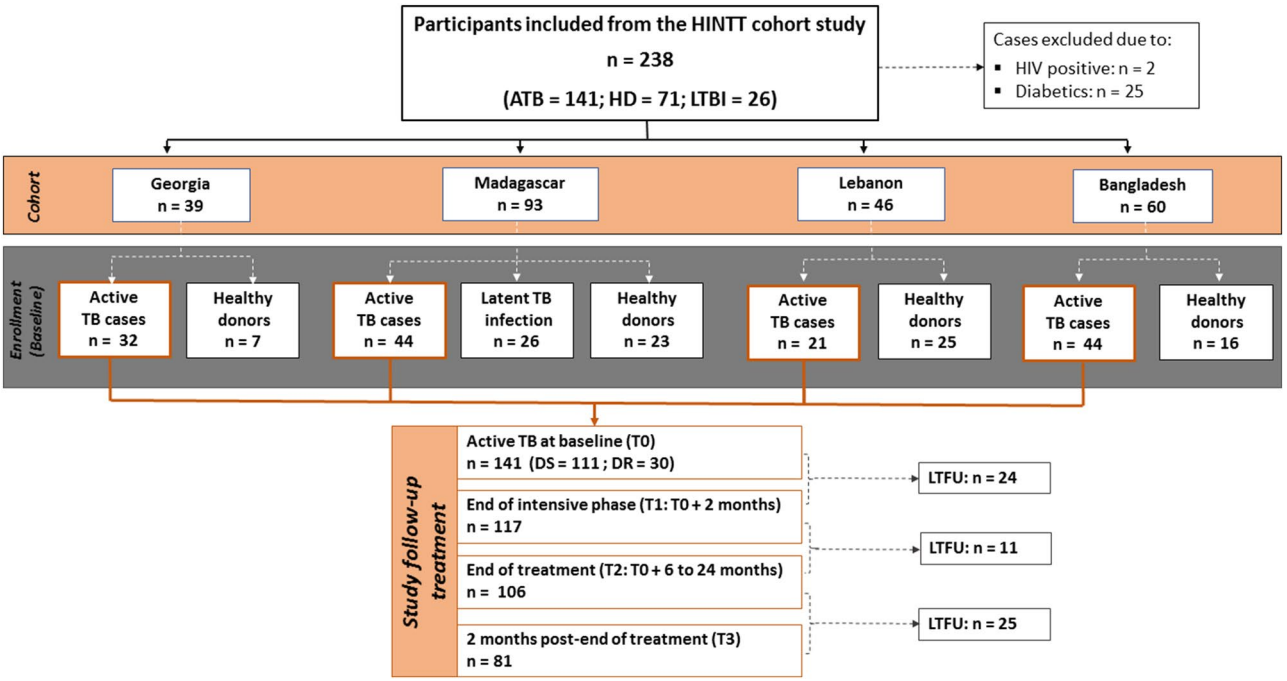

Figure 4. Flow diagram describing the enrollment and exclusion of participants with active TB, latent TB infection, and healthy donor participants from the different cohorts. ATB patients were followed-up at four different time points: at baseline (T0), ATB patients who didn't their TB treatment and followed throughout antibiotic therapy: at month 2 (T1), at the end of treatment (T2), and 2 months after treatment completion (T3). *TB* Tuberculosis, *ATB* active TB, *LTBI* Latent TB infection, *HD* healthy donors, *HIV* human immunodeficiency virus, *DS* drug-susceptible, *DR* drug-resistant, *LTFU* lost to follow-up.

staining method and/or Auramine O staining. In addition to positive culture, active TB status was defined by positive Xpert MTB/RIF (Cepheid). Patients were re-evaluated by sputum smear and culture during the intensive phase of treatment (T1) thereafter at the end of treatment (T2) and 2-months after treatment completion (T3) to confirm that they were successfully treated and cured. Drug susceptibility testing (DST) methods were performed according to standard protocols[53].

Demographic and clinical data collection. At enrollment and at each follow-up visit, medical history, clinical and demographic data were collected using standardized questionnaires to feed the cloud-based database system CASTOR (CASTOR Electronic Data Capture, Version 1.4, Netherlands).

Blood collection process. A minimum of 3 mL of whole blood for transcriptomic analysis and 5 mL for the Interferon-γ release assays were drawn from each participant. For transcriptomic analysis, specimens were directly collected in Tempus Blood RNA Tubes (Applied Biosystems, 4342792), vigorously shaken, and stored at − 80 °C. Of note, in Madagascar and Bangladesh, blood samples were first collected in lithium heparin tubes and then transferred in Tempus Blood RNA Tubes for transcriptomic analysis.

RNA extraction process and complementary DNA (cDNA) synthesis. Frozen Tempus Blood RNA tubes were thawed and RNA was manually extracted using the MagMAX™ for Stabilized Blood Tubes RNA Isolation Kit (Applied Biosystems by Thermo Fisher Scientific, 4451893) following the manufacturer's instructions. RNA elution was performed by adding 30 µL of Elution Buffer. The purified RNA was transferred to a nuclease-free tube, assessed for quantity and quality (Nanodrop spectrophotometer), and stored at − 80 °C until needed. The cDNA was synthetized using the Applied High Capacity RNA to cDNA kit (Applied Biosystems by Thermo Fisher Scientific, 4387406). The RT reaction mix was prepared as follows: 10 µL of 2xRT buffer mix, 1 µL of 20 × RT Enzyme, and 3 µL of nuclease-free water. Then 6 µL of purified RNA/negative control samples were added and proceeded using random hexamer primers (1 h 37 °C, 5 min 95 °C and hold 4 °C). cDNA was then 1:5 diluted (nuclease-free water) and stored at − 20 °C for long-term conservation.

Pre-amplification PCR. Prepared cDNA was pre-amplified using specific sequences of TaqMan primer-probes as previously described by Penn-Nicholson et al.[26]. 5 µL of 2 × PCR mix (TaqMan Universal PCR Master Mix 2×) (Applied Biosystems by Thermo Fisher Scientific, 4304437) with 2.5 µL of the specific primers-probes mix (PPM 0.6×), composed of primers of the 6 genes (listed in Supplementary Table 1) (Applied Biosystems by Thermo Fisher Scientific) was mixeded. Then 2.5 µL of the diluted cDNA/negative control samples were added and the mixture was incubated 10 min at 95 °C followed by 16 cycles of amplification at 95 °C for 15 s, 60 °C for

4 min, and hold at 4 °C. The pre-amplified PCR products were diluted 1:25 with nuclease-free water and stored at − 20 °C for long-term conservation.

Quantitative Real-Time PCR (qRT-PCR) assay and gene expression analysis. For every target to amplify, 4 µL of pre-amplified DNA was subjected to a real time nucleic acid amplification using 10 µL of TaqMan Universal PCR Master Mix (Applied Biosystems by Thermo Fisher Scientific), 1 µL of primers-probe mix (20×) and 4 µL of nuclease-free water using the following conditions: 2 min at 50 °C, 10 min at 95 °C, followed by 95 °C for 15 s and 60 °C for 1 min for 40 cycles. For analytical reasons, all the PCR reactions were performed in duplicate.

RISK6 score generation. Polymerase chain reaction signals were analyzed using CFX Manager Software version 3.1 (BioRad) in regression mode and expressed as cycle threshold (Ct) values. The step-by-step procedure for computing the 6-gene signature (RISK6) scores was performed as described by Penn-Nicholson et al.[26]. Briefly, the mean of Ct values was calculated for every targeted genes and combined to generate a score. The score was computed with R script available on https://bitbucket.org/satvi/risk6/src/master/.

QuantiFERON-TB Gold Plus and IGRAs-rmsHBHA assays. 1 mL of whole blood was collected directly into each of the QFT-P tubes (Qiagen, Hilden, Germany, 622526) (Nil: Negative Control, TB-Antigens (TB1/TB2) and Mitogen: Positive control) and an extra 1 mL of blood was collected in a heparin tube and stimulated with 10 µg/mL of rmsHBHA (UNICATT, Rome, Italy[10101010]). After 16–24 h incubation at 37 °C, plasma samples were harvested and stored at − 80 °C prior subjected to QFT-P ELISA (Qiagen, Hilden, Germany, 622120), following the manufacturer instructions. Briefly, 50 µL of plasma samples were tested, optical density results were compared to log-normalized values from freshly reconstituted IFN-γ kit standards. To account for potential immunomodulation phenomena unrelated with TB treatment, baseline IFN-γ level values (Nil tubes) were subtracted from antigen-stimulated IFN-γ values (TB1, TB2, Mitogen and rmsHBHA). According to the kit's sensitivity range, the maximum for IFN-γ level values was set at 10 IU/mL and negative values were rescaled to 0.

Statistical analysis. All statistical analyses were performed with R studio (version 4.0.3) software[54]. Graphs were created using the ggplot2 packages[55]. Statistical evaluation of the performance of RISK6 was done by calculating the Area Under the receiver operating characteristic curve (ROC AUC) and associated 95% confidence intervals (CI) using the pROC in R[56]. Discrete variables were analyzed using Fisher's Exact test with Bonferroni's post-hoc test. Normality was assessed using the Shapiro–Wilk Normality Test. Normal, continuous variables were analyzed with Student's t-test. Non-normal, continuous variables were analyzed with the Mann–Whitney test or the Kruskal–Wallis rank-sum test with Dunn's Kruskal–Wallis Multiple Comparisons post-hoc test. Repeated measures of non-independent continuous variables were analyzed using the Friedman rank-sum test, with Wilcoxon–Nemenyi–McDonald–Thompson's post-hoc test. Non-parametric data were presented as median ± IQR and the statistical significance cut-off was considered as a p value of < 0.05. For logistic regression analyses, variables were first evaluated in univariate analyses, then multivariate analyses were performed. Adjustment variables were selected as follows: sociodemographic variables of known clinical importance (e.g., sex, country of origin), TB risk factors (e.g., smoking), and additional sociodemographic variables that were at least moderately associated ($p < 0.10$) with the outcome in univariate analyses (e.g., prison). Irrelevant adjustment variables were then removed by backward model selection. The combination of variables that minimized the Akaike Information Criterion (AIC) for most tested predictors, while including important adjustment variables, was selected.

Data availability

The RISK6 scores and associated clinical data for all cohorts can be found in Supplementary Tables 2–7.

Received: 9 April 2021; Accepted: 21 June 2021
Published online: 01 July 2021

References

1. World Health Organisation. Global Tuberculosis Report. (2020).
2. Pai, M. *et al.* Tuberculosis. *Nat. Rev. Dis. Primers* **2**, 16076 (2016).
3. Goletti, D. *et al.* Can we predict tuberculosis cure? What tools are available?. *Eur. Respir. J.* **52**, 1801089 (2018).
4. World Health Organisation. Guidelines for treatment of drug-susceptible tuberculosis and patient care. (2017).
5. Parrish, N. M. & Carroll, K. C. Role of the clinical mycobacteriology laboratory in diagnosis and management of tuberculosis in low-prevalence settings. *J. Clin. Microbiol.* **49**, 772–776 (2011).
6. Goletti, D., Lee, M. R., Wang, J. Y., Walter, N. & Ottenhoff, T. H. M. Update on tuberculosis biomarkers: From correlates of risk, to correlates of active disease and of cure from disease. *Respirology* **23**, 455–466 (2018).
7. Petrone, L. *et al.* Evaluation of IP-10 in Quantiferon-Plus as biomarker for the diagnosis of latent tuberculosis infection. *Tuberculosis (Edinb)* **111**, 147–153 (2018).
8. Petruccioli, E. *et al.* Effect of HIV-infection on QuantiFERON-plus accuracy in patients with active tuberculosis and latent infection. *J. Infect.* **80**, 536–546 (2020).
9. Petruccioli, E. *et al.* Effect of therapy on Quantiferon-Plus response in patients with active and latent tuberculosis infection. *Sci. Rep.* **8**, 15626 (2018).
10. Delogu, G. *et al.* Methylated HBHA produced in *M. smegmatis* discriminates between active and non-active tuberculosis disease among RD1-responders. *PLoS One* **6**, e18315 (2011).

11. Chiacchio, T. *et al.* Immune characterization of the HBHA-specific response in *Mycobacterium tuberculosis*-infected patients with or without HIV infection. *PLoS ONE* **12**, e0183846 (2017).
12. Tang, J. *et al.* QuantiFERON-TB Gold Plus combined with HBHA-Induced IFN-gamma release assay improves the accuracy of identifying tuberculosis disease status. *Tuberculosis (Edinb)* **124**, 101966 (2020).
13. Sali, M. *et al.* Combined use of Quantiferon and HBHA-based IGRA supports tuberculosis diagnosis and therapy management in children. *J. Infect.* **77**, 526–533 (2018).
14. Chedid, C. *et al.* Relevance of QuantiFERON-TB gold plus and heparin-binding hemagglutinin interferon-gamma release assays for monitoring of pulmonary tuberculosis clearance: A multicentered study. *Front. Immunol.* **11**, 616450 (2020).
15. Davies, P. D. & Pai, M. The diagnosis and misdiagnosis of tuberculosis. *Int. J. Tuberc. Lung Dis.* **12**, 1226–1234 (2008).
16. Diagnostic Standards and Classification of Tuberculosis in Adults and Children. *Am. J. Respir. Crit. Care. Med.* **161**, 1376–1395 (2000).
17. Steingart, K. R. *et al.* Xpert(R) MTB/RIF assay for pulmonary tuberculosis and rifampicin resistance in adults. *Cochrane Database Syst. Rev.* **2014**, CD009593 (2014).
18. Singhania, A. *et al.* A modular transcriptional signature identifies phenotypic heterogeneity of human tuberculosis infection. *Nat. Commun.* **9**, 2308 (2018).
19. World Health Organisation. Foundation for Innovative New Diagnostics. Pipeline Report 2020 Tuberculosis Diagnostics. (2020).
20. Wallis, R. S. *et al.* Tuberculosis biomarkers discovery: Developments, needs, and challenges. *Lancet Infect. Dis.* **13**, 362–372 (2013).
21. Kik, S. V. *et al.* An evaluation framework for new tests that predict progression from tuberculosis infection to clinical disease. *Eur. Respir. J.* **52**, 1800946 (2018).
22. Denkinger, C. M. *et al.* Defining the needs for next generation assays for tuberculosis. *J. Infect. Dis.* **211**(Suppl 2), S29-38 (2015).
23. Zak, D. E. *et al.* A blood RNA signature for tuberculosis disease risk: A prospective cohort study. *Lancet* **387**, 2312–2322 (2016).
24. Esmail, H., Cobelens, F. & Goletti, D. Transcriptional biomarkers for predicting development of tuberculosis: Progress and clinical considerations. *Eur. Respir. J.* **55**, 1901957 (2020).
25. Scriba, T. J. *et al.* Biomarker-guided tuberculosis preventive therapy (CORTIS): A randomised controlled trial. *Lancet Infect. Dis.* **21**, 354–365 (2021).
26. Penn-Nicholson, A. & Mbandi, S. K. RISK6, a 6-gene transcriptomic signature of TB disease risk, diagnosis and treatment response. *Sci. Rep.* **10**, 8629 (2020).
27. World Health Organization. High-priority target product profiles for new tuberculosis diagnostics: report of a consensus meeting. (2014).
28. Sweeney, T. E., Braviak, L., Tato, C. M. & Khatri, P. Genome-wide expression for diagnosis of pulmonary tuberculosis: A multicohort analysis. *Lancet Respir. Med.* **4**, 213–224 (2016).
29. Blankley, S. *et al.* The application of transcriptional blood signatures to enhance our understanding of the host response to infection: The example of tuberculosis. *Philos. Trans. R. Soc. Lond. B Biol. Sci.* **369**, 20130427 (2014).
30. Berry, M. P. *et al.* An interferon-inducible neutrophil-driven blood transcriptional signature in human tuberculosis. *Nature* **466**, 973–977 (2010).
31. Maertzdorf, J. *et al.* Concise gene signature for point-of-care classification of tuberculosis. *EMBO Mol. Med.* **8**, 86–95 (2016).
32. Sambarey, A. *et al.* Unbiased identification of blood-based biomarkers for pulmonary tuberculosis by modeling and mining molecular interaction networks. *EBioMedicine* **15**, 112–126 (2017).
33. Kaforou, M. *et al.* Detection of tuberculosis in HIV-infected and -uninfected African adults using whole blood RNA expression signatures: A case-control study. *PLoS Med.* **10**, e1001538 (2013).
34. Laux da Costa, L. *et al.* A real-time PCR signature to discriminate between tuberculosis and other pulmonary diseases. *Tuberculosis (Edinb.)* **95**, 421–425 (2015).
35. Warsinske, H., Vashisht, R. & Khatri, P. Host-response-based gene signatures for tuberculosis diagnosis: A systematic comparison of 16 signatures. *PLoS Med.* **16**, e1002786 (2019).
36. Warsinske, H. C. *et al.* Assessment of validity of a blood-based 3-gene signature score for progression and diagnosis of tuberculosis, disease severity, and treatment response. *JAMA Netw. Open* **1**, e183779 (2018).
37. Turner, C. T. *et al.* Blood transcriptional biomarkers for active pulmonary tuberculosis in a high-burden setting: A prospective, observational, diagnostic accuracy study. *Lancet Respir. Med.* **8**, 407–419 (2020).
38. Beynon, F. *et al.* Correlation of Xpert MTB/RIF with measures to assess *Mycobacterium tuberculosis* bacillary burden in high HIV burden areas of Southern Africa. *Sci. Rep.* **8**, 5201 (2018).
39. Miranda, P. *et al.* Sustained elevated levels of C-reactive protein and ferritin in pulmonary tuberculosis patients remaining culture positive upon treatment initiation. *PLoS One* **12**, e0175278 (2017).
40. Sane Schepisi, M. *et al.* Immune status and serial quantiferon-TB gold in-tube screening for latent *Mycobacterium tuberculosis* infection among HIV-infected persons in a country with a low tuberculosis incidence. *J. Infect. Dis.* **211**, 1852–1853 (2015).
41. Won, D., Park, J. Y., Kim, H. S. & Park, Y. Comparative results of QuantiFERON-TB gold in-tube and QuantiFERON-TB gold plus assays for detection of tuberculosis infection in clinical samples. *J. Clin. Microbiol.* **58**, e01854-e1919 (2020).
42. MacLean, E. & Broger, T. A 10-gene signature for the diagnosis and treatment monitoring of active tuberculosis using a molecular interaction network approach. *EBioMedicine* **16**, 22–23 (2017).
43. Sambarey, A. *et al.* Meta-analysis of host response networks identifies a common core in tuberculosis. *NPJ Syst. Biol. Appl.* **3**, 4 (2017).
44. Thompson, E. G. *et al.* Host blood RNA signatures predict the outcome of tuberculosis treatment. *Tuberculosis (Edinb.)* **107**, 48–58 (2017).
45. Darboe, F. *et al.* Detection of tuberculosis recurrence, diagnosis and treatment response by a blood transcriptomic risk signature in HIV-infected persons on antiretroviral therapy. *Front. Microbiol.* **10**, 1441 (2019).
46. Satproedprai, N. *et al.* Diagnostic value of blood gene expression signatures in active tuberculosis in Thais: A pilot study. *Genes Immun.* **16**, 253–260 (2015).
47. Cliff, J. M. *et al.* Distinct phases of blood gene expression pattern through tuberculosis treatment reflect modulation of the humoral immune response. *J. Infect. Dis.* **207**, 18–29 (2013).
48. Bloom, C. I. *et al.* Detectable changes in the blood transcriptome are present after two weeks of antituberculosis therapy. *PLoS One* **7**, e46191 (2012).
49. Francisco, N. M. *et al.* Diagnostic accuracy of a selected signature gene set that discriminates active pulmonary tuberculosis and other pulmonary diseases. *J. Infect.* **75**, 499–510 (2017).
50. van Rensburg, I. C. & Loxton, A. G. Transcriptomics: The key to biomarker discovery during tuberculosis?. *Biomark. Med.* **9**, 483–495 (2015).
51. Sodersten, E. *et al.* Diagnostic accuracy study of a novel blood-based assay for identification of TB in people living with HIV. *J. Clin. Microbiol.* **4**, 213 (2020).
52. Komurian-Pradel, F. *et al.* Enhancing research capacities in infectious diseases: The GABRIEL network, a joint approach to major local health issues in developing countries. *Clin. Epidemiol. Glob. Health* **1**, 40–43 (2013).
53. World Health Organisation. WHO Consolidated Guidelines on Tuberculosis, Module 4: Treatment - Drug-Resistant Tuberculosis Treatment. (2020).
54. R Core Team. *R: A Language and Environment for Statistical Computing*. R Foundation for Statistical Computing. (2021).

55. Wickham, H. *ggplot2: Elegant Graphics for Data Analysis* (Springer, 2016).
56. Robin, X. *et al.* pROC: An open-source package for R and S+ to analyze and compare ROC curves. *BMC Bioinform.* **12**, 77 (2011).

Acknowledgements
We are grateful for the inventors of a patent on RISK6 signature, the SATVI Clinical and Laboratory Team. This work was supported by Fondation Mérieux. We thank the patients and volunteer participants, as well as the local healthcare staff in each clinical site for their excellent assistance. We would like to thank Dr. Matthieu SCHOENHALS head of the immunology of infectious diseases unit of IPM for his assistance.

Author contributions
J.H. conceived and designed the study, and initiated this project in partnership with N.R., M.H., N.T., S.Ba. and D.G. Patient recruitment, follow-up and data collection was done by E.K., M.U., S.Bi., R.N., P.R., C.R., P.H., J.R., A.R. and R.B. The experiments were performed by R.B., M.N. and S.P. and J.H. performed statistical analysis with contribution from C.C. Data analysis and interpretation of results was implemented by R.B., M.N., J.H. and S.P. The manuscript was written by R.B., and all authors have read, reviewed and approved the final manuscript.

Competing interests
The authors declare no competing interests.

Additional information
Supplementary Information The online version contains supplementary material available at https://doi.org/10.1038/s41598-021-93059-1.

Correspondence and requests for materials should be addressed to R.B. or J.H.

Reprints and permissions information is available at www.nature.com/reprints.

Publisher's note Springer Nature remains neutral with regard to jurisdictional claims in published maps and institutional affiliations.

The HINTT working group within the GABRIEL network

Graciela Russomando[13], Chyntia Carolina Díaz Acosta[13] & Rossana Arenas[14]

[13]Instituto de Investigaciones en Ciencias de la Salud, National University of Asunción, Asunción, Paraguay. [14]Hospital General de San Lorenzo, MSPyBS, Asunción, Paraguay.

2. Study 2: Evaluation of protein biomarkers for diagnosis and monitoring of treatment response

Summary

There is a need for rapid non-sputum-based tests to identify and treat patients infected with *M. tuberculosis*. In this study we aim to measure and compare the expression of a selected panel of human plasma proteins in patients with active pulmonary tuberculosis (ATB) throughout anti-TB treatment (from baseline to the end of treatment), in *M. tuberculosis* infected individuals (TBI) and healthy donors (HD) to identify a host-protein signature useful for both TB diagnosis and treatment monitoring. We evaluated seven human host proteins CLEC3B, SELL, IGFBP3, IP10, CD14, ECM1 and C1Q. These markers were measured in the plasma isolated from an HIV-negative prospective cohort of ATB, TBI and HD. The protein signatures were assessed using a Luminex xMAP® to quantify the plasmatic levels in unstimulated blood of the different clinical group. We also assessed the protein levels at baseline and during the 6-months ATB treatment, to compare the plasma protein levels between culture slow and fast converters that may contribute to monitor the TB treatment outcome. Protein signatures were defined using the CombiROC algorithm and multivariate models. The studied plasma host proteins showed different levels between the clinical groups and during the TB treatment. Six of the plasma proteins showed significant differences in normalised median fluorescence intensities when comparing ATB vs HD or TBI groups while ECM1 protein revealed a significant difference between fast and slow sputum culture converters after 2 months following treatment ($p = 0.006$). The expression of a four-host protein markers (CLEC3B-ECM1-IP10-SELL) was significantly different between ATB from HD or TBI groups (respectively, $p < 0.05$). The expression of the same signature was significantly different between the slow vs the fast sputum culture converters after 2 months of treatment (*p-value* < 0.05). The results suggest a promising 4 host-plasma marker signature that would be associated with both TB diagnosis and treatment monitoring.

scientific reports

Check for updates

OPEN

Plasma host protein signatures correlating with *Mycobacterium tuberculosis* activity prior to and during antituberculosis treatment

Mame Diarra Bousso Ndiaye[1]✉, Paulo Ranaivomanana[1], Lova Tsikiniaina Rasoloharimanana[1], Voahangy Rasolofo[1], Rila Ratovoson[1], Perlinot Herindrainy[2], Julio Rakotonirina[3], Matthieu Schoenhals[1], Jonathan Hoffmann[4,5] & Niaina Rakotosamimanana[1,5]✉

There is a need for rapid non-sputum-based tests to identify and treat patients infected with *Mycobacterium tuberculosis* (*Mtb*). The overall objective of this study was to measure and compare the expression of a selected panel of human plasma proteins in patients with active pulmonary tuberculosis (ATB) throughout anti-TB treatment (from baseline to the end of treatment), in Mtb-infected individuals (TBI) and healthy donors (HD) to identify a putative host-protein signature useful for both TB diagnosis and treatment monitoring. A panel of seven human host proteins CLEC3B, SELL, IGFBP3, IP10, CD14, ECM1 and C1Q were measured in the plasma isolated from an HIV-negative prospective cohort of 37 ATB, 24 TBI and 23 HD. The protein signatures were assessed using a Luminex xMAP® to quantify the plasmatic levels in unstimulated blood of the different clinical group as well as the protein levels at baseline and at three timepoints during the 6-months ATB treatment, to compare the plasma protein levels between culture slow and fast converters that may contribute to monitor the TB treatment outcome. Protein signatures were defined using the CombiROC algorithm and multivariate models. The studied plasma host proteins showed different levels between the clinical groups and during the TB treatment. Six of the plasma proteins (CLEC3B, SELL, IGFBP3, IP10, CD14 and C1Q) showed significant differences in normalised median fluorescence intensities when comparing ATB vs HD or TBI groups while ECM1 revealed a significant difference between fast and slow sputum culture converters after 2 months following treatment ($p = 0.006$). The expression of a four-host protein markers (CLEC3B-ECM1-IP10-SELL) was significantly different between ATB from HD or TBI groups (respectively, $p < 0.05$). The expression of the same signature was significantly different between the slow vs the fast sputum culture converters after 2 months of treatment ($p < 0.05$). The results suggest a promising 4 host-plasma marker signature that would be associated with both TB diagnostic and treatment monitoring.

Tuberculosis (TB) is one of the deadliest diseases caused by a single infectious agent as approximately 10 million people are infected each year. As reported by the World Health Organisation (WHO), the mortality rate was 1.5 million from TB in 2020[1].

The diagnosis of TB is mainly lying on clinical symptoms followed by bacteriological or molecular confirmation of the presence of *Mycobacterium tuberculosis* (Mtb). Once diagnosed the treatment of TB requires antibiotic multitherapies that last at least 6 months and treatment failure as well as relapse can occur[2]. These outcomes are

[1]Institut Pasteur de Madagascar, Antananarivo, Madagascar. [2]United States Agency for International Development (USAID), Antananarivo, Madagascar. [3]Centre Hospitalier Universitaire de Soins et Santé Publique Analakely (CHUSSPA), Antananarivo, Madagascar. [4]Medical and Scientific Department, Fondation Mérieux, Lyon, France. [5]These authors contributed equally: Jonathan Hoffmann and Niaina Rakotosamimanana. ✉email: ndiayemame@pasteur.mg; niaina@pasteur.mg

associated with severe adverse effects and long treatment durations that induce a lack of patient adherence to the treatment thus promoting the emergence of drug-resistance[3]. According to the WHO, globally one third of all TB cases are still not notified, and many patients' samples do not undergo drug-susceptibility testing (DST). Improved TB prevention and control depend critically on the development of a simple, readily accessible rapid test to detect TB and monitor the effect of its treatment. These tests should achieve the WHO Target Product Profile (TPP) recommendations in terms of performances for a non-sputum based screening/triage test (at a sensitivity of > 90%, the minimum specificity as set out in this TPP should be ≥ 70%), for an initial TB diagnostic test to replace sputum based tests (at minimum 60% sensitivity, the minimum specificity should be > 98%) and for a confirmatory test (at minimum 65% sensitivity, the minimum specificity should be > 98%)[4].

Monitoring TB treatment adherence and effects relies on *Mtb* detection by sputum smear microscopy and culture when possible. Sputum smear microscopy is highly sample- and operator-dependent and has poor sensitivity. The bacteriological confirmation of TB with mycobacterial culture takes from 3 to 6 weeks and it takes longer to obtain the DST results.

On the other hand, molecular tests based on the detection of the mycobacterial DNA like the GeneXpert or the line probe assay showed good specificity/sensitivity and allow rapid identification of antibiotic-resistant *Mtb* strain. However, they may have some limitations, due to the bacterial DNA that can be detected from both live and dead cells.

The development of TB immunodiagnostic tests like the tuberculin skin test (TST) and the interferon gamma release assay (IGRA) offers an alternative to sputum based tests by assessing the peripheral immune response for the identification of individuals infected with *Mtb* but, these tests lack accuracy to monitor treatment. Diagnostic approaches based on non-sputum based tests like the evaluation of host plasma protein, transcriptomic or phenotypic signatures for treatment monitoring, screening or triage showed some relevant clinical advantages[5–11].

A proteomic study notably described a panel of host protein biomarkers that would help to differentiate active TB from other forms of respiratory disease in non-HIV infected patients[8]. Some of these proteins were particularly described as having potential important roles during the active TB and treatment. The tetranectin, also known as C type LECtin domain family 3 member B (CLEC3B), and extracellular matrix protein 1 (ECM1), are involved in tissue modification and remodeling[12,13] as well as in pro-/anti-inflammatory and fibrogenic properties and regulating Th2 cell migration[14,15]. The insulin-like growth factor (IGF) pathway 3 (IGFBP3) are regulated in patients with active TB (ATB)[6,8]. SELL is involved in leukocyte addressing, adhesion, migration, signal transduction and has been shown to discriminate TB from other respiratory diseases[16,17]. Soluble CD14 (sCD14) is known for its role in the recognition pathologies in the lungs including active TB[18–22]. C1q, the first subcomponent of the classical complement cascade was used to discriminate ATB from latent TB infection[23–25]. Interferon gamma inducible protein 10 (IP10) is known as a marker for TB infection and was recently described to be involved as an indicator for sputum culture conversion and treatment monitoring[26]. A combination of IP-10 and RANTES has shown good performance in diagnostic and monitoring in pulmonary TB management[27–29].

The present study aims to compare the expression of these proteins previously described as plasma host markers related to TB, CLEC3B, SELL, IGFBP3, IP10, CD14, ECM1 and C1Q, in different human clinical groups (ATB, TBI, and HD) and during anti-TB treatment to identify a putative host protein signature useful for both TB diagnosis and treatment monitoring.

Results

Sociodemographic and clinical characteristics. A total of 37 patients with bacteriologically confirmed pulmonary tuberculosis (ATB), 23 individuals with asymptomatic tuberculosis infection (TBI), and 24 healthy donors (HD) were enrolled in the study. The sociodemographic and clinical characteristics of the participants at baseline are summarized in Table 1. Among patients with ATB, 16.2% reported previous TB infection. All the 37 TB patients successfully achieved their TB treatment. No drug resistance was reported amongst the ATB group. At baseline, 32.4% (12/37) of the ATB cases were reported as negative by smear microscopy, while 40.5% (15/37) were high grade (2+ or 3+) positive smear and 27% (10/37) were low grade (1+ or scanty) positive smear.

The white blood cell count (WBC) was higher in patients with ATB compared to respectively TBI or HD (8870/mm^3 (6350–11,360), 7340/mm^3 (5875–9230) and 6760/mm^3 (5920–7132.5) respectively, $p < 0.001$). In contrast, the proportion of lymphocytes in the WBC count was lower in ATB group than in TBI and HD groups (17.8% [95% CI 13–23.9], 35.2% [95% CI 30.1–41.4] and 43.1% [95% CI 38.25–52.67] respectively, $p < 0.001$). Retrospectively "Slow converter" profile was assigned to 32.4% (12/37) of ATB patients. QFT-P assay result was positive for 67.6% (25/37) of ATB cases at baseline.

Evaluation of single host protein markers related to clinical group and mycobacterial load variations. The differences in normalized MFI ratio of each marker were separately assessed and compared between the three studied clinical groups as well as during the ATB treatment (Fig. 1). When comparing the protein levels in ATB vs HD or in ATB vs TBI, significant differences of normalized MFI ratio were observed for all markers except for ECM1 ($p > 0.05$) (Fig. 1A).

A significant difference in normalized MFI ratios was observed for SELL levels when comparing TBI to HD ($p = 0.046$). The use of plasma measure of sCD14 and SELL to distinguish ATB from HD reached respective sensitivity of 97% [95% CI 85–99] and specificity of 96% [95% CI 80–10] for sCD14 and a sensitivity of 97% [95% CI 86–99], specificity of 100% [95% CI 85–100] for SELL (Fig. 2C). sCD14 and SELL distinguished also TBI from ATB (Fig. 2B). Simplex detection of these 2 markers did not discriminate TBI from HD (Fig. 2A).

Due to the various sputum smear microscopy observed at baseline for the ATB patients that may influence the immune response and the plasma protein levels, we wondered if the expression of these markers and the mycobacterial loads were correlated. The levels of the plasma proteins were thus stratified to the sputum smear

	ATB	TBI	HD	
	N = 37	N = 23	N = 24	*p* value
Patient demographics				
Age (years)	28 (22–43)	35 (24.5–44.5)	29.5 (23.25–36.25)	0.22
Sex (male)	59.5% (22/37)	34.8% (8/23)	20.8% (5/24)	0.015
BMI at inclusion	17.27 (16.16–18.48)	NA	NA	
Risk factors and comorbidities				
Smoking	40.5% (15/37)	NA	NA	
Alcohol abuse	40.5% (15/37)	NA	NA	
Jail detention history	2.7% (1/37)	NA	NA	
Chronic HCV infection	2.7% (1/37)	NA	NA	
History of TB				
Previous TB	16.2% (6/37)	NA	NA	
Previous TB treatment outcome				
Cured and completed	50% (3/6)	NA	NA	
Treatment failure	16.7% (1/6)	NA	NA	
Outcome not evaluated or unknown	33.3% (2/6)	NA	NA	
TB characteristics at inclusion				
Drug-susceptible Mtb	100% (37/37)	NA	NA	
Pulmonary TB	100% (37/37)	NA	NA	
Sputum smear microscopy at inclusion				
High grade (2+ or 3+)	40.5% (15/37)	NA	NA	
Low grade (1+ or scanty)	27% (10/37)	NA	NA	
Negative	32.4% (12/37)	NA	NA	
Treatment regimen				
2HRZE/2HR	97.3% (36/37)	NA	NA	
Slow converters	32.4% (12/37)	NA	NA	
Fast converters	67.6% (25/37)	NA	NA	
WBC absolute count at inclusion (/mm^3)	8870 (6350–11,360)	7340 (5875–9230)	6760 (5920–7132.5)	0.009
Lymphocyte at inclusion (% of WBC)	17.8 (13–23.9)	35.2 (30.1–41.4)	43.1 (38.25–52.67)	< 0.001
Monocytes at inclusion (% of WBC)	9.8 (7–11.5)	7.2 (6.6–7.75)	7.65 (6.8–9.47)	0.001
Hemoglobin at inclusion (g/dL)	11.9 (11–13.1)	14.4 (13.6–15.35)	14.35 (13–15.1)	< 0.001
Neutrophils at inclusion (% of WBC)	70.1 (62.7–77.5)	52 (45.7–58.56)	44.6 (33.57–48.82)	< 0.001
Eosinophil at inclusion (% of WBC)	1 (0.5–1.9)	2.6 (1.91–4.99)	2.71 (2.18–4.28)	< 0.001
Basophils at inclusion (% of WBC)	0.4 (0.1–0.6)	0.6 (0.5–0.85)	0.75 (0.5–0.89)	< 0.001
BCG vaccination	91.9% (34/37)	NA	NA	
Positive QuantiFERON-TB gold plus at baseline	67.6% (25/37)	100% (23/23)	0% (0/24)	

Table 1. Sociodemographic data of patients. N(IQR); %(n/N).

microscopy grades at baseline we observed for the ATB (Fig. 1B). Among the seven markers, IGFBP3, IP10, and sCD14, had a significant difference of normalized MFI ratio between negative and high-grade positive smears: $p = 0.029$, 0.030, and 0.037 respectively. No significant difference was noted when comparing the expression of those 3 host proteins between patients with low- vs high-grade nor between negative smear grade vs low-grade (Fig. 1B).

ECM1 plasma levels differ according to the sputum culture conversion. Regarding the treatment monitoring, all the 37 ATB patients had achieved sputum conversion at the end of treatment (T2). A significantly higher ($p = 0.006$) level of ECM1 normalized MFI at baseline was observed in patients with fast culture conversion status compared to those of the slow converters (Fig. 3). ROC curve analysis of plasma ECM1 levels distinguished the two clinical groups between "fast converters" and "slow converters" at baseline with an AUC of 0.773, sensitivity of 75% [95% CI 47–91], and specificity of 80% [95% CI 61–91] (Fig. 2D).

Identification and evaluation of a four host plasma protein signature between the clinical groups. A CombiROC algorithm was used to identify the best plasma marker combinations that first allowed to distinguish the three clinical groups (ATB, TBI, and HD). A set of 120 signatures were obtained from the seven studied markers (Supplementary tables 2–8). These signatures were ranked according to their decreasing Area Under the Receiver Operating characteristic Curve (AUC) values, then, the number and the relevance of the combined markers involved in each signature. The "ECM1-CLEC3B-IP10-SELL" combination was the most

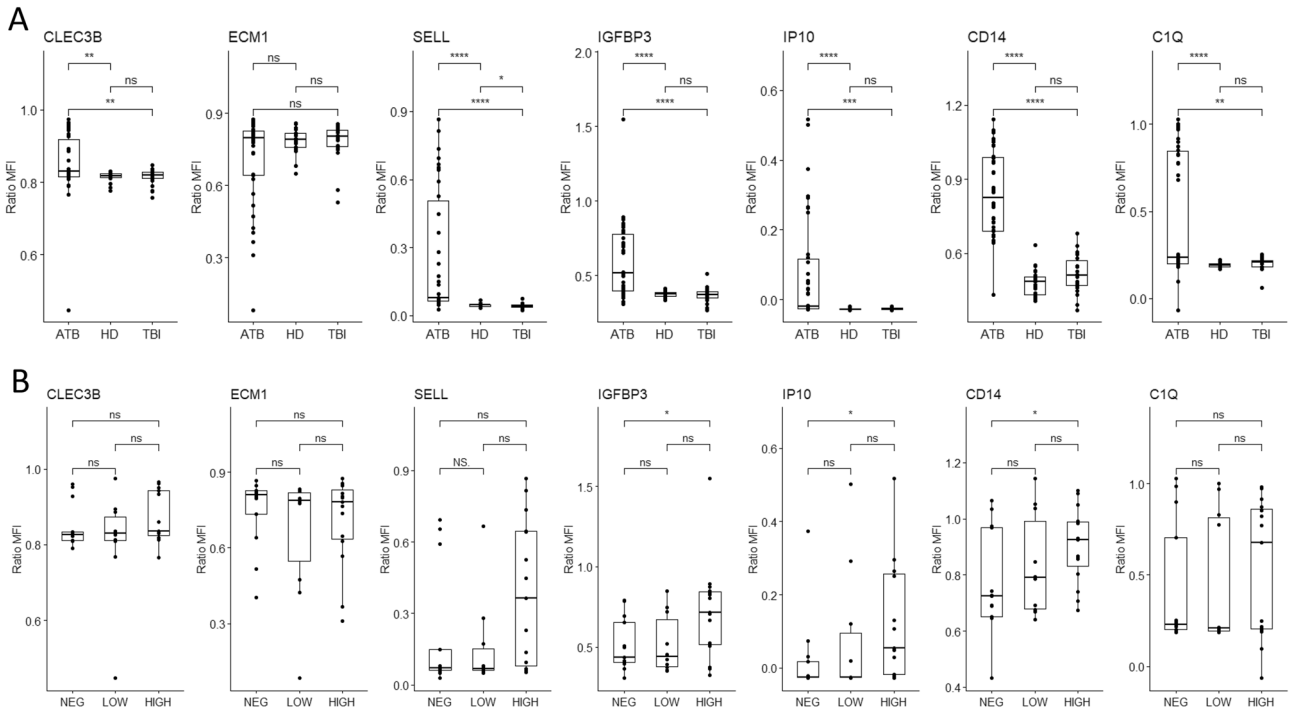

Figure 1. Evaluation of single host protein markers related to clinical group and mycobacterial load variations. (**A**) Comparison of markers expression in different clinical groups. (**B**) Comparison of markers expression and mycobacterial load variation. Data are given as median + interquartile range. Each black dot represents one patient. Data were compared using the Mann–Whithney U test with correction apply to adjust *p* values. $^{*}p<0.05$; $^{**}p<0.01$; $^{***}p<0.001$.

relevant to stratify the clinical groups regarding the selected parameters. This protein combination reached an AUC of 0.95, corresponding to a sensitivity of 95% and specificity of 92% when comparing the ATB protein levels to those of the HD group (Table 2). This same signature also showed an AUC of 0.87 for a treatment monitoring assay, corresponding to a sensitivity of 83%, and specificity of 84% in identifying fast or slow converters at baseline prior to TB treatment.

For the discrimination between ATB and TBI individuals, the AUC value was 0.929 corresponding to a sensitivity of 89% and specificity of 91%.

After comparing the protein levels observed from TBI to those of HD, a lower performance was observed compared to the latest groups with an AUC value of 0.74 corresponding to a sensitivity of 56% and specificity of 96%.

Discussion

The plasma host expression variations of seven proteins in patients with ATB (with different time-points from baseline to the end of anti-TB treatment), subjects with *Mtb* infection and healthy donors has been assessed in this study. Among the seven proteins targeted, our results suggest that a signature of four plasma proteins seems useful for both TB diagnostic and treatment monitoring. Nevertheless, its diagnostic/prognostic performance must be confirmed in a large-scale clinical study. To date, few studies have demonstrated the existence of a unique signature fulfilling the WHO TPPs recommendations for both purposes[4].

Several studies have already described marker signatures of interest for TB triage[28–31]. Chegou et al., identified signatures on QFT supernatants using the same technology (i.e. Luminex xMAP® technology) for TB diagnosis. A biosignature including IFN-γ, MIP-1β, TGF-α in unstimulated plasma, and antigen-specific TGF-α and VEGF has been described with acceptable AUC of 0.81 to discriminate between group of patients with TB disease or other respiratory diseases (ORD)[32]. In another study, a five-marker (IL-1β, IL-23, ECM1, HCC1, fibrinogen) biosignature was identified in saliva for TB diagnosis with an optimal AUC of 0.88[33]. In both studies, TPPs recommendations for a triage test were not reached, and the utility of these signatures in treatment monitoring was not evaluated.

In the present study, the protein markers expression in the plasma were assessed using a multiplex assay developed on the xMAP platform and were then analysed individually or in combined panels to establish a signature associating both TB detection and treatment monitoring. The four host-plasma marker signatures (ECM1-CLEC3B-IP10-SELL) selected in our study would meet the recommendations for a non-sputum-based assay, however, it needs to be evaluated in a larger scale sample size study population, allowing to better define the diagnostic/prognostic performance of this assay.

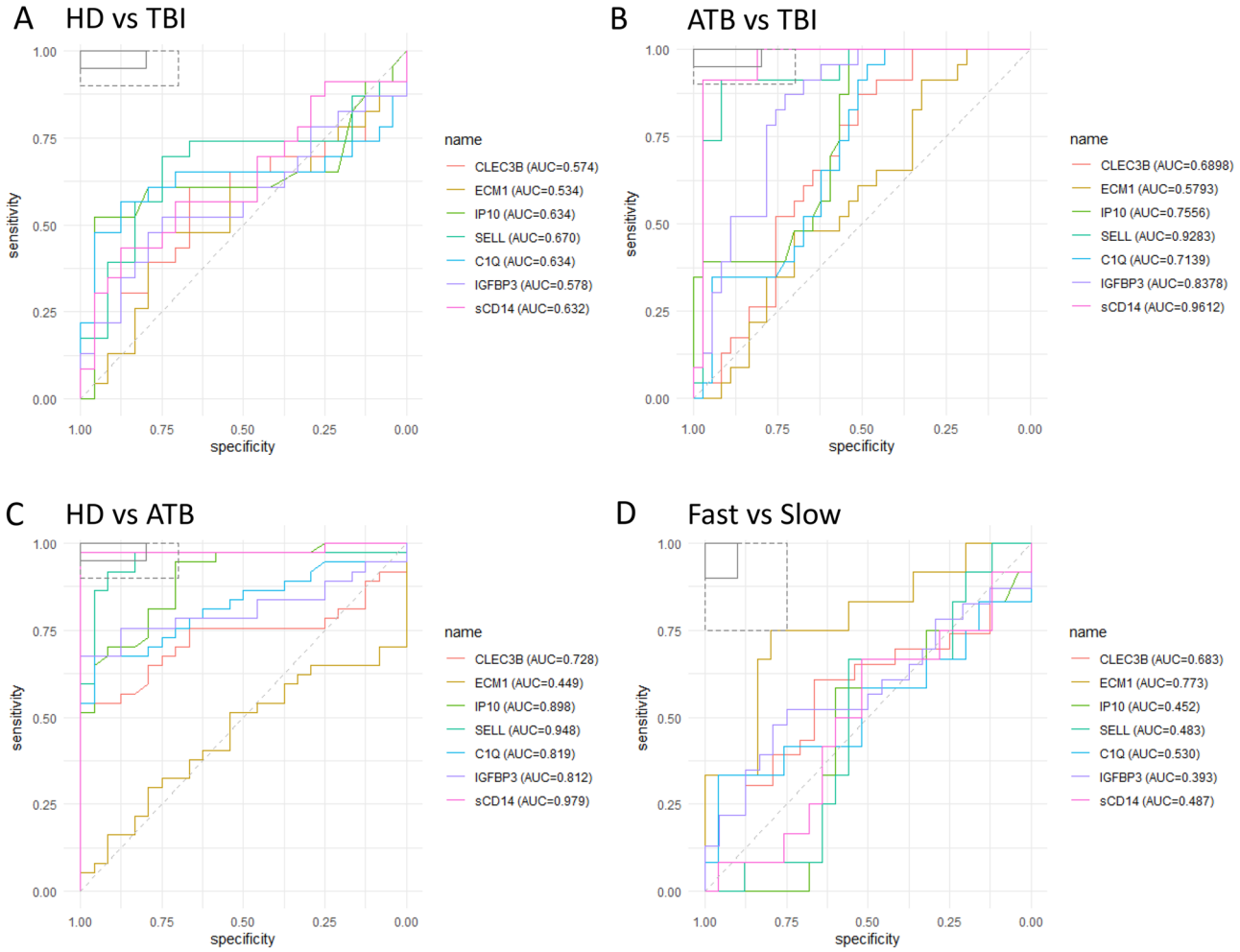

Figure 2. Receiver operating characteristic (ROC) curve analysis of biomarkers for triage and TB treatment. ROC curves for comparing the performance of different markers between healthy donors (HD) and TB infected (TBI) (**A**), active TB infection (ATB) vs. TBI (**B**), HD vs. ATB (**C**), and finally Fast and Slow treatment responders, are shown. In the top left box, the solid and dashed lines represent the respective optimal and minimum criteria set by the WHO in the target product profile (TPP) for a triage test for TB.

Regarding the host proteins detected with our xMAP panel, ECM1 has already been described as a potential TB treatment monitoring marker[34]. This marker, along with other proteins, can distinguish fast from slow responders in sample comparisons at baseline and 8 weeks after TB treatment, using the a complex multiplexed, aptamer-based proteomic technology, SOMAscan[34]. In our study, we demonstrate that the level of ECM1 changes significantly prior to TB treatment and the issue of the sputum culture conversion after 2 months of therapy. This host marker might be of interest to identify at baseline patients who would require close follow-up during the intensive phase of treatment. The use of this type of marker could also help refine therapeutic trials aimed at shortening treatment or evaluating shorter TB treatment regimens.

After combining different plasma proteins, we showed that the combination of ECM1, CLEC3B, IP10 and SELL generated the best AUC to discriminate (1) ATB from HD groups (95% sensitivity and 92% specificity), and (2) fast vs slow sputum culture converters at baseline (83%sensitivity and of 84% specificity). If the diagnostic/prognostic performance of this four host-plasma marker signature (ECM1-CLEC3B-IP10-SELL) are confirmed to meet the TPP recommendations for both purposes, this potential signature will present several assets : its detection can directly be measured from unstimulated plasma (as already described elsewhere[27,28,35]) or directly assessed for instance on a xMAP® luminex platform from which results interpretation is not biased by the analytes concentrations determination. On this latter point, it has been shown that normalized MFI ratios are generally a better choice than absolute concentration values for statistical analysis as it does not require background subtraction for differentialanalysis[36,37]. Host biomarkers detection from unstimulated plasma might be of interest for the diagnosis of paucibacillary forms of TB (i.e., childhood TB and/or extra-pulmonary TB).

The present study has limitations. The evaluation was only carried out on a limited sample size of patient cohorts that do not allow to powerfully assess the diagnostic value of these proteins as TB biomarkers. The efficacy of the treatment such as the success or the treatment failure cannot be evaluated in this study, as none of the patients had a treatment failure nor drug-resistance profile after the 6-months treatment period. These

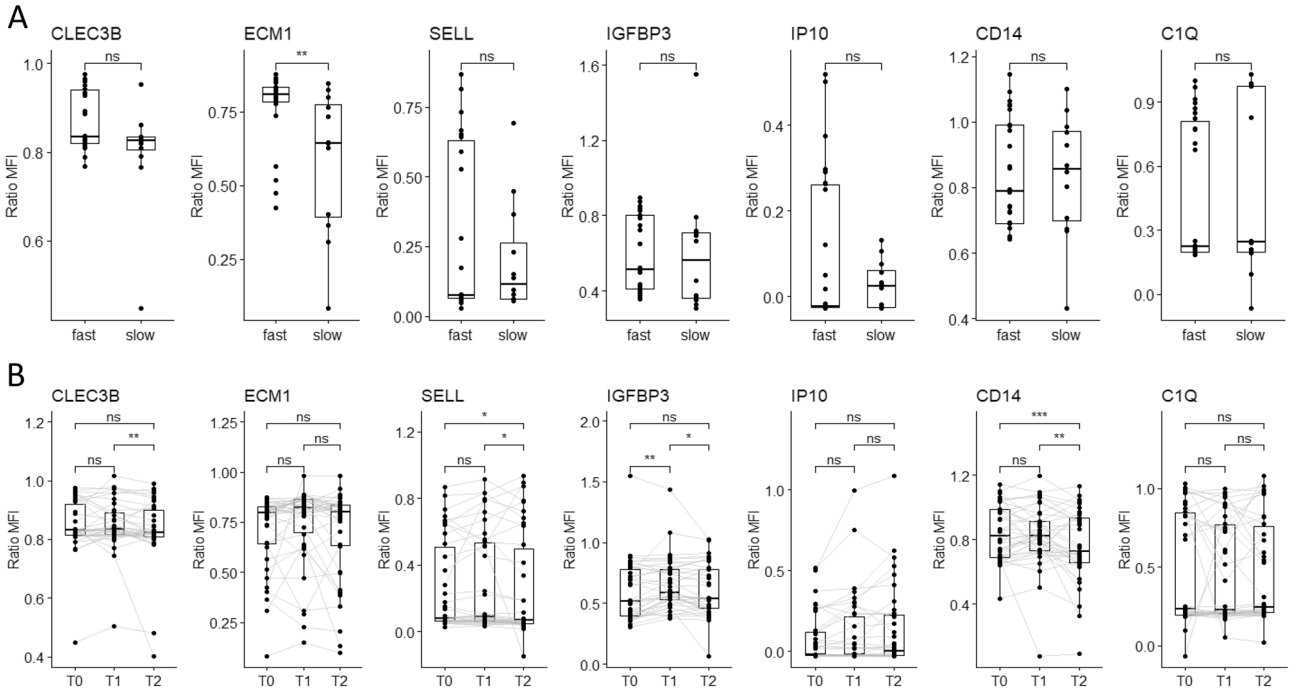

Figure 3. Plasma markers levels for treatment monitoring. (**A**) Comparison of markers expression in Fast vs Slow. (**B**) Dynamics of plasma markers over the course of TB therapy (n = 37 per timepoint). Data are given as median with interquartile range. Each black dot represents one patient, Grey lines connect data points from the same patient T0: baseline. T1: baseline + 2 months. T2: end of treatment. Data were compared using the Wilcoxon–paired test or Mann-Whithney U test with correction apply to adjust *p* values. $^{*}p < 0.05$; $^{**}p < 0.01$; $^{***}p < 0.001$.

Purpose	Groups	AUC	SE	SP	CutOff	ACC	TN	TP	FN	FP	NPV	PPV
Clinical group comparisons												
	ATB vs HD	0.958	0.946	0.917	0.412	0.934	22	35	2	2	0.917	0.946
	ATB vs TBI	0.929	0.892	0.913	0.536	0.9	21	33	4	2	0.84	0.943
	HD vs TBI	0.741	0.565	0.958	0.564	0.766	23	13	10	1	0.697	0.929
Treatment monitoring												
	Fast vs Slow converters	0.87	0.833	0.84	0.272	0.838	21	10	2	4	0.913	0.714

Table 2. Performance of CLEC3B-ECM1-IP10-SELL signature for comparison of clinical groups and TB treatment monitoring. *AUC* area under the ROC curve, *SE* sensitivity, *SP* specificity, *PPV* positive predictive value, *NPV* negative predictive value, *ACC* accuracy.

results need to be validated in larger scale studies using diverse endemic and genetically different populations to further appreciate the robustness of the biosignatures.

In conclusion, the present study identified four host-plasma proteins marker that can potentially be useful as biological markers for both TB diagnostic and treatment monitoring. The diagnostic and prognostic performances of these protein markers must be confirmed in larger clinical studies. Implementing such protein markers or biosignatures in limited resource countries and/or those countries with the highest TB incidences could help to improve the diagnosis and the global management of TB.

Materials and methods

Study design and population. All the participants were recruited in Antananarivo, Madagascar. Between January to April 2019, active TB patients (ATB) were enrolled from the individuals presenting TB symptoms addressed for TB diagnosis at the main anti-tuberculosis centre of Madagascar at the Centre Hospitalier Universitaire de Soins et Santé Publique in Analakely. Inclusion criteria for ATB are pulmonary TB diagnosed patients adult, ≥ 18 years old patients identified using both bacteriological and/or molecular tests, ie. scoring positive for pulmonary TB with Mtb detection either by sputum smear microscopy and/or by Xpert MTB/RIF Ultra and/or sputum culture on Lowenstein-Jensen (LJ) media.

Healthy volunteer donors (HD), recruited as a control group were clinically asymptomatic adults (≥ 18 years old) without any sign of TB and without known TB contact. For the study, QuantiFERON-TB Gold (QFT-P)

Markers	Full name	Function
CLEC3B	C-type lectin domain family 3 member B/Tetranectin	Transport/tissue remodelling[47]
ECM1	Extracellular Matrix Protein 1	Tissue development and remodelling[48]
sCD14	Monocyte differentiation antigen sCD14 soluble	Immune response[49]
SELL	Selectin L/CD26L	Cell migration and adhesion[50]
IGFBP3	Insulin-like growth factor-binding protein 3	Cell proliferation[51]
C1q	Complement component	Complement[52]
IP10	Interferon gamma-induced protein 10/CXCL10	Immune response[53]

Table 3. List of host markers evaluated in this study.

plus was performed on the healthy volunteers and those positive to QFT-P (ie. IFN-γ production ≥ 0.35 IU/mL in response to TB1 and TB2 stimulation) were classified in the TBI group. Pregnant women, HIV-positive individuals, people living with known diabetes mellitus comorbidity and patients under immunocompromising treatment were excluded from this study.

Mycobacteriological procedures. ATB diagnosis was based on both bacteriological and molecular tests. At least one sputum sample was collected at inclusion (T0) for Xpert MTB/RIF Ultra (Cepheid) or culture testing on solid culture Lowenstein–Jensen media and tested by smear microscopy for the presence of acid-fast bacilli (AFB) using the Ziehl–Neelsen staining method and/or Auramine O staining. Smear microscopy results were classified as negative smear, low-grade positive smear (1+ or scanty) and high-grade positive smear (2+ or 3+). Confirmed TB patients were re-evaluated by sputum smear and culture during the intensive phase of their treatment (T1) thereafter at the end of treatment (T2) and 2-months after treatment completion (T3) to confirm that they were successfully treated and cured. Drug susceptibility testing (DST) methods were performed according to standard protocols[38].

TB treatment and follow-up. Confirmed TB patients were put on Directly Observed Treatment Strategy and received a 6 months treatment with four antibiotics Rifampicin (R), Isoniazid (H), Ethambutol (E) and Pyrazinmide (Z) according to Madagascar standard protocols (2EHRZ/4RH)[39]. During their treatment, TB patients were followed up at inclusion (T0), after 2 months of treatment (T1), at the end of therapy (T2); 6 months for drug susceptible patients. Sputum culture conversion at T1 was used to define three patient subsets: fast converters (definitive culture conversion between T0 and T1), slow converters (definitive culture conversion between T1 and T2), and patients with poor treatment outcome (positive culture results at T2: treatment failure; or positive culture at T3: relapse) (Supplementary figure 1).

Blood collection process. A minimum of 6 mL of peripheral whole blood were collected from each participant: 1 mL was collected in EDTA tubes for whole blood cell counting with the Sysmex XT-2100i haematology cell counter according to manufacturer instructions, and 5 mL were drawn in Lithium heparin tubes for IGRA.

For QFT-P assay, 1 mL of whole blood was collected directly into each of the four QFT-P tubes (Qiagen, Hilden, Germany, 622526) provided by the QFT-P kit (Nil: Negative Control, TB-Antigens (TB1/TB2) and Mitogen: Positive control). After 16–24 h incubation at 37 °C, plasma samples were harvested and stored at − 80 °C prior to measures using QFT-P ELISA Kit (Qiagen, Hilden, Germany, 622120), according to the manufacturer instructions. Briefly, 50 µL of plasma samples were used and optical density (OD) results were compared to log-normalized values from a freshly reconstituted IFN-γ standard kit. To consider any potential immunomodulation phenomena unrelated with TB treatment, baseline IFN-γ level values (Nil tubes) were subtracted from antigen-stimulated IFN-γ values (TB1, TB2 and Mitogen). According to the kit's sensitivity range, the maximum for IFN-γ level values was set at 10 IU/mL and negative values were rescaled to zero.

Luminex xMAP® assay set-up. In the framework of this study a multiplex detection panel of CLEC3B, SELL, IGFBP3, IP10, CD14, ECM1 and C1Q in plasma has been set-up using the Luminex xMAP® technology (Table 3). Coupling of antibodies to beads was performed according to the manufacturer's instruction43. All antibodies, recombinant proteins and bead regions used in this study are listed in supplementary table 1. After coupling confirmation, reaction parameters including the capture antibody concentration, the detection of antibody concentration, and the number of washing steps were tested to optimize the assay protocol. The optimal assay protocol generated a mixture of each antibody-coupled microsphere that was diluted in an assay buffer to 50 beads of each region per µL. 50 µL of bead suspensions and 50 µL of assay buffer were pipetted into each well. Standard curves were obtained using a tenfold dilution in an assay buffer of recombinant proteins (10000 ng/mL to 0.01 ng/mL) that were also used as positive controls. Each 96 well plate received 50 µL of standard, plasma or assay buffer only (blanks), bringing the final volume to 150 µL per well. Plates were incubated for 30 min on a plate shaker, then washed with an assay buffer. A mixture of biotinylated detection antibodies (4 µg/mL) was added to each well and incubated for 30 min. The beads were washed and incubated with PE-labelled streptavidin SAPE (diluted to 4 µg/mL in assay buffer) for 30 min. The beads were washed and then resuspended in a 100 µL assay buffer before analysis on the MAGPIX Luminex platform. All incubations were performed in the

dark, at room temperature on a shaker. To normalize the data and eliminate interpolation bias, median fluorescence intensity (MFI) ratios were evaluated as follow:

$$Normalized\ MFI\ ratio = \frac{MFI\ x - MFI\ min}{MFI\ max - MFI\ min}$$

The MFI min and max correspond to the MFI values of the protein given at the concentration 0.01 ng/mL (min) and 1000 ng/mL (max). X represents the sample.

Statistical analysis. At enrolment and at each follow-up visit for the TB patients, medical history, pseudonymized clinical and demographic data were collected using standardized questionnaires and stored in a secured cloud-based database system (CASTOR Electronic Data Capture, Version 1.4, Netherlands)[40].

Data analyses were performed using R software version 4.0.3[41]. Due to the studied sample size, discrete variables were analysed using Fisher's Exact test with Bonferroni's post-hoc correction test[42]. Normality was assessed using the Shapiro–Wilk Normality test. Normal, continuous variables were analyzed with Student's t-test. Non-normal, continuous variables were analyzed with the Mann–Whitney test or the Kruskal–Wallis rank-sum test with Dunn's Kruskal–Wallis Multiple Comparisons post-hoc test[43]. Repeated measures of non-independent continuous variables were analyzed using the Friedman rank-sum test, with Wilcoxon-Nemenyi-McDonald-Thompson's post-hoc test[44]. For both ROC analyses and logistic regression, model performance metrics (respectively, AUC and the C-statistic) were corrected for optimism using bootstrap to assess model validity as described elsewhere[45]. Combinatorial analysis of multiple biomarkers to define the best marker combinations of the tested plasma markers was done using the CombiROC package[46]. The combinations with the highest AUC, sensitivity and specificity values were considered for selection of efficient immune biomarker signatures. Computation and selection of optimal biomarker combinations by integrative ROC.

Ethics statement. The study protocol was reviewed and approved by the Ministry of Public Health and the Ethical Committee for Biomedical Research of Madagascar (Reference number: n°099–MSANP/CERBM). All study participants provided written informed consent. All research was performed in accordance with relevant guidelines and regulations.

Data availability

All raw data will be shared upon request to the corresponding author.

Received: 29 July 2022; Accepted: 28 November 2022
Published online: 30 November 2022

References

1. World Health Organization. *Global Tuberculosis Report 2021* (World Health Organization, 2021).
2. Goletti, D. *et al.* Can we predict tuberculosis cure? What tools are available?. *Eur. Respir. J.* **52**, 1801089 (2018).
3. Mirzayev, F. *et al.* World Health Organization recommendations on the treatment of drug-resistant tuberculosis, 2020 update. *Eur. Respir. J.* **57**, 2003300 (2021).
4. World Health Organisation. Foundation for Innovative New Diagnostics. Pipeline Report 2021 Tuberculosis Diagnostics. (2021).
5. Bayaa, R. *et al.* Multi-country evaluation of RISK6, a 6-gene blood transcriptomic signature, for tuberculosis diagnosis and treatment monitoring. *Sci. Rep.* **11**, 13646 (2021).
6. Bark, C. M. *et al.* Identification of host proteins predictive of early stage *Mycobacterium tuberculosis* infection. *EBioMedicine* **21**, 150–157 (2017).
7. Suliman, S. *et al.* Four-gene pan-African blood signature predicts progression to tuberculosis. *Am. J. Respir. Crit. Care Med.* **197**, 1198–1208 (2018).
8. Achkar, J. M. *et al.* Host protein biomarkers identify active tuberculosis in HIV uninfected and co-infected individuals. *EBioMedicine* **2**, 1160–1168 (2015).
9. Mpande, C. A. M. *et al.* Immune profiling of *Mycobacterium tuberculosis*-specific T cells in recent and remote infection. *EBioMedicine* **64**, 103233 (2021).
10. Chedid, C. *et al.* In-depth immunophenotyping with mass cytometry during TB treatment reveals new T-cell subsets associated with culture conversion. *Front. Immunol.* **13**, 853572 (2022).
11. Srivastava, S. *et al.* Aptamers: An emerging tool for diagnosis and therapeutics in tuberculosis. *Front. Cell. Infect. Microbiol.* **11**, 656421 (2021).
12. Lu, P. *et al.* Extracellular matrix degradation and remodeling in development and disease. *Cold Spring Harb. Perspect. Biol.* **3**, a005058 (2011).
13. Chan, I. The role of extracellular matrix protein 1 in human skin. *Clin. Exp. Dermatol.* **29**, 52–56 (2004).
14. Li, Z. *et al.* ECM1 controls TH2 cell egress from lymph nodes through re-expression of S1P1. *Nat. Immunol.* **12**, 178–185 (2011).
15. Zhang, Y. *et al.* ECM1 is an essential factor for the determination of M1 macrophage polarization in IBD in response to LPS stimulation. *Proc. Natl. Acad. Sci. USA* **117**, 3083–3092 (2020).
16. Wedepohl, S. *et al.* l-Selectin—A dynamic regulator of leukocyte migration. *Eur. J. Cell Biol.* **91**, 257–264 (2012).
17. Ivetic, A., Hoskins Green, H. L. & Hart, S. J. L-selectin: A major regulator of leukocyte adhesion, migration and signaling. *Front. Immunol.* **10**, 1068 (2019).
18. Singer, S. N. *et al.* Plasma host protein biomarkers correlating with increasing *Mycobacterium tuberculosis* infection activity prior to tuberculosis diagnosis in people living with HIV. *BioMedicine* **75**, e103787 (2022).
19. Liu, Y. *et al.* Soluble CD14 as a diagnostic biomarker for smear-negative HIV-associated tuberculosis. *Pathogens* **7**, 26 (2018).
20. Druszczynska, M. *et al.* Two-year follow-up study of *Mycobacterium tuberculosis* antigen-driven IFN-γ responses and macrophage sCD14 levels after tuberculosis contact. *Indian J. Microbiol.* **56**, 205–213 (2016).
21. Wang, P.-H. *et al.* The dynamic change of immune checkpoints and CD14+ monocytes in latent tuberculosis infection. *Biomedicines* **9**, 1479 (2021).
22. Chen, J. *et al.* Serum sCD14, PGLYRP2 and FGA as potential biomarkers for multidrug-resistant tuberculosis based on data-independent acquisition and targeted proteomics. *J. Cell. Mol. Med.* **24**, 12537–12549 (2020).

23. Cai, Y. *et al.* Increased complement C1q level marks active disease in human tuberculosis. *PLoS ONE* **9**, e92340 (2014).
24. Dijkman, K. *et al.* Systemic and pulmonary C1q as biomarker of progressive disease in experimental non-human primate tuberculosis. *Sci. Rep.* **10**, 6290 (2020).
25. Lubbers, R. *et al.* Complement component C1q as serum biomarker to detect active tuberculosis. *Front. Immunol.* **9**, 2427 (2018).
26. Stefanescu, S. *et al.* Prediction of treatment outcome with inflammatory biomarkers after 2 months of therapy in pulmonary tuberculosis patients: Preliminary results. *Pathogens* **10**, 789 (2021).
27. Kumar, N. P. *et al.* Plasma chemokines as immune biomarkers for diagnosis of pediatric tuberculosis. *BMC Infect. Dis.* **21**, 1055 (2021).
28. Togun, T. *et al.* A three-marker protein biosignature distinguishes tuberculosis from other respiratory diseases in Gambian children. *EBioMedicine* **58**, 102909 (2020).
29. Strzelak, A. *et al.* Diagnostic value of IP-10 level in plasma and bronchoalveolar lavage fluid in children with tuberculosis and other lung diseases. *Diagnostics (Basel)* **12**, 840 (2022).
30. Chendi, B. H. *et al.* A plasma 5-marker host biosignature identifies tuberculosis in high and low endemic countries. *Front. Immunol.* **12**, 608846 (2021).
31. Chegou, N. N. *et al.* Diagnostic performance of a seven-marker serum protein biosignature for the diagnosis of active TB disease in African primary healthcare clinic attendees with signs and symptoms suggestive of TB. *Thorax* **71**, 785–794 (2016).
32. Chegou, N. N. *et al.* Africa-wide evaluation of host biomarkers in QuantiFERON supernatants for the diagnosis of pulmonary tuberculosis. *Sci. Rep.* **8**, 2675 (2018).
33. Jacobs, R. *et al.* Diagnostic potential of novel salivary host biomarkers as candidates for the immunological diagnosis of tuberculosis disease and monitoring of tuberculosis treatment response. *PLoS ONE* **11**, e0160546 (2016).
34. Nahid, P. *et al.* Aptamer-based proteomic signature of intensive phase treatment response in pulmonary tuberculosis. *Tuberculosis (Edinb)* **94**, 187–196 (2014).
35. Kumar, N. P. *et al.* Plasma chemokines are baseline predictors of unfavorable treatment outcomes in pulmonary tuberculosis. *Clin. Infect. Dis.* **73**, e3419–e3427 (2021).
36. Breen, E. J., Polaskova, V. & Khan, A. Bead-based multiplex immuno-assays for cytokines, chemokines, growth factors and other analytes: Median fluorescence intensities versus their derived absolute concentration values for statistical analysis. *Cytokine* **71**, 188–198 (2015).
37. Breen, E. J., Tan, W. & Khan, A. The statistical value of raw fluorescence signal in Luminex xMAP based multiplex immunoassays. *Sci. Rep.* **6**, 26996 (2016).
38. World Health Organization. *WHO Consolidated Guidelines on Tuberculosis: Module 4: Treatment: Drug-Susceptible Tuberculosis Treatment* (World Health Organization, 2022).
39. World Health Organization. *Guidelines for Treatment of Drug-Susceptible Tuberculosis and Patient Care* (World Health Organization, 2017).
40. Castor - Top-Rated eClinical Data Management Platform. *Castor.* https://www.castoredc.com/.
41. R Core Team. *The Comprehensive R Archive Network*. https://cran.r-project.org/ (2020).
42. Kim, T. K. Understanding one-way ANOVA using conceptual figures. *Korean J. Anesthesiol.* **70**, 22–26 (2017).
43. Dunn, O. J. Multiple comparisons using rank sums. *Technometrics* **6**, 241–252 (1964).
44. Pedro, H. D. S. P. *et al.* Clinical and epidemiological profiles of individuals with drug-resistant tuberculosis. *Mem. Inst. Oswaldo Cruz* **110**, 235–248 (2015).
45. Smith, G. C. S., Seaman, S. R., Wood, A. M., Royston, P. & White, I. R. Correcting for optimistic prediction in small data sets. *Am. J. Epidemiol.* **180**, 318–324 (2014).
46. Mazzara, S. *et al.* CombiROC: An interactive web tool for selecting accurate marker combinations of omics data. *Sci. Rep.* **7**, 45477 (2017).
47. UniProt. https://www.uniprot.org/uniprotkb/P05452/entry.
48. UniProt. https://www.uniprot.org/uniprotkb/Q16610/entry.
49. UniProt. https://www.uniprot.org/uniprotkb/P08571/entry.
50. UniProt. https://www.uniprot.org/uniprotkb/P14151/entry.
51. UniProt. https://www.uniprot.org/uniprotkb/P17936/entry.
52. UniProt. https://www.uniprot.org/uniprotkb/P02745/entry.
53. UniProt. https://www.uniprot.org/uniprotkb/P02778/entry.

Acknowledgements

We would like to thank all the patients and volunteers who agreed to participate in the study. MDBN benefited of a Scholarship from the Fondation Mérieux.

Author contributions

M.D.B.N., J.H. and N.R. wrote the original draft. M.D.B.N. and J.H. developed the assay and validated the multiplex test. J.H. and N.R. supervised the study. M.D.B.N. and J.H. did statistical analysis. M.D.B.N., P.R., T.R., V.R., M.S., J.H., R.R., P.H., J.R. and N.R. reviewed the paper. All authors approved the final manuscript.

Funding

This work was supported by Fondation Mérieux.

Competing interests

The authors declare no competing interests.

Additional information

Supplementary Information The online version contains supplementary material available at https://doi.org/10.1038/s41598-022-25236-9.

Correspondence and requests for materials should be addressed to M.D.B.N. or N.R.

3. Study 3: Using a Multiplex Serological Assay to Estimate Time Since SARS-CoV-2 Infection and Past Clinical Presentation in Malagasy Patients

Summary

In the context of 2019 coronavirus (COVID-19) pandemic caused by severe acute respiratory syndrome coronavirus 2 (SARS-CoV-2), efficient serological assays are needed to accurately describe the humoral responses against the virus. We developed and validated a Luminex xMAP® technology based multiplex serological assay targeting specific IgM and IgG antibodies against the SARS-CoV-2 Spike subunit 1 (S1), Spike subunit 2 (S2), Spike Receptor Binding Domain (RBD) and the Nucleocapsid Protein (NP). Blood samples collected periodically for 12 months from 43 patients diagnosed with COVID-19 in Madagascar were tested for these antibodies. A random forest algorithm was used to build a predictive model of time since infection and symptom presentation. The performance of the multiplex serological assay was evaluated for the detection of SARS-CoV-2 anti-IgG and anti-IgM antibodies. Both sensitivity and specificity were equal to 100% (89.85-100) for S1, RBD and NP (S2 had a lower specificity = 95%) for IgG at day 14 after enrolment. This multiplex assay compared with two commercialized ELISA kits, showed a higher sensitivity. Principal Component Analysis was performed on serologic data to group patients according to time of sample collection and clinical presentations. The random forest algorithm built by this approach predicted symptom presentation and time since infection with an accuracy of 87.1% (95% CI = 70.17-96.37, p-value = 0.0016), and 80% (95% CI = 61.43-92.29, p-value = 0.0001) respectively. This study demonstrates that the statistical model predicts time since infection and previous symptom presentation using IgM and IgG response to SARS-CoV2. This tool may be useful for global surveillance, discriminating recent- and past- SARS-CoV-2 infection, and assessing disease severity.

Using a multiplex serological assay to estimate time since SARS-CoV-2 infection and past clinical presentation in Malagasy patients

Authors: Mame Diarra Bousso NDIAYE[1], Lova Tsikiniaina RASOLOHARIMANANA[1], Solohery Lalaina RAZAFIMAHATRATRA[1], Rila RATOVOSON[1], Voahangy RASOLOFO[1], Paulo RANAIVOMANANA[1], Laurent RASKINE[2], Jonathan HOFFMANN[2], Rindra RANDREMANANA[1], Niaina RAKOTOSAMIMANANA[1], Matthieu SCHOENHALS[1*]

Affiliations:

[1]Institut Pasteur de Madagascar, Antananarivo, Madagascar

[2]Medical and Scientific Department, Fondation Mérieux, Lyon, France

*Corresponding author:

schoenhals@pasteur.mg

Immunology of infectious diseases Unit, Institut Pasteur de Madagascar, BP 1274, Antananarivo, Madagascar

Keywords:

SARS-CoV-2 antibodies; COVID-19 seroprevalence; prediction model; Madagascar; symptom presentation; time since infection

Abstract

Background: The world is facing a 2019 coronavirus (COVID-19) pandemic caused by severe acute respiratory syndrome coronavirus 2 (SARS-CoV-2). In this context, efficient serological assays are needed to accurately describe the humoral responses against the virus. These tools could potentially provide temporal and clinical characteristics and are thus paramount in developing-countries lacking sufficient ongoing COVID-19 epidemic descriptions.

Methods: We developed and validated a Luminex xMAP® multiplex serological assay targeting specific IgM and IgG antibodies against the SARS-CoV-2 Spike subunit 1 (S1), Spike subunit 2 (S2), Spike Receptor Binding Domain (RBD) and the Nucleocapsid Protein (NP). Blood samples collected periodically for 12 months from 43 patients diagnosed with COVID-19 in Madagascar were tested for these antibodies. A random forest algorithm was used to build a predictive model of time since infection and symptom presentation.

Findings: The performance of the multiplex serological assay was evaluated for the detection of SARS-CoV-2 anti-IgG and anti-IgM antibodies. Both sensitivity and specificity were equal to 100% (89.85-100) for S1, RBD and NP (S2 had a lower specificity = 95%) for IgG at day 14 after enrolment. This multiplex assay compared with two commercialized ELISA kits, showed a higher sensitivity. Principal Component Analysis was performed on serologic data to group patients according to time of sample collection and clinical presentations. The random forest algorithm built by this approach predicted symptom presentation and time since infection with an accuracy of 87.1% (95% CI = 70.17-96.37, p-value = 0.0016), and 80% (95% CI = 61.43-92.29, p-value = 0.0001) respectively.

Interpretation: This study demonstrates that the statistical model predicts time since infection and previous symptom presentation using IgM and IgG response to SARS-CoV2. This tool may be useful for global surveillance, discriminating recent- and past- SARS-CoV-2 infection, and assessing disease severity.

Fundings: This study was funded by the French Ministry for Europe and Foreign Affairs through the REPAIR COVID-19-Africa project coordinated by the Pasteur International Network association. WANTAI reagents were provided by WHO AFRO as part of a Sero-epidemiological "Unity" Study Grant/Award Number: 2020/1019828-0 P.O 202546047 and Initiative 5% grant n°AP-5PC–2018–03-RO.

Introduction

Coronavirus disease 2019 (COVID-19) is caused by severe acute respiratory syndrome coronavirus 2 (SARS-CoV-2)1. As of the 8 April 2022 the WHO has reported 494 million confirmed cases and more than 6 million deaths worldwide from this disease2. Most people infected with SARS-CoV-2 have mild to moderate respiratory illness and recover without the need for specific treatment3. However, the elderly and those with underlying medical conditions such as cardiovascular disease, diabetes, chronic respiratory disease and cancer are more likely to develop severe presentations.

PCR-based tests are widely used to diagnose active infection to SARS-CoV-2 4–7. The two most common target genes are open reading frame 1ab (ORF1ab) and nucleocapsid protein (NP). The SARS-CoV-2 genome encodes 20 proteins including 16 non-structural and 4 structural proteins. The infected patient's immune system will produce antibodies against all of these viral proteins in the serum. Most SARS-CoV-2 developed serological tests target antibodies against spike glycoprotein (S), or nucleocapsid protein (NP) antigen because of the high antigenicity of those proteins. The S protein consists of two subunits: S1 and S28,9. S1 allows the binding and entry into target cells. Through its receptor binding domain (RBD), S1 interacts with the human angiotensin-converting enzyme 2 (ACE2) receptor. The RBD of the S1 subunit is the primary target of neutralizing antibodies10. NP plays the main role in the genomic replication, transcription and packaging of the virus11. It has been shown that Anti-NP antibodies are more sensitive for the SARS-CoV-2 detection than the antibodies developed against Spike proteins for the detection of an early infection that are however more specific12.

Antibodies to SARS-CoV-2 are produced a few days to weeks after viral infection13. The presence of antibodies indicates that a person has been infected with the COVID-19 virus, whether the individual has severe or mild disease, or even asymptomatic infection.

Quantification of antibody levels can be very informative. It is an important indicator associated with the duration of the disease, time since infection, severity of symptoms. Moreover, in the case of COVID-19 infection, patients with mild or moderate disease may also experience prolonged symptoms presentation, known as Long COVID14.

IgM antibodies are produced during the early stages of infection, whereas IgG antibodies, which have a higher target protein affinity, are markers of the immune response developed later after infection but persist over time and provide longer protection against the antigen. In the humoral response against SARS-CoV-2, IgG or IgM appears to increase within 20 days of symptom onset15–17.

Serological tests are commonly used to detect a virus circulation in the population and provide an indication about the proportion of this population that may be immunized against the virus. Since the beginning of the pandemic, more than 200 serological tests dedicated to detect SARS-CoV-2 have been developed 18.

A better characterization of the humoral response to SARS-CoV-2 infection would be of great value in estimating the time of infection, or retrospectively the patient's clinical presentation. Studies have shown that by measuring antibodies in serum samples from infected patients, it is possible to estimate the time since infection and to assess the serologic reconstruction of past SARS-CoV-2 transmission19.

Serological diagnostic tests generally classify a sample as positive if the measured antibody level is above a defined threshold. In this study, we developed and validated a multiplex serological tool based on the Luminex xMAP® technology, evaluated its performance against 4 antigens (S1, S2, RBD and NP) for the detection of SARS-CoV-2 specific IgM and IgG antibodies in a cohort of COVID-19 confirmed patients. Indeed, the serological responses are context specific and may be influenced by the circulation of multiple coronaviruses strains, genetic background and endemic pathogen circulation20,21. The serological data collected were then used to estimate the time since infection and to retrospectively describe symptomatic presentations.

Materials and methods

Development of a Luminex xMAP® multiplex assay

- **Bead coupling**

The first step in the development of the assay was the coupling of the beads with the SARS-CoV-2 S1, S2, RBD and NP antigens. Coupling of the proteins onto the microspheres was performed according to the manufacturer's instructions[22]. The carboxylated magnetic beads (MagPlex™) and the coupling kit (Luminex, 40-50016) were supplied by Luminex Corporation (Austin, TX, USA). The recombinant proteins used are listed in the supplementary table 1. Briefly, 5.10^6 microspheres were transferred to low-binding tubes, positioned into Dynamag-spin magnet (Invitrogen, 12320D), and resuspended in 500µl activation buffer (0.1 mol/L sodium phosphate, pH 6.2). Then, 10 µL of Sulfo-NHS (50 g/L) and 10µl EDC (50 g/L) were added and the suspension was incubated for 20 min in the dark at room temperature (RT). The activated microspheres were washed twice in the activation buffer. 5µg of recombinant protein for 10^6 beads (diluted in activation buffer to a total of 500 mL), were added and the mixture was spun down for 2 h in the dark. After incubation, the microspheres were three times washed in wash buffer. Finally, the beads were resuspended in 1ml of wash buffer and stored at 4°C in the dark. The coupled beads were counted with Malassez cells to adjust the concentration. The following bead regions were used: MC10012-01 (Spike S1), MC10013-01 (Spike S2), MC10014-01 (Spike RBD), MC10015-01 (Nucleocapsid).

For confirmation of coupling, a dilution range (0.625 - 4µg/mL) of goat anti-human IgG Fc labelled with phycoerythrin detection antibody (Thermo Fisher Scientific, H10104) was tested with the antigen-coupled beads. The median fluorescence intensity (MFI) was detected by a standard PMT.

- **Validation of the 4 Plex assay**

The coupling was confirmed using a dilution of the detection antibodies (Supplementary figure 1A). MFI levels related to the antibodies concentration of 2µg/mL was defined as the saturation concentration and was used for the downstream experiments.

The detection limit for antibodies quantification was then assessed. The linearity zone indicating the detection range was found between 0.1 ng/mL and 1000 ng/mL for all four antibodies tested (Supplementary figure 1B). The repeatability and the reproducibility of the assay were evaluated with the intra-assay variation (intra-assay CV) and the inter-assay variation (inter-assay CV) respectively (Table 1).

Cross-reactivity of the multiplexed assay was evaluated by testing mixed sets of coupled beads, individual specific antibodies and individual detection antibodies (IgG or IgM) to determine any cross-reacting antigens with the non-targeted beads.

The lower limit of detection (LOD) of the test was defined as the mean blank MFI + 3 Standard deviation (SD). Lower limit of quantification (LLOQ) estimation was based on repeated sample measurements (n=6) with 0.01, 0.1, or 1 ng/mL of antibody, whereas upper limit of quantification (ULOQ) was based on repeated sample measurements (n=6) with 100, 1000, or 10000 ng/mL. Inter-assay and intra-assay variations was assessed by analyzing multiple replicates (intra-assay n=12, inter-assay n=6) of a control sample with a known concentration for each protein.

Multiplex Luminex assay

After verifying that the coefficient of variation (CV) for the number of beads counted in each region is less than 15%, all beads were mixed. The volume of mix to be dispensed was set to have 1000 beads/region/well. Each well received 100µl of positive control, plasma (diluted to 1:100) and assay buffer only (blanks). Round-bottom polystyrene 96-well microplates (Costar, CORNING_ 3915) were used. The plate was incubated for 30 min on a plate shaker, then placed 60s on a plate magnet to pull down magnetic microspheres and washed with assay buffer. This washing step was repeated twice. Detection antibodies (4 µg/ml) were added to each well and incubated for 30 min (100µl/well). Microspheres were then washed twice and resuspended in 120µL of assay buffer before analysis on the MagPix™ instrument supplied by Luminex Corporation (Austin, TX, USA). All incubations were performed in the dark, at room temperature, on a plate shaker (900 rpm).

The fluorescence background was determined by the mean of MFI + 3 SD. The MFI shown in the figures is the median fluorescence minus the fluorescence background. Cut-off limits for the determination of positive antibodies in the SARS-CoV-2 infected individuals were determined by receiver operating characteristics (ROC) analysis.

Comparison with the ELISA kits

The performance of the Luminex test was compared to two commercial ELISA kits: ID Screen® SARS-CoV-2-N IgG Indirect ELISA (SARSCoV2S-8P, ID.Vet, Grabels, France) which detects antibodies (IgG) directed against the nucleocapsid (N) of the SARS -CoV-2 in human serum or plasma, and the WANTAI SARS-CoV-2 Ab ELISA (WS-1096, Beijing Wantai Biological Pharmacy Enterprise Co., Ltd.) which determines IgA, IgG, IgM antibodies to the SARS-CoV-2 Spike RBD antigen.

Study population and sample collection

The FFX (first few cases) cohort from the Institut Pasteur of Madagascar was described in a previously study[23]. Among the FFX cohort, 43 Malagasy patients with positive SARS-CoV-2 PCR tests were included in the present study. These patients were enrolled from 3 different Hospitals of Antananarivo Madagascar: They were followed at 7-day intervals, at least until day 21, or longer until their PCR was negative. Patients were followed-up at home for one year (at months 1, 3, 6, and 12 of their SARS-CoV-2 test diagnosis). Of the 43, only 13 completed the 12-month visits. All participants were screened for comorbidities. Informed consent forms were obtained from all patients prior to enrolment in the study, in accordance with the FFX core protocol. All patients' characteristics are summarized in Table 1. This study protocol obtained ethical approval from the Biomedical Research Ethics

Committee of Madagascar (n°. 058/MSANP/SG/AGMED/CERBM, March 30, 2020 and amendment n°109/MSANP/SG/AGMED/CERBM, June 24, 2020). As negative control, 40 pre-epidemic sera collected in 2015 from Malagasy individuals were tested.

Participants had peripheral blood samples collected during follow-up at each timepoint. Blood was collected in two 5mL heparin tubes. Serum was separated from the red fraction of blood (red and white blood cells) and stored at -80°C.

Statistical analysis

Luminex data were analysed using the Prism version 9 software (GraphPad, La Jolla, CA). The Mann Whitney test was used to compare differences in MFI between symptomatic and non-symptomatic participants and to compare positive and negative samples for anti-SARS-CoV-2 antibodies. ROC curves were generated to determine the detection thresholds, sensitivity and specificity values. We compared PCA scores by performing Wilcoxon signed rank exact test and Mann-Whitney tests.

We performed a Random Forest analysis and a PCA analysis for prediction and estimation of time to infection and symptom presentation. The random forest analysis was performed using a validation set approach, which involves randomly dividing the data into two sets: one set is used to train the model and the other set is used to test the model. In our case, 80% of the data set was used for training a linear regression model and 20% was used to evaluate the performance of the model. This set of analyses was performed on R using the packages random Forest version 4.6-14 and FactoMineR version 2.4 and ggplot for PCA. The R-Scripts used for this study are available in the Statistical tools for high-throughput data analysis (STHDA) website[24].

Results

Performance of the Luminex xMAP® assay for the serological detection of SARS-CoV-2

We investigated the levels of anti-IgM and anti-IgG targeting S1, S2, RBD and NP between the pre-epidemic negative control (n=40) and positive patients at different timepoints after a positive PCR test (n=62) from the FFX cohort described in the methods section, based on the MFI generated by the Luminex test (Table 1). For each combined target, MFI levels in positive patients were significantly higher than in negative controls (Figure 1A and 1B). Moreover, we observed that the MFI intensity was 4-fold higher for IgGs (median MFI=10771) than for IgMs (median MFI=1280).

Two pre-epidemic negative samples strongly expressed anti-S2 IgGs (MFI >10,000). To ensure that this was a coronavirus non-specific signal, we tested these samples for anti-S2 IgGs from seasonal human coronaviruses OC43, NL63, 229E and HKU1 and found positivity for anti-S2 IgGs from OC43 and HKU1 in one sample and positivity for anti-S2 IgGs from NL63 in the other sample, suggesting cross reactivity between the SARS-CoV-2 S2 antigen subunit and antibodies developed against seasonal human coronaviruses Spike proteins (Supplementary Figure 2).

Sensitivity (se), specificity (sp), and threshold values were obtained using ROC curves. For IgM, specificity reached 95% for all of the antigens. The S1 had better performance for IgM (AUC= 0.96; $p<0.0001$). In contrast, NP had the lowest diagnostic score among the four antibodies (AUC=0.81; $p<0.0001$) (Table 3 and Figure 1B). For IgG antibody detection, all targets had sensitivity and specificity values > 95%, unlike IgM antibodies (Table 3 and Figure 1B). The threshold of protein detection was set with the highest possible specificity value.

Two hundred and fifty eight samples from 43 patients collected between day 1 and day 180 were tested with two commercially available kits. 16.27% of samples were negative for SARS-CoV-2 antibodies (n=42) with the Wantai kit and 30.23% with the ID.Vet kit (n=78). Sera from these negative patients were then tested for SARS-CoV-2 IgM and IgG antibodies using the Luminex xMAP® assay. Of the negative sera tested with the ID.Vet kit, 39.74% (31/78) were positive for IgG NP antibodies. For the negative Wantai, 54.76% (23/42) were positive for anti-RBD IgM and IgG antibodies (Supplementary Figure 3). The developed Luminex xMAP® assay is able to detect more seropositivity compared to the ELISAs assay regarding the sensitivity of the multiplex test.

COVID-19 symptomatic individuals produce more RBD-specific IgM

We investigated the difference in antibodies levels between symptomatic (n=35) and asymptomatic COVID-19 patients (n=8). No differences were found when anti-S1, S2, RBD, and NP IgG were studied and only the MFI values associated with anti-RBD IgM were significantly higher in symptomatic patients compared to asymptomatic ones (*p-value* 0.0333) (Figure 2). This trend was confirmed using commercial IDVET (anti-NP IgG) and Wantai (anti-RBD IgM and IgG) kits but no significant difference was observed.

IgM and IgG responses to SARS-CoV-2 show distinct patterns over time

To assess IgM and IgG antibody seroconversion, survival curves for the four antigens were plotted. More than 60% of patients had IgG positive antibodies specific for S1, RBD, and NP in the first 20 days before decreasing at 3 months (Figure 3). For IgG, antibodies decreased by day 180, but the majority of patients remained positive at 1-year post-infection (day 365) (Figure 3). For anti-S2 IgM, 79% (34/43) of patients had subthreshold MFI values

at 6 months. At 1-year post-infection, seroconversion rates were 100%, 76%, 72%, and 71% for anti-S1, S2, RBD, and NP IgM respectively.

For IgG antibody detection, we observed the same antibody seroconversion kinetics for all four antigens. 1/43 patients showed late IgG antibody conversion at day 21 and 2/43 showed seroconversion 3 months after the day of symptom onset (Figure 3). After the first year of infection, the seroconversion rate was 95%, 100%, 100%, and 95% for anti-S1, S2, RBD, and NP IgG, respectively.

Seroconversion curves showed that by day 1, more than 50% of all patients had seroconverted and showed anti-S1 IgG or IgM seropositivity. These patients reached more than 80% seroconversion at 6 months of follow-up (Figure 4 and Supplementary Table 2). The IgM antibody seroconversion rate at day 1 was 41.86%, 50%, and 30.23% for anti-S2, anti-RBD, and anti-NP antibodies, respectively. At 6 months, these rates increased but did not exceed 55% for anti-NP IgM (Supplementary Table 2).

At day 7, over 90% of the cohort is positive for anti-S1 IgM. After 90 days of the infection, less than 40% of patients are positive for anti-RBD. For S2 and RBD, from day 1 to day 180, the positivity range is between 60% and 30%, before decreasing at 23% and 8% for anti-S2 and anti-RBD respectively. For anti-NP IgM, the positivity range is between 40% and 20% during the 6 first months of infection and reached 40% at 12 months (Figure 5).

For IgG detection, antibody positivity against all targets was greater than 60% on day 1 and increased during follow-up to more 80%, with the exception of anti-NP, which decreased to 60% at 12 months (Figure 5).

Time since infection and clinical presentation impact on serology results

The observed distinct antibody-dependent kinetics enabled us to investigate the possibility of estimating time since infection and, potentially, prior clinical presentation.

A principal component analysis (PCA) was performed using the combination of all variables (IgM and IgG). The PCA profiles were mostly separated when divided by infection date group (Figure 6A). Dimension 1 explained 56.4% of the total observed variance, compared with 19.1% for Dimension 2 (Supplementary Figure 4). The main variables explaining the variance described by Dimensions 1 and 2 were MFIs of RBD-targeting IgM and IgG, with the least contributing variable being MFIs of anti-S2 IgM. (Figure 6A).

The coordinates on Dim 1 and Dim 2 of the PCA were used to describe a score for each individual (Figure 6). Patients in the cohort were divided into 4 infection groups: 21 days, 90 days, 180 days, 365 days of infection and negative group. The Dim 1 score was highest at day 21 and decreased significantly over time ($P<0.0001$) (Figure 6B). A ROC analysis was performed to characterize each group. In doing so, we found that samples collected at 3 months versus 1 year showed the best discrimination (AUC = 0.98, 95% CI = 0.94 – 1; Specificity = 100% and sensitivity = 94.44%) (Figure 6D). We found good discriminations between samples collected at 6 months and 1 year (AUC = 0.89, 95% CI = 0.79 – 0.99; Specificity = 100% and sensitivity = 75%) (Figure 6D and Table 4). Samples collected at 3- and 6-months post-infection, however, were difficult to distinguish, suggesting stable humoral profiles at these timepoints (AUC = 0.68, 95% CI = 0.55 – 0.80; Specificity = 97.22% and sensitivity = 33.33%) (Table 4).

Analysis of symptom presentation was performed using the scores obtained for Dim 1 and Dim 2 (Figure 7B and C). There was a significant decrease in the Dim 1 score for the asymptomatic group compared to the symptomatic

group (p= 0.0088). These results were confirmed when the Dim1 score was added to the Dim 2 score. There was no difference between these two groups on Dim 2.

ROC curves were performed to identify the discrimination between the symptomatic and the asymptomatic groups. This test revealed that the best discrimination between the two groups was obtained with the addition of Dim1 and Dim2 values (AUC = 0.71, 95% CI = 0.59 – 82; Specificity = 95.24% and sensitivity = 36.84%) (Figure 7D and Table 5).

Antibody responses describe time since infection and symptom presentation

A random forest classification model was used to estimate the date since SARS-CoV-2 infection and symptom presentation based on antibody expression. After removing the late converters (N=7), 116 samples from D21 to 1-year post-infection and 40 negative samples, were analysed. The model was trained on 126 samples (80% of the sample size). The model estimated 100 (32/32), 44.83% (16/29), 77.58% (45/58), and 0% were uninfected, infected for less than 3 months, 3-6 months, and 1 year, respectively (Table 6). For assessment of symptom presentation, the model predicted 93.42% (71/76) of symptom presentations but could not predict asymptomatic presentations (only 5.88% (1/17) of asymptomatic presentations were predicted) (Table 7).

The model was validated on the 30 remaining samples (20% of the sample size). The prediction accuracy was 80% (95% CI = 61.43-92.29, p-value = 0.0001) for the estimation of time since infection and 87.1% (95% CI = 70.17-96.37, p-value = 0.0016) for symptom presentation.

Discussion

Accurate SARS-CoV-2 seroprevalence data are key to better understand the burden of the SARS-CoV-2. Using the seroprevalence to further define time since infection and clinical presentation can be an important tool to better address and improve the response against COVID-19 especially in countries with poor diagnostic capacity.

In the present study we developed a multiplex assay to detect human anti-S1, anti-S2, anti-RBD and anti-NP IgM and IgG antibodies. With the developed assay, we were able to observe the kinetics of antibody responses in patients with SARS-CoV-2 infection from day 1 to 12 months.

The first validation step allowed us to determine the performance of the test by measuring the sensitivity and specificity values. It is known that the NP protein is well conserved within the coronavirus family (96% amino acid homology with SARS-Cov-1). Even if we obtained a fair sensitivity of 42%, we wanted to be as specific as possible for this assay even with IgM. Moreover, when testing a pool of pre-epidemic negative samples (2015), we found 2 patients strongly expressing anti-S2 IgG (MFI >10,000). These individuals were also positive for IgGs anti-S2 subunits of seasonal coronaviruses, suggesting high S2 cross-reactivity (Supplementary figure 2). It is also known that there is an active circulation of human coronaviruses (OC43=7.1%, NL63=3.7, 229E=0.7% HKU1=1%) in Madagascar[20,21].

Once the in-house Luminex xMAP® assay was validated, we compared the results obtained with 2 commercial ELISAs. Among all sera tested, 42/258 were considered negative with the Wantai kit and 78/258 with the ID.Vet kit. These negative samples were then tested with the Luminex xMAP® and respectively 23/42 and 31/78 were found positive using our in-house assay. These results confirmed that the Luminex xMAP® assay is more sensitive

than the Wantai which is itself more sensitive than ID.Vet kit. Indeed, it has been described several times that Luminex xMAP® assay is more sensitive than conventional ELISA[25–27].

In the present study cohort, SARS-CoV-2 specific IgM and IgG were measured in symptomatic and asymptomatic COVID-19 confirmed patients. We noted no significant difference in antibodies to each of the targets, with the exception of anti RBD IgM. In general, it appears that IgM antibodies were higher in the symptomatic group than in the asymptomatic group. For IgG detection, the opposite trend was observed, with asymptomatic antibody levels being higher than those in the symptomatic group. These results have been described in several cohorts, with significant differences between these groups[13,15,28]. In the present cohort, only 8 patients were asymptomatic. The non-significant difference observed could be explained by the sample size.

We used this test to study the kinetics of seroconversion in patients over 1 year. IgG antibodies of anti S1, S2, RBD and NP persisted overtime. During follow-up, we noticed that for 3 of the patients, antibodies seroconversion occurred only at 6 months. IgG seroconversion usually occur around the fifth and seventh day of symptom onset[29,30]. This seemingly surprising results could be explained by the fact that for these patients, either an infection by SARS-CoV-2 virus occurred between M3 and M6 after a possibly false-positive PCR test result was given at day 0, or a SARS-CoV-2 reinfection occurred after an initial infection that did not lead to seroconversion, or for these individuals' seroconversion occurred almost 6 months after the initial infection. Indeed, the PCR test can have false-positive PCR results; one false-positive PCR can yield 6.3% meaning that these COVID-19 patients may have an initially false-positive RT-PCR result[31].

To visualize of the serological data, we performed a principal component analysis. Using dimensions 1 or 2 of the PCA as scores, ROC curves derived from these scores on dimension 1 showed an AUC of 0.98 for classification between infections from 3 months to 1 year and an AUC of 0.88 from 6 months to 1 year. The antibodies that contribute the most in the first dimension 1 are the anti-RBD IgGs. These results show that the decrease in MFI but persistence of seropositivity of anti-RBD IgGs over time seems to be a good marker for the discrimination of infections older than 1 year. Indeed, we found a persistence of anti-RBD IgG of more than 90% after one year of infection (Figure 5). Dim 1 score of the PCA showed a significant decrease in the asymptomatic group compared to the symptomatic but no discrimination of symptomatic presentations versus asymptomatic ones could be achieved using the Dim2 score. Indeed, a subgroup of symptomatic seems to be segregated (high Dim2 score) from a larger mixed presentation group (low Dim2 score). Obtained scores showed a significant decrease of the asymptomatic one compared to symptomatic ones.

The random forest model made a few misclassifications within groups, however, the accuracy rate was >80% for predicting the time of infection and predicting symptom presentation. Symptomatic patients were classified better than non-symptomatic ones suggesting the existence of 2 biological groups of individuals: either symptomatic (IgM^{high}) or a group of mixed presentations. This however may be because there are more symptomatic patients than asymptomatic patients in our cohort or because symptom presentation may be a subjective feeling. Nevertheless, it seems that IgM-producing individuals always feel symptomatic.

This study has several limitations, including sample size. This study was conducted on 43 patients who were followed for up to one year. But of these patients, only 13 completed the 12-month visit. The intervals of the group we chose for the estimation of time after infection could not give the best results. This observation is related to the

fact that the number of patients in each interval class was too small, resulting in the misclassification of 3 months in the 6-months group and infections > 3 months and 1 year in the 3 to 6-months group, which contains patients of 6 months and 3 months at the same time. We believe that these data need to be validated with a larger cohort.

A great asset of this study is the approach of using principal component analysis and a regression and classification model to retrospectively determine the time to infection and clinical symptoms presentation from a cohort of patients followed for one year and potentially over a year. Our group and others have shown that exposure to emerging VOCs can impact both the T-cell and the B-cell repertoires[32,33]. Indeed, in Madagascar, it was shown that during the second epidemic wave in 2021, antibody affinity gradually shifted towards VOC^{Beta}. These multiple antigen affinities and their evolution following successive immunisations, whether they be vaccinal or “natural", could be integrated in a more complex model and thoroughly describe a history of populational exposure to SARS-CoV-2.

The results of this study can be used for surveillance of a population where exposure to SARS-CoV-2 is poorly established. This innovative approach could help to investigate spatio-temporal dynamics and epidemiological surveillance of other infectious diseases. Moreover, this serological infection timing tool could be used in cohorts of individuals exposed to other pathogens and comorbidities associated to SARS-CoV-2, such as *Mycobacterium Tuberculosis*, to study the impact of co-infections as risk factors provided the response to both pathogens does not impact the humoral response to either pathogens or its impact is integrated to the model. This may help evaluate the impact of the ongoing COVID-19 pandemic on other public health priorities such as tuberculosis, HIV, malaria or other respiratory diseases[34–37].

Declaration of interests:

We declare no competing interests.

Acknowledgments:

We would like to thank to the patients and volunteers that accepted to participate to the study.

Fundings:

The study was funded by the French Ministry for Europe and Foreign Affairs through the REPAIR COVID-19-Africa project coordinated by the Pasteur International Network association. WANTAI reagents were provided by WHO AFRO as part of a Sero-epidemiological "Unity" Study Grant/Award Number: 2020/1019828-0 P.O 202546047 and Initiative 5% grant n°AP-5PC–2018–03-RO.

Data sharing:

All raw data will be shared upon request to the corresponding author.

Contributors:

MDBN and TR developed the methodology and validated the multiplex test. MS supervised the study. MDBN and TR accessed and cleaned the raw data, MDBN did statistical analysis. SR, RR, VR, NR, LR, JH, RR and PR reviewed the paper, MDBN and MS wrote the original draft. All authors approved the final manuscript.

References

1. Wu F, Zhao S, Yu B, Chen Y-M, Wang W, Song Z-G, et al. A new coronavirus associated with human respiratory disease in China. Nature. 2020 Mar;579(7798):265–9.

2. WHO Coronavirus (COVID-19) Dashboard. Available from: https://covid19.who.int

3. Tang B, Bragazzi NL, Li Q, Tang S, Xiao Y, Wu J. An updated estimation of the risk of transmission of the novel coronavirus (2019-nCov). Infect Dis Model. 2020;5:248–55.

4. Corman VM, Landt O, Kaiser M, Molenkamp R, Meijer A, Chu DK, et al. Detection of 2019 novel coronavirus (2019-nCoV) by real-time RT-PCR. Euro Surveill. 2020 Jan;25(3).

5. Wang W, Xu Y, Gao R, Lu R, Han K, Wu G, et al. Detection of SARS-CoV-2 in Different Types of Clinical Specimens. JAMA. 2020 May 12;323(18):1843–4.

6. Wang D, Hu B, Hu C, Zhu F, Liu X, Zhang J, et al. Clinical Characteristics of 138 Hospitalized Patients With 2019 Novel Coronavirus–Infected Pneumonia in Wuhan, China. JAMA. 2020 Mar 17;323(11):1061.

7. Rakotosamimanana N, Randrianirina F, Randremanana R, Raherison MS, Rasolofo V, Solofomalala GD, et al. GeneXpert for the diagnosis of COVID-19 in LMICs. Lancet Glob Health. 2020 Dec;8(12):e1457–8.

8. Wang M-Y, Zhao R, Gao L-J, Gao X-F, Wang D-P, Cao J-M. SARS-CoV-2: Structure, Biology, and Structure-Based Therapeutics Development. Front Cell Infect Microbiol. 2020;10:587269.

9. Duan L, Zheng Q, Zhang H, Niu Y, Lou Y, Wang H. The SARS-CoV-2 Spike Glycoprotein Biosynthesis, Structure, Function, and Antigenicity: Implications for the Design of Spike-Based Vaccine Immunogens. Front Immunol. 2020;11:576622.

10. Premkumar L, Segovia-Chumbez B, Jadi R, Martinez DR, Raut R, Markmann AJ, et al. The receptor-binding domain of the viral spike protein is an immunodominant and highly specific target of antibodies in SARS-CoV-2 patients. Science Immunology. 2020 Jun 1;5(48).

11. Hurst KR, Koetzner CA, Masters PS. Identification of In Vivo-Interacting Domains of the Murine Coronavirus Nucleocapsid Protein. J Virol. 2009 Jul 15;83(14):7221–34.

12. Burbelo PD, Riedo FX, Morishima C, Rawlings S, Smith D, Das S, et al. Sensitivity in Detection of Antibodies to Nucleocapsid and Spike Proteins of Severe Acute Respiratory Syndrome Coronavirus 2 in Patients With Coronavirus Disease 2019. J Infect Dis. 2020 May 19;jiaa273.

13. Al-Jighefee HT, Yassine HM, Al-Nesf MA, Hssain AA, Taleb S, Mohamed AS, et al. Evaluation of Antibody Response in Symptomatic and Asymptomatic COVID-19 Patients and Diagnostic Assessment of New IgM/IgG ELISA Kits. Pathogens. 2021 Feb;10(2):161.

14. Callard F, Perego E. How and why patients made Long Covid. Social Science & Medicine. 2021 Jan 1;268:113426.

15. Long Q-X, Liu B-Z, Deng H-J, Wu G-C, Deng K, Chen Y-K, et al. Antibody responses to SARS-CoV-2 in patients with COVID-19. Nat Med. 2020 Jun;26(6):845–8.

16. Jin Y, Wang M, Zuo Z, Fan C, Ye F, Cai Z, et al. Diagnostic value and dynamic variance of serum antibody in coronavirus disease 2019. International Journal of Infectious Diseases. 2020 May;94:49–52.

17. Zhao J, Yuan Q, Wang H, Liu W, Liao X, Su Y, et al. Antibody Responses to SARS-CoV-2 in Patients With Novel Coronavirus Disease 2019. Clinical Infectious Diseases. 2020 Nov 19;71(16):2027–34.

18. Test directory. FIND. Available from: https://www.finddx.org/covid-19/test-directory/

19. Pelleau S, Woudenberg T, Rosado J, Donnadieu F, Garcia L, Obadia T, et al. Kinetics of the Severe Acute Respiratory Syndrome Coronavirus 2 Antibody Response and Serological Estimation of Time Since Infection. The Journal of Infectious Diseases. 2021 Nov 16;224(9):1489–99.

20. Razanajatovo NH, Richard V, Hoffmann J, Reynes J-M, Razafitrimo GM, Randremanana RV, et al. Viral Etiology of Influenza-Like Illnesses in Antananarivo, Madagascar, July 2008 to June 2009. PLoS One. 2011 Mar 3;6(3).

21. Hoffmann J, Rabezanahary H, Randriamarotia M, Ratsimbasoa A, Najjar J, Vernet G, et al. Viral and Atypical Bacterial Etiology of Acute Respiratory Infections in Children under 5 Years Old Living in a Rural Tropical Area of Madagascar. PLoS One. 2012 Aug 17;7(8).

22. Luminex Corporation. xMAP Cookbook A collection of methods and protocols for developing multiplex assays with xMAP® Technology. BR402139. Available from: http://info.luminexcorp.com/en-us/research/download-the-xmap-cookbook

23. Ratovoson R, Razafimahatratra R, Randriamanantsoa L, Raberahona M, Rabarison HJ, Rahaingovahoaka FN, et al. Household transmission of COVID-19 among the earliest cases in Antananarivo, Madagascar. Influenza Other Respir Viruses. 2022 Jan;16(1):48–55.

24. Bagging and Random Forest Essentials - Articles - STHDA. Available from: http://www.sthda.com/english/articles/35-statistical-machine-learning-essentials/140-bagging-and-random-forest-essentials/

25. Weiss S, Klingler J, Hioe C, Amanat F, Baine I, Arinsburg S, et al. A High-Throughput Assay for Circulating Antibodies Directed Against the S Protein of Severe Acute Respiratory Syndrome Coronavirus 2. The Journal of Infectious Diseases. 2020 Oct 13;222(10):1629–34.

26. Mariën J, Ceulemans A, Michiels J, Heyndrickx L, Kerkhof K, Foque N, et al. Evaluating SARS-CoV-2 spike and nucleocapsid proteins as targets for antibody detection in severe and mild COVID-19 cases using a Luminex bead-based assay. Journal of Virological Methods. 2021 Feb;288:114025.

27. Drouot L, Hantz S, Jouen F, Velay A, Lamia B, Veber B, et al. Evaluation of Humoral Immunity to SARS-CoV-2: Diagnostic Value of a New Multiplex Addressable Laser Bead Immunoassay. Front Microbiol. 2020 Nov 26;11:603931.

28. Xiao T, Wang Y, Yuan J, Ye H, Wei L, Liao X, et al. Early Viral Clearance and Antibody Kinetics of COVID-19 Among Asymptomatic Carriers. Front Med. 2021;8.

29. Amanat F, Stadlbauer D, Strohmeier S, Nguyen THO, Chromikova V, McMahon M, et al. A serological assay to detect SARS-CoV-2 seroconversion in humans. Nat Med. 2020 Jul;26(7):1033–6.

30. Orner EP, Rodgers MA, Hock K, Tang MS, Taylor R, Gardiner M, et al. Comparison of SARS-CoV-2 IgM and IgG seroconversion profiles among hospitalized patients in two US cities. Diagn Microbiol Infect Dis. 2021 Apr;99(4):115300.

31. Sung H, Han M-G, Yoo C-K, Lee S-W, Chung Y-S, Park J-S, et al. Nationwide External Quality Assessment of SARS-CoV-2 Molecular Testing, South Korea - Volume 26, Number 10—October 2020 - Emerging Infectious Diseases journal - CDC.

32. Reynolds CJ, Gibbons JM, Pade C, Lin K-M, Sandoval DM, Pieper F, et al. Heterologous infection and vaccination shapes immunity against SARS-CoV-2 variants. 2022;11.

33. Razafimahatratra SL, Ndiaye MDB, Rasoloharimanana LT, Dussart P, Sahondranirina PH, Randriamanantany ZA, et al. Seroprevalence of ancestral and Beta SARS-CoV-2 antibodies in Malagasy blood donors. The Lancet Global Health. 2021 Oct;9(10):e1363–4.

34. Calcagno A, Ghisetti V, Burdino E, Trunfio M, Allice T, Boglione L, et al. Co-infection with other respiratory pathogens in COVID-19 patients. Clinical Microbiology and Infection. 2021 Feb;27(2):297–8.

35. Alosaimi B, Naeem A, Hamed ME, Alkadi HS, Alanazi T, Al Rehily SS, et al. Influenza co-infection associated with severity and mortality in COVID-19 patients. Virol J. 2021 Dec;18(1):127.

36. Gatechompol S, Avihingsanon A, Putcharoen O, Ruxrungtham K, Kuritzkes DR. COVID-19 and HIV infection co-pandemics and their impact: a review of the literature. AIDS Res Ther. 2021 May 5;18(1):28.

37. Al Lawati R, Al Busaidi N, Al Umairi R, Al Busaidy M, Al Naabi HH, Khamis F. COVID-19 and Pulmonary Mycobacterium Tuberculosis Coinfection. Oman Med J. 2021 Sep;36(5):e298.

Figure legends:

Figure 1: Performance of the luminex 4-plex assay. (A) Boxplot representing MFI levels for of S1. S2. RBD. NP between negative samples (40) and positive samples (N=34) IgM and IgG. Negative samples are pre-endemic sera collected in 2015. Positive samples are collected from hospitalized patients with a positive PCR for SARS-Cov-2. Receiving Operating Characteristic (ROC) curve obtained with MFI of negative and positive

Figure 2: Boxplot representing MFI levels for of S1. S2. RBD. NP between symptomatic (n=35. dark green) and non-symptomatic patients (N=8. light green) IgM and IgG. Data were compared using the Mann-Whitney test. *: $p < 0.05$, ns: non significative

Figure 3: Kinetics of seroconversion with 7 timepoints from day 1 to day 365. (A) line plot of antibody detection in 43 hospitalized patients. Each line represent a patient. Dashed line and grey area indicate the cut off of positivity. (B) Seroconversion curves during the follow up. Only the event seropositivation is considered.

Figure 4 : Seroconversion and seroreversion in IgM and IgG antibodies over 365 days of follow-up. A and B, Kaplan-Meier plots of patients with IgM and IgG seroconversion, respectively. C and D, Kaplan-Meier plots of patients with IgM and IgG seroreverted respectively.

Figure 5: Seroprevalence of IgM and IgG in the FFX cohort. Antibody seroprevalence from day 1 to Month 12 (day 365) for anti-SARS-Cov-2 S1 (blue), S2 (grey), RBD (green) and NP (red) with error bars of the 43 patients of the FFX cohort.

Figure 6: PCA representing time since infection using serology results. Principal component analysis (PCA) was performed on the expression of anti-S1, anti-S2, anti-RBD and anti-NP IgM and IgG. A. Explanation of variance between early infections (day 21), 3-month infections (day 90), 6-month (day 180) and 1-year infections (day 365). N= 36 samples at each time point except 12 months (n=8) and Negative (n=40). Each point represents one patient. Color coding represents infection date groups. The axes represent principal components 1 (Dimension 1, Dim1) and 2 (Dimension 2, Dim2) and the percentages indicate their contribution to the total observed variance. Axis values represent individual PCA scores. The concentration ellipses correspond to 90% data coverage. Arrows represent the contribution of each IgG and IgM to the variance described by Dim1 and Dim2. B. Distribution of individual PCA score values as a function of infection date and time point, for Dim1. Data were compared using the Wilcoxon rank sum test. ****: $p<0.0001$. and Mann- Whitney test ****: $p<0.0001$ for comparisons between negative and 12 month. C. Distribution of individual PCA score values as a function of infection date and time point, for Dim2. Data were compared using the Wilcoxon rank sum test. ****: $p<0.0001$. and Mann- Whitney test ****: $p<0.0001$ for comparisons between negative and 12 month. D. Receiving Operating Characteristic (ROC) curve obtained PCA Scores for Dim1. Color coding represents ROC of comparison for different infection date groups

Figure 7: PCA representing clinical presentation using serology results. Principal component analysis (PCA) was performed on the expression of anti-S1, anti-S2, anti-RBD and anti-NP IgM and IgG. A. Explanation of

variance between among Symptomatic (N=95) and asymptomatic (N=21) patients all timepoints combined. Each point represents one patient. Color coding represents infection groups. The axes represent principal components 1 (Dimension 1, Dim 1) and 2 (Dimension 2,Dim 2) and the percentages indicate their contribution to the total observed variance. Axis values represent individual PCA scores. The concentration ellipses correspond to 90% data coverage. Arrows represent the contribution of each IgG and IgM to the variance described by Dim 1 and Dim 2. B. Distribution of individual PCA score values as a function of symptom presentation groups and time point, for Dim 1. Data were compared using the Mann-Whitney test. **: $p<0.01$ ****: $p<0.0001$ for comparisons between negative and 12 month. C. Distribution of individual PCA score values as a function of symptom presentation groups and time point, for Dim 2. Data were compared using the Mann-Whitney test. **: $p<0.01$ ****: $p<0.0001$ for comparisons between negative and 12 month. D. Receiving Operating Characteristic (ROC) curve obtained PCA Scores for Dim 1 and Dim 2.

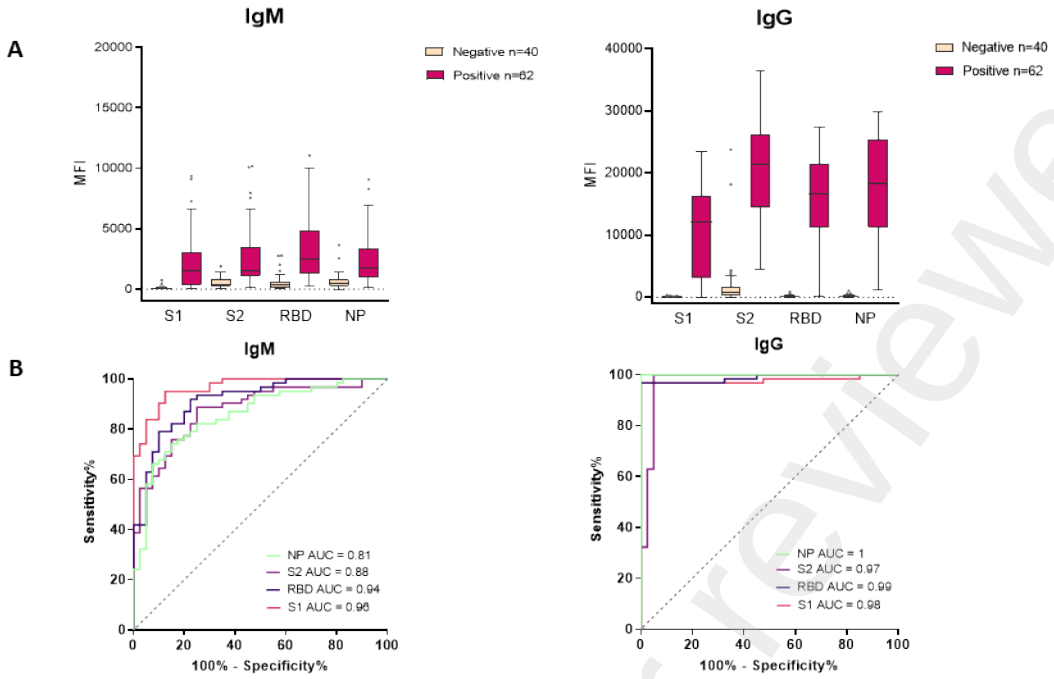

Figure 1: Performance of the luminex 4-plex assay. (A) Boxplot representing MFI levels for of S1. S2. RBD. NP between negative samples (40) and positive samples (N=34) IgM and IgG. Negative samples are pre-endemic sera collected in 2015. Positive samples are collected from hospitalized patients with a positive PCR for SARS-Cov-2. All differences between positive and negative patients are significant. Receiving Operating Characteristic (ROC) curve obtained with MFI of negative and positive.

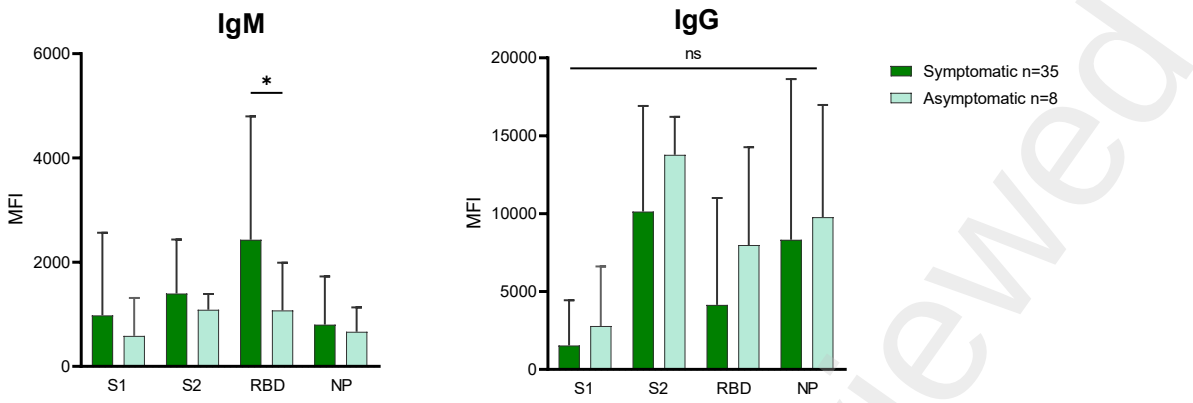

Figure 2: Boxplot representing MFI levels for of S1. S2. RBD. NP between symptomatic (n=35. dark green) and non symptomatic patients (N=8. light green) IgM and IgG. Data were compared using the Mann-Whitney test. *: p <0.05, ns: non significative.

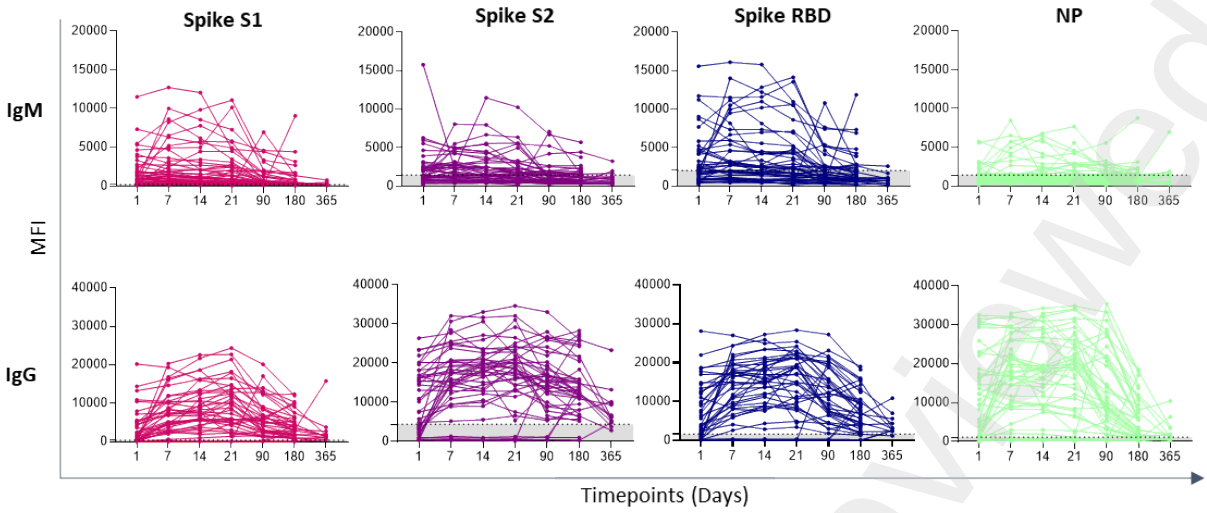

Figure 3: Kinetics of seroconversion with 7 timepoints from day 1 to day 365. (A) line plot of antibody detection in 43 hospitalized patients. Each line represent a patient. Dashed line and grey area indicate the cut off of positivity. (B) Seroconversion curves during the follow up. Only the event seropositivation is considered.

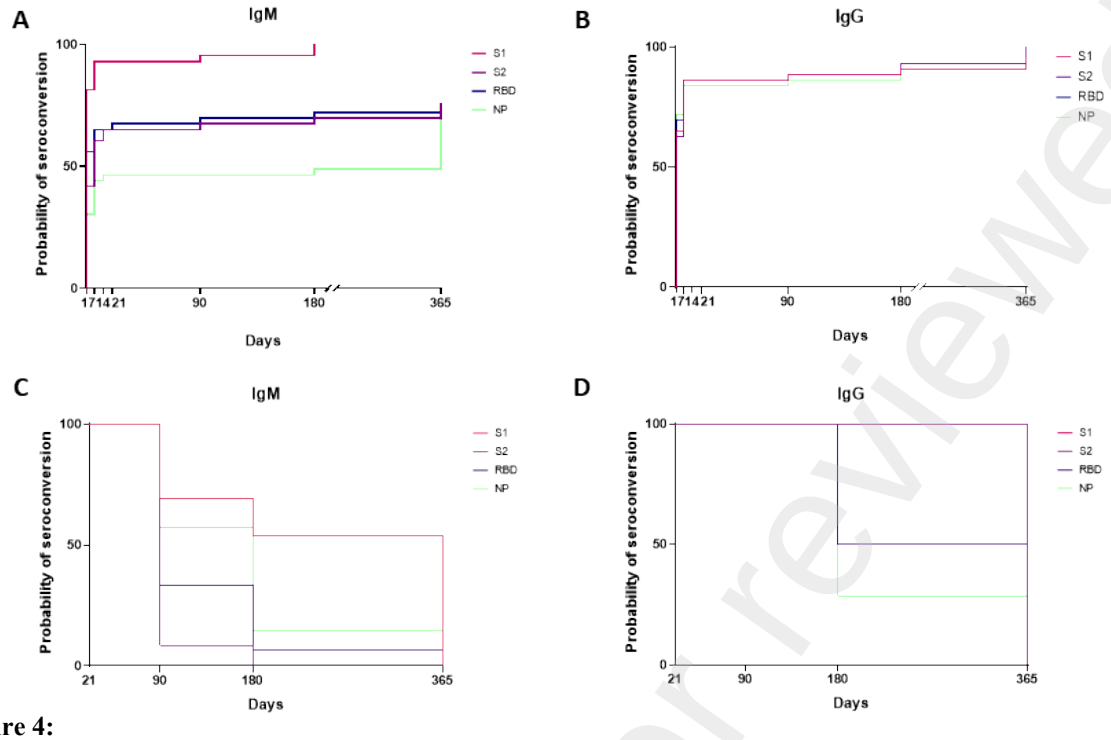

Figure 4:

Seroconversion and seroreversion in IgM and IgG antibodies over 365 days of follow-up. A and B, Kaplan-Meier plots of patients with IgM and IgG seroconversion, respectively. C and D, Kaplan-Meier plots of patients with IgM and IgG seroreverted respectively.

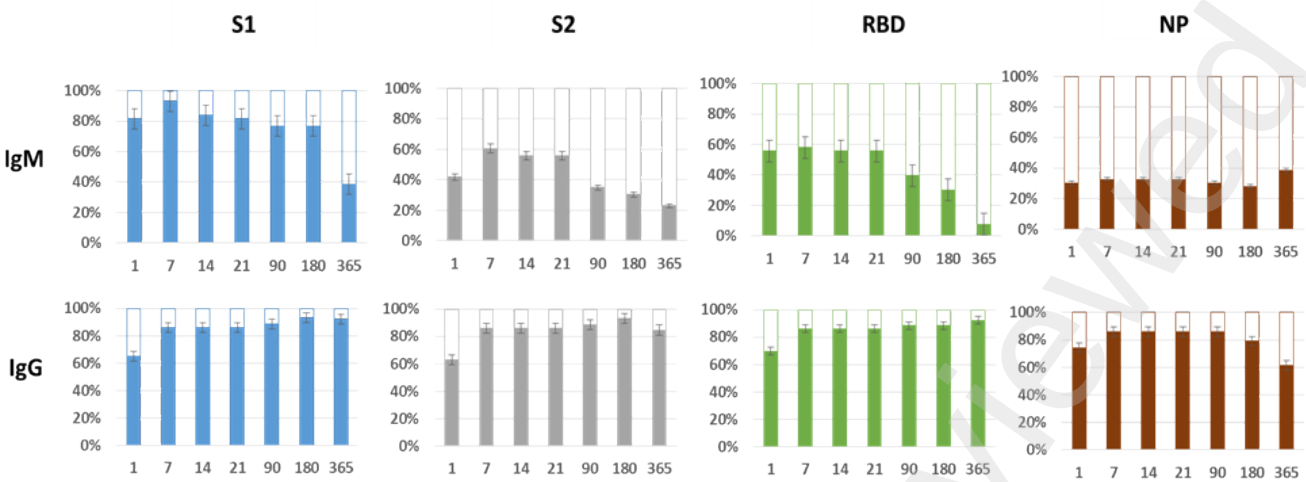

Figure 5: Seroprevalence of IgM and IgG in the FFX cohort. Antibody seroprevalence from day 1 to Month 12 (day 365) for anti-SARS-Cov-2 S1 (blue), S2 (grey), RBD (green) and NP (red) with error bars of the 43 patients of the FFX cohort.

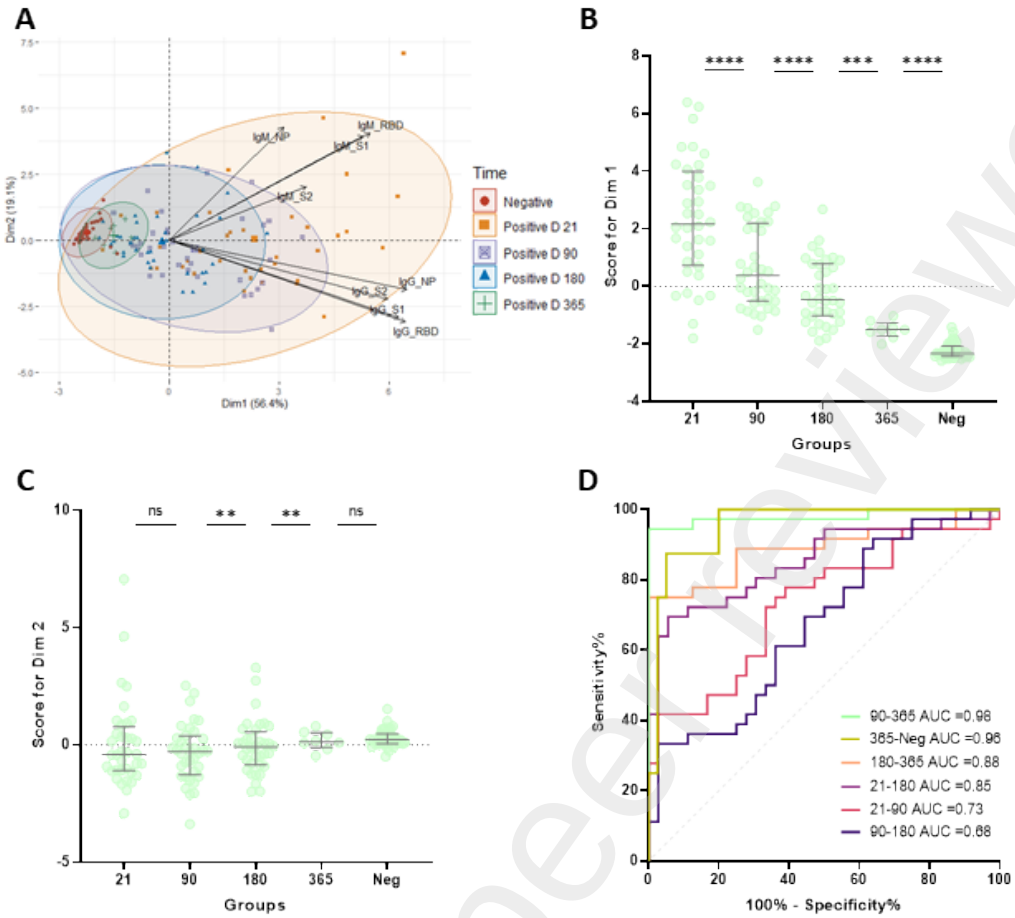

Figure 6: PCA representing time since infection using serology results. Principal component analysis (PCA) was performed on the expression of anti-S1, anti-S2, anti-RBD and anti-NP IgM and IgG. A. Explanation of variance between early infections (day 21), 3-month infections (day 90), 6-month (day 180) and 1-year infections (day 365). N= 36 samples at each time point except 12 months (n=8) and Negative (n=40). Each point represents one patient. Color coding represents infection date groups. The axes represent principal components 1 (Dimension 1, Dim1) and 2 (Dimension 2,Dim2) and the percentages indicate their contribution to the total observed variance. Axis values represent individual PCA scores. The concentration ellipses correspond to 90% data coverage. Arrows represent the contribution of each IgG and IgM to the variance described by Dim1 and Dim2.
B. Distribution of individual PCA score values as a function of infection date and time point, for Dim1. Data were compared using the Wilcoxon rank sum test. ****: $p<0.0001$. and Mann-Whitney test ****: $p<0.0001$ for comparisons between negative and 12 month. C. Distribution of individual PCA score values as a function of infection date and time point, for Dim2. Data were compared using the Wilcoxon rank sum test. ****: $p<0.0001$. and Mann-Whitney test ****: $p<0.0001$ for comparisons between negative and 12 month. D. Receiving Operating Characteristic (ROC) curve obtained PCA Scores for Dim1. Color coding represents ROC of comparison for different infection date groups

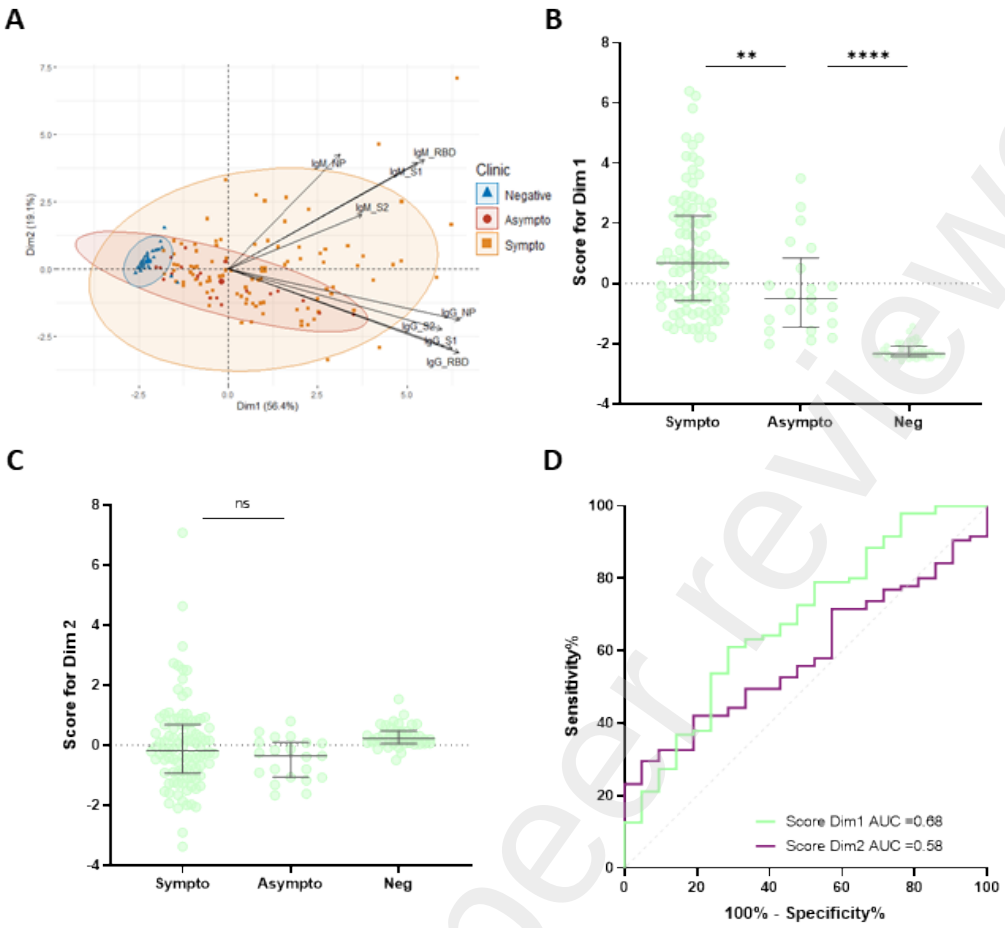

Figure 7: **PCA representing clinical presentation using serology results**. Principal component analysis (PCA) was performed on the expression of anti-S1, anti-S2, anti-RBD and anti-NP IgM and IgG. A. Explanation of variance between among Symptomatic (N=95) and asymptomatic (N=21) patients all timepoints combined . Each point represents one patient. Color coding represents infection groups. The axes represent principal components 1 (Dimension 1, Dim 1) and 2 (Dimension 2,Dim 2) and the percentages indicate their contribution to the total observed variance. Axis values represent individual PCA scores. The concentration ellipses correspond to 90% data coverage. Arrows represent the contribution of each IgG and IgM to the variance described by Dim 1 and Dim 2.

B. Distribution of individual PCA score values as a function of symptom presentation groups and time point, for Dim 1. Data were compared using the Mann-Whitney test. **: $p<0.01$ ****: $p<0.0001$ for comparisons between negative and 12 month

C. Distribution of individual PCA score values as a function of symptom presentation groups and time point, for Dim 2. Data were compared using the Mann-Whitney test. **: $p<0.01$ ****: $p<0.0001$ for comparisons between negative and 12 month

D. Receiving Operating Characteristic (ROC) curve obtained PCA Scores for Dim 1 and Dim 2 .

List of tables:

Table 1: Characteristics of the cohorts

Patients of the study	Evaluation
Sample collection date	March 2020 - July 2020
Number included	43
Number of samples	271
Gender	
Male	42% (18/43)
Female	58% (25/43)
Age (years)	43 (15-71)
Symptoms	
Symptomatic	81% (35/43)
Non symptomatic	19% (8/43)
Comorbidities	
Diabetes	7% (3/43)
Asthma	2.3% (1/43)
Obesity	2.3% (1/43)
Cardiovascular disease	7% (3/43)
Negative controls	
Collection date	2015
Number included	40

Table 2: Validation luminex assay. Characteristics of validation for the luminex assay. LLoQ: Lower Limit Of Quantification. ULoQ: Upper Limit Of Quantification. CV intra essai < 10%CV inter essai <15%.

	Spike S1	Spike S2	Spike RBD	NP
CV% intra assay	2.87	2.14	2.53	2.21
CV% inter assay	3.08	3.12	2.96	3.38
LLoQ Ab (ng/mL)	0.1	0.1	0.1	0.1
ULoQ Ab (ng/mL)	1000	1000	1000	1000

Table 3: Performance of the 4-plex assay. Sensitivity and specificity of the luminex antibody assay for antigen in multiplex

		AUC	95% CI	p value	cut off	Sensitivity %	95% CI	Specificity %	95% CI
IgM	**S1**	0.96	0.94 - 0.99	< 0.0001	> 201.90	83.87	72.79 – 91.00	95.00	83.50 - 99.11
	S2	0.88	0.81 - 0.94	< 0.0001	> 1437	56.45	44.09 - 68.06	97.50	87.12 - 99.87
	RBD	0.94	0.89 - 0.99	< 0.0001	> 2036	62.90	50.46 - 73.84	95.00	83.50 - 99.11
	Np	0.81	0.71 - 0.91	< 0.0001	> 1404	58.06	45.676 - 9.52	95.00	83.50 - 99.11
IgG	**S1**	0.98	0.95 – 1.00	< 0.0001	> 335.70	96.77	88.98 - 99.43	97.50	87.12 - 99.87
	S2	0.97	0.94 – 1.00	< 0.0001	> 4396	100.00	94.17 – 100.00	95.00	83.50 - 99.11
	RBD	0.99	0.97 – 1.00	< 0.0001	> 1613	96.77	88.98 - 99.43	100.00	91.24 – 100.00
	Np	1.00	1.00 - 1.00	< 0.0001	> 1114	100.00	94.17 – 100.00	100.00	91.24 – 100.00

Table 4: Discrimination of different time of infection groups using PCA dimensions as scores

	AUC	95% CI	p value	cut off	Sensitivity %	95% CI	Specificity %	95% CI
<1 month - 3 month	0.73	0.61 - 0.85	0.0008	> 2.84	41.67	27.14 - 57.80	97.22	85.83 - 99.86
<1 month - 6 month	**0.85**	**0.76 - 0.94**	**<0.0001**	**> 1.61**	**63.89**	**47.58 - 77.52**	**97.22**	**85.83 - 99.86**
3 month - 6 month	0.68	0.55 - 0.80	0.0106	> 1.76	33.33	20.21 - 49.67	97.22	85.83 - 99.86
3 month - 12 month	**0.98**	**0.94 - 1.00**	**<0.0001**	**> -1.00**	**94.44**	**81.86 - 99.01**	**100.00**	67.56 - 100.00
6 month - 12 month	**0.89**	0.79 - 0.99	0.0007	> -0.99	75.00	58.93 - 86.25	100.00	67.56 - 100.00
12 month - Negative	0.96	0.90 - 1.00	<0.0001	> -1.59	75.00	40.93 - 95.56	97.5	87.12 - 99.87

Table 5: Symptom presentation discrimination using PCA dimensions as scores

	AUC	95% CI	p value	cut off	Sensitivity %	95% CI	Specificity %	95% CI
Dim1	0.68	0.55 - 0.81	0.0093	> 2.56	21.05	14.06 - 30.29	95.24	77.33 - 99.76
Dim2	0.59	0.47 - 0.70	0.2215	> 0.46	29.47	21.25 - 39.29	95.24	77.33 - 99.76
Dim1 + Dim2	0.71	0.59 - 0.82	0.0033	> 0.93	36.84	27.83 - 46.88	95.24	77.33 - 99.76

Table 6: Estimation of the date of infection on the training set. % (N)

		Reference			
		Negative	**< 3 month**	**3 - 6 month**	**1 year**
Prediction	**Negative**	**100** (32/32)	0	0	0
	< 3 month	0	**44.83** (16/29)	55,17 (13/29)	0
	3 - 6 month	0	17.24 (10/58)	**77.58** (45/58)	5.17 (3/58)
	1 year	14.29 (1/7)	0	85.71 (6/7)	**0**

Table 7: Prediction of symptom presentation on the training set. % (N)

		Reference		
		Negative	**Asympto**	**Sympto**
Prediction	**Negative**	**100** (32/32)	0	0
	Asympto	0	**5.88 (1/17)**	94.12 (16/17)
	Sympto	0	6.58(5/76)	**93.42** (71/76)

4. Study 4: Cross-impact study between SARS-CoV-2 and tuberculosis infections (in preparation)

Summary:

Conducted in the context of the emergence of SARS-CoV-2 and the subsequent pandemic, the present study aims to describe the seroprevalence of COVID-19 in a contact cohort of TB patients and to assess the impact that may have SARS-CoV-2 infection on TB progression. We know that people with TBI are at risk of developing the disease in their lifetime. This risk is higher during the first two years after exposure to the bacteria. Here is to find out whether SARS-CoV-2 infection could also be a risk for the progression of TB disease.

In the APRECIT study conducted in Madagascar, 1030 contacts of bacteriologically confirmed patients with active TB were recruited and followed for 18 months. During this follow-up, venous blood samples were taken. The serodiagnosis test based on Luminex technology, developed for this study was used to measure SARS-CoV-2 antibodies. The developed assay targets IgG and IgM directed against the Spike protein subunits (S1, S2, RBD) and the nucleocapsid protein (N). We described a high seroprevalence of SARS-CoV-2 infection in the cohort. At inclusion, the seroprevalence was 50% IgM and 70% IgG. An increase of this seroprevalence was observed during the follow-up reaching over 90%. Furthermore, we described the progression of tuberculosis by analysing the QFT-P and anti- SARS-CoV-2 antibody levels of these patients. Our results did not show a difference between progressors and non-progressors in the household contacts for anti-SARS-CoV-2 specific humoral response and specific TB IFN-γ response. Further investigations are needed to assess the correlation between both respiratory infections.

Clinical demographic data

389 microbiologically confirmed TB patients were identified for 1030 household contacts recruited. Those HHC were followed during 18 months. For this present study, we excluded individuals who received COVID-19 vaccine leading to 974 household contacts. Among them 861 of them were followed to 6 months. 770 of them completed the 12 months visit and 511 completed all visits (Figure 1).

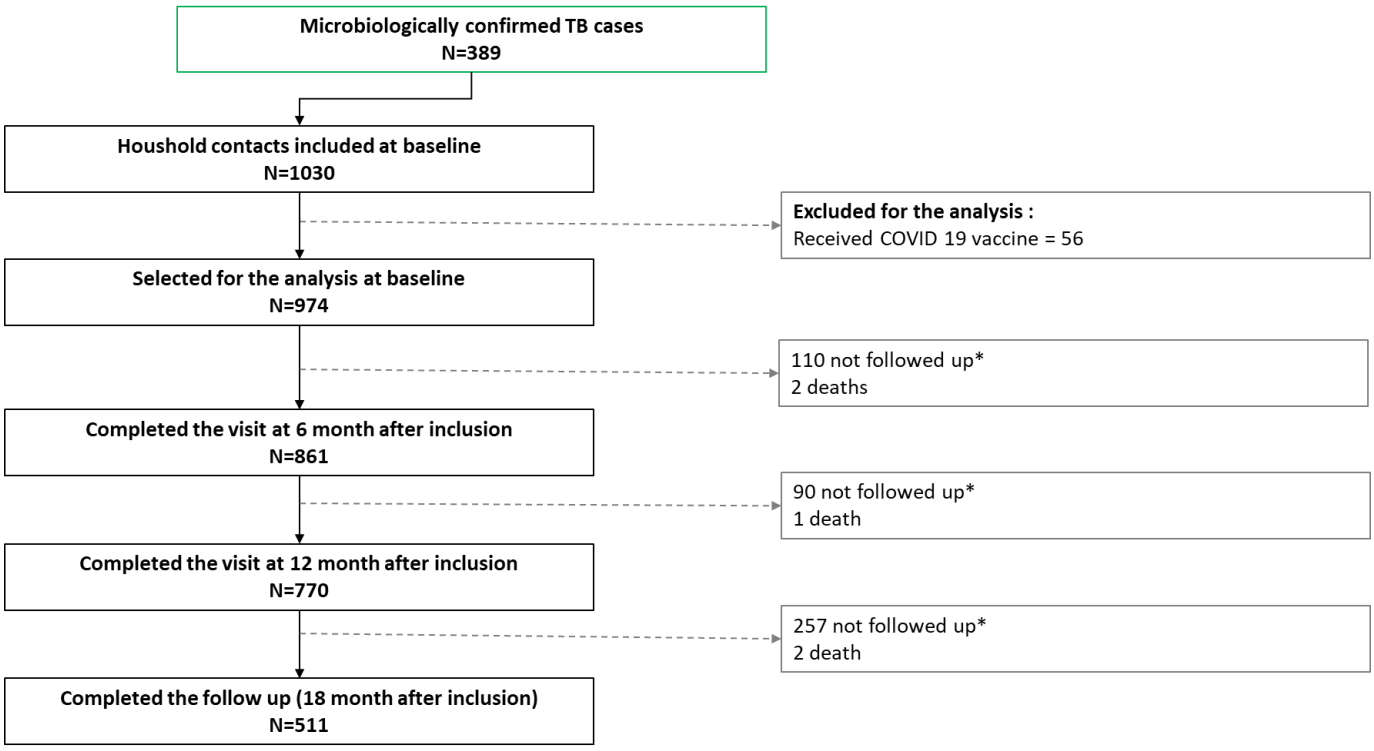

Figure 1: Patient inclusions between December 2020 and December 2021. *Not followed up group include: lost to follow up because of house moving or other reasons and refusals of follow-ups

Demographic information on the Cohort.

389 ATB patients were recruited for 974 HHC recruited. Among ATB patients, 36% were female and for HHC patients 58% (Table 1). The mean age is ATB and for HHC. I this latter cohort, the predominant age group is [10-25[that represents 38.9%. The BCG vaccination reached 91%. We noticed 97.6% and 99.2% of HIV negative in ATB and HHC respectively. 67,3% of HHC had a positive TST result. The QuantiFERON positivity rate for HHC varied slightly between 58 and 66.6% during the follow-up. TB T.SPOT-TB was 49.8% positive and increased during the follow-up to 70.7% at M18(Table 1).

Individuals with positive results for both QFT-P and T.SPOT-TB (IGRA positive), 61.8% at the enrolment.

During the HHC follow-up, 1 individual progressed from TBI to ATB and 12 progressed to ATB at M6 for a total of 15 progressors over 974 (1.54%).

Table 1:**Sociodemographic data of patients**

		ATB	Household contacts			
			M0	M6	M12	M18
N		389	974	861	770	511
Age mean (SD)		36.04 (13.33)	23.96 (17.72)	-	-	-
Age group N (%)	[0-5]		81 (8.3)	-	-	-
	]5-10[		151 (15.5)	-	-	-
	[10-25[		379 (38.9)	-	-	-
	[25-40[		184 (18.9)	-	-	-
	[40-60[		128 (13.1)	-	-	-
	> 60		51 (5.2)	-	-	-
Gender female N(%)		140 (36.0)	565 (58.0)	-	-	-
Smoking N(%)		88 (22.6)	88 (9.0)	-	-	-
Previous TB history N(%)		32 (8.2)	26 (2.7)	-	-	-
BCG vaccinated N(%)		357 (91.8)	905 (92.9)	-	-	-
HIV Negative N(%)		324 (97.6)	946 (99.2)	-	-	-
TST N(%)						
	< 5 mm		238 (24.7)	-	-	-
	5 à 10 mm		78 (8.1)	-	-	-
	>=10mm		649 (67.3)	-	-	-
QFT-P N(%)						
	Positive	221 (59.2)	532 (58.0)	514 (65.6)	482 (63.9)	303 (66.6)
	Negative	49 (13.1)	330 (36.0)	196 (25.0)	230 (30.5)	152 (33.4)
	Indeterminate	103 (27.6)	55 (6.0)	74 (9.4)	42 (5.6)	0 (0.0)
T.SPOT-TB N(%)						
	Positive	261 (68.1)	474 (49.8)	514 (67.5)	422 (69.1)	224 (70.7)
	Negative	105 (27.4)	404 (42.5)	187 (24.6)	149 (24.4)	69 (21.8)
	Indeterminate	17 (4.4)	73 (7.7)	60 (7.9)	40 (6.5)	24 (7.6)
IGRA Positive N(%)		173 (88.7)	381 (61.9)	331 (61.3)	300 (61.5)	186 (58.9)
Progressors N(%)		-	0(0.0)	1 (0.1)	13(1.4)	15 (2.93)

Mean (SD), N(%)

IGRA response by age group during the follow-up period

The evolution of the response to IFN-γ in the cohort and by age groups during the 18 months of follow-up was then analysed. Overall, we observe a predominance of positive IGRA results, followed by negative results and a small proportion of undetermined results (Figure 2).

Concerning the QFT-P results, the proportion of positive results varies from 43% to 64% at M0, from 50% to 75% at M6, from 42% to 71% at M12 and from 40% to 75% at M18. We noticed that the age group [0-5] have a generally lower positive IGRA result compared to the other age groups.

The same trend is observed for T.SPOT-TB results with a steady increase in the percentage of positivity during the follow-up. The proportion of positives ranged from 35% to 52% at M0, 60% to 73% at M6, 62% to 77% at M12 and 55% to 81% at M18

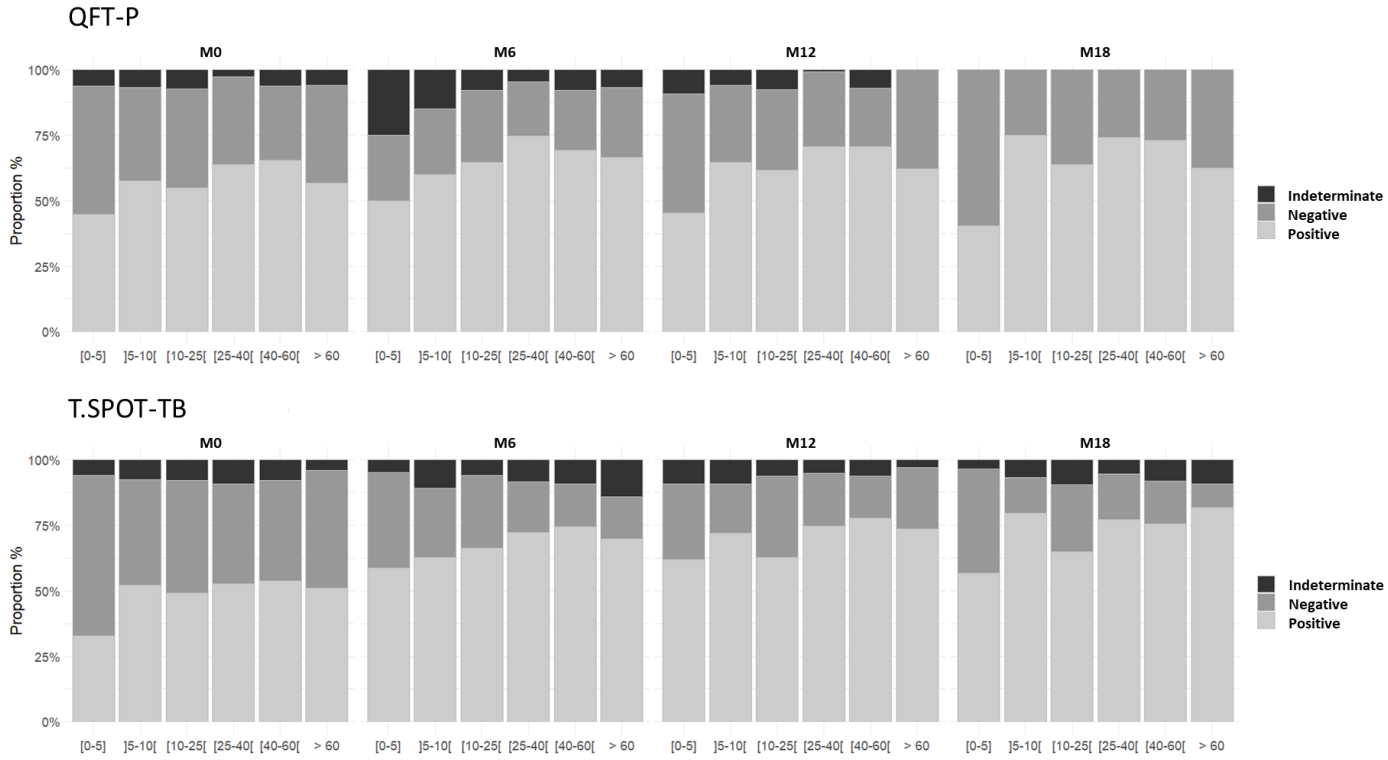

Figure 2: IGRA response by age group during the follow-up period. Stacked plot of QFT-P result and T.SPOT-TB results in different age groups. y axis represents proportion in percent of each sub-group. axis represents different age classes

COVID-19 infections in a cohort of TB contacts

Over 493 Household contacts recruited and followed up during 18 months, the results serology Luminex SARS CoV 2 have shown a seroprevalence of overall antibodies a 82% at baseline going during the follow-up timenpoints up to 98% of seroprevalence M18 (Figure 3). IgM SARS-CoV-2 was detected in 50% of the population and this seroprevalence decreased during the follow-up to 25%. This shows the high circulation of SARS-CoV-2 in this cohort which can be extrapolated to the Malagasy population of Antananarivo.

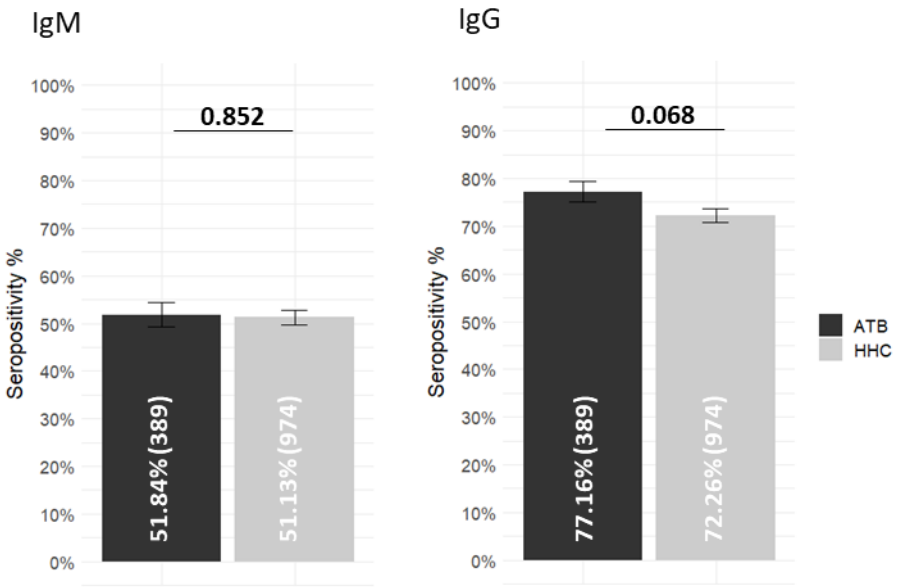

Figure 3: Comparison of IgM and IgG seropositivity between ATB and HHC. Bar plot represents seropositivity in percent. Error bars represent standard error of the Mean (SEM). Data were compared using an analysis of variance model.

We assessed the COVID seroprevalence in the two populations of ATB and HHC. Regarding the expression of IgM anti-SARS-CoV-2, we have 51.84% of seropositivity in ATB against 51.13% in HHC (Figure 3). Global IgG antibodies seropositivity rates were 77.26% and 77.16% for ATB and HHC respectively. No significant difference was found comparing these two groups.

IgM and IgG seropositivity during HHC follow up

The IgM and IgG seroprevalence was studied as a function of age, in the contact cohort (Figure 4). The IgM seroprevalence between M0 and M6 is around 50% for all age groups, and decreases significantly during the follow-up. Only the seroprevalence in the [40-60] class remains high at M18. IgG seroprevalence ranged from 60% to 75% at M0 depending on the age group. It increases substantially during the follow-up to reach seropositivity ranges between 95% and 100%.

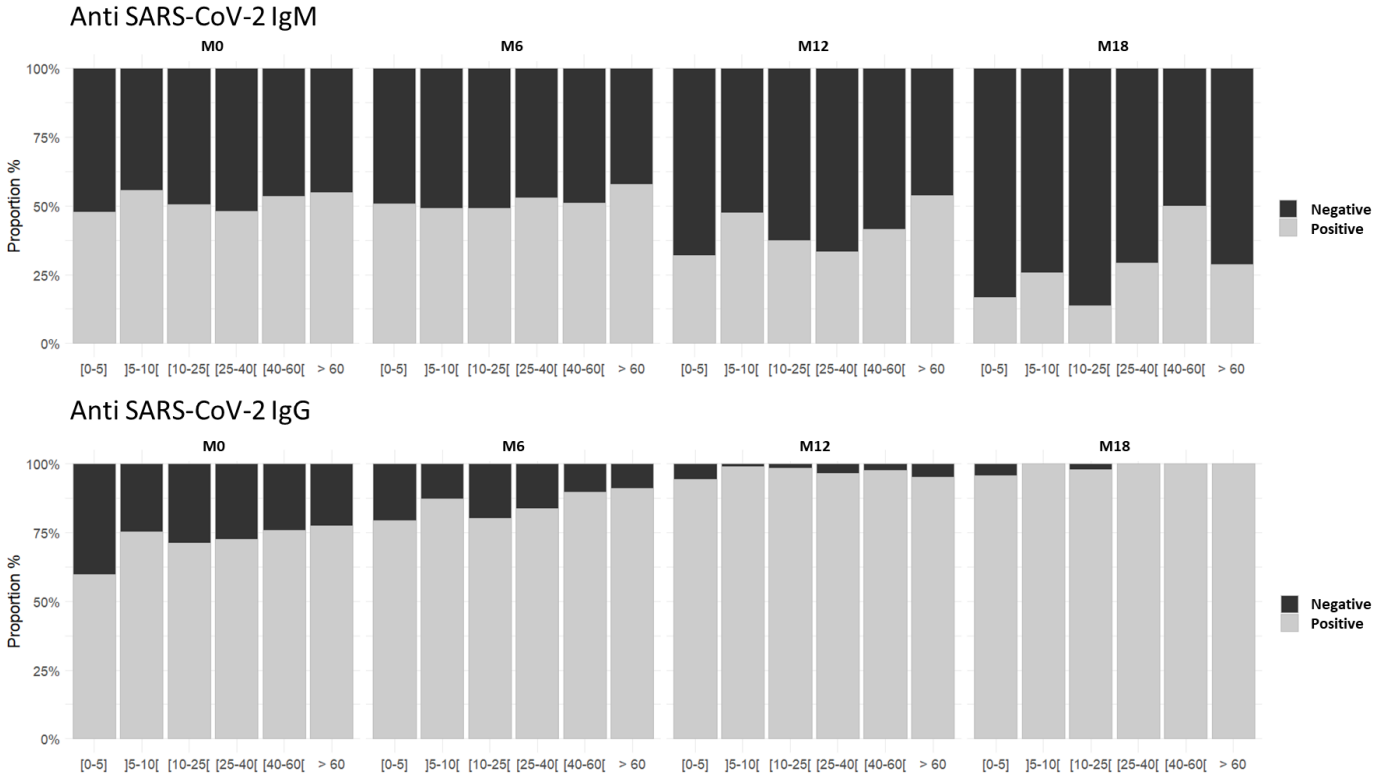

Figure 4 : IgM and IgG seropositivity during HHC follow up. Stacked plot of anti-SARS-CoV-2 IgM and anti-SARS-CoV-2 IgG seroprevalence in different age groups. y axis represents proportion in percent of each sub-group. x axis represents different age classes

We then studied the evolution of COVID seroprevalence during the follow-up in the HHC. To do so, the cohort was divided into 2 groups: the IGRA positive with a positive test for QFT-P and for T.SPOT-TB and the IGRA negative concerning patients who had a QFT-P and a negative T.SPOT-TB result (Figure 4).

Our results showed an IgM seroprevalence ranging from 46% to 30% at M0 for the IGRA-negative and a seroprevalence of 55.98% to 37.84% at M18 (Figure 4). Regarding

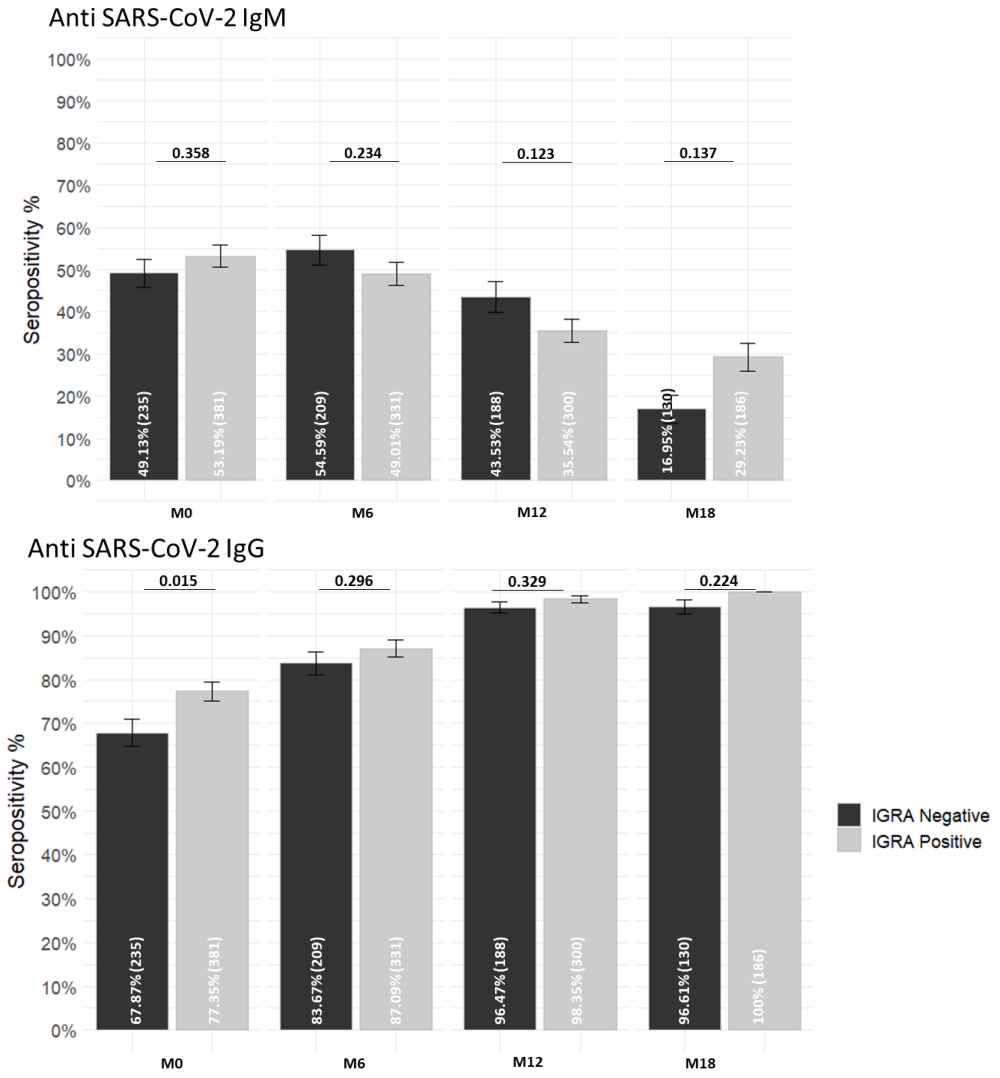

Figure 5: IgM and IgG seropositivity during HHC follow up. Bar plot represents seropositivity in percent. Error bars represent standard error of the Mean (SEM). Data were compared using Fisher exact test.

IgG, the seroprevalence increased during the follow-up, from 69.81% to 100% for IGRA negative and from 78.71% to 100% for IGRA positive.

Antibody dynamic during HHC follow up

We measured the seroprevalence rate of contacts during the 18 months of follow-up (Figure 5). Regarding less of the target, anti-SARS-CoV-2 IgG increased significantly in the cohort during the follow-up. This increase slows down and remains stagnant

between M12 and M18. IgM antibodies were hight at M0 and remained hight at M6 before decreasing significantly during the follow-up (p-value <0.001).

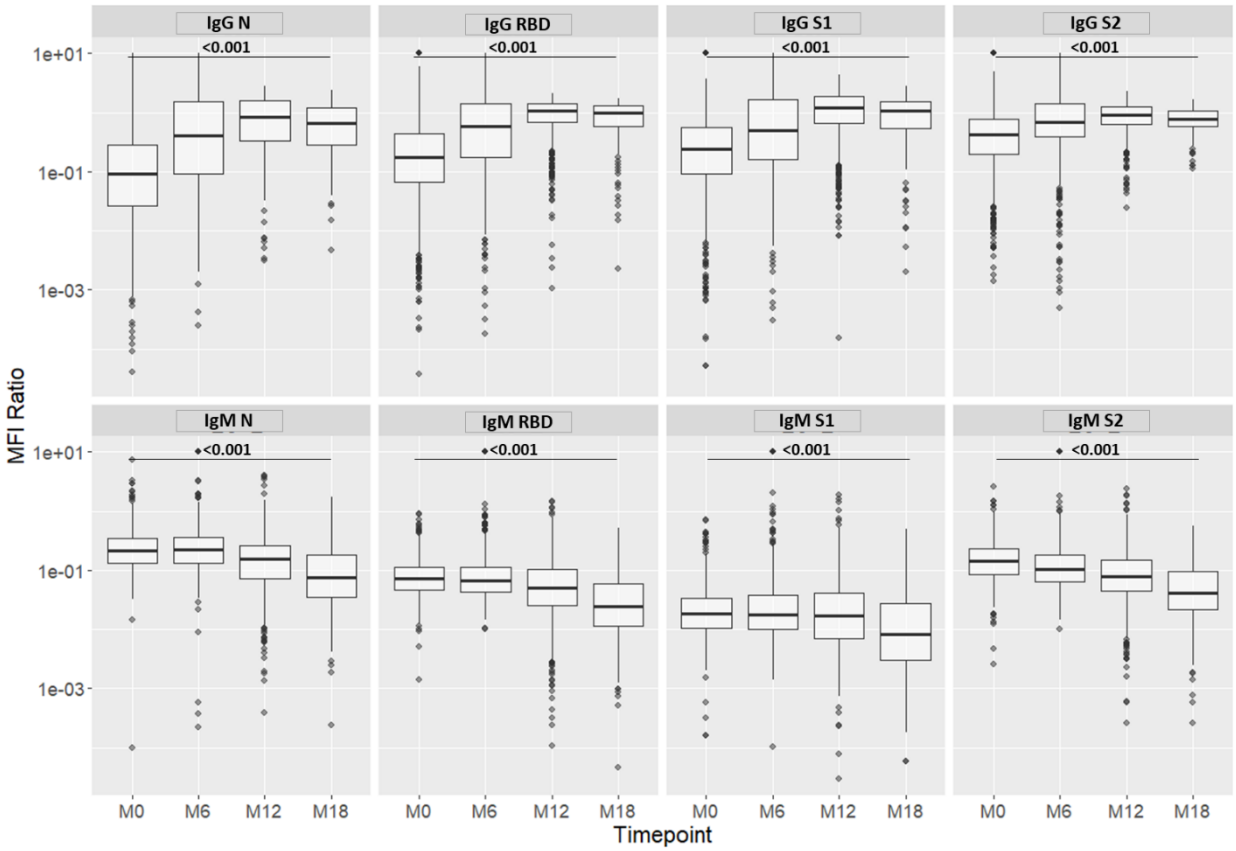

Figure 6: Evaluation of specific SARS-CoV-2 antibodies during follow up. Boxplot represents median and interquartile range in ratio of Median of Fluorescence Intensity (MFI). Each black dot represents one patient. Data were compared using the Mann-Whitney U test with Holm–Bonferroni correction method apply to adjust p-values.

Comparative analysis of non-progressors and progressors among HHC at baseline

Throughout the follow up of this cohort, 15 patients progressed to ATB. The mean age of the latter group of progressors is 31.57 years, ranging from 10 to 60 years old (Table 2). Seven among the progressors were women and 6.7% (1/15) were smokers. They did not report previous TB and 86.7% were BCG vaccinated versus 93% for non-progressors. The T.SPOT-TB results seem to show a higher seropositivity result for progressors (73.3%) than for non-progressors (49.5%), but the difference was not significant.

Table 2: Sociodemographic data of progressors versus non progressors at baseline

	Non Progressors	Progressors	p-value
	N=959	N=15	
Age (years) mean (SD)	23.84 (17.74)	31.57 (15.45)	0.094
Age group N (%)			0.346
[0-5]	81 (8.4)	0 (0.0)	0.481
]5-10[	151 (15.7)	0 (0.0)	0.189
[10-25[	372 (38.8)	7 (46.7)	0.723
[25-40[	179 (18.7)	5 (33.3)	0.268
[40-60[	126 (13.1)	2 (13.3)	1.000
> 60	50 (5.2)	1 (6.7)	1.000
Sex (Female) N (%)	558 (58.2)	7 (46.7)	0.527
Smoking N (%)	87 (9.1)	1 (6.7)	1.000
BMI at Baseline mean (SD)	20.20 (12.69)	20.36 (4.15)	0.961
Previous TB history N (%)	932 (97.2)	15 (100.0)	0.805
BCG vaccinated N (%)	892 (93.0)	13 (86.7)	0.477
HIV Negative N (%)	931 (99.0)	15 (100.0)	1.000
TST N (%)			0.288
< 5 mm	236 (24.8)	2 (14.3)	0.552
5 à 10 mm	78 (8.2)	0 (0.0)	0.533
>=10mm	637 (67.0)	12 (85.7)	0.232
QFT-P N (%)			0.609
Positive	523 (58.0)	9 (60.0)	1.000
Negative	324 (35.9)	6 (40.0)	0.956
Indeterminate	55 (6.1)	0 (0.0)	0.661
T.SPOT-TB N (%)			0.153
Positive	463 (49.5)	11 (73.3)	0.115
Negative	400 (42.7)	4 (26.7)	0.324
Indeterminate	73 (7.8)	0 (0.0)	0.524
IGRA Positive N (%)	373 (61.7)	8 (72.7)	0.663
IgM Positive N (%)	508 (51.3)	5 (46,7)	0.921
IgG Positive N (%)	711 (72.2)	12 (78,6)	0.818

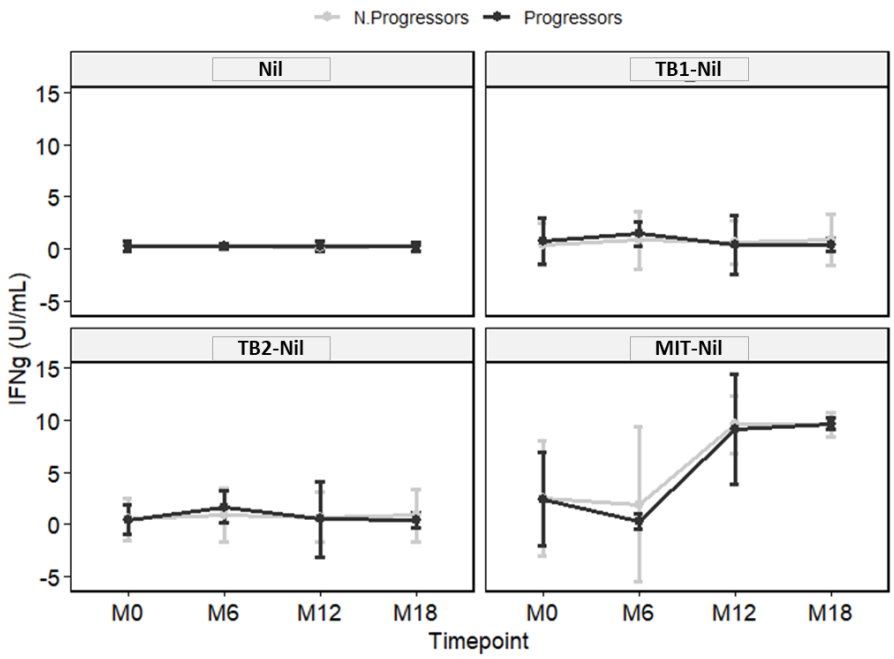

Figure 7: Evaluation of IFN-γ response during follow up. Dots represent median and interquartile range in UI/mL. Progressors are in grey and non-progressors in black.

Subsequently, analysis on the quantitative data for TB infection and SARS-CoV-2 infection were performed.

IFN-γ levels in TB1 and TB2 minus negative control (Nil) were analysed in non-progressors and progressors (Figure 7). TB1-Nil and TB2-Nil showed a slight increase in IFN-γ at M6 before a decrease to baseline. A similar trend was observed between progressors and non-progressors. No significant difference was observed between these two groups of patients.

Furthermore, serological data from anti-SARS-CoV-2 antibody assays were used to compare progressors and non-progressors (Table 3).

We compared the medians between progressors and non-progressors for anti-S1, anti-S2, anti-RBD and anti-N IgG and IgM. During follow-up, IgM, regardless of the target, decreased in both groups while IgG increased over time. No significant difference was observed between progressors and non-progressors (Table 3).

Table 3: comparative analysis between progressors and non-progressors

		Non-progressors	Progressors	
		Median	Median	*p-value*
IgM N				
	M0	0.215	0.222	0.634
	M6	0.220	0.226	0.988
	M12	0.121	0.105	0.655
	M18	0.016	-0.004	0.840
IgM RBD				
	M0	0.071	0.062	0.898
	M6	0.066	0.057	0.817
	M12	0.045	0.044	0.748
	M18	0.014	0.008	0.400
IgM S1				
	M0	0.019	0.024	0.935
	M6	0.017	0.016	0.607
	M12	0.014	0.020	0.480
	M18	0.006	0.002	0.276
IgM S2				
	M0	0.146	0.104	0.232
	M6	0.104	0.164	0.665
	M12	0.072	0.073	0.866
	M18	0.027	0.040	0.961
IgG N				
	M0	0.025	0.089	0.449
	M6	0.145	0.027	0.246
	M12	0.811	0.429	0.193
	M18	0.657	0.555	0.864
IgG RBD				
	M0	0.125	0.211	0.179
	M6	0.416	0.054	0.077
	M12	1.047	0.886	0.418
	M18	0.979	0.906	0.900
IgG S1				
	M0	0.117	0.214	0.196
	M6	0.310	0.049	0.051
	M12	1.169	1.139	0.678
	M18	1.033	0.997	0.967
IgG S2				
	M0	0.333	0.379	0.579
	M6	0.596	0.302	0.419
	M12	0.908	0.718	0.314
	M18	0.780	0.926	0.752

Discussion:

The purpose of this study is to assess the impact of COVID infection on the outcome of TBI. First, the seroprevalence of SARS-CoV-2 infection was assessed, in the context of a pandemic in Madagascar just after a first wave of COVID-19. Our results revealed a high prevalence of anti-SARS-CoV-2 antibodies in the cohort. This seroprevalence remains quite high with 77.26% and 75.44% of IgG positive responses for ATB and HHC respectively at baseline. This is not surprising as a similar seroprevalence has been previously reported for the Malagasy population[172,173]. The HHC were followed up to 18 months. 15 among them progressed to ATB. A high prevalence of IgG antibodies was observed among those progressors reaching 78.6% (12/15).

Children under 5 years of age in the present cohort, generally had relatively lower IFN-γ responses following QFT-P or T.SPOT-TB than was obtained in the other groups. This is probably related to the fact that between 0-5 years, the functional capacity of the immune system appears to be limited, leading to a reduced capacity to generate protective cellular and humoral immunity after immunisation and an increased risk of disease[174].

It is known that men, people over 65 years old and smokers are at greater risk of progressing to a critical or fatal condition as a result. Co-morbidities such as hypertension, diabetes, cardiovascular disease and respiratory disease can also significantly affect the prognosis of COVID-19. Recent studies have shown that tuberculosis is one of those comorbidities. Indeed, studies have reported how the severity of COVID was affected by TB[175].

However, little information remains available on the relationship between COVID-19 and tuberculosis. We analysed antibodies response over the 18 month follow up between progressors and non-progressors. No significant difference was found between progressors and non-progressors. There is still slight information about the impact that Covid may have on TBI. A study conducted by Motta et al. reported coincident TB in their own cohort and in an earlier co-infection cohort, suggesting that

TB may not be a major determinant of mortality[176]. Another one reported a series of cases of nosocomial transmission of SARS-CoV-2 among patients hospitalised with TB, noting that they are generally unaffected[177].

In a meta-analysis, Sarkar et al. colleagues concluded that patients with TB have an increased risk of mortality when co-infected with SARS-CoV-2 (hazard ratio = 2.10 CI, 1.75-2.51)[178]. In Zambia a post-mortem surveillance study reported the presence of TB in 22/71 (31%) of patients who died with a positive SARS-CoV-2 RT-PCR testing[179].

According to an Italian study, LTBI/TB results were not affected by COVID-19 in Italian TB reference centres during the first pandemic wave. Other more cell-based studies report higher IFN-γ production in TBI/COVID co-infected patients compared to covid-only patients[170].

To our knowledge, this is the only study reporting a longitudinal follow up of HHC of TB patients in order to investigate the possible correlation between COVID infection and TB progression. The results we present in this study remain mostly descriptive at the moment, given that the follow-up of the cohort has not yet been completed. We are considering a modelling approach applied to these data in order to capture to the dynamics of TB and SARS-CoV-2 infection. The present study was focus in the humoral response to SARS-CoV-2 infection, we plan to analyse the cellular response of SARS-CoV-2 patients of these progressors. Further effort is therefore needed to better understand the impact of COVID infection and TB progression.

Materials and methods

Study design and population

All the participants were recruited in Analamanga region of Madagascar. Between December 2020 and December 2021, active TB patients (ATB) were enrolled from the individuals presenting TB symptoms addressed for TB diagnosis at several anti-tuberculosis centres of Madagascar. Inclusion criteria for ATB are pulmonary TB diagnosed patients adult, ≥18 years old patients identified using both bacteriological and/or molecular tests, ie. scoring positive for pulmonary TB with Mtb detection either by sputum smear microscopy and/or by Xpert MTB/RIF Ultra and/or sputum culture on Lowenstein-Jensen (LJ) media.

Household contacts (HHC), of these ATB patients were recruited as a group of clinically asymptomatic adults without any sign of TB and living under the same roof. For the study, QuantiFERON-TB Gold (QFT-P -P) plus and T.SPOT-TB assay were performed on the HHC and those positive to QFT-P -P (ie. IFN-γ production ≥ 0.35 IU/mL in response to TB1 and TB2 stimulation) and positive T.SPOT-TB test results were classified in the IGRA positive group. A total of 4 visits were carried out per household over a 18-month period, at the baseline (M0), 6 months (M6) after enrolment, 12 months (M12) and 18 months (M18). Blood sampling was performed at each visit.

HHC progressors from TBI towards active TB disease during the 18-month project period, were referred to the nearest TBSC, where they received anti-tuberculous treatment and a personalized clinical follow-up.

Blood collection process.

All tests and clinical evaluations are carried out within the framework of the conventional screening and management algorithm defined by the NTCP of Madagascar. At baseline (study enrolment) a whole-blood sample will be drawn from a consent ATB case for testing IGRA (QuantiFERON-TB Gold plus, T-SPOT TB) and a nasopharyngeal swab will be done for SARS-CoV-2 diagnostic.

A minimum of 9 ml of peripheral whole blood were collected from each participant: 1ml was collected in EDTA tubes for HIV testing and COVID-19 serological testing, and 8ml were drawn in Lithium heparin tubes for IGRA.

For QFT-P assay, 1mL of whole blood was collected directly into each of the four QFT-P tubes (Qiagen, Hilden, Germany, 622526) provided by the QFT-P -P kit (Nil: Negative Control, TB-Antigens (TB1/TB2) and Mitogen: Positive control). After 16–24 h incubation at 37 °C, plasma samples were harvested and stored at − 80 °C prior to measures using QFT-P ELISA Kit (Qiagen, Hilden, Germany, 622120), according to the manufacturer instructions. Briefly, 50µL of plasma samples were used and optical density (OD) results were compared to log-normalized values from a freshly reconstituted IFN-γ standard kit. To consider any potential immunomodulation phenomena unrelated with TB treatment, baseline IFN-γ level values (Nil tubes) were subtracted from antigen-stimulated IFN-γ values (TB1, TB2 and Mitogen). According to the kit's sensitivity range, the maximum for IFN-γ level values was set at 10 IU/mL and negative values were rescaled to zero.

For T.SPOT-TB assay (Oxford Immunotec, Ltd., Abingdon, UK), PBMCs were isolated from whole blood, about 1 million cells used for assay 250000cells per condition. Briefly, the cell suspension was seeded onto T-SPOT.TB plates and incubated with ESAT-6 (Panel A), CFP-10 (Panel B), positive control, or negative control, respectively. A 100 µl cell suspension was then added into corresponding microwells, and these were cultured in an incubator with 5% CO2 at 37 °C. Microwells were then washed with phosphate buffer solution (PBS), before adding secondary antibody solution into each well, and the assay was incubated for 1 h at 2–8 °C. Subsequently, revelation step by adding chromogenic agent. Plate was incubated in de dark for 7 to 12 min before termination with distilled water. The spots were counted measured, using AID EliSpot/FluoroSpot Reader Systems (Advanced Imaging Devices GmbH Strassberg Germany). Spots results were interpreted according to the manufacturer manual.

IGRA status was defined using QFT-P and T.SPOT-TB. An individual is considered as IGRA positive with a positive test for QFT-P and for T.SPOT-TB and the IGRA negative when the QFT-P result and T.SPOT-TB result are both negative

COVID-19 serodiagnosis testing

We used the Luminex xMAP® assay described previously in the section 3 of the chapter 2

Statistical analysis

Data were analysed using R studio (2022.07.2). The Shapiro-Wilk test showed that antibodies MFI were non-normally distributed. Therefore, comparisons between groups were made using the Mann-Whitney U test or Wilcoxon signed rank test. For anti-SARS-CoV-2 antibody seroprevalence analysis, a fisher exact test was performed to compare groups. Statistical comparison on sociodemographic data weas performed with Pearson's Chi-squared test.

Chapter 3: Discussion and perspectives

1. Performance of RISK6 test for TB diagnosis and monitoring of treatment response

TB remains one of the major infectious causes of death globally. In this study, we aimed to evaluate the performance of the RISK6 signature[149], in a blood-based RT-PCR test from six-gene human transcriptomic signature, to detect TB and to monitor the TB treatment.

We evaluated the performance of RISK6 signature as a screening test for TB and showed that it displayed similar performance in the four different cohorts including Bangladesh, Madagascar, Georgia and Lebanon with near-identical ROC AUC values (>0.90). Furthermore, RISK6 signature satisfied the TPP minimum criteria set by the WHO for a non–sputum-based screening test[11]. Notably, the RISK6 signature showed an acceptable performance as a screening test for discriminating between ATB patients and HD. Moreover, while RISK6 signature seems to meet or exceeded the WHO TPP criteria, only two among the previous signatures (Sweeney3 and Sambarey10) satisfied the sensitivity and specificity set by the WHO for a triage test[93,180,181]. Besides, while these previous signatures have shown promise as diagnostic tests, it should be noted that results of a three gene signature were not generalizable, while other signatures require measurement of a high number of genes, thus limiting their possible application in resource-limited settings[93,143].

We also showed that the RISK6 signature allowed to distinguish the participants into TB infection clinical groups. The RISK6 signature demonstrated indeed a significantly higher score in ATB individuals at baseline compared to those with LTBI (IGRA-positive based). In addition a 20-gene signature set that also discriminated ATB patients from LTBI and healthy controls[182]. In our study, at >90% sensitivity, RISK6 signature discriminated ATB from both LTBI and HD with a specificity >70% which met the WHO TPP for a triage test for TB. This is consistent with a previous study showing that a 3-gene transcriptomic signature was significantly higher in ATB patients versus LTBI individuals[93].

An additional observation from our study is that RISK6 signature scores directly correlate with sputum smear grade. This may represent a useful tool in the identification of patients with high transmission risk.

Data obtained from the RISK6 signature is consistent with previous studies suggesting that transcriptomic signatures could be used as a powerful tool to monitor TB treatment response[142,145,180]. When used to monitor the TB treatment, we showed that the RISK6 signature scores returned to baseline levels (similar to scores observed in the HD participants) after the completion of the 6 months TB treatment , which confirmed previous data published by Penn-Nicholson et al., but contrasted with another transcriptomic study showing that normal levels were reached 12 months after the treatment initiation[142,149].

The RISK6 signature relies on the use of qRT-PCR that detects acceptable levels of gene expression that allow to be integrated into clinical poor settings in contrast to other complex methods. These genes can be used as alternatives or to strengthen existing closed RT-PCR systems like the Genexpert-HR that uses the 3-gene signature[154].Besides, this signature requires the measurement of a small number of genes with subsequent reduced complexity and costs. Moreover, a key advantage of RISK6 is that it is a blood-based test, which is an easily accessible sample. Blood transcriptomic tests will improve the diagnosis of TB allowing faster treatment and thus reduction of transmission, especially in children, HIV co-infected TB patients. In such populations, microbiological tests are not always feasible due to the limited ability to produce good quality sputum samples or due to low bacterial loads in their samples.

This study highlights the performance of a 6 genes signature promising for TB diagnosis, that can be used has a non-sputum-based test validation studies are needed for children and HIV-positive patients.

2. A 4 host protein biomarkers signature for diagnosis and monitoring of treatment response

In the second part of results obtained from this work, a four plasma host biomarkers signature for TB diagnosis and treatment monitoring was described and assesed. We evaluated the plasma protein expression variations of seven proteins in respectively patients with ATB or TBI compare to healthy donors. Among the seven proteins targeted, we identified a signature of four plasma proteins useful for both TB diagnostic and treatment monitoring. To date, few studies have demonstrated the existence of a unique signature fulfilling the WHO TPPs recommendations for both purposes[11]. In the present study, the protein markers expression in the plasma were assessed using a multiplex assay developed for both TB detection and treatment monitoring. The four host-plasma marker signatures (ECM1-CLEC3B-IP10-SELL) selected in our study would meet the recommendations for a non-sputum-based assay, however, it needs to be evaluated in a larger scale sample size study population, allowing to better define the diagnostic/prognostic performance of this assay. The identified signature might be of interest to identify at baseline patients who would require close follow-up during the intensive phase of treatment. The use of this type of marker could also help refine therapeutic trials aimed at shortening treatment or evaluating shorter TB treatment regimens. We showed that the four host-plasma marker signatures generated the best AUC to discriminate 1) ATB from HD groups (95% sensitivity and 92% specificity), and 2) fast vs slow sputum culture converters at baseline (83% sensitivity and 84% specificity). However, these results need to be validated in larger scale studies using diverse endemic and genetically different populations to further appreciate the robustness of the biosignatures. Host biomarkers detection from plasma might be of interest for the diagnosis of paucibacillary forms of TB (i.e., childhood TB and/or extra-pulmonary TB). One of the main advantages of this test is that it is plasma-based, which is an easily accessible sample, beside the simplicity of the technology (ELISA) that implies reduced costs. This test could be further translated into a point of care test

using DBS, which is even more convenient in terms of transportation and volume of sample, especially in low and middle-income countries.

3. Cross-impact study between SARS-CoV-2 and tuberculosis infections

We developed a multiplex assay to detect human anti-S1, anti-S2, anti-RBD and anti-N IgM and IgG antibodies. With this serodiagnosis assay, we evaluated the seroprevalence of SARS-CoV-2 infection in a population of TB patients and their household contacts. Our results revealed a high prevalence of anti-SARS-CoV-2 antibodies in the cohort (over 70% for IgG). This seroprevalence was similar between ATB and HHC. The same trend was reported among progressors. When assessing the correlation between SARS-CoV-2 infection and progression to active TB, no statistical differences were observed between the humoral response and the progression to active disease, suggesting that a SARS-CoV-2 infection is not a risk factor for TB.

In a study published by Petrone et al., the results showed that patients with symptomatic COVID-19 and latent or active TB infection had significantly higher IFN-γ levels in response to the TB1 and TB2 antigens of QuantiFERON-TB Gold plus, compared with patients with COVID-19 alone[170]. Moreover, patients with COVID-19 or COVID-19 and TBI expressed significantly more IFN-γ in response to SARS-CoV-2 antigen compared to patients with COVID-19/active TB co-infection[170]. These results are quite different from what we found. Compared to our work, this study is describing IFN response in patients still infected with COVID-19.

However, we did not investigate further the cellular responses where more complex relationship and risk were described[169]. Indeed, they found that COVID-19 patients displayed reduced frequency of Mycobacterium tuberculosis–specific CD4+ T cells, with possible implications for TB disease progression[169]. Therefore, if these results are confirmed by other studies, it would be very reassuring for patients as we know that COVID-19 has already had a great effect on the management of TB in this world, but we were not / still not sure of the impact at the clinical and biological level.

4. The future of TB diagnosis

Finding innovative and more effective diagnostic tools can be a breaking point to tackle the TB outbreak worldwide. These advances in biomarkers and diagnostics are fully in line with the latest WHO recommendations to reduce the testing time and simplifying the use of these tools by dispensing with sputum to allow more efficient screening and more accessible testing. This last point is very important because in some countries with a high incidence of TB but very limited ressources (i.e., Madagascar), which are also less developed countries, where accessibility to diagnostics is a real challenge. There is a lack of simple, rapid and inexpensive tests that can be implemented in laboratories in low-resource countries. Recently developed innovative tools, such as the detection of molecular markers of LAM in exhaled breath condensate samples, face mask samples or the detection of blood biomarkers, represent the future of TB diagnosis. Such tools, once validated in terms of diagnostic performance, would allow for easier and less invasive screening of patients, which would also lead to faster identification and management of TB patients. However, despite advances in TB diagnostic research, there is still room for improvement, especially in the diagnosis of TB in vulnerable populations such as children.

In publication 1 of the present work, we demonstrated the performance of the RISK6 host gene signature as a non-sputum-based diagnostic test that responds to the WHO TPP diagnostic test. This tool, based on RTqPCR, is easy to implement in countries. This tool has been tested in 4 different settings. In publication 2, we describe a signature based on host proteins to discriminate between ATB and HD, ATB and TBI and also to predict the response to treatment. This test was developed on a Luminex platform using a small amount of plasma (i.e., 10 µL). Finally, we have developed a serodiagnosis test for SARS-CoV-2 based on Luminex technology. The tool is fully developed and validated in Madagascar and provides information on the time of infection and the presentation of symptoms. Based on this test another improvement has been made,

allowing differentiation of infection caused by a VOC. These tests have been designed and developed by researchers. However, there is a huge gap between the innovative breakthroughs made in the laboratories and the tests that are commercially available. There is a big effort to be made to fill this breach.

Still in this perspective of making tests simple and affordable to the populations, the above-mentioned tests are being evaluated on the basis of DBS which uses less blood and raises less constraints of preservation but also on simpler devices such as automated PCR cartridges. We hope that the results of these studies will be beneficial for the future.

Conclusion

Tuberculosis remains a global health concern. It is now more important than ever to eradicate this disease due to the damage it causes and despite the existing tools available to tackle it. Developing point-of-care, biomarker-based, non-sputum-based diagnostics is a major priority. In the present thesis project, we evaluated and identified molecular biomarker signatures for the diagnosis and treatment monitoring of TB.

This study provides strong evidence in the performance of molecular markers as non-sputum-based tool for triage and treatment monitoring, meeting the WHO TPP criteria. The two biosignature describe here are host response-based signature enabling to stratify patients according to their TB infection status, as well as for monitoring patients during treatment.

Furthermore, the results suggested that the presence of specific anti-SARS-CoV-2 humoral response does not correlate with risk of disease progression in TB household contacts. This represents a positive point, as we know that the COVID-19 pandemic has caused much concern in the management of TB. Further research is needed to better characterise the specific cellular response of co-infected patients.

The results obtained in this study need to be confirmed by larger clinical studies. The implementation of non-sputum-based tests using host biomarkers in resource-limited countries and in countries with the highest incidence of TB could contribute to improving the diagnosis and overall management of TB. Indeed, these simple tests are much needed to reduce the spread and transmission of the disease.

This work has allowed us to bring evidence to the science and control of TB through innovative approaches to the diagnosis of TB but also to the understanding of TB/COVID co-infection and the risk of progression. However, this result should be confirmed in larger cohorts. And above all, a validation step of the tool would be essential. It is only once validated that these tools could be optimised and improved in

formats and technological means more adapted to resource-poor countries where TB diagnosis could be simplified and thus participate in the control and eradication of this disease.

References

1. World Health Organization. Global tuberculosis report 2021 [Internet]. Geneva: World Health Organization; 2021 [cited 2022 Jan 12]. Available from: https://apps.who.int/iris/handle/10665/346387

2. World Health Organization. Global tuberculosis report 2022 [Internet]. Geneva: World Health Organization; 2022 [cited 2022 Oct 31]. Available from: https://apps.who.int/iris/handle/10665/363752

3. Pai M, Behr MA, Dowdy D, Dheda K, Divangahi M, Boehme CC, et al. Tuberculosis. Nat Rev Dis Primers. 2016 Dec 22;2(1):16076.

4. The end TB strategy [Internet]. [cited 2022 Aug 26]. Available from: https://www.who.int/publications-detail-redirect/WHO-HTM-TB-2015.19

5. Goletti D, Arlehamn CSL, Scriba TJ, Anthony R, Cirillo DM, Alonzi T, et al. Can we predict tuberculosis cure? What tools are available? European Respiratory Journal [Internet]. 2018 Nov 1 [cited 2022 Jun 6];52(5). Available from: https://erj.ersjournals.com/content/52/5/1801089

6. Parrish NM, Carroll KC. Role of the Clinical Mycobacteriology Laboratory in Diagnosis and Management of Tuberculosis in Low-Prevalence Settings. Journal of Clinical Microbiology. 2011 Mar;49(3):772–6.

7. Davies PDO, Pai M. The diagnosis and misdiagnosis of tuberculosis [State of the art series. Tuberculosis. Edited by I. D. Rusen. Number 1 in the series]. The International Journal of Tuberculosis and Lung Disease. 2008 Nov 1;12(11):1226–34.

8. Steingart KR, Schiller I, Horne DJ, Pai M, Boehme CC, Dendukuri N. Xpert® MTB/RIF assay for pulmonary tuberculosis and rifampicin resistance in adults. Cochrane Database of Systematic Reviews [Internet]. 2014 [cited 2022 Dec 29];(1). Available from: https://www.cochranelibrary.com/cdsr/doi/10.1002/14651858.CD009593.pub3/full

9. Nogueira BMF, Krishnan S, Barreto-Duarte B, Araújo-Pereira M, Queiroz ATL, Ellner JJ, et al. Diagnostic biomarkers for active tuberculosis: progress and challenges. EMBO Molecular Medicine. 2022 Dec 7;14(12):e14088.

10. MacLean E, Broger T, Yerlikaya S, Fernandez-Carballo BL, Pai M, Denkinger CM. A systematic review of biomarkers to detect active tuberculosis. Nat Microbiol. 2019;4(5):748–58.

11. Branigan D, Deborggraeve S, Kohli M, MacLean E, McKenna L, Ruhwald M. Steady progress to bring TB diagnosis closer to the point of care. 2021;42.

12. Kik SV, Schumacher S, Cirillo DM, Churchyard G, Boehme C, Goletti D, et al. An evaluation framework for new tests that predict progression from tuberculosis infection to clinical disease. European Respiratory Journal [Internet]. 2018 Oct 1 [cited 2022 Dec 29];52(4). Available from: https://erj.ersjournals.com/content/52/4/1800946

13. World Health Organization. Consensus meeting report: development of a target product profile (TPP) and a framework for evaluation for a test for predicting progression from tuberculosis infection to active disease [Internet]. World Health Organization; 2017 [cited 2022 Dec 29]. Report No.: WHO/HTM/TB/2017.18. Available from: https://apps.who.int/iris/handle/10665/259176

14. Denkinger CM, Kik SV, Cirillo DM, Casenghi M, Shinnick T, Weyer K, et al. Defining the needs for next generation assays for tuberculosis. J Infect Dis. 2015 Apr 1;211 Suppl 2(Suppl 2):S29-38.

15. World Health Organization. Global tuberculosis report 2020 [Internet]. Geneva: World Health Organization; 2020 [cited 2022 Jan 12]. Available from: https://apps.who.int/iris/handle/10665/336069

16. Hershkovitz I, Donoghue HD, Minnikin DE, May H, Lee OYC, Feldman M, et al. Tuberculosis origin: The Neolithic scenario. Tuberculosis. 2015 Jun;95:S122–6.

17. Gutierrez MC, Brisse S, Brosch R, Fabre M, Omaïs B, Marmiesse M, et al. Ancient Origin and Gene Mosaicism of the Progenitor of Mycobacterium tuberculosis. Ramakrishnan L, editor. PLoS Pathog. 2005 Aug 19;1(1):e5.

18. Sakula A. Robert Koch: centenary of the discovery of the tubercle bacillus, 1882. Thorax. 1982 Apr 1;37(4):246–51.

19. Frith J. History of Tuberculosis. Part 1 - Phthisis, consumption and the White Plague. 2014;22(2):7.

20. texte AA du, Ibn Sīnā A Ḥusayn ibn ʿAbd A (0980 1037) A du texte. Le Canon d'Avicenne. [Internet]. 1447 [cited 2022 Dec 8]. Available from: https://gallica.bnf.fr/ark:/12148/btv1b84061787

21. Henri Boisvert. La découverte du bacille de la tuberculose par Robert Koch. Histoire des sciences médicales [Internet]. 1982 [cited 2022 Dec 29]; Available from: https://www.biusante.parisdescartes.fr/sfhm/hsm/HSMx1982x016x002/HSMx1982x016x002x0093.pdf

22. Mazana JS. Tuberculosis and its eponyms: Charles Mantoux (1877-1947). Revista Española de Sanidad Penitenciaria. 2009;11(1):17–23.

23. Duthie MS, Reed SG. Skin tests for the detection of Mycobacterial infections: achievements, current perspectives, and implications for other diseases. Appl Microbiol Biotechnol. 2021;105(2):503–8.

24. LUCA S, MIHAESCU T. History of BCG Vaccine. Maedica (Bucur). 2013 Mar;8(1):53–8.

25. Sakula A. Selman Waksman (1888–1973), discoverer of streptomycin: A centenary review. British Journal of Diseases of the Chest. 1988 Jan;82:23–31.

26. Chakraborty S, Rhee KY. Tuberculosis Drug Development: History and Evolution of the Mechanism-Based Paradigm. Cold Spring Harb Perspect Med. 2015 Aug;5(8):a021147.

27. F. Barnes P, A. Barrows S. Tuberculosis in the 1990s. Annals of Internal Medicine [Internet]. 1993 [cited 2022 Dec 29]; Available from: https://www.acpjournals.org/doi/10.7326/0003-4819-119-5-199309010-00009

28. Cole ST, Brosch R, Parkhill J, Garnier T, Churcher C, Harris D, et al. Deciphering the biology of Mycobacterium tuberculosis from the complete genome sequence. Nature. 1998 Jun;393(6685):537–44.

29. Brosch R, Gordon SV, Marmiesse M, Brodin P, Buchrieser C, Eiglmeier K, et al. A new evolutionary scenario for the Mycobacterium tuberculosis complex. Proceedings of the National Academy of Sciences. 2002 Mar 19;99(6):3684–9.

30. TB profile [Internet]. [cited 2022 Dec 8]. Available from: https://worldhealthorg.shinyapps.io/tb_profiles/?_inputs_&entity_type=%22country%22&lan=%22EN%22&iso2=%22MG%22

31. Madagascar Overview [Internet]. World Bank. [cited 2022 Dec 29]. Available from: https://www.worldbank.org/en/country/madagascar/overview

32. Chandra RK. Nutrition, immunity and infection: From basic knowledge of dietary manipulation of immune responses to practical application of ameliorating suffering and improving survival. Proc Natl Acad Sci U S A. 1996 Dec 10;93(25):14304–7.

33. Gupta KB, Gupta R, Atreja A, Verma M, Vishvkarma S. Tuberculosis and nutrition. Lung India. 2009;26(1):9–16.

34. Turner RD, Bothamley GH. Cough and the Transmission of Tuberculosis. The Journal of Infectious Diseases. 2015 May 1;211(9):1367–72.

35. Wurie FB, Lawn SD, Booth H, Sonnenberg P, Hayward AC. Bioaerosol production by patients with tuberculosis during normal tidal breathing: implications for transmission risk. Thorax. 2016 Jun 1;71(6):549–54.

36. Gralton J, Tovey E, McLaws ML, Rawlinson WD. The role of particle size in aerosolised pathogen transmission: A review. Journal of Infection. 2011 Jan 1;62(1):1–13.

37. C. B. Beggs, C. J. Noakes, P. A. Sleigh, L. A. Fletcher, K. Siddiqi JW. The transmission of tuberculosis in confined spaces: an analytical review of alternative epidemiological models. JAMA: The Journal of the American Medical Association. 2003;280(13):1200-a-1200.

38. Johnson KR, Braden CR, Cairns KL, Field KW, Colombel AC, Yang Z, et al. Transmission of Mycobacterium tuberculosis from medical waste. JAMA. 2000 Oct 4;284(13):1683–8.

39. Sharma SK, Mohan A, Kohli M. Extrapulmonary tuberculosis. Expert Review of Respiratory Medicine. 2021 Jul 3;15(7):931–48.

40. O'Garra A, Redford PS, McNab FW, Bloom CI, Wilkinson RJ, Berry MPR. The Immune Response in Tuberculosis. Annual Review of Immunology. 2013;31(1):475–527.

41. Dheda K. Tuberculosis, A practical guide to diagnosis and management of latent and active TB. Biomérieux. 2022;16076.

42. Supply P, Brosch R. The Biology and Epidemiology of Mycobacterium canettii. Adv Exp Med Biol. 2017;1019:27–41.

43. de Jong BC, Antonio M, Gagneux S. Mycobacterium africanum—Review of an Important Cause of Human Tuberculosis in West Africa. PLoS Negl Trop Dis. 2010 Sep 28;4(9):e744.

44. Silva ML, Cá B, Osório NS, Rodrigues PNS, Maceiras AR, Saraiva M. Tuberculosis caused by Mycobacterium africanum: Knowns and unknowns. PLoS Pathog. 2022 May 26;18(5):e1010490.

45. Smith NH, Crawshaw T, Parry J, Birtles RJ. Mycobacterium microti: More Diverse than Previously Thought. J Clin Microbiol. 2009 Aug;47(8):2551–9.

46. Rodríguez S, Bezos J, Romero B, de Juan L, Álvarez J, Castellanos E, et al. Mycobacterium caprae Infection in Livestock and Wildlife, Spain. Emerg Infect Dis. 2011 Mar;17(3):532–5.

47. Pérez de Val B, Perea C, Estruch J, Solano-Manrique C, Riera C, Sanz A, et al. Generalized tuberculosis due to Mycobacterium caprae in a red fox phylogenetically related to livestock breakdowns. BMC Vet Res. 2022 Sep 20;18:352.

48. Cousins DV, Bastida R, Cataldi A, Quse V, Redrobe S, Dow S, et al. Tuberculosis in seals caused by a novel member of the Mycobacterium tuberculosis complex: Mycobacterium pinnipedii sp. nov. International Journal of Systematic and Evolutionary Microbiology. 2003 Sep 1;53(5):1305–14.

49. Ramakrishnan T, Harshey RM. Rate of ribonucleic acid chain growth in Mycobacterium tuberculosis H37Rv. J BACTERIOL. 1977;129.

50. Virulence factors of the Mycobacterium tuberculosis complex [Internet]. [cited 2022 Dec 11]. Available from: https://www.tandfonline.com/doi/epdf/10.4161/viru.22329?needAccess=true&role=button

51. Chiaradia L, Lefebvre C, Parra J, Marcoux J, Burlet-Schiltz O, Etienne G, et al. Dissecting the mycobacterial cell envelope and defining the composition of the native mycomembrane. Sci Rep. 2017 Oct 9;7(1):12807.

52. Brennan PJ. Structure, function, and biogenesis of the cell wall of Mycobacterium tuberculosis. Tuberculosis (Edinb). 2003;83(1–3):91–7.

53. Maitra A, Munshi T, Healy J, Martin LT, Vollmer W, Keep NH, et al. Cell wall peptidoglycan in Mycobacterium tuberculosis: An Achilles' heel for the TB-causing pathogen. FEMS Microbiology Reviews. 2019 Sep 1;43(5):548–75.

54. Hmama Z, Sendide K, Talal A, Garcia R, Dobos K, Reiner NE. Quantitative analysis of phagolysosome fusion in intact cells: inhibition by mycobacterial lipoarabinomannan

and rescue by an 1alpha,25-dihydroxyvitamin D3-phosphoinositide 3-kinase pathway. J Cell Sci. 2004 Apr 15;117(Pt 10):2131–40.

55. Chan J, Fan XD, Hunter SW, Brennan PJ, Bloom BR. Lipoarabinomannan, a possible virulence factor involved in persistence of Mycobacterium tuberculosis within macrophages. Infect Immun. 1991 May;59(5):1755–61.

56. Ottenhoff THM, Kaufmann SHE. Vaccines against Tuberculosis: Where Are We and Where Do We Need to Go? PLOS Pathogens. 2012 May 10;8(5):e1002607.

57. Abdallah AM, Gey van Pittius NC, DiGiuseppe Champion PA, Cox J, Luirink J, Vandenbroucke-Grauls CMJE, et al. Type VII secretion — mycobacteria show the way. Nat Rev Microbiol. 2007 Nov;5(11):883–91.

58. Reed MB, Domenech P, Manca C, Su H, Barczak AK, Kreiswirth BN, et al. A glycolipid of hypervirulent tuberculosis strains that inhibits the innate immune response. Nature. 2004 Sep;431(7004):84–7.

59. Pai M, Denkinger CM, Kik SV, Rangaka MX, Zwerling A, Oxlade O, et al. Gamma Interferon Release Assays for Detection of Mycobacterium tuberculosis Infection. Clinical Microbiology Reviews. 2014 Jan;27(1):3–20.

60. Prezzemolo T, Guggino G, La Manna MP, Di Liberto D, Dieli F, Caccamo N. Functional Signatures of Human CD4 and CD8 T Cell Responses to Mycobacterium tuberculosis. Front Immunol. 2014 Apr 22;5:180.

61. Lyadova IV, Panteleev AV. Th1 and Th17 Cells in Tuberculosis: Protection, Pathology, and Biomarkers. Mediators of Inflammation. 2015 Nov 10;2015:e854507.

62. Torrado E, Cooper AM. IL-17 and Th17 cells in tuberculosis. Cytokine Growth Factor Rev. 2010 Dec;21(6):455–62.

63. Li HM, Wang LJ, Huang Q, Pan HF, Zhang TP. Exploring the association between Th17 pathway gene polymorphisms and pulmonary tuberculosis. Frontiers in Immunology [Internet]. 2022 [cited 2022 Dec 31];13. Available from: https://www.frontiersin.org/articles/10.3389/fimmu.2022.994247

64. Keane J, Remold HG, Kornfeld H. Virulent Mycobacterium tuberculosis strains evade apoptosis of infected alveolar macrophages. J Immunol. 2000 Feb 15;164(4):2016–20.

65. Flynn JL, Chan J. Immune cell interactions in tuberculosis. Cell. 2022 Dec;185(25):4682–702.

66. Koch A, Mizrahi V. Mycobacterium tuberculosis. Trends in Microbiology. 2018 Jun;26(6):555–6.

67. Brett K, Dulong C, Severn M. Treatment of Tuberculosis: A Review of Guidelines [Internet]. Canadian Agency for Drugs and Technologies in Health; 2020 [cited 2022 May 13]. Available from: https://www.ncbi.nlm.nih.gov/books/NBK562947/

68. 2022_pipeline_TB_vaccines_final.pdf [Internet]. [cited 2022 Dec 12]. Available from: https://www.treatmentactiongroup.org/wp-content/uploads/2022/10/2022_pipeline_TB_vaccines_final.pdf

69. Wallis RS, Kim P, Cole S, Hanna D, Andrade BB, Maeurer M, et al. Tuberculosis biomarkers discovery: developments, needs, and challenges. The Lancet Infectious Diseases. 2013 Apr 1;13(4):362–72.

70. Zumla A, Wallis R, Klein N, Oleson O, Lang H, Vahedi M, et al. Joint TDR/EC expert consultation on biomarkers in tuberculosis : report of the joint TDR/EC expert consultation to evaluate the potential roles of biomarkers in the management of HIV-infected and HIV-uninfected patients with tuberculosis, Geneva, Switzerland, 2-3 July 2008 [Internet]. World Health Organization; 2009 [cited 2022 Dec 25]. Available from: https://apps.who.int/iris/handle/10665/44105

71. Gandhi NR, Nunn P, Dheda K, Schaaf HS, Zignol M, Soolingen D van, et al. Multidrug-resistant and extensively drug-resistant tuberculosis: a threat to global control of tuberculosis. The Lancet. 2010 May 22;375(9728):1830–43.

72. Lange C, Abubakar I, Alffenaar JWC, Bothamley G, Caminero JA, Carvalho ACC, et al. Management of patients with multidrug-resistant/extensively drug-resistant tuberculosis in Europe: a TBNET consensus statement. European Respiratory Journal. 2014 Jul 1;44(1):23–63.

73. Abubakar I, Pimpin L, Ariti C, Beynon R, Mangtani P, Sterne J a. C, et al. Systematic review and meta-analysis of the current evidence on the duration of protection by bacillus Calmette-Guérin vaccination against tuberculosis. Health Technol Assess. 2013 Sep;17(37):1–372, v–vi.

74. Mangtani P, Abubakar I, Ariti C, Beynon R, Pimpin L, Fine PEM, et al. Protection by BCG Vaccine Against Tuberculosis: A Systematic Review of Randomized Controlled Trials. Clinical Infectious Diseases. 2014 Feb 15;58(4):470–80.

75. Kuan R, Muskat K, Peters B, Arlehamn CSL. BCG vaccine efficacy, immune correlates of protection and antigen-specific T cell responses. J Intern Med. 2020 Dec;288(6):651–60.

76. Cobat A, Gallant CJ, Simkin L, Black GF, Stanley K, Hughes J, et al. Two loci control tuberculin skin test reactivity in an area hyperendemic for tuberculosis. J Exp Med. 2009 Nov 23;206(12):2583–91.

77. Hoff ST, Peter JG, Theron G, Pascoe M, Tingskov PN, Aggerbeck H, et al. Sensitivity of C-Tb: a novel RD-1-specific skin test for the diagnosis of tuberculosis infection. European Respiratory Journal. 2016 Mar 1;47(3):919–28.

78. LIOFeron®IGRA | Lionex [Internet]. [cited 2023 Jan 1]. Available from: https://lionex.de/product/lioferon/

79. Dong Y, Demaria S, Sun X, Santori FR, Jesdale BM, De Groot AS, et al. HLA-A2-restricted CD8+-cytotoxic-T-cell responses to novel epitopes in Mycobacterium

tuberculosis superoxide dismutase, alanine dehydrogenase, and glutamine synthetase. Infect Immun. 2004 Apr;72(4):2412–5.

80. LIAISON QuantiFERON-TB Gold Plus [Internet]. [cited 2023 Jan 1]. Available from: https://www.qiagen.com/us/products/diagnostics-and-clinical-research/tb-management/liaison-quantiferon-tb-gold-plus-us

81. Tuberculosis (TB) | The T-SPOT.TB test | Oxford Immunotec [Internet]. T-Spot International. [cited 2023 Jan 1]. Available from: https://www.tspot.com/uk/why-the-t-spot-tb-test/screening-matters/

82. Steingart KR, Henry M, Ng V, Hopewell PC, Ramsay A, Cunningham J, et al. Fluorescence versus conventional sputum smear microscopy for tuberculosis: a systematic review. Lancet Infect Dis. 2006 Sep;6(9):570–81.

83. Bishop PJ, Neumann G. The history of the Ziehl-Neelsen stain. Tubercle. 1970 Jun;51(2):196–206.

84. Kommareddi S, Abramowsky CR, Swinehart GL, Hrabak L. Nontuberculous mycobacterial infections: Comparison of the fluorescent auramine-o and Ziehl-Neelsen techniques in tissue diagnosis. Human Pathology. 1984 Nov 1;15(11):1085–9.

85. Asmar S, Drancourt M. Rapid culture-based diagnosis of pulmonary tuberculosis in developed and developing countries. Front Microbiol. 2015 Nov 3;6:1184.

86. Dinnes J, Deeks J, Kunst H, Gibson A, Cummins E, Waugh N, et al. A systematic review of rapid diagnostic tests for the detection of tuberculosis infection. Health Technol Assess. 2007 Jan;11(3):1–196.

87. Agarwal S, Caplivski D, Bottone EJ. Disseminated tuberculosis presenting with finger swelling in a patient with tuberculous osteomyelitis: a case report. Annals of Clinical Microbiology and Antimicrobials. 2005 Nov 3;4(1):18.

88. World Health Organization. Lateral flow urine lipoarabinomannan assay (LF-LAM) for the diagnosis of active tuberculosis in people living with HIV: policy update 2019 [Internet]. Geneva: World Health Organization; 2019 [cited 2022 Dec 13]. Available from: https://apps.who.int/iris/handle/10665/329479

89. World Health Organization. The use of lateral flow urine lipoarabinomannan assay (LF-LAM) for the diagnosis and screening of active tuberculosis in people living with HIV: policy guidance [Internet]. Geneva: World Health Organization; 2015 [cited 2022 Dec 13]. 62 p. Available from: https://apps.who.int/iris/handle/10665/193633

90. Kerkhoff AD, Sossen B, Schutz C, Reipold EI, Trollip A, Moreau E, et al. Diagnostic sensitivity of SILVAMP TB-LAM (FujiLAM) point-of-care urine assay for extra-pulmonary tuberculosis in people living with HIV. European Respiratory Journal [Internet]. 2020 Feb 1 [cited 2023 Jan 1];55(2). Available from: https://erj.ersjournals.com/content/55/2/1901259

91. Cabibbe AM, Spitaleri A, Battaglia S, Colman RE, Suresh A, Uplekar S, et al. Application of Targeted Next-Generation Sequencing Assay on a Portable Sequencing

Platform for Culture-Free Detection of Drug-Resistant Tuberculosis from Clinical Samples. J Clin Microbiol. 2020 Sep 22;58(10):e00632-20.

92. Sibandze DB, Kay A, Dreyer V, Sikhondze W, Dlamini Q, DiNardo A, et al. Rapid molecular diagnostics of tuberculosis resistance by targeted stool sequencing. Genome Med. 2022 May 19;14(1):52.

93. Sweeney TE, Braviak L, Tato CM, Khatri P. Genome-wide expression for diagnosis of pulmonary tuberculosis: a multicohort analysis. The Lancet Respiratory Medicine. 2016 Mar;4(3):213–24.

94. Togun T, Hoggart CJ, Agbla SC, Gomez MP, Egere U, Sillah AK, et al. A three-marker protein biosignature distinguishes tuberculosis from other respiratory diseases in Gambian children. EBioMedicine. 2020 Aug;58:102909.

95. Brock M, Hanlon D, Zhao M, Pollock NR. Detection of mycobacterial lipoarabinomannan in serum for diagnosis of active tuberculosis. Diagnostic Microbiology and Infectious Disease. 2020 Feb 1;96(2):114937.

96. Broger T, Tsionksy M, Mathew A, Lowary TL, Pinter A, Plisova T, et al. Sensitive electrochemiluminescence (ECL) immunoassays for detecting lipoarabinomannan (LAM) and ESAT-6 in urine and serum from tuberculosis patients. PLOS ONE. 2019 Apr 18;14(4):e0215443.

97. Kalra M, Khuller GK, Grover A, Behera D, Wanchu A, Verma I. Utility of a combination of RD1 and RD2 antigens as a diagnostic marker for tuberculosis. Diagnostic Microbiology and Infectious Disease. 2010 Feb 1;66(2):153–61.

98. Kashyap RS, Rajan AN, Ramteke SS, Agrawal VS, Kelkar SS, Purohit HJ, et al. Diagnosis of tuberculosis in an Indian population by an indirect ELISA protocol based on detection of Antigen 85 complex: a prospective cohort study. BMC Infect Dis. 2007 Jul 10;7:74.

99. Kashyap RS, Dobos KM, Belisle JT, Purohit HJ, Chandak NH, Taori GM, et al. Demonstration of Components of Antigen 85 Complex in Cerebrospinal Fluid of Tuberculous Meningitis Patients. Clinical and Vaccine Immunology. 2005 Jun;12(6):752–8.

100. Turbawaty DK, Sugianli AK, Soeroto AY, Setiabudiawan B, Parwati I. Comparison of the Performance of Urinary *Mycobacterium tuberculosis* Antigens Cocktail (ESAT6, CFP10, and MPT64) with Culture and Microscopy in Pulmonary Tuberculosis Patients. International Journal of Microbiology. 2017 Oct 18;2017:e3259329.

101. Menozzi FD, Reddy VM, Cayet D, Raze D, Debrie AS, Dehouck MP, et al. Mycobacterium tuberculosis heparin-binding haemagglutinin adhesin (HBHA) triggers receptor-mediated transcytosis without altering the integrity of tight junctions. Microbes Infect. 2006 Jan;8(1):1–9.

102. Pethe K, Alonso S, Biet F, Delogu G, Brennan MJ, Locht C, et al. The heparin-binding haemagglutinin of M. tuberculosis is required for extrapulmonary dissemination. Nature. 2001 Jul 12;412(6843):190–4.

103. Menozzi FD, Rouse JH, Alavi M, Laude-Sharp M, Muller J, Bischoff R, et al. Identification of a heparin-binding hemagglutinin present in mycobacteria. J Exp Med. 1996 Sep 1;184(3):993–1001.

104. Masungi C, Temmerman S, Van Vooren JP, Drowart A, Pethe K, Menozzi FD, et al. Differential T and B cell responses against Mycobacterium tuberculosis heparin-binding hemagglutinin adhesin in infected healthy individuals and patients with tuberculosis. J Infect Dis. 2002 Feb 15;185(4):513–20.

105. Sun Z, Nie L, Zhang X, Li Y, Li C. Mycobacterial heparin-binding haemagglutinin adhesion-induced interferon & antibody for detection of tuberculosis. Indian J Med Res. 2011 Apr;133:421–5.

106. Abebe F, Belay M, Legesse M, K L M C F, Ottenhoff THM. IgA and IgG against Mycobacterium tuberculosis Rv2031 discriminate between pulmonary tuberculosis patients, Mycobacterium tuberculosis-infected and non-infected individuals. PLoS One. 2018;13(1):e0190989.

107. Shin AR, Lee KS, Lee JS, Kim SY, Song CH, Jung SB, et al. Mycobacterium tuberculosis HBHA protein reacts strongly with the serum immunoglobulin M of tuberculosis patients. Clin Vaccine Immunol. 2006 Aug;13(8):869–75.

108. Yang CS, Lee JS, Lee HM, Shim TS, Son JW, Jung SS, et al. Differential cytokine levels and immunoreactivities against Mycobacterium tuberculosis antigens between tuberculous and malignant effusions. Respir Med. 2008 Feb;102(2):280–6.

109. Meier NR, Jacobsen M, Ottenhoff THM, Ritz N. A Systematic Review on Novel Mycobacterium tuberculosis Antigens and Their Discriminatory Potential for the Diagnosis of Latent and Active Tuberculosis. Front Immunol [Internet]. 2018 [cited 2020 Feb 25];9. Available from: https://www.frontiersin.org/articles/10.3389/fimmu.2018.02476/full

110. Delogu G, Chiacchio T, Vanini V, Butera O, Cuzzi G, Bua A, et al. Methylated HBHA produced in M. smegmatis discriminates between active and non-active tuberculosis disease among RD1-responders. PLoS One. 2011 Mar 29;6(3):e18315.

111. Chegou NN, Sutherland JS, Malherbe S, Crampin AC, Corstjens PLAM, Geluk A, et al. Diagnostic performance of a seven-marker serum protein biosignature for the diagnosis of active TB disease in African primary healthcare clinic attendees with signs and symptoms suggestive of TB. Thorax. 2016 Sep;71(9):785–94.

112. Chegou NN, Sutherland JS, Namuganga AR, Corstjens PL, Geluk A, Gebremichael G, et al. Africa-wide evaluation of host biomarkers in QuantiFERON supernatants for the diagnosis of pulmonary tuberculosis. Sci Rep. 2018 Feb 8;8(1):2675.

113. Jacobs R, Malherbe S, Loxton AG, Stanley K, van der Spuy G, Walzl G, et al. Identification of novel host biomarkers in plasma as candidates for the immunodiagnosis of tuberculosis disease and monitoring of tuberculosis treatment response. Oncotarget. 2016 Sep 6;7(36):57581–92.

114. Jacobs R, Maasdorp E, Malherbe S, Loxton AG, Stanley K, Spuy G van der, et al. Diagnostic Potential of Novel Salivary Host Biomarkers as Candidates for the Immunological Diagnosis of Tuberculosis Disease and Monitoring of Tuberculosis Treatment Response. PLOS ONE. 2016 Aug 3;11(8):e0160546.

115. Chedid C, Kokhreidze E, Tukvadze N, Banu S, Uddin MKM, Biswas S, et al. Relevance of QuantiFERON-TB Gold Plus and Heparin-Binding Hemagglutinin Interferon-γ Release Assays for Monitoring of Pulmonary Tuberculosis Clearance: A Multicentered Study. Front Immunol [Internet]. 2021 [cited 2021 Feb 2];11. Available from: https://www.frontiersin.org/articles/10.3389/fimmu.2020.616450/full?&utm_source=Email_to_authors_&utm_medium=Email&utm_content=T1_11.5e1_author&utm_campaign=Email_publication&field=&journalName=Frontiers_in_Immunology&id=616450

116. Chedid C, Kokhreidze E, Tukvadze N, Banu S, Uddin MKM, Biswas S, et al. Association of baseline white blood cell counts with tuberculosis treatment outcome: a prospective multicentered cohort study. Int J Infect Dis. 2020 Nov;100:199–206.

117. Rakotosamimanana N, Richard V, Raharimanga V, Gicquel B, Doherty TM, Zumla A, et al. Biomarkers for risk of developing active tuberculosis in contacts of TB patients: a prospective cohort study. Eur Respir J. 2015 Oct;46(4):1095–103.

118. Yong YK, Tan HY, Saeidi A, Wong WF, Vignesh R, Velu V, et al. Immune Biomarkers for Diagnosis and Treatment Monitoring of Tuberculosis: Current Developments and Future Prospects. Frontiers in Microbiology [Internet]. 2019 [cited 2022 Dec 25];10. Available from: https://www.frontiersin.org/articles/10.3389/fmicb.2019.02789

119. Adekambi T, Ibegbu CC, Cagle S, Kalokhe AS, Wang YF, Hu Y, et al. Biomarkers on patient T cells diagnose active tuberculosis and monitor treatment response [Internet]. American Society for Clinical Investigation; 2015 [cited 2022 Dec 27]. Available from: https://www.jci.org/articles/view/77990/pdf

120. Riou C, Berkowitz N, Goliath R, Burgers WA, Wilkinson RJ. Analysis of the Phenotype of Mycobacterium tuberculosis-Specific CD4+ T Cells to Discriminate Latent from Active Tuberculosis in HIV-Uninfected and HIV-Infected Individuals. Frontiers in Immunology [Internet]. 2017 [cited 2022 Dec 27];8. Available from: https://www.frontiersin.org/articles/10.3389/fimmu.2017.00968

121. Borrego F, Robertson MJ, Ritz J, Peña J, Solana R. CD69 is a stimulatory receptor for natural killer cell and its cytotoxic effect is blocked by CD94 inhibitory receptor. Immunology. 1999 May;97(1):159–65.

122. Yong YK, Tan HY, Saeidi A, Rosmawati M, Atiya N, Ansari AW, et al. Decrease of CD69 levels on TCR Vα7.2+CD4+ innate-like lymphocytes is associated with impaired cytotoxic functions in chronic hepatitis B virus-infected patients. Innate Immun. 2017 Jul 1;23(5):459–67.

123. Nikolova M, Markova R, Drenska R, Muhtarova M, Todorova Y, Dimitrov V, et al. Antigen-specific CD4- and CD8-positive signatures in different phases of Mycobacterium tuberculosis infection. Diagnostic Microbiology and Infectious Disease. 2013 Mar 1;75(3):277–81.

124. Yan ZH, Zheng XF, Yi L, Wang J, Wang XJ, Wei PJ, et al. CD137 is a Useful Marker for Identifying CD4+ T Cell Responses to Mycobacterium tuberculosis. Scand J Immunol. 2017 May;85(5):372–80.

125. Millington KA, Innes JA, Hackforth S, Hinks TSC, Deeks JJ, Dosanjh DPS, et al. Dynamic Relationship between IFN-γ and IL-2 Profile of Mycobacterium tuberculosis-Specific T Cells and Antigen Load1. The Journal of Immunology. 2007 Apr 15;178(8):5217–26.

126. Sester U, Fousse M, Dirks J, Mack U, Prasse A, Singh M, et al. Whole-Blood Flow-Cytometric Analysis of Antigen-Specific CD4 T-Cell Cytokine Profiles Distinguishes Active Tuberculosis from Non-Active States. PLOS ONE. 2011 Mar 15;6(3):e17813.

127. Sutherland JS, Adetifa IM, Hill PC, Adegbola RA, Ota MOC. Pattern and diversity of cytokine production differentiates between Mycobacterium tuberculosis infection and disease. European Journal of Immunology. 2009;39(3):723–9.

128. Ahmed MIM, Ntinginya NE, Kibiki G, Mtafya BA, Semvua H, Mpagama S, et al. Phenotypic Changes on Mycobacterium Tuberculosis-Specific CD4 T Cells as Surrogate Markers for Tuberculosis Treatment Efficacy. Frontiers in Immunology [Internet]. 2018 [cited 2023 Jan 2];9. Available from: https://www.frontiersin.org/articles/10.3389/fimmu.2018.02247

129. Streitz M, Tesfa L, Yildirim V, Yahyazadeh A, Ulrichs T, Lenkei R, et al. Loss of Receptor on Tuberculin-Reactive T-Cells Marks Active Pulmonary Tuberculosis. PLOS ONE. 2007 Aug 15;2(8):e735.

130. Adekambi T, Ibegbu CC, Kalokhe AS, Yu T, Ray SM, Rengarajan J. Distinct Effector Memory CD4+ T Cell Signatures in Latent Mycobacterium tuberculosis Infection, BCG Vaccination and Clinically Resolved Tuberculosis. PLoS One. 2012 Apr 24;7(4):e36046.

131. Mpande CAM, Rozot V, Mosito B, Musvosvi M, Dintwe OB, Bilek N, et al. Immune profiling of Mycobacterium tuberculosis-specific T cells in recent and remote infection. EBioMedicine. 2021 Feb;64:103233.

132. Hiza H, Hella J, Arbués A, Magani B, Sasamalo M, Gagneux S, et al. Case–control diagnostic accuracy study of a non-sputum CD38-based TAM-TB test from a single milliliter of blood. Sci Rep. 2021 Jun 23;11(1):13190.

133. Fang Y, Wang N, Tang L, Yang XJ, Tang Y, Li L, et al. Evaluation of Mycobacterium tuberculosis specific antigen-stimulated CD27−CD38+IFN-γ+CD4+ T cells for discrimination of active tuberculosis. BMC Infectious Diseases. 2022 Dec 1;22(1):899.

134. Estévez O, Anibarro L, Garet E, Martínez A, Pena A, Barcia L, et al. Multi-parameter flow cytometry immunophenotyping distinguishes different stages of tuberculosis infection. Journal of Infection. 2020 Jul 1;81(1):57–71.

135. Balfour A, Schutz C, Goliath R, Wilkinson KA, Sayed S, Sossen B, et al. Functional and Activation Profiles of Mucosal-Associated Invariant T Cells in Patients With Tuberculosis and HIV in a High Endemic Setting. Front Immunol. 2021;12:648216.

136. Parlato S, Chiacchio T, Salerno D, Petrone L, Castiello L, Romagnoli G, et al. Impaired IFN-α-mediated signal in dendritic cells differentiates active from latent tuberculosis. PLoS One. 2018 Jan 10;13(1):e0189477.

137. Qaqish A, Huang D, Chen CY, Zhang Z, Wang R, Li S, et al. Adoptive Transfer of Phosphoantigen-Specific γδ T Cell Subset Attenuates Mycobacterium tuberculosis Infection in Nonhuman Primates. The Journal of Immunology. 2017 Jun 15;198(12):4753–63.

138. Abebe F. Immunological basis of early clearance of Mycobacterium tuberculosis infection: the role of natural killer cells. Clinical and Experimental Immunology. 2021 Apr 1;204(1):32–40.

139. Hamada Y, Penn-Nicholson A, Krishnan S, Cirillo DM, Matteelli A, Wyss R, et al. Are mRNA based transcriptomic signatures ready for diagnosing tuberculosis in the clinic? - A review of evidence and the technological landscape. eBioMedicine. 2022 Jul 15;82:104174.

140. Mulenga H, Zauchenberger CZ, Bunyasi EW, Mbandi SK, Mendelsohn SC, Kagina B, et al. Performance of diagnostic and predictive host blood transcriptomic signatures for Tuberculosis disease: A systematic review and meta-analysis. PLoS One. 2020 Aug 21;15(8):e0237574.

141. Zak DE, Penn-Nicholson A, Scriba TJ, Thompson E, Suliman S, Amon LM, et al. A prospective blood RNA signature for tuberculosis disease risk. Lancet. 2016 Jun 4;387(10035):2312–22.

142. Berry MPR, Graham CM, McNab FW, Xu Z, Bloch SAA, Oni T, et al. An interferon-inducible neutrophil-driven blood transcriptional signature in human tuberculosis. Nature. 2010 Aug;466(7309):973–7.

143. Kaforou M, Wright VJ, Oni T, French N, Anderson ST, Bangani N, et al. Detection of Tuberculosis in HIV-Infected and -Uninfected African Adults Using Whole Blood RNA Expression Signatures: A Case-Control Study. Cattamanchi A, editor. PLoS Med. 2013 Oct 22;10(10):e1001538.

144. Mendelsohn SC, Fiore-Gartland A, Penn-Nicholson A, Mulenga H, Mbandi SK, Borate B, et al. Validation of a host blood transcriptomic biomarker for pulmonary tuberculosis in people living with HIV: a prospective diagnostic and prognostic accuracy study. Lancet Glob Health. 2021 Jun;9(6):e841–53.

145. Darboe F, Mbandi SK, Naidoo K, Yende-Zuma N, Lewis L, Thompson EG, et al. Detection of Tuberculosis Recurrence, Diagnosis and Treatment Response by a Blood Transcriptomic Risk Signature in HIV-Infected Persons on Antiretroviral Therapy. Front Microbiol. 2019 Jun 26;10:1441.

146. Scriba TJ, Fiore-Gartland A, Penn-Nicholson A, Mulenga H, Kimbung Mbandi S, Borate B, et al. Biomarker-guided tuberculosis preventive therapy (CORTIS): a randomised controlled trial. The Lancet Infectious Diseases. 2021 Jan;S1473309920309142.

147. Mendelsohn SC, Mbandi SK, Fiore-Gartland A, Penn-Nicholson A, Musvosvi M, Mulenga H, et al. Prospective multicentre head-to-head validation of host blood transcriptomic biomarkers for pulmonary tuberculosis by real-time PCR. Commun Med (Lond). 2022 Mar 10;2:26.

148. Blankley S, Graham CM, Turner J, Berry MPR, Bloom CI, Xu Z, et al. The Transcriptional Signature of Active Tuberculosis Reflects Symptom Status in Extra-Pulmonary and Pulmonary Tuberculosis. PLoS One. 2016 Oct 5;11(10):e0162220.

149. Penn-Nicholson A, Mbandi SK, Thompson E, Mendelsohn SC, Suliman S, Chegou NN, et al. RISK6, a 6-gene transcriptomic signature of TB disease risk, diagnosis and treatment response. Sci Rep [Internet]. 2020 May 25 [cited 2020 Jun 10];10. Available from: https://www.ncbi.nlm.nih.gov/pmc/articles/PMC7248089/

150. Bayaa R, Ndiaye MDB, Chedid C, Kokhreidze E, Tukvadze N, Banu S, et al. Multi-country evaluation of RISK6, a 6-gene blood transcriptomic signature, for tuberculosis diagnosis and treatment monitoring. Sci Rep. 2021 Dec;11(1):13646.

151. Turner CT, Gupta RK, Tsaliki E, Roe JK, Mondal P, Nyawo GR, et al. Blood transcriptional biomarkers for active pulmonary tuberculosis in a high-burden setting: a prospective, observational, diagnostic accuracy study. The Lancet Respiratory Medicine. 2020 Apr;8(4):407–19.

152. Moreira FMF, Verma R, Pereira dos Santos PC, Leite A, da Silva Santos A, de Araujo RCP, et al. Blood-based host biomarker diagnostics in active case finding for pulmonary tuberculosis: A diagnostic case-control study. EClinicalMedicine. 2021 Mar 6;33:100776.

153. Södersten E, Ongarello S, Mantsoki A, Wyss R, Persing DH, Banderby S, et al. Diagnostic Accuracy Study of a Novel Blood-Based Assay for Identification of Tuberculosis in People Living with HIV. J Clin Microbiol. 2021 Feb 18;59(3):e01643-20.

154. Sutherland JS, van der Spuy G, Gindeh A, Thuong NTT, Namuganga A, Owolabi O, et al. Diagnostic Accuracy of the Cepheid 3-gene Host Response Fingerstick Blood Test in a Prospective, Multi-site Study: Interim Results. Clinical Infectious Diseases. 2021 Sep 22;ciab839.

155. Hamada Y, Cirillo DM, Matteelli A, Penn-Nicholson A, Rangaka MX, Ruhwald M. Tests for tuberculosis infection: landscape analysis. European Respiratory Journal [Internet]. 2021 Nov 1 [cited 2022 Dec 26];58(5). Available from: https://erj.ersjournals.com/content/58/5/2100167

156. Ahmadzai H, Huang S, Hettiarachchi R, Lin JL, Thomas PS, Zhang Q. Exhaled breath condensate: a comprehensive update. Clinical Chemistry and Laboratory Medicine. 2013 Jul 1;51(7):1343–61.

157. Davis MD, Montpetit A, Hunt J. Exhaled Breath Condensate—an overview. Immunol Allergy Clin North Am. 2012 Aug;32(3):363–75.

158. Davis MD, Montpetit AJ. Exhaled Breath Condensate: An Update. Immunology and Allergy Clinics of North America. 2018 Nov 1;38(4):667–78.

159. Mosquera-Restrepo SF, Zuberogoïtia S, Gouxette L, Layre E, Gilleron M, Stella A, et al. A Mycobacterium tuberculosis fingerprint in human breath allows tuberculosis detection. Nat Commun. 2022 Dec 14;13(1):7751.

160. Chen D, Bryden WA, Wood R. Detection of Tuberculosis by The Analysis of Exhaled Breath Particles with High-resolution Mass Spectrometry. Sci Rep. 2020 May 6;10(1):7647.

161. Williams CM, Abdulwhhab M, Birring SS, Kock ED, Garton NJ, Townsend E, et al. Exhaled Mycobacterium tuberculosis output and detection of subclinical disease by face-mask sampling: prospective observational studies. The Lancet Infectious Diseases. 2020 May 1;20(5):607–17.

162. WHO Coronavirus (COVID-19) Dashboard [Internet]. [cited 2021 Apr 1]. Available from: https://covid19.who.int

163. Tadolini M, Codecasa LR, García-García JM, Blanc FX, Borisov S, Alffenaar JW, et al. Active tuberculosis, sequelae and COVID-19 co-infection: first cohort of 49 cases. Eur Respir J [Internet]. 2020 Jul 9 [cited 2020 Nov 2];56(1). Available from: https://www.ncbi.nlm.nih.gov/pmc/articles/PMC7251245/

164. Western Cape Department of Health in collaboration with the National Institute for Communicable Diseases SA. Risk Factors for Coronavirus Disease 2019 (COVID-19) Death in a Population Cohort Study from the Western Cape Province, South Africa. Clinical Infectious Diseases. 2021 Oct 1;73(7):e2005–15.

165. Sy KTL, Haw NJL, Uy J. Previous and active tuberculosis increases risk of death and prolongs recovery in patients with COVID-19. Infect Dis (Lond). 2020 Dec;52(12):902–7.

166. Song WM, Zhao JY, Zhang QY, Liu SQ, Zhu XH, An QQ, et al. COVID-19 and Tuberculosis Coinfection: An Overview of Case Reports/Case Series and Meta-Analysis. Front Med (Lausanne). 2021;8:657006.

167. Rajamanickam A, Kumar NP, Padmapriyadarsini C, Nancy A, Selvaraj N, Karunanithi K, et al. Latent tuberculosis co-infection is associated with heightened levels of humoral, cytokine and acute phase responses in seropositive SARS-CoV-2 infection. J Infect. 2021 Sep;83(3):339–46.

168. Madan M, Baldwa B, Raja A, Tyagi R, Dwivedi T, Mohan A, et al. Impact of Latent Tuberculosis on Severity and Outcomes in Admitted COVID-19 Patients. Cureus [Internet]. 2021 Nov 25 [cited 2022 Dec 23];13(11). Available from: https://www.cureus.com/articles/78004-impact-of-latent-tuberculosis-on-severity-and-outcomes-in-admitted-covid-19-patients

169. Riou C, du Bruyn E, Stek C, Daroowala R, Goliath RT, Abrahams F, et al. Relationship of SARS-CoV-2–specific CD4 response to COVID-19 severity and impact of HIV-1 and

tuberculosis coinfection. Journal of Clinical Investigation. 2021 Jun 15;131(12):e149125.

170. Petrone L, Petruccioli E, Vanini V, Cuzzi G, Gualano G, Vittozzi P, et al. Coinfection of tuberculosis and COVID-19 limits the ability to in vitro respond to SARS-CoV-2. International Journal of Infectious Diseases. 2021 Mar;S1201971221001764.

171. Flores-Lovon K, Ortiz-Saavedra B, Cueva-Chicaña LA, Aperrigue-Lira S, Montes-Madariaga ES, Soriano-Moreno DR, et al. Immune responses in COVID-19 and tuberculosis coinfection: A scoping review. Frontiers in Immunology [Internet]. 2022 [cited 2022 Dec 23];13. Available from: https://www.frontiersin.org/articles/10.3389/fimmu.2022.992743

172. Schoenhals M, Rabenindrina N, Rakotondramanga JM, Dussart P, Randremanana R, Heraud JM, et al. SARS-CoV-2 antibody seroprevalence follow-up in Malagasy blood donors during the 2020 COVID-19 Epidemic. eBioMedicine [Internet]. 2021 Jun 1 [cited 2023 Feb 2];68. Available from: https://www.thelancet.com/journals/ebiom/article/PIIS2352-3964(21)00212-7/fulltext

173. Razafimahatratra SL, Ndiaye MDB, Rasoloharimanana LT, Dussart P, Sahondranirina PH, Randriamanantany ZA, et al. Seroprevalence of ancestral and Beta SARS-CoV-2 antibodies in Malagasy blood donors. The Lancet Global Health. 2021 Oct;9(10):e1363–4.

174. Kollmann TR, Kampmann B, Mazmanian SK, Marchant A, Levy O. Protecting the Newborn and Young Infant from Infectious Diseases: Lessons from Immune Ontogeny. Immunity. 2017 Mar 21;46(3):350–63.

175. du Bruyn E, Stek C, Daroowala R, Said-Hartley Q, Hsiao M, Schafer G, et al. Effects of tuberculosis and/or HIV-1 infection on COVID-19 presentation and immune response in Africa. Nat Commun. 2023 Jan 12;14(1):188.

176. Motta I, Centis R, D'Ambrosio L, García-García JM, Goletti D, Gualano G, et al. Tuberculosis, COVID-19 and migrants: Preliminary analysis of deaths occurring in 69 patients from two cohorts. Pulmonology. 2020 Aug;26(4):233–40.

177. Stochino C, Villa S, Zucchi P, Parravicini P, Gori A, Raviglione MC. Clinical characteristics of COVID-19 and active tuberculosis co-infection in an Italian reference hospital. Eur Respir J. 2020 Jul;56(1):2001708.

178. Sarkar S, Khanna P, Singh AK. Impact of COVID-19 in patients with concurrent co-infections: A systematic review and meta-analyses. J Med Virol. 2021 Apr;93(4):2385–95.

179. Mwananyanda L, Gill CJ, MacLeod W, Kwenda G, Pieciak R, Mupila Z, et al. Covid-19 deaths in Africa: prospective systematic postmortem surveillance study. BMJ. 2021 Feb 17;372:n334.

180. Sambarey A, Devaprasad A, Mohan A, Ahmed A, Nayak S, Swaminathan S, et al. Unbiased Identification of Blood-based Biomarkers for Pulmonary Tuberculosis by

Modeling and Mining Molecular Interaction Networks. EBioMedicine. 2016 Dec 21;15:112–26.

181. Warsinske H, Vashisht R, Khatri P. Host-response-based gene signatures for tuberculosis diagnosis: A systematic comparison of 16 signatures. PLoS Med. 2019 Apr;16(4):e1002786.

182. Singhania A, Verma R, Graham CM, Lee J, Tran T, Richardson M, et al. A modular transcriptional signature identifies phenotypic heterogeneity of human tuberculosis infection. Nat Commun. 2018 Jun 19;9(1):2308.

APPENDIX

1. Communications

- **33rd European Congress of Clinical Microbiology and Infectious Diseases (ECCMID) 2023.** Poster presentation titled: "Plasma host protein signatures correlating with Mycobacterium tuberculosis activity prior to and during antituberculosis treatment". Copenhagen, Denmark- 16 April 2023

- **PhD student day of the Institut Pasteur de Madagascar**. Institut Pasteur de Madagascar – 04 November 2022
    - 1st prize winner of the best poster presentation: "Plasma host protein signatures correlating with Mycobacterium tuberculosis activity prior to and during antituberculosis treatment".
    - Participation in the "My thesis in 180 seconds" contest.

- **53nd World Conference on Lung Health (The Union)**. Oral presentation titled: "Identification of host protein biomarker signatures for diagnosis and treatment monitoring of tuberculosis infection in Madagascar using a multiplex assay". Online – 8-11 November 2022

- **EMBO Workshop on Tuberculosis 2022**. Poster presentation titled: "Plasma host protein signatures correlating with Mycobacterium tuberculosis activity prior to and during antituberculosis treatment" Institut Pasteur Paris, France – 12-16 September 2022

- **11th GABRIEL network meeting**: oral presentation titled "APRECIT Project". Veyrier-du-lac, France – November 7-10 2021

- **52nd World Conference on Lung Health (The Union**): oral presentation titled: "Development and evaluation of a multiplex assay for detection of SARS-CoV-2 IgM and IgG antibodies: a serological tool for Covid- 19 surveillance in Madagascar". Online - 19-22 october 2021

- **6th edition of the doctoral school SDSV day**. Poster presentation entitled: "Multi-country validation of RISK6, a 6-gene transcriptomic signature, for tuberculosis diagnosis and treatment outcome monitoring" – Online – 23 march 2021

2. Other original publications

2.1. Seroprevalence of ancestral and Beta SARS-CoV-2 antibodies in Malagasy blood donors

Summary:

Following the second wave of COVID-19 in Madagascar in June 2020 and the emergence of VOCs worldwide, we wanted to determine the proportion of Beta infections among blood donors with anti-protein N IgG seropositivity. We monitored the ability of seropositive blood donor samples to bind either the ancestral receptor binding domain (RBD) or the same one including three specific mutations found in Beta and used this information to define the proportion of individuals who seroconverted due to Beta infection. Increasing affinities for the Beta peak RBD were found in 2021 samples. The proportion of Beta-induced seropositivity increased throughout the last epidemic wave, from 4-5% (1-2-12-5) in January to 5-6% (1-5-15-1) in February, 15-4% (9-0-25-0) in March, 54-5% (46-4-62-4) in April and 63-1% (56-8-69-0) in May. These results suggest that this variant was introduced shortly after it was first described in October 2020 in South Africa, and that the variant was responsible for two-thirds of the infections observed in May 2021, at the peak of the epidemic wave in early 2021. Our data describe both the dynamics of the early 2021 epidemic wave in Antananarivo, Madagascar, and how Beta contributed to it, partially escaping natural immunisation the previous natural immunisation. Beta has been described in Madagascar, but the Beta has been described in Madagascar, but the proportion of infections due to this variant has not been continuously monitored due to under-screening for COVID-19 in the general population and sub-optimal identification of the variant in positive samples.

Seroprevalence of ancestral and Beta SARS-CoV-2 antibodies in Malagasy blood donors

We recently described that, during the first wave of the COVID-19 epidemic in early 2020, the seroprevalence of anti-SARS-CoV-2 IgG antibodies among blood donors in Antananarivo, Madagascar, sharply increased from 0·0% to 43·5% (95% CI 43·3–43·8).[1] This sudden increase was associated with what seems to have been sufficient population immunisation to dramatically slow down virus circulation; a reproducible pattern found in all five investigated regions of the country and five major cities,[1] including the capital city of Antananarivo with 1 275 207 residents.[2]

High seroprevalence (in 255 [44·9%] of 568 people) was also described in Manaus, Brazil, in late 2020; however, it was not sufficient to avoid a second epidemic wave in January, 2021, due to circulation of the P.1 (Gamma) variant, which eludes the human immune response to the ancestral variant that was prevalent earlier in 2020.[3] Similar immune evasion of B.1.351 (also known as the Beta variant of concern) was also described in South Africa and has led to a major second wave.[4] Similar to these two countries, high seroprevalence was not sufficient to prevent Madagascar from having a second major peak in early 2021. Introductions of Beta in the country were first detected in early February, 2021 (GISAID accession IDs EPI_ISL_1660263, _1660266, _1660268, _1660270, _1660272-75, _1660278-79, _1660283-84 and _1660286-290), but the degree to which this variant contributed to the last epidemic wave remains unclear.

In 2020–21, we continuously monitored natural immunisation of the population of Antananarivo by sampling the city's blood donors from the Regional Blood Transfusion Centre in Antananarivo, as previously described[1] (from Oct 1, 2020, to May 26, 2021; mean of 421·9 samples per month, 3375 total samples; appendix p 3). The serum samples were analysed at the Infectious Diseases Immunology Unit of the Pasteur Institute of Madagascar, for antibodies against the SARS-CoV-2 nucleocapsid (N) protein, spike receptor binding domain (RBD),

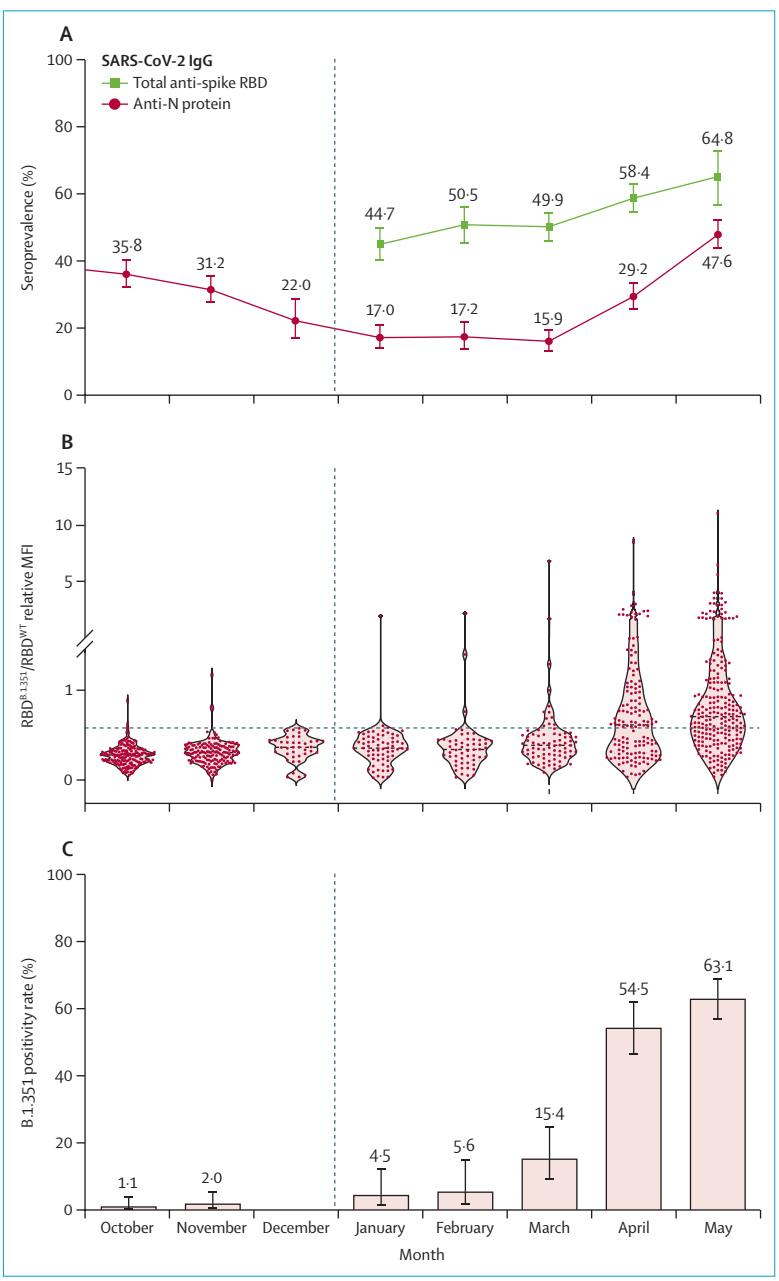

Figure: **Blood donor monthly anti-SARS-CoV-2 IgG seropositivity and Beta positivity rates in seropositive samples**

(A) Anti-N protein IgG and anti-spike RBD total Ig seroprevalences. (B) Anti-spike RBD^{Beta} to anti-spike RBD^{WT} MFI ratio among samples positive for anti-N protein IgG. (C) Beta positivity rate, as the rate of samples for which the RBD^{Beta} to RBD^{WT} MFI ratio was greater than a prespecified threshold that was based on samples from October, 2020 (when Beta variant was first identified; appendix pp 2–3). Error bars indicate 95% CIs. N=nucleocapsid. RBD=receptor binding domain. WT=wild-type. MFI=mean fluorescence intensity.

See Online for appendix

and Beta spike RBD (specific to RBDs containing mutations of Beta; appendix pp 1–2). Anti-N protein IgG seroprevalences reached their lowest point (since the summer of 2020) in March, 2021 (15·9% seropositive [95% CI 12·9–19·4], n=497), then sharply increased to a peak (47·6% [43·3–52·0], n=500) in May, 2021. Seroprevalence for total anti-spike RBD antibodies (IgA, IgG, and IgM), which are known to be more persistent,[5] increased from 49·9% (45·5–54·3) seropositivity to 64·8% (56·1–72·6) during the same period (figure A, appendix p 3).

To determine the proportion of infections caused by Beta among blood donors with seropositivity for anti-N protein IgG, we monitored the capacity of seropositive blood donor samples to bind either the ancestral RBD or the same subunit comprising three specific mutations found in Beta (appendix p 2), and used this information to define the proportion of individuals who had seroconverted due to infection with Beta. Increasing affinities for the Beta spike RBD were found in 2021 samples (figure B). The proportion of Beta-induced seropositivities increased throughout the last epidemic wave from 4·5% (1·2–12·5) in January to 5·6% (1·5–15·1) in February, 15·4% (9·0–25·0) in March, 54·5% (46·4–62·4) in April, and 63·1% (56·8–69·0) in May (figure C, appendix p 3). These results suggest an introduction of this variant soon after its first description in October, 2020, in South Africa,[4] and that the variant was responsible for two-thirds of the observed infections in May, 2021, at the peak of the early 2021 epidemic wave.

Our data describe both the dynamics of the early 2021 epidemic wave in Antananarivo, Madagascar, and how Beta contributed to it, partially escaping previous natural immunisation. Beta has been described in Madagascar, but the proportion of infections due to this variant have not been continuously monitored due to undertesting for COVID-19 in the general population and suboptimal variant identification in positive samples. Monitoring blood donors for both general SARS-CoV-2 and variant-specific antibody seroprevalences might be a useful tool when, as with Beta, serological responses seem to be affected.[6]

Vaccination of the general Malagasy population should be intensified, yet adapted to a population highly naturally immunised by exposure to ancestral SARS-CoV-2, variant Beta, or both. Early detection of new variants that might affect the course of the epidemic should be continuously monitored for immediate public health decision making.

We declare no competing interests.

*Solohery Lalaina Razafimahatratra, Mame Diarra Bousso Ndiaye, Lova Tsikiniaina Rasoloharimanana, Philippe Dussart, Paquerette Hanitriniala Sahondranirina, Zely Arivelo Randriamanantany, *Matthieu Schoenhals*

schoenhals@pasteur.mg

Institut Pasteur de Madagascar, Antananarivo BP1274, Madagascar (SLR, MDBN, LTR, PD, MS); Ministry of Public Health (Madagascar), Antananarivo, Madagascar (PHS, ZAR)

1 Schoenhals M, Rabenindrina N, Rakotondramanga JM, et al. SARS-CoV-2 antibody seroprevalence follow-up in Malagasy blood donors during the 2020 COVID-19 epidemic. *EBioMedicine* 2021; **68:** 103419.

2 Institut National de la Statistique Madagascar. Troisieme recensement général de la population et de l'habitation (RGPH-3). 2020. https://madagascar.unfpa.org/sites/default/files/pub-pdf/resultat_globaux_rgph3_tome_01.pdf (accessed Aug 11, 2021).

3 Faria NR, Mellan TA, Whittaker C, et al. Genomics and epidemiology of the P.1 SARS-CoV-2 lineage in Manaus, Brazil. *Science* 2021; **372:** 815–21.

4 Tegally H, Wilkinson E, Giovanetti M, et al. Detection of a SARS-CoV-2 variant of concern in South Africa. *Nature* 2021; **592:** 438–43.

5 Dan JM, Mateus J, Kato Y, et al. Immunological memory to SARS-CoV-2 assessed for up to 8 months after infection. *Science* 2021; **371:** eabf4063.

6 Madhi SA, Baillie V, Cutland CL, et al. Efficacy of the ChAdOx1 nCoV-19 Covid-19 vaccine against the B.1.351 variant. *N Engl J Med* 2021; **384:** 1885–98.

2.2. Different PPD-stimulated cytokine responses from patients infected with genetically distinct Mycobacterium tuberculosis complex lineages

Summary:

The genetic diversity of Mycobacterium tuberculosis complex (MTBC) influences the immune response of the host, which may affect the immunodiagnostic tests and biomarker assessment studies used for tuberculosis (TB). This study aimed to determine whether the mycobacterial-antigen-stimulated cytokine responses vary with the genotype of the MTBC infecting the patient.

Eighty-one patients with confirmed active pulmonary TB were recruited, and MTBC clinical strains were isolated from their sputum for bacterial lineage single-nucleotide polymorphism typing. Whole blood was drawn from the patients to measure the purified protein derivative (PPD)-stimulated cytokine responses (GM-CSF, IFN-g, IL-1β, IL-2, IL-4, IL-5, IL-6, IL-7, IL-8, IL-10, TNF-α, IFN-α, IL-12, eotaxin, IL-13, IL-15, IL-17, MIP1-α, MIP1-β, MCP1, IL1RA, IP10, IL2R, MIG) with the Luminex multiplex immunoassay.

Of the 24 cytokines studied, three were produced differentially in whole blood dependent on the infecting lineage of MTBC. Decreased production of IL-17 was observed in patients infected with modern lineages compared with patients infected with ancestral lineages (*p-value* <0.01), and production of IFN-g and IL-2 was significantly decreased in patients infected with lineage 4 strains compared with patients infected with lineage 3 strains (*p-value* <0.05).

MTBC strains belonging to lineage 4 induced a decreased whole-blood PPD-stimulated pro- inflammatory cytokine response.

International Journal of Infectious Diseases 104 (2021) 725–731

Contents lists available at ScienceDirect

International Journal of Infectious Diseases

journal homepage: www.elsevier.com/locate/ijid

Different PPD-stimulated cytokine responses from patients infected with genetically distinct *Mycobacterium tuberculosis* complex lineages

Paulo Ranaivomanana[1], Marie Sylvianne Rabodoarivelo[1], Mame Diarra Bousso Ndiaye, Niaina Rakotosamimanana[*], Voahangy Rasolofo

Mycobacteria Unit, Institut Pasteur de Madagascar, B.P. Ambatofotsikely, Antananarivo, Madagascar

ARTICLE INFO

Article history:
Received 10 November 2020
Received in revised form 8 January 2021
Accepted 30 January 2021

Keywords:
Tuberculosis
Mycobacterium tuberculosis complex lineages
Cytokine
Antigen stimulation
Whole blood

ABSTRACT

Objectives: The genetic diversity of *Mycobacterium tuberculosis* complex (MTBC) influences the immune response of the host, which may affect the immunodiagnostic tests and biomarker assessment studies used for tuberculosis (TB). This study aimed to determine whether the mycobacterial-antigen-stimulated cytokine responses vary with the genotype of the MTBC infecting the patient.

Methods: Eighty-one patients with confirmed active pulmonary TB were recruited, and MTBC clinical strains were isolated from their sputum for bacterial lineage single-nucleotide polymorphism typing. Whole blood was drawn from the patients to measure the purified protein derivative (PPD)-stimulated cytokine responses (GM-CSF, IFN-γ, IL-1β, IL-2, IL-4, IL-5, IL-6, IL-7, IL-8, IL-10, TNF-α, IFN-α, IL-12, eotaxin, IL-13, IL-15, IL-17, MIP1-α, MIP1-β, MCP1, IL1RA, IP10, IL2R, MIG) with the Luminex multiplex immunoassay.

Results: Of the 24 cytokines studied, three were produced differentially in whole blood dependent on the infecting lineage of MTBC. Decreased production of IL-17 was observed in patients infected with modern lineages compared with patients infected with ancestral lineages ($P < 0.01$), and production of IFN-γ and IL-2 was significantly decreased in patients infected with lineage 4 strains compared with patients infected with lineage 3 strains ($P < 0.05$).

Conclusion: MTBC strains belonging to lineage 4 induced a decreased whole-blood PPD-stimulated pro-inflammatory cytokine response.

Introduction

With approximately 10 million new cases and 1.4 million deaths in 2019 (World Health Organization, 2019), tuberculosis (TB) remains a major public health problem. To optimize the TB control effort with accurate diagnostic tools, it is essential to better understand the interaction between *Mycobacterium tuberculosis* complex (MTBC) and the human immune system.

Measurement of MTBC antigen-specific interferon-gamma (IFN-γ) remains the main immunological readout for TB vaccine and TB infection assessment (Beveridge et al., 2008). In addition to the human host immune status, the genetic diversity of MTBC plays a role in the host immune response and TB infection (Chae and Shin, 2018; Rutaihwa et al., 2019). Several studies, including the authors' previous research in Madagascar, have reported that stimulation of peripheral blood mononuclear cells (PBMCs) with MTBC antigens showed variability in the IFN-γ response across phylogenetic lineages of MTBC (Rakotosamimanana et al., 2010). MTBC-specific responses have already proven to be useful in the diagnosis of MTBC infection as this is the concept behind IFN-γ release assays (IGRAs) (Clifford et al., 2018). Moreover, antigen-specific polyfunctional CD4 cells expressing several cytokines simultaneously, such as IFN-γ, tumour necrosis factor alpha (TNF-α) and interleukin-2 (IL-2), have been reported to have protective correlates against TB and/or can be used to distinguish TB-related status (Smith et al., 2016; Lewinsohn et al., 2017; Tanner et al., 2020). There is increasing and promising evidence regarding the diagnostic potential of other MTBC-antigen-stimulated cytokine biomarkers to identify individuals infected with TB (Essone et al.,

* Corresponding author at: Mycobacteria Unit, Institut Pasteur de Madagascar, B.P. 1274, Ambatofotsikely, 101 Antananarivo, Madagascar.
E-mail address: niaina@pasteur.mg (N. Rakotosamimanana).
[1] Equal contribution.

https://doi.org/10.1016/j.ijid.2021.01.073

2014; Chen et al., 2015; Wang et al., 2018; Korma et al., 2020). However, the wide range of cytokine responses that differ significantly across the major phylogenetic lineages of MTBC may affect the inflammatory phenotypes, and this has to be considered when evaluating immunodiagnostic tools (Portevin et al., 2011).

This study aimed to determine whether whole-blood mycobacterial-antigen-stimulated cytokine responses vary with the infecting MTBC lineage. This may constitute an important factor to consider in the development of novel intervention strategies.

Materials and methods

Participants

Newly sputum-positive adults with TB were recruited from the main antituberculosis centres in Antananarivo, Madagascar between August 2007 and June 2010. Patients who gave their informed consent to participate were interviewed and examined. TB cases were defined as two sputum samples positive on smear microscopy examination and confirmed by culture on Lowenstein–Jensen (LJ) medium. Venous blood was drawn in sodium heparin vacutainer tubes (Becton–Dickinson, Franklin Lakes, NJ, USA) for Luminex assay (10 mL), and a dry Vacutainer tube for a human immunodeficiency virus (HIV) test (1 mL). HIV-positive subjects were excluded from the study. Those patients with complete biological tests were included in the study analyses. This study was approved by the National Ethics Committee of the Ministry of Health of Madagascar (Approval No. 158-SANPFPS, 10 May 2007).

Mycobacteriological procedures

Sputum samples isolated from patients with TB were decontaminated using the sodium lauryl sulfate method, and stained using the acid-fast bacilli test (auramine method) for smear microscopy examination under a fluorescence microscope (×40). The remaining decontaminated specimen was inoculated into two tubes of standard LJ medium for MTBC colony confirmation.

SNP typing

Five previously described single-nucleotide polymorphisms (SNPs) from the MTBC genome (*Rv 3221c*_0085n, *Rv 2952*_0526n, *Rv 3804c*_00112n, *katG*463 and *pstS1*_1055) were used to classify the LJ growth culture colonies into phylogenetic lineages of MTBC (lineages 1, 2, 3, 4 and bovis, respectively) (Comas et al., 2009). In addition, a specific SNP on the MTBC *gyrA* gene (Rv 0006_1842) was used to classify the strains into modern or ancestral lineages based on TbD1 deletion (Table 1). Briefly, bacterial DNA was extracted from LJ colonies as described previously (Van Embden et al., 1993). Taqman allelic discrimination assay was performed for SNP typing using StepOne software (Applied Biosystems, Foster City, CA, USA). Ten nanograms of bacterial DNA was added to the polymerase chain reaction (PCR) mixture containing 6 μL QuantiTect Probe PCR Master Mix 2X [PCR buffer, HotStar Taq DNA polymerase, dNTP, passive reference dye ROX and 8 mM $MgCl_2$ (Qiagen, Hilden, Germany)], 0.25 μL forward and reverse primers 10 μM (Sigma), and 1 μL Taqman probe 10 μM labelled with FAM (6-carboxyfluoresceine) or VIC (Applied Biosystems). Details of primers and probes are given in Table 1. Amplification was performed using a StepOne Thermocycler (Applied Biosystems) and consisted of 15 min of denaturing at 95 °C, followed by 40 cycles at 94 °C for 15 s and 60 °C for 1 min, and a final extension at 60 °C for 30 s.

Cytokine/chemokine assessment

For each participant, whole blood was plated in a 24-well plate in duplicate (1 mL/well) and stimulated with purified protein derivative (PPD) (Tubersol 1 μg/mL; Sanofi Pasteur, Lyon, France) for 24 h in a 37 °C/5% CO_2 incubator. Phorbol myristate acetate (Sigma # P 8139, 1 μg/mL) was used as the positive control and phosphate-buffered saline was used as the negative control. After stimulation, the supernatant plasma was collected and stored at −70 °C for further cytokine measurement. Plasma concentrations of granulocyte-macrophage colony-stimulating factor (GM-CSF), IFN-γ, IL-1β, IL-2, IL-4, IL-5, IL-6, IL-8, IL-10, TNF-α, IFN-α, IL-12, eotaxin, IL-13, IL-15, IL-17, macrophage inflammatory proteins (MIP)1-α, MIP1-β, monocyte chemoattractant protein 1 (MCP1), IL1RA, IL-7, interferon gamma-induced protein 10 (IP10), IL2R and monokine induced by IFN-γ (MIG) were measured by Luminex technology using Milliplex TMMAP kits (MilliporeSigma, Burlington, MA, USA) in accordance with the manufacturer's instructions. Briefly, 50 μL of biological fluid or the standard was incubated with antibody-linked beads for 2 h, washed twice with wash solution, and incubated for 1 h with biotinylated secondary antibodies. Following incubation for 30 min with streptavidin-PE, data were acquired on the Luminex 100IS. At least 100 events were acquired for each analyte. Values above or below the standard curves were replaced, respectively, by the lowest or highest concentrations measured.

Table 1
Sequence information of primers and probes (minor groove binder probes) used in this study to classify *Mycobacterium tuberculosis* complex strains into different lineages by Taqman polymerase chain reaction single-nucleotide polymorphism (SNP) genotyping.

Lineage	SNP name	Primer sequences	Amplicon size	Probe sequences
Lineage 1	Rv3221c_ 0085n	F: 5′-TGT CAA CGA AGG CGA TCA GA R: 5′-GAC CGT TCC GGC AGC TT	100 bp	Wild-type probe: FAM-ACAAGGGCGACGTC Mutant probe: VIC-ACAAGGGCGACATC
Lineage 2	Rv2952_ 0526n	F: 5′-CCT TCG ATG TTG TGC TCA ATG T R: 5′-CAT GCG GCG ATC TCA TTG T	142 bp	Wild-type probe: FAM-CCCAGGAGGGTAC Mutant probe: VIC-CCCAGGAAGGTACT
Lineage 3	Rv3804c_0012s	F: 5′- GCA TGG ATG CGT TGA GAT GA R: 5′- CGA GTC GAC GCG ACA TAC C	92 bp	Wild-type probe: VIC-AAGAATGCAGCTTGTTGA Mutant probe: FAM-AAGAATGCAGCTTGTCGA
Lineage 4	Rv1908c_1389n	F: 5′- CCG AGA TTG CCA GCC TTA AG R: 5′- GAA ACT AGC TGT GAG ACA GTC AAT CC	64 bp	Wild-type probe: VIC-CCAGATCCTGGCATC Mutant probe: FAM-CAGATCCGGGCATC
Bovis	Rv0934_1055n	F: 5′- CAC CGA CGG CAA CAA GGC CTC R: 5′- TTC ACC ACC GCG GGC GGC AGC GGC T	69 bp	Wild-type probe: FAM-ACCAGGTTCATTTCC Mutant probe: VIC-ACCAGGCTCATTTCC
TbD1	Rv0006_1842s	F: 5′- CCA GCC CGA GGA ACG CAT CGC CCA R: 5′- AGC ACC AGG TAC GGG GCG TCG G	69 bp	Wild-type probe: FAM-TCCAGATTCGCGGCT Mutant probe: VIC-TCCAGATCCGCGGCT

R, reverse; F, forward.
Primer and probe sequences were reported from Stucki et al. (2012) and Gagneux et al. (2006).

Table 2
Basic epidemiological data of participants.

	Lineage 1	Lineage 2	Lineage 3	Lineage 4	Total
Age (mean ± SD)	32 ± 9	27 ± 9	28 ± 4	27 ± 8	27 ± 9
Sex, *n* (%)					
Male	4 (50)	3 (60)	9 (90)	34 (59)	50 (62)
Female	4 (50)	2 (40)	1 (10)	24 (41)	31 (38)
BCG status, *n* (%)					
Vaccinated	7 (88)	4 (80)	8 (80)	40 (71)	59 (73)
Non-vaccinated	1 (13)	1 (20)	2 (20)	18 (29)	22 (27)

SD, standard deviation; BCG, Bacillus Calmette–Guérin.

Statistical analysis

Statistical analysis was performed using GraphPad Prism Version 6 (GraphPad, San Diego, CA, USA). The mean values of duplicate PPD-stimulated samples were considered. Each assessed cytokine was compared according to the infecting MTBC lineage using Dunn's test to consider multiple comparisons. $P < 0.05$ was considered to indicate statistical significance.

Results

Study participants

Eighty-one patients with TB were included in this study. Clinical isolates had been genotyped and immunological data by Luminex were complete. All participants were HIV negative. Table 2 shows the basic epidemiological data of the participants. The mean age of the patients was 27 (standard deviation 9) years. Seventy-two percent of patients were reported as vaccinated with Bacillus Calmette–Guérin (BCG) based on the presence of a BCG scar.

Classification of MTB isolates by SNP typing

The distribution of the isolates across MTBC lineages is shown in Figure 1. The four major lineages of MTBC (Lineages 1, 2, 3 and 4) were found in this study. Lineage 4 was predominant (n = 58, 71.6%), followed by lineage 3 (n = 10, 12.34%), lineage 1 (n = 8, 9.88%) and lineage 2 (n = 5, 6.17%). Based on SNP typing of the Rv 0006_1842 region, which allows classification of the strains into ancestral and modern lineages, those strains belonging to lineage 1 were classified as the ancestral lineage and lineages 2, 3 and 4 were classified as the modern lineage, as expected.

PPD-stimulated cytokine responses according to bacterial lineage

Regarding the pro-inflammatory cytokines (TNF-α, IL-6, IL-1β and IL-17), the concentration of IL-17 was significantly higher in whole blood from patients infected with MTBC of ancestral lineage compared with patients infected with MTBC of modern lineage (P = 0.005) (Figure 2G). This difference was significant between patients infected with lineage 1 and lineage 4 strains (Figure 2H, P = 0.004). No significant difference in TNF-α, IL-6 and IL-1β was observed between patients infected with different lineages of MTBC (Figure 2).

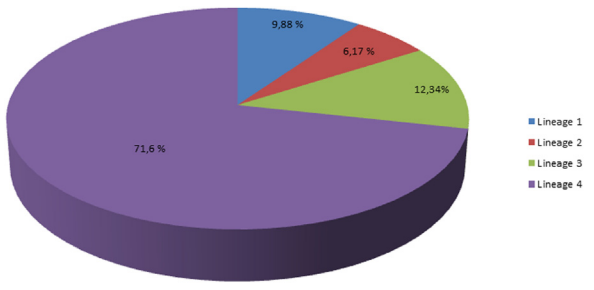

Figure 1. Distribution of *Mycobacterium tuberculosis* complex isolates according to their phylogenetic lineage (n = 81).

Whole-blood production of PPD-stimulated IL-2 and IFN-γ were significantly lower in patients infected with lineage 4 strains compared with those infected with lineage 3 strains (P = 0.004 and P = 0.02, respectively; Figure 3B, D). There were no significnat differences in the concentrations of Th2 cytokines (IL-4 and IL-10) (Figure 4). No significant differences in the other cytokines measured (GM-CSF, IFN-α, eotaxin, IL-7, IL-8, IL-12, IL-13, IL-15, MIP1-α, MIP1-β, MCP1, IL1RA, IP10, IL2R and MIG) were observed between patients infected with different lineages of MTBC.

No significant difference in cytokine production was observed between BCG-vaccinated and unvaccinated patients.

Discussion

This study evaluated the PPD-stimulated cytokine responses from patients with TB infected with different phylogenetical lineages of MTBC. PPD has long been used as an antigen for diagnosing infection based on delayed-type hypersensitivity. The decision to use PPD in this study was based on the highly complex PPD protein components (Prasad et al., 2013) that can give a first overview of the influence of infecting strains on antigen-stimulated cytokine production before further investigation using more specific Mtb proteins. Some of these biomarkers, specifically IL-17, were found to differ between patients infected with ancestral and modern lineages of MTBC, while the production of IL-2 and IFN-γ differed significantly between patients with active TB infected with lineage 3 and lineage 4 (both modern lineages). The MTBC lineages have been shown to be phylogeographically associated with specific human populations where immune responses to infection vary between the different lineages of MTBC, suggesting their propensity to adapt in different human population (Gagneux et al., 2006; Caws et al., 2008; Valcheva et al., 2010; Portevin et al., 2011; Clarke et al., 2016). The present observations suggest that the infecting MTBC could also affect the downstream ex-vivo mycobacterial-antigen-stimulated cytokines, and may have implications for TB immunodiagnostic and biomarker assessment tests. There is no gold standard to date for latent TB infection assays; IGRAs have been reported to perform well, especially compared with the tuberculin skin test, for the detection of TB infection, but several sources of variability can affect IGRA results when comparing different IGRAs or when comparing the performance of IGRAs with other latent TB infection assays (Gilani and Sergent, 2020). There is room for improvement in IGRA performance. PPD-stimulated cytokine responses may be influenced by BCG vaccination or BCG putative protection, particularly in the case of latent TB assays. However, as the population in the present study were active TB patients, the use of BCG would not influence cytokine production significantly, as confirmed by the absence of a significant difference in cytokine production between BCG-vaccinated and unvaccinated groups.

The inflammatory response of patients infected by MTBC ensures local innate control of bacterial infection by phagocyte cells (Van Crevel et al., 2002; Korbel et al., 2008), and also induces an adaptative immune response by formation of granulomas (Cooper, 2009). Of all the lymphocyte-derived cytokines studied, IL-2, IL-5, IL-17 and IFN-γ were induced differentially between the MTBC lineages. Patients infected with an ancestral lineage of MTBC had a significantly higher IL-17 response than patients infected with a modern lineage of MTBC. IL-17 and IL-17-producing innate lymphoid cells were reported to play a protective role during acute infection with hypervirulent MTBC (Gopal et al., 2014; Domingo-

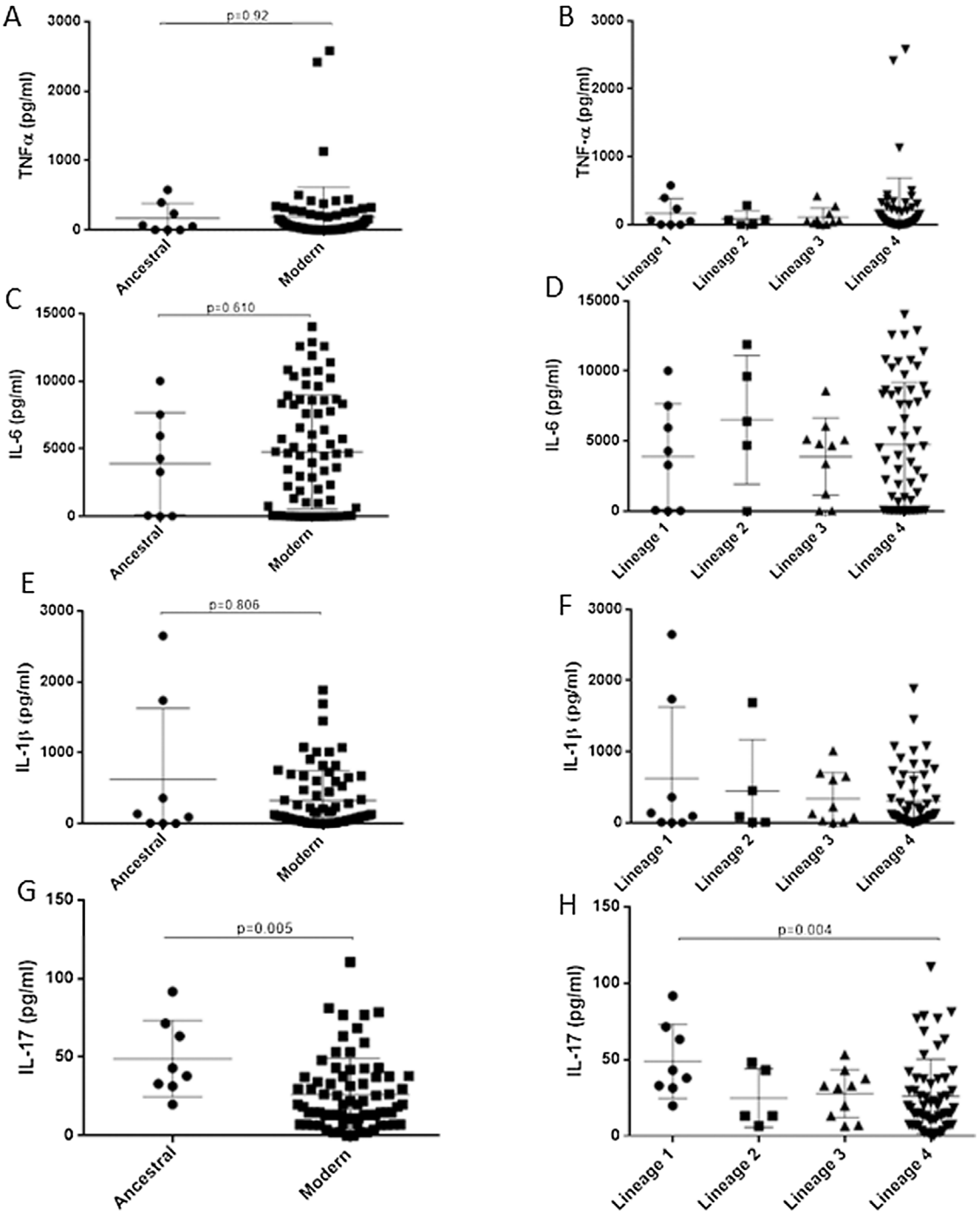

Figure 2. Pro-inflammatory tumour necrosis factor (TNF)-α, interleukin (IL)-6, IL-1β and IL-17 secretions after purified protein derivative stimulation of whole blood from patients with tuberculosis (TB) infected with ancestral and modern *Mycobacterium tuberculosis* complex (MTBC) strains (A, C, E, G), and patients with TB infected with different lineages of MTBC (B, D, F, H). Data represent mean and standard deviation.

Gonzalez et al., 2017; Ardain et al., 2019). The MTBC-strain-specific role of IL-17 in the control of TB infection has been observed in different models. Mourik et al. (2019) reported higher IL-17 and IFN-γ levels in the lungs of mice infected with a laboratory lineage 4 strain compared with mice infected with a lineage 1 strain, and this was associated with a T-cell response against infection in these infectious models. In the context of human infection with multi-drug-resistant MTBC, IL-17-producing T cells were associated with immunopathology, possibly lowering the efficacy of the second-line drugs employed during treatment (Basile et al., 2011). As MDR MTBC strains have lower fitness compared with their susceptible counterparts (Gagneux, 2009), these data suggest a role for the infecting MTB strain lineage in the variation of IL-17 production during infection. A decrease in IL-17 response after infection with a modern MTBC strain may contribute to confer resistance to the host immune response, which can correlate with enhanced bacterial virulence (Bottai et al., 2020).

Within the modern lineages of MTBC, PPD stimulation of whole blood drawn from patients infected with a lineage 4 strain displayed decreased IL-2 and IFN-γ responses compared with

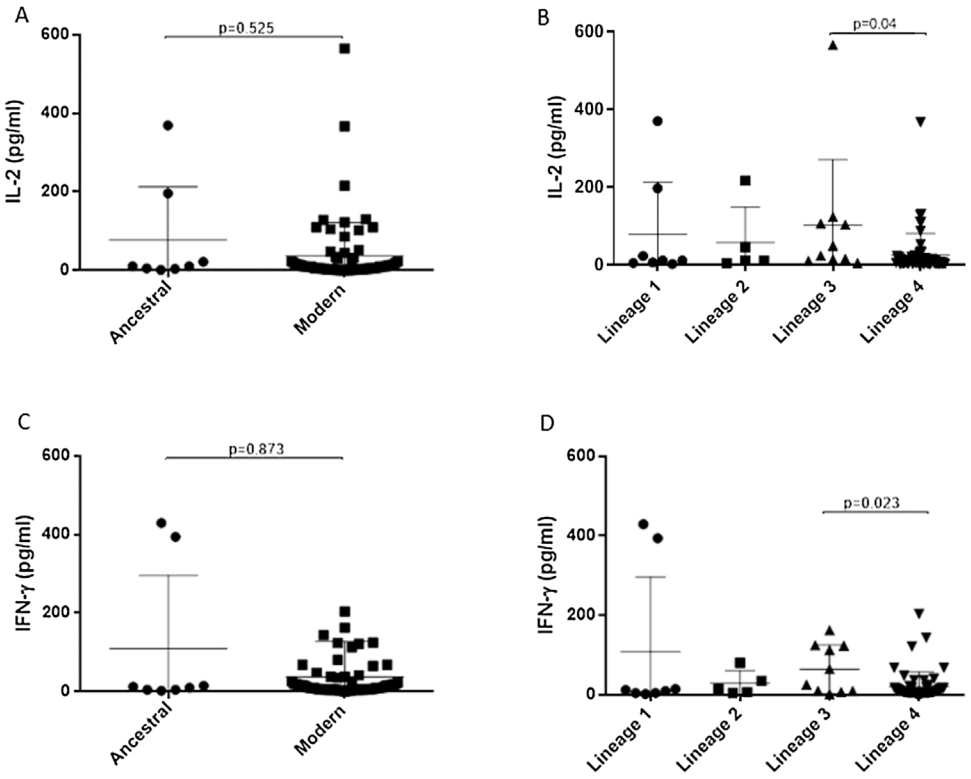

Figure 3. Th1-related interleukin (IL)-2 and interferon (IFN)-γ cytokine secretions after purified protein derivative stimulation of whole blood from patients with tuberculosis (TB) infected with ancestral and modern *Mycobacterium tuberculosis* complex (MTBC) strains (A, C), and patients with TB infected with different lineages of MTBC (B, D). Data represent mean and standard deviation.

patients infected with a lineage 3 strain. This is inconsistent with the authors' previous study in human ex-vivo PPD-stimulated PBMC cells, where lineage 2 and lineage 3 strains (both modern lineages) induced lower IFN-γ responses compared with lineage 4 strains (Rakotosamimanana et al., 2010). Although these two studies involved two independent cohorts with two different methods (enzyme-linked immunosorbent assay and enzyme-linked immunosorbent spot), this observed difference in the IFN-γ response between whole-blood and PBMC PPD-stimulation assays highlights the importance of the methodological approach when considering differences in the immune response compartmental localization. Such a difference was reported for transcriptomic expression between whole blood and PBMCs (He et al., 2019). While lymphocytes and monocytes in PBMCs play significant roles in the immune response, they remain a subset of all immune cells and do not include other cell types (eosinophils and neutrophils) nor the plasma matrix that directly reflects the patient's responsiveness to immune stimuli. A low plasmatic IFN-γ level was reported to be associated with disseminated infection and higher virulence of MTBC (Lopez et al., 2003; Kong et al., 2007; Sarkar et al., 2012). Other factors could also be related to this difference, such as genetic background or epidemiological differences in the study populations, as well as differences in immune regulation by MTBC lineages that could occur at sub-lineage level.

The same observation as with IFN-γ was observed for IL-2, where PPD-stimulated whole blood from patients infected with lineage 4 strains exhibited significantly lower IL-2 compared with patients infected with lineage 3 strains. IL-2 is crucial for T-cell differentiation (Pipkin et al., 2010), generation of memory T cells (Kahan et al., 2015; Kaartinen et al., 2017) and enhancement of the CD8+ cell response (West et al., 2013). In a recent study, IL-2 was shown to restore T-cell dysfunction, exhaust immunity induced by persistent MTBC stimulation (Liu et al., 2019), and be effective for the treatment of MDR-TB (Johnson et al., 1998; You et al., 2016). More importantly, IL-2 was reported to have higher diagnostic value than IFN-γ, but lacks the ability to discriminate between infection states. Clifford et al. (2018) reported that combining IL-2 and IFN-γ may achieve greater sensitivity for the detection of TB infection irrespective of the stimulant used, and the present study suggested that MTBC lineage 4 strains may influence IL-2 and IFN-γ production.

This study did not detect differential production of TNF-α, IL-1β and IL-6 between patients infected with different lineages of MTBC, while studies from in-vitro-infected human macrophages found that lineage 2 strains induced less TNF-α, IL-1β and IL-6 than non-Beijing strains (Wang et al., 2010; Chen et al., 2014). It was also reported that infection with modern lineages of MTBC induces a weaker pro-inflammatory response than infection with ancestral lineages in cellular assays of infection (Portevin et al., 2011; Van Laarhoven et al., 2013). These differences compared with the present study could suggest that there are more complex interactions in whole blood that stabilize the cytokine production found in in-vitro or intrinsic anti-inflammatory properties in macrophages or cellular models.

In summary, PPD stimulation of whole blood from patients with TB triggers variable cytokine responses depending on the infecting phylogenetic lineage of MTBC. Patients infected with lineage 4 strains showed decreased production of Th1 cytokines IFN-γ and IL-2 compared with lineage 3 strains, and decreased production of IL-17 compared with lineage 1 strains. This study provides additional evidence that MTBC genotype influences the type and magnitude of the immune response to infection in a human host.

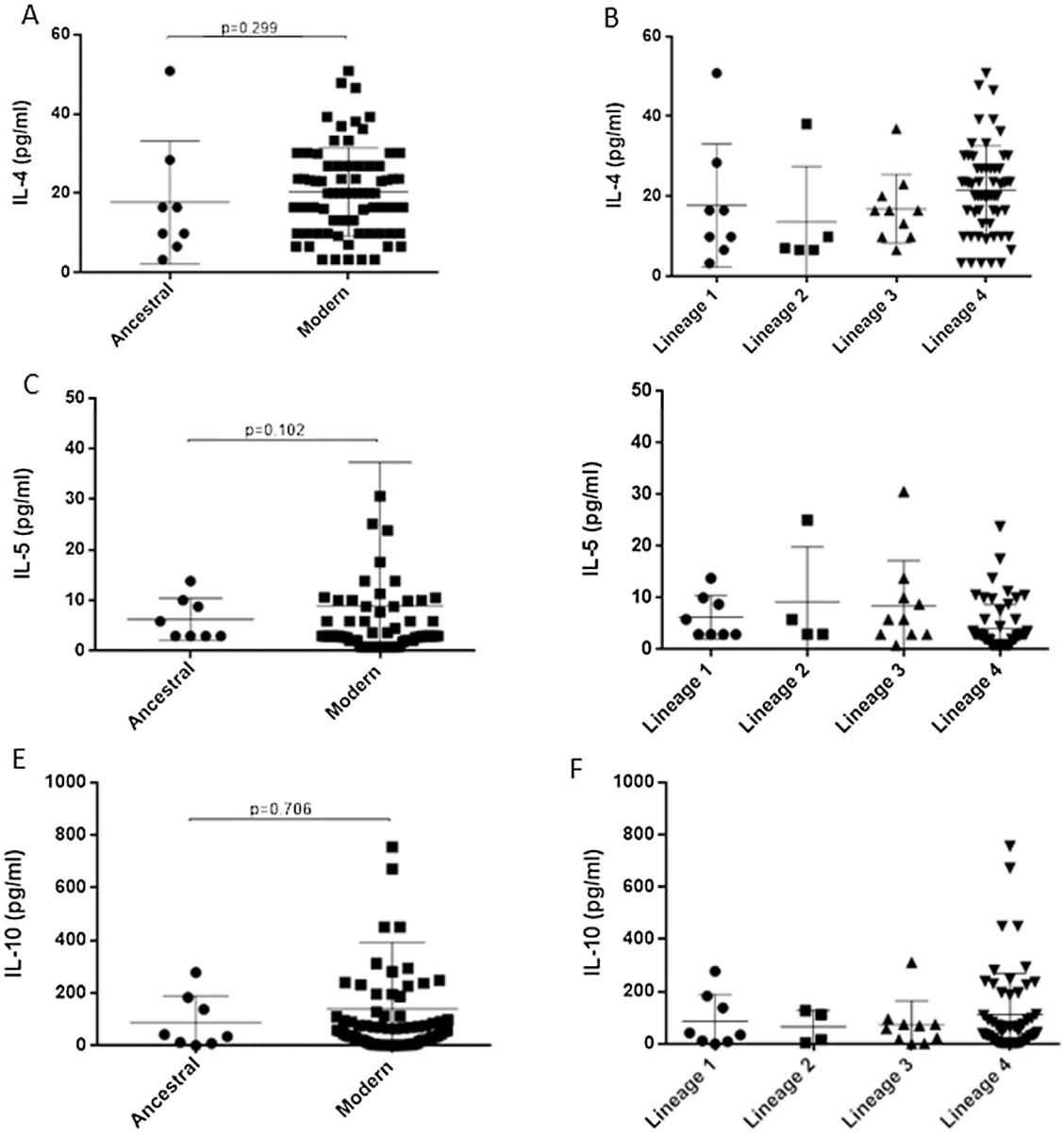

Figure 4. Th2-related interleukin (IL)-4, IL-5 and IL-10 secretions after purified protein derivative stimulation of whole blood from patients with tuberculosis (TB) infected with ancestral and modern *Mycobacterium tuberculosis* complex (MTBC) strains (A, C, E), and patients with infected with different lineages of MTBC (B, D, F). Data represent mean and standard deviation.

The reduced pro-inflammatory cytokines elicited by lineage 4 strains could be considered as a mechanism that contributes to the success of this lineage in terms of disease progression and transmission. The large lineage to lineage variations in immune response observed in whole blood after mycobacterial antigen stimulation must be considered when designing new strategies for immunotherapy or immunodiagnostics, and can help to adapt the strategies used when designing future biomarkers for TB.

Contributions

VR conceived the study, and initiated the project together with NR, PR and SR. PR and SR undertook the biological sample experiments. NR and VR designed the probes and primers. PR analysed the data and wrote the first draft of the manuscript. All authors contributed to the content and have given their final approval.

Funding

This study was funded by the Pasteur Institute (Programmes Transversaux de Recherche, PTR202).

Ethical approval

This study was registered and approved by the National Ethics Committee of the Ministry of Health of Madagascar (Approval No. 158-SANPFPS, 10 May 2007). All patients gave their written, informed consent.

Conflict of interest

None declared.

Acknowledgments

The authors wish to thank the study participants and the healthcare staff at the Dispensaire Antituberculeux de l'Institut d'Hygiène Sociale and the Centre de Santé de Base niveau II (CSB II) Isotry. The authors also wish to thank Mrs Elie Vololonirina and Mrs Rondroarivelo Lucia Rasoahanitralisoa from the Mycobacteria Unit, Institut Pasteur de Madagascar; and Mrs Roxane Simeone and Mrs Caroline Demangel from Institut Pasteur in Paris for their help and advice.

Appendix A. Supplementary data

Supplementary material related to this article can be found, in the online version, at doi:https://doi.org/10.1016/j.ijid.2021.01.073.

References

Ardain A, Domingo-Gonzalez R, Das S, Kazer SW, Howard NC, Singh A, et al. Group 3 innate lymphoid cells mediate early protective immunity against tuberculosis. Nature 2019;570:528–32.

Basile JI, Geffner LJ, Romero MM, Balboa L, Sabio y García C, Ritacco V, et al. Outbreaks of *Mycobacterium tuberculosis* MDR strains induce high IL-17 T-cell response in patients with MDR tuberculosis that is closely associated with high antigen load. J Infect Dis 2011;204:1054–64.

Beveridge NE, Fletcher HA, Hughes J, Pathan AA, Scriba TJ, Minassian A, et al. A comparison of IFNgamma detection methods used in tuberculosis vaccine trials. Tuberculosis (Edinb) 2008;88:631–40.

Bottai D, Frigui W, Sayes F, Di Luca M, Spadoni D, Pawlik A, et al. TbD1 deletion as a driver of the evolutionary success of modern epidemic *Mycobacterium tuberculosis* lineages. Nat Commun 2020;11:684.

Caws MG, Thwaites S, Dunstan TR, Hawn, Lan NT, Thuong NT, et al. The influence of host and bacterial genotype on the development of disseminated disease with *Mycobacterium tuberculosis.* PLoS Pathog 2008;4:e1000034.

Chae H, Shin SJ. Importance of differential identification of *Mycobacterium tuberculosis* strains for understanding differences in their prevalence, treatment efficacy, and vaccine development. J Microbiol 2018;56:300–11.

Chen YY, Chang JR, Huang WF, Hsu SC, Kuo SC, Sun JR, et al. The pattern of cytokine production in vitro induced by ancient and modern Beijing *Mycobacterium tuberculosis* strains. PLoS One 2014;9:e94296.

Chen T, Lin J, Wang W, Fleming J, Chen L, Wang Y, et al. Cytokine and antibody based diagnostic algorithms for sputum culture-positive pulmonary tuberculosis. PLoS One 2015;10:e0144705.

Clarke C, Van Helden P, Miller M, Parsons S. Animal-adapted members of the *Mycobacterium tuberculosis* complex endemic to the southern African subregion. J S Afr Vet Assoc 2016;87:1–7.

Clifford V, Tebruegge M, Zufferey C, Germano S, Forbes B, Cosentino L, et al. Cytokine biomarkers for the diagnosis of tuberculosis infection and disease in adults in a low prevalence setting. Tuberculosis 2018;114:91–102.

Comas I, Homolka S, Niemann S, Gagneux S. Genotyping of genetically monomorphic bacteria. DNA sequencing in *Mycobacterium tuberculosis* highlights the limitations of current methodologies. PLoS One 2009;4:e7815.

Cooper AM. Cell-mediated immune responses in tuberculosis. Ann Rev Immunol 2009;27:393–422.

Domingo-Gonzalez R, Das S, Griffiths KL, Ahmed M, Bambouskova M, Gopal R, et al. Interleukin-17 limits hypoxia-inducible factor 1alpha and development of hypoxic granulomas during tuberculosis. JCI Insight 2017;2(19).

Essone PN, Chegou NN, Loxton AG, Stanley K, Kriel M, van der Spuy G, et al. Host cytokine responses induced after overnight stimulation with novel *M. tuberculosis* infection phase-dependent antigens show promise as diagnostic candidates for TB disease. PLoS One 2014;9:e102584.

Gagneux S. Fitness cost of drug resistance in *Mycobacterium tuberculosis*. Clin Microbiol Infect 2009;15:66–8.

Gagneux SK, DeRiemer T, Van M, Kato-Maeda BC, de Jong S, Narayanan M, et al. Variable host-pathogen compatibility in *Mycobacterium tuberculosis*. Proc Natl Acad Sci U S A 2006;103:2869–73.

Gilani B, Sergent SR. Interferon test. Treasure Island, FL: StatPearls; 2020.

Gopal RL, Monin S, Slight U, Uche E, Blanchard BA, Junecko R, et al. Unexpected role for IL-17 in protective immunity against hypervirulent *Mycobacterium tuberculosis* HN878 infection. PLoS Pathog 2014;10:e1004099.

He D, Yang CX, Sahin B, Singh A, Shannon CP, Oliveria JP, et al. Whole blood vs PBMC: compartmental differences in gene expression profiling exemplified in asthma. Allergy Asthma Clin Immunol 2019;15:67.

Johnson B, Bekker LG, Ress S, Kaplan G. Recombinant interleukin 2 adjunctive therapy in multidrug-resistant tuberculosis. Novartis Found Symp 1998;217:99–106.

Kaartinen T, Luostarinen A, Maliniemi P, Keto J, Arvas M, Belt H, et al. Low interleukin-2 concentration favors generation of early memory T cells over effector phenotypes during chimeric antigen receptor T-cell expansion. Cytotherapy 2017;19:689–702.

Kahan SM, Wherry EJ, Zajac AJ. T cell exhaustion during persistent viral infections. Virology 2015;479:180–93.

Kong Y, Cave MD, Zhang L, Foxman B, Marrs CF, Bates JH, et al. Association between *Mycobacterium tuberculosis* Beijing/W lineage strain infection and extrathoracic tuberculosis: insights from epidemiologic and clinical characterization of the three principal genetic groups of *M. tuberculosis* clinical isolates. J Clin Microbiol 2007;45:409–14.

Korbel DS, Schneider BE, Schaible UE. Innate immunity in tuberculosis: myths and truth. Microbes Infect 2008;10:995–1004.

Korma W, Mihret A, Chang Y, Tarekegn A, Tegegn M, Tuha A, et al. Antigen-specific cytokine and chemokine gene expression for diagnosing latent and active tuberculosis. Diagnostics 2020;10:716.

Lewinsohn DA, Lewinsohn DM, Scriba TJ. Polyfunctional CD4+ T cells as targets for tuberculosis vaccination. Front Immunol 2017;8:1262.

Liu X, Li F, Niu H, Ma L, Chen J, Zhang Y, et al. IL-2 restores T-cell dysfunction induced by persistent *Mycobacterium tuberculosis* antigen stimulation. Front Immunol 2019;10:2350.

Lopez BD, Aguilar H, Orozco M, Burger C, Espitia V, Ritacco L, et al. A marked difference in pathogenesis and immune response induced by different *Mycobacterium tuberculosis* genotypes. Clin Exp Immunol 2003;133:30–7.

Mourik BC, de Steenwinkel JE, de Knegt GJ, Huizinga R, Verbon A, Ottenhoff TH, et al. *Mycobacterium tuberculosis* clinical isolates of the Beijing and East-African Indian lineage induce fundamentally different host responses in mice compared to H37Rv. Sci Rep 2019;9:1–11.

Pipkin ME, Sacks JA, Cruz-Guilloty F, Lichtenheld MG, Bevan MJ, Rao A. Interleukin-2 and inflammation induce distinct transcriptional programs that promote the differentiation of effector cytolytic T cells. Immunity 2010;32:79–90.

Portevin D, Gagneux S, Comas I, Young D. Human macrophage responses to clinical isolates from the *Mycobacterium tuberculosis* complex discriminate between ancient and modern lineages. PLoS Pathog 2011;7:e1001307.

Prasad TSK, Verma R, Kumar S, Nirujogi RS, Sathe GJ, Madugundu AK, et al. Proteomic analysis of purified protein derivative of *Mycobacterium tuberculosis*. Clin Proteome 2013;10:1–9.

Rakotosamimanana N, Raharimanga V, Andriamandimby SF, Soares JL, Doherty TM, Ratsitorahina M, et al. Variation in gamma interferon responses to different infecting strains of *Mycobacterium tuberculosis* in acid-fast bacillus smear-positive patients and household contacts in Antananarivo, Madagascar. Clin Vaccine Immunol 2010;17:1094–103.

Rutaihwa LK, Sasamalo M, Jaleco A, Hella J, Kingazi A, Kamwela L, et al. Insights into the genetic diversity of *Mycobacterium tuberculosis* in Tanzania. PLoS One 2019;14:e0206334.

Sarkar R, Lenders L, Wilkinson KA, Wilkinson RJ, Nicol MP. Modern lineages of *Mycobacterium tuberculosis* exhibit lineage-specific patterns of growth and cytokine induction in human monocyte-derived macrophages. PLoS One 2012;7:e43170.

Smith SG, Zelmer A, Blitz R, Fletcher HA, Dockrell HM. Polyfunctional CD4 T-cells correlate with in vitro mycobacterial growth inhibition following *Mycobacterium bovis* BCG-vaccination of infants. Vaccine 2016;34:5298–305.

Stucki D, Malla B, Hostettler S, Huna T, Feldmann J, Yeboah-Manu D, et al. Two new rapid SNP-typing methods for classifying *Mycobacterium tuberculosis* complex into the main phylogenetic lineages. PLoS One 2012;7:e41253.

Tanner IS, Stephanie A, Harris MK, O'Shea, Deniz C, Daniel O, et al. Tools for assessing the protective efficacy of TB vaccines in humans: in vitro mycobacterial growth inhibition predicts outcome of in vivo mycobacterial infection. Front Immunol 2020;10:2983.

Valcheva V, Mokrousov I, Panaiotov S, Bachiiska E, Zozio T, Sola C, et al. Bulgarian specificity and controversial phylogeography of *Mycobacterium tuberculosis* spoligotype ST125_BGR. FEMS Immunol Med Microbiol 2010;59:90–9.

Van Crevel R, Ottenhoff TH, van der Meer JW. Innate immunity to *Mycobacterium tuberculosis*. Clin Microbiol Rev 2002;15:294–309.

Van Embden JD, Cave MD, Crawford JT, Dale JW, Eisenach KD, Gicquel B, et al. Strain identification of *Mycobacterium tuberculosis* by DNA fingerprinting: recommendations for a standardized methodology. J Clin Microbiol 1993;31:406–9.

Van Laarhoven A, Mandemakers JJ, Kleinnijenhuis J, Enaimi M, Lachmandas E, Joosten LA, et al. Low induction of proinflammatory cytokines parallels evolutionary success of modern strains within the *Mycobacterium tuberculosis* Beijing genotype. Infect Immun 2013;81:3750–6.

Wang C, Peyron P, Mestre O, Kaplan G, Van Soolingen D, Gao Q, et al. Innate immune response to *Mycobacterium tuberculosis* Beijing and other genotypes. PLoS One 2010;5:e13594.

Wang S, Li Y, Shen Y, Wu J, Gao Y, Zhang S, et al. Screening and identification of a six-cytokine biosignature for detecting TB infection and discriminating active from latent TB. J Transl Med 2018;16:206.

West EE, Jin HT, Rasheed AU, Penaloza-MacMaster P, Ha SJ, Tan WG, et al. PD-L1 blockade synergizes with IL-2 therapy in reinvigorating exhausted T cells. J Clin Invest 2013;123:2604–15.

World Health Organization. Global tuberculosis report 2018 WHO/CDS/TB/201820. Geneva: WHO; 2019.

You E, Kim MH, Lee WI, Kang SY. Evaluation of IL-2, IL-10, IL-17 and IP-10 as potent discriminative markers for active tuberculosis among pulmonary tuberculosis suspects. Tuberculosis 2016;99:100–8.

3. Résumé en français

Avant l'émergence de la pandémie de coronavirus (COVID-19), la tuberculose (TB) était la première maladie mortelle causé agent infectieux, devant le VIH. En 2021, 10,6 millions de personnes ont contracté la maladie et 1,6 million en sont mortes, dont 187000 co-infectées par le VIH. L'Organisation mondiale de la santé (OMS) estime qu'entre un quart et un tiers de la population mondiale est infectée par *Mycobacterium tuberculosis (M. tuberculosis)*, de manière asymptomatique, c'est-à-dire dans un état où des bactéries viables persistent sans qu'il y ait de tuberculose cliniquement active. L'infection tuberculeuse latente (ITL) constitue un réservoir à partir duquel la tuberculose-maladie continuera d'émerger, et représente donc un défi majeur pour l'effort mondial visant à mettre fin à l'épidémie de tuberculose. 20 % des personnes exposées à un bacille du complexe Mycobacterium (dont le plus connu est *M. tuberculosis*) développent une primo-infection tuberculeuse. L'infection sera le plus souvent latente, avec environ 5 à 10 % de risque de développer une forme active de la maladie au cours de leur vie. Ce risque est beaucoup plus élevé chez les enfants, chez les personnes dont le système immunitaire est affaibli : personnes vivant avec le VIH, en état de malnutrition, ou diabétiques ; comme on l'observe surtout dans les pays du Sud.

L'OMS a élaboré la stratégie "End TB", qui vise à réduire le nombre de décès dus à la tuberculose de 95% et le taux d'incidence de 90% d'ici 2035. L'objectif est d'atteindre des notifications de cas similaires à ceux observés dans les pays où l'incidence de la tuberculose est faible (moins de 8 cas pour 100 000 habitants). Pour atteindre cet objectif, l'OMS préconise, entre autres, d'intensifier la recherche de nouveaux outils de pronostic de l'évolution de l'infection latente et de diagnostic de la tuberculose afin de surmonter les limites actuelles dans ce domaine.

Le diagnostic actuel de la tuberculose repose sur des tests basés sur les expectorations, notamment le frottis microscopique et la culture, qui sont également utilisés pour surveiller la réponse au traitement antituberculeux. Cependant, les tests de TB basés

sur les expectorations présentent des limites, notamment la longue durée de culture et le manque de sensibilité et de spécificité de la microscopie à frottis. Des tests moléculaires, tels que GeneXpert MTB/RIF ou ULTRA, sont également réalisés à partir d'échantillons de crachats. En outre, bien que les tests moléculaires soient plus sensibles pour le diagnostic de la tuberculose pulmonaire, leur sensibilité reste limitée chez les patients atteints de tuberculose pulmonaire paucibacillaire. En outre, les échantillons d'expectoration peuvent être difficiles à obtenir dans certaines populations comme c'est le cas chez les enfants. Il est donc essentiel de s'appuyer non seulement sur un diagnostic précoce, mais aussi sur des biomarqueurs pour surveiller l'efficacité du traitement. Dans ce contexte, l'OMS a déclaré qu'il existe un besoin urgent de tests de tuberculose alternatifs non basés sur l'expectoration, remplissant les critères minimaux et optimaux à respecter pour un test de diagnostic ou de suivi de la réponse au traitement de la tuberculose. Il est donc essentiel de mettre au point de nouveaux tests TB basés sur des biomarqueurs à partir d'échantillons autres que les expectorations afin de développer des outils rapides et peu coûteux. Ces tests devraient être basés sur des échantillons biologiques accessibles, tels que le sang ou l'urine, pratiques pour les applications sur le terrain, et pourraient être mis en œuvre dans des pays à faibles ressources.

Alors que le monde est confronté à la pandémie de COVID-19, il est important de veiller à ce que les services et les opérations essentiels à la résolution des problèmes de santé de longue date continuent de protéger la vie des personnes atteintes de tuberculose. Nos connaissances sur la co-infection entre le COVID-19 et la TB sont assez limitées. Nous avons trouvé intéressant d'étudier la concomitance de ces deux maladies. Dans ce manuscrit de thèse, une revue de la littérature a été établie présentant la tuberculose et ses principales problématiques, puis les objectifs énoncés, avant de présenter les publications et les résultats obtenus, et enfin les résultats ont été discutés afin de tirer des conclusions finales et des perspectives.

L'objectif global de cette thèse était d'évaluer et de développer de nouveaux outils de diagnostic de la tuberculose non basés sur l'expectoration, conformément aux besoins prioritaires de la recherche sur la tuberculose conseillée par l'OMS. Ainsi, nous nous sommes concentrés sur l'évaluation de nouveaux tests sanguins pour le diagnostic de la tuberculose et sur l'identification de biomarqueurs simples et rapides pour le diagnostic de l'infection tuberculeuse mais aussi pour le suivi de la réponse au traitement de la tuberculose chez l'adulte. Dans le contexte de la pandémie de COVID-19, nous nous sommes intéressés à étudier la co-infection SARS-CoV-2 et la Tuberculose mais aussi au risque de progression de la TB suite à la co-infection par le SARS-CoV-2. A cette fin, nous avons évalué la performance d'une nouvelle signature transcriptomique sang-homme, RISK6, dans le contexte du diagnostic et du suivi du traitement de la TB. Ensuite, nous avons identifié des dosages de biomarqueurs plasmatiques en utilisant la plateforme Luminex x-MAP®, pour le suivi du traitement de la TB et pour discriminer entre TB active et ITL. Ensuite, nous avons développé un outil de sérodiagnostic pour le COVID-19 et décrit un modèle statistique pour dater l'infection par le virus SARS-CoV-2 et la présentation clinique. Cet outil a été utilisé rétrospectivement pour déterminer la séroprévalence de COVID-19 et dater l'infection par le SARS-CoV-2 chez les contacts intradomicillaires des patients atteints de TB active. Grâce à ces données, nous avons évalué le risque de progression des patients tuberculeux de la cohorte APRECIT.

Nous pensons que les résultats de cette thèse de doctorat apportent de nouvelles avancées dans le domaine de la recherche sur la tuberculose en proposant de nouveaux outils simples et rapides pour le diagnostic et le suivi du traitement de la tuberculose, qui pourraient passer de la recherche clinique aux applications cliniques, mais aussi aider à la compréhension de l'infection tuberculeuse COVID-19.

Dans la publication 1 de cette thèse, nous avons évalué la performance de RISK6, une signature transcriptomique à partir sang, pour le dépistage et le suivi du traitement de la tuberculose. Les performances de RISK6 ont été évaluées dans le cadre d'une étude

prospective multicentrique menée au Bangladesh, en Géorgie, au Liban et à Madagascar. Des patients adultes non immunodéprimés présentant une tuberculose pulmonaire active (ATB) confirmée par des examens bactériologiques, une infection tuberculeuse latente (ITL) et des donneurs sains (HD) ont été recrutés. Les patients atteints de tuberculose pulmonaire active ont été suivis pendant et après le traitement. Les scores RISK6 sanguins ont été évalués par PCR quantitative en temps réel et évalués par l'aire sous la courbe de la caractéristique récepteur (AUC ROC). La performance de RISK6 pour discriminer l'ATB de l'HD a atteint une AUC de 0,94 (IC 95 % 0,89-0,99), avec une sensibilité de 90,9 % et une spécificité de 87,8 %, atteignant ainsi les critéres de l'OMS pour un test de dépistage de la tuberculose non basé sur l'expectoration. En outre, RISK6 a donné une AUC de 0,93 (IC à 95 % : 0,85-1), avec une sensibilité de 90,9 % et une spécificité de 88,5 %, pour distinguer l'ATB de la tuberculose légère. De plus, RISK6 a montré une meilleure performance (AUC 0,90, IC 95 % 0,85-0,94) que l'IGRA-rmsHBHA (AUC 0,75, IC 95 % 0,69-0,82) pour différencier les stades d'infection tuberculeuse. Enfin, les scores de la signature RISK6 ont significativement diminué après 2 mois de traitement contre la TB et ont continué à baisser progressivement jusqu'à la fin du traitement pour atteindre les scores obtenus en HD.

Dans la publication 2, nous avons mesuré et comparé l'expression d'un panel sélectionné de protéines plasmatiques de l'hôte, chez des patients d'ATB suivi tout au long du traitement antituberculeux, chez des individus infectés d'une ITL et chez des donneurs sains afin d'identifier une signature protéique de l'hôte utile à la fois pour le diagnostic de la TB et pour le suivi du traitement. Nous avons évalué sept protéines hôtes: CLEC3B, SELL, IGFBP3, IP10, CD14, ECM1 et C1Q. Les marqueurs protéiques ont été évaluées à l'aide d'un Luminex xMAP® pour quantifier les niveaux plasmatiques dans le sang non stimulé des différents groupes cliniques. Nous avons également évalué les niveaux de protéines avant et pendant les 6 mois de traitement par ATB, chez les convertisseurs lents et rapides de la culture. Les signatures protéiques ont été définies à l'aide de l'algorithme CombiROC et de modèles multivariés. Les protéines plasmatiques de l'hôte étudiées ont montré des niveaux différents entre les groupes

cliniques et pendant le traitement de la tuberculose. Six des protéines plasmatiques ont montré des différences significatives en comparant les groupes ATB vs HD ou ITL, tandis que la protéine ECM1 a révélé une différence significative entre les convertisseurs de culture rapides et lents après 2 mois de traitement (*p-value*= 0,006). L'expression d'une signature de quatre marqueurs de l'hôte (CLEC3B-ECM1-IP10-SELL) était significativement différente entre les groupes ATB et HD ou ITL (respectivement, p < 0,05). L'expression de la même signature était significativement différente entre les convertisseurs de culture d'expectoration lents et rapides après 2 mois de traitement (valeur p< 0,05). Les résultats suggèrent une signature prometteuse de 4 marqueurs plasmatique qui serait associée à la fois au diagnostic de la tuberculose et au suivi du traitement.

Enfin, nous avons développé un test de sérodiagnostic pour le SARS-CoV-2 basé sur la technologie Luminex détectant les anticorps anti-IgG et IgM dirigé contre les régions Spike 1 (S1), Spike 2 (S2), la RBD et la Nucléocapside (N). La performance du test sérologique multiplex a été évaluée pour la détection des anticorps anti-IgG et anti-IgM du SARS-CoV-2. La sensibilité et la spécificité étaient toutes deux égales à 100% (89,85-100) pour S1, RBD et N (S2 avait une spécificité plus faible = 95%) pour les IgG au jour 14 après l'inscription. Ce test multiplex, comparé à deux kits ELISA commercialisés, a montré une plus grande sensibilité.

Ces résultats montrent la performance des marqueurs moléculaires comme outil non basé sur l'expectoration pour le triage et le suivi du traitement, répondant aux critères de l'OMS. Les deux biosignatures (transcriptomique et plasmatique) décrites dans ce manuscrit sont des signatures basées sur la réponse de l'hôte permettant de stratifier les patients en fonction de leur statut d'infection tuberculeuse, ainsi que pour le suivi des patients pendant le traitement.

Dans le contexte de l'émergence du SARS-CoV-2 et de la pandémie qui a suivi, nous avons cherché à décrire la séroprévalence du COVID-19 dans une cohorte de contacts de patients tuberculeux et à évaluer l'impact que peut avoir l'infection par le SARS-

CoV-2 sur la progression de la tuberculose. Nous savons que les personnes infectés par la *M. tuberculosis* sont à risque de développer la maladie au cours de leur vie. Ce risque est plus élevé au cours des deux premières années après l'exposition à la bactérie. Il s'agit ici de savoir si l'infection par le SARS-CoV-2 pourrait également constituer un risque pour la progression de la tuberculose. Dans l'étude APRECIT menée à Madagascar, 1030 contacts de patients atteints de tuberculose active confirmée bactériologiquement ont été recrutés et suivis pendant 18 mois. Au cours de ce suivi, des échantillons de sang veineux ont été prélevés. Le test de sérodiagnostic basé sur la technologie Luminex, développé pour cette étude a été utilisé pour mesurer les anticorps du SARS-CoV-2. Le test développé cible les IgG et IgM dirigés contre les sous-unités de la protéine spike (S1, S2, RBD) et la protéine de la nucléocapside (N). Nous avons décrit une séroprévalence élevée de l'infection par le SARS-CoV-2 dans la cohorte. A l'inclusion, la séroprévalence était de 50% d'IgM et 70% d'IgG. Une augmentation de cette séroprévalence a été observée au cours du suivi atteignant plus de 90%. Par ailleurs, nous avons décrit la progression de la tuberculose en analysant les taux de QFT-P et d'anticorps anti-SARS-CoV-2 de ces patients. Nos résultats n'ont pas montré de différence entre les progressifs et les non-progressifs chez les contacts familiaux pour la réponse humorale spécifique anti-SARS-CoV-2 et la réponse IFN-γ spécifique à la tuberculose. Des investigations supplémentaires sont nécessaires pour évaluer la corrélation entre les deux infections respiratoires.

Les résultats obtenus dans cette thèse doivent être confirmés par des études cliniques de plus grande envergure. La mise en œuvre de tests non basés sur les expectorats et utilisant des biomarqueurs de l'hôte dans les pays à ressources limitées où l'incidence de la tuberculose est la plus élevée pourrait contribuer à améliorer le diagnostic et la prise en charge globale de la tuberculose. En effet, ces tests simples sont nécessaires pour réduire la propagation et la transmission de la maladie.

Ce travail nous a permis d'apporter plus d’informations à la science aidant au contrôle de la tuberculose grâce à des approches innovantes pour le diagnostic de la

tuberculose mais aussi pour la compréhension de la co-infection TB/COVID-19 et du risque de progression. Ces outils une fois validés pourraient être optimisés et améliorés dans des formats simplifiés et plus adaptés aux pays en voie de developpement où le diagnostic de la TB reste problématique.